

DEVELOPMENT OF A PERCEPTION ORIENTED TEXTURE-BASED IMAGE RETRIEVAL SYSTEM FOR WALLPAPERS

A Doctoral Thesis
submitted in partial fulfilment of the requirement for the
award of
Doctor of Philosophy
from Middlesex University

Author:

Yu Qian

School of Computing Science

Middlesex University

June 2008

Abstract

Due to advances in computer technology, large image collections have been digitised and archived in computers. Image management systems are therefore developed to retrieve relevant images. Because of the limitations of text-based image retrieval systems, Content-Based Image Retrieval (CBIR) systems have been developed. A CBIR system usually extracts global or local contents of colour, shape and texture from an image to form a feature vector that is used to index the image. Plethora methods have been developed to extract these features, however, there is very little in the literature to study the closeness of each method to human perception.

This research aims to develop a human perception oriented content-based image retrieval system for the Museum of Domestic Design & Architecture (MoDA) wallpaper images. Since texture has been widely regarded as the main feature for these images and applied in CBIR systems, psychophysical experiments were conducted to study the way human perceive texture and to evaluate five popular computational models for texture representations: Grey Level Co-occurrence Matrices (GLCM), Multi-Resolution Simultaneous Auto-Regressive (MRSAR) model, Fourier Transform (FT), Wavelet Transform (WT) and Gabor Transform (GT). By analyzing experimental results, it was found that people consider directionality and regularity to be more important in terms of texture than coarseness. Unexpectedly, none of the five models appeared to represent human perception of texture very well. It was therefore concluded that classification is needed before retrieval in order to improve retrieval performance and a new classification algorithm based on directionality and regularity for wallpaper images was developed. The experimental result showed that the evaluation algorithm worked effectively and the evaluation experiments confirmed the necessity of the classification step in the development of CBIR system for MoDA collections.

Acknowledgements

I would like to thank the director of my research, Dr. Xiaohong Gao, for her guidance in this project and constructive criticism on the thesis. I am also grateful for her encouragement throughout the project.

I would also like to express my deepest appreciation to Miss Zoë Hendon, my supervisor, for her unconditional support and expertise on MoDA images.

I would like to pay my special tribute to late Prof. Colin Tully, whose guidance and encouragement helped me in many ways during the project.

Many thanks go to the staff and research students of Middlesex University for the discussions, support and help with the experiments. Special thanks go to Dr. Christian Huyck, Dr Roman Belavkin, Dr Arumugam Siri Bavan, Dr. Getha Abeysinghe, Mr. William McDonald, Mr. Richard Lumb, Ms. Maggie Wood, Ms. Emma Shaw, Ms. Diane Coxon, Dr. Kok Fong Tan, Ms Amala Rajan, and my friends Ms Jenny Wang, Ms Evelyn Chuan, who helped me with the experiments.

I offer my gratitude and sincere thanks to my parents for their encouragement, love and support. All my love goes to my husband, Dr. Kunbin Hong, for his enduring encouragement and taking care of all the home affairs during my writing. Thanks also go to my baby son, Hanying, who made so much effort to be “quiet” while I was writing.

Thanks and acknowledgement go to MoDA (Museum of Domestic Design & Architecture), Middlesex University for providing wallpaper images for this research.

This work is financially supported by the School of Computing Science, Middlesex University, whose support is gratefully acknowledged.

Contents

CAPTIONS	5
List of Figures	5
List of Tables	8
1. INTRODUCTION	9
2. LITERATURE REVIEW	11
2.1 Text-Based Image Retrieval	11
2.2 Content-Based Image Retrieval (CBIR)	12
2.3 Methods in Content-Based Image Retrieval	15
2.3.1 <i>Visual Feature Extraction</i>	15
2.3.1.1 <i>Colour</i>	15
2.3.1.2 <i>Texture</i>	19
2.3.1.3 <i>Shape</i>	21
2.3.2 <i>Similarity Measurements</i>	24
2.3.3 <i>Relevance Feedback</i>	25
2.4 Some Samples of CBIR System	27
2.5 MoDA and its Collections	32
2.6 Current Research Work on Wallpaper Images	33
2.6.1 <i>Texture-Based Wallpaper Retrieval</i>	33
2.6.2 <i>Symmetry Groups Based Wallpaper Retrieval</i>	34
2.7 The Importance of Human Visual Perception in CBIR for Wallpaper Images	36
3. METHODS	39
3.1 Computational Texture Features	39
3.1.1 <i>Grey Level Co-occurrence Matrices (GLCM)</i>	40
3.1.2 <i>Multi-Resolution Simultaneous Auto-Regressive (MRSAR) Model</i>	42
3.1.3 <i>Fourier Transform (FT)</i>	43
3.1.4 <i>Wavelet Transform (WT)</i>	45
3.1.5 <i>Gabor Transform (GT)</i>	47

3.2 Methods for the Data Analysis	51
3.2.1 <i>Psychophysical Scaling---Choice Score Method</i>	51
3.2.1.1 Obtaining Rankings	51
3.2.1.2 Obtaining Interval Scale---Choice Score Method.....	52
3.2.2 <i>Rank Correlation --- Spearman's Rank Correlation Coefficient</i>	53
3.3 Radon Transform	55
4. PSYCHOPHYSICAL EXPERIMENTS	58
4.1 Experiment One: Texture Feature Perception.....	58
4.1.1 <i>Experimental Preparation</i>	59
4.1.1.1 Sample Selection.....	59
4.1.1.2 Subject Selection.....	60
4.1.2 <i>Experimental Procedure</i>	60
4.1.2.1 Subject Training.....	60
4.1.2.2 Obtaining Rankings	62
4.2 Experiment Two: Human Visual Similarity	63
4.3 Summary.....	63
5. EXPERIMENTAL RESULTS AND DATA ANALYSIS	65
5.1 Results of Experiment One	65
5.1.1 <i>Rankings</i>	65
5.1.2 <i>Raw Data Analysis and Pre-Processing</i>	66
5.1.3 <i>Psychophysical Scaling</i>	67
5.2 Results of Experiment Two	69
5.2.1 <i>Rankings</i>	69
5.2.2 <i>Raw Data Analysis and Pre-Processing</i>	69
5.2.3 <i>Psychophysical Scaling</i>	71
5.3 Comparison between Computational Texture Methods and Human Visual Perception	71
5.3.1 <i>Comparison between Computational Texture Representations and Visual Texture Features</i>	71
5.3.2 <i>Comparison Similarity Measurements between Computational Texture Methods and Subjects</i>	73
5.3.3 <i>Data Analysis and Discussion</i>	74

5.4 Relationships between Visual Similarity Measurements and Visual Texture	
Features	76
5.4.1 Rank Correlation between Visual Similarity Measurements and Visual Texture Features	77
5.4.2 Data Analysis and Discussion	78
5.5 Summary	80
6. IMAGE RETRIEVAL FOR WALLPAPER IMAGES	81
6.1 Image Classification	81
6.1.1 Classification Based on Directionality	82
6.1.1.1 Directionality Representations	84
6.1.1.2 Classification Based on Directionality	91
6.1.2 Classification Based on Regularity	92
6.1.2.1 Regularity Representations	93
6.1.2.2 Classification Based on Regularity	96
6.1.3 Classification Based on Directionality and Regularity	97
6.2 Image Retrieval	98
6.3 A Content-Based Image Retrieval System for Wallpaper Images	100
6.4 Summary	101
7. RESULTS OF CLASSIFICATION AND RETRIEVAL	103
7.1 Results for Classification	103
7.1.1 Classification Based on Directionality	104
7.1.1.1 Results	104
7.1.1.2 Analysis	108
7.1.2 Classification Based on Regularity	109
7.1.2.1 Results	109
7.1.2.2 Analysis	113
7.1.3 Classification Based on Directionality and Regularity	114
7.1.3.1 Results	114
7.1.3.2 Analysis	117
7.2 Results for Image Retrieval after Classification	117
7.2.1 Results	118
7.2.1 Analysis	127

7.3 A GUI for Wallpaper Images.....	128
7.4 Summary.....	130
8. CONCLUSIONS AND FUTURE WORK.....	132
8.1 Conclusions.....	132
8.2 Contributions.....	133
8.3 Future Work.....	135
REFERENCES	137
APPENDICES.....	146

Captions

List of Figures

Figure 2.1 Basic framework of a CBIR system	13
Figure 2.2 Example of colour query	14
Figure 2.3 Texture query in satellite image databases	14
Figure 2.4 Shape query in trademark image databases	15
Figure 2.5 QBIC on-line demo	28
Figure 2.6 NeTra on-line demo.....	28
Figure 2.7 Blobworld on-line demo.....	29
Figure 2.8 MARS on-line demo.....	30
Figure 2.9 Some samples from MoDA	32
Figure 2.10 On-line search engine based on text in MoDA	32
Figure 2.11 Repeated pattern syntheses.....	35
Figure 2.12 Artlandia :graphic design software and one demo	35
Figure 3.1 Graphical illustration of co-occurrence matrices	41
Figure 3.2 Pixel X neighbourhood V5 (d=2), V7 (d=3), V9 (d=4)	42
Figure 3.3 Fourier transform of images	44
Figure 3.4 Process of 2-scale Wavelet transform of image	46
Figure 3.5 3-scale Wavelet transform of an image.....	46
Figure 3.6 Visualization of 24 Gabor filters with 4 scales and 6 orientations in the frequency domain.....	49
Figure 3.7 Gabor transform of an image with one Gabor filter ($s=3$ and $\theta = 120^\circ$)... 50	50
Figure 3.8 Significance of Spearman's rank correlation coefficient	54
Figure 3.9 Geometry of the Radon transformation	56
Figure 3.10 Edge image and its Radon transform.....	56
Figure 3.11 Straight line detection (in red) using Radon transform	57
Figure 4.1 Experimental samples.....	59
Figure 4.2 Texture images from Brodatz database	61
Figure 4.3 Example for ranking from fineness to coarseness.....	62
Figure 4.4 Example for ranking from regularity to irregularity.....	62
Figure 4.5 Example for ranking from directionality to non-directionality	62

Figure 5.1 Image ranking based on psychophysical scaling of coarseness (from fineness to coarseness).....	68
Figure 5.2 Image ranking based on psychophysical scaling of regularity (from regularity to irregularity).....	68
Figure 5.3 Image ranking based on psychophysical scaling of directionality (from directionality to non-directionality).....	68
Figure 5.4 Comparing retrieval results between subjects and five computational methods for query 9	76
Figure 5.5 Comparison between ranking results based on human visual similarity and ranking results based on visual texture feature for query 5	79
Figure 5.6 Comparison between ranking results based on human visual similarity and ranking results based on visual texture feature for query 8	79
Figure 6.1 An overview of framework for wallpaper image retrieval	81
Figure 6.2 Classification tree based on regularity and directionality	82
Figure 6.3 Wallpaper images and their Fourier power spectrum, direction histogram and Radon transform.....	83
Figure 6.4 Classification based on directionality.....	84
Figure 6.5 Radon transform of edge images	88
Figure 6.6 Directionality representations in Radon transform.....	90
Figure 6.7 Directionality features of 40 training sample images.....	91
Figure 6.8 Classification based on regularity	93
Figure 6.9 Visualizing the correlation coefficient matrix $c(i, j)$, $C(d)$ of images in horizontal and vertical direction	94
Figure 6.10 Regularity features of 40 training sample images	97
Figure 6.11 Flow of classification based on directionality and regularity.....	98
Figure 6.12 Diagram for content-based image retrieval system for wallpaper images	102
Figure 7.1 Ranking from directionality to non-directionality by subjects.....	105
Figure 7.2 Classification based on directionality for ten sample images	105
Figure 7.3 Some correctly classified directional textures and non-directional textures and their directionality representations.....	107
Figure 7.4 Misclassified textures and their directionality representations	108
Figure 7.5 Ranking from regularity to irregularity by subjects	110

Figure 7.6 Classification based on regularity for ten samples images.....	110
Figure 7.7 Some correctly classified regular textures and irregular textures and their <i>REG</i> values in horizontal and vertical direction respectively	112
Figure 7.8 Misclassified textures and their <i>REG</i> values in horizontal and vertical direction	113
Figure 7.9 Classification based on directionality and regularity for ten sample images	115
Figure 7.10 Misclassified textures	116
Figure 7.11 Nine query images selected from MoDA collections.....	119
Figure 7.12 Average precision for nine queries after classification	122
Figure 7.13 Average precision for nine queries before classification	123
Figure 7.14 Comparison retrieval results before and after classification by GLCM for query 3	125
Figure 7.15 Comparison retrieval results before and after classification by WT for query 7	126
Figure 7.16 Interface of content-based image retrieval for wallpaper images	129

List of Tables

Table 2.1 Summary of techniques in some CBIR systems	31
Table 3.1 Rankings	52
Table 5.1 The average rank correlation between texture features calculated by computational methods and visual texture features perceived by subjects.....	73
Table 5.2 Coefficients of rank correlation between computational methods and subjects for seven queries	74
Table 5.3 Coefficients of rank correlation between perceived similarity measurements and visual texture features for seven queries	78
Table 6.1 Directionality features of images	91
Table 6.2 Regularity features of images	96
Table 6.3 Rankings based on coarseness, regularity, and directionality	99
Table 6.4 Coefficients of the rank correlation between texture features.....	99
Table 7.1 True Positive, False Positive, False Negative and False Positive.....	103
Table 7.2 Classification results based on directionality for 100 test images.....	106
Table 7.3 Classification results based on regularity for 100 test images.....	111
Table 7.4 Classification results based on directionality and regularity for 100 images..	116
Table 7.5 Coefficients of rank correlation between subjects and computational methods for image retrieval after classification.....	118
Table 7.6 Comparison of retrieval results before and after classification by using five computational texture methods.....	119
Table 7.7 Four sets for retrieving images	121
Table 7.8 Average precision and mean average precision for nine queries after classification	123
Table 7.9 Average precision and mean average precision for nine queries before classification	124
Table 7.10 Comparison retrieval results before and after classification by using five computational texture methods for nine queries in dataset of one hundred images ..	124
Table 7.11 Query time.....	127

1. Introduction

In the past decade, due to the development of advanced technology in computer hardware and digital cameras, large collections of various images have been digitised and archived in computer. These databases have applications in numerous fields, including criminal identification, geographic information systems, trademark retrieval, medical image archiving and art image indexing. Effective image indexing and retrieval methods are very important for the success of image database development.

Currently, there are two main image retrieval techniques: text-based and content-based image retrieval.

Traditionally, images are indexed using textual descriptions annotated by domain experts [1]. The limitation with this system is the subjectivity of textual descriptions. In reality, textual description cannot include an enumeration of all the objects and their visual characteristics, especially their spatial relationship.

Content-Based Image Retrieval (CBIR) [2-4] was hence developed in the early 1990s to overcome the drawbacks encountered by text-based systems. CBIR systems index images using the visual contents that an image is carrying, such as colour, texture, shape and location. A CBIR system can automatically extract these visual features from an image and define the relative search/matching functions to perform retrieval.

However, most current CBIR systems only extract low-level visual features, which are mathematical representations of colour, shape, and texture, whilst users tend to use high-level concepts to retrieve images. Human perception of image similarity is subjective and task-dependent. Some progress has been made towards closing the gap between high level concepts and low level features, for example, relevance feedback is incorporated into CBIR system in order to establish the link between high-level concepts and low-level features, however there is little literature

considering human visual perception in content-based image retrieval (how a user interprets an image and performs retrieval).

The aim of this research was two fold: to investigate human perception in conducting image retrieval and to evaluate the existing five texture models in performing CBIR by comparison with human perception, an area has not previously been well researched. The wallpapers from Museum of Domestic and Architecture (MoDA) have been applied in this study, leading to the development of CBIR systems for MoDA images that are currently indexed using textual descriptions. Since texture is the dominant feature represented in these images, it was the focus of this research. Five texture models widely applied in extracting texture features in CBIR were assessed in comparison with human perception.

The structure for this thesis is organised as follows. A literature review is given in Chapter 2 describing the background and basic techniques in Content-Based Image Retrieval (CBIR). Chapter 3 describes some methods applied in this research. Chapter 4 details the experimental methodology employed. The experimental results and analyses are presented in Chapter 5. Based on experimental results, the developed CBIR system for MoDA images is described in Chapters 6 and 7. Finally, the overall conclusions and recommendations for future work will be presented in Chapters 8. The final two sections are the References and Appendices.

2. Literature Review

Due to the rapid development of digital cameras and computer technology, large numbers of images are collected and stored in computers. Systematic management of these image data is therefore very important for future applications in order to retrieve images effectively and efficiently. Two approaches are most commonly used, one is text-based image retrieval and the other is content-based image retrieval.

2.1 Text-Based Image Retrieval

Text-based image retrieval can be traced back to the 1980s[1]. Traditionally, images are indexed by text descriptions, such as keywords, filenames, etc. These systems first annotate an image with text written by domain experts and then perform image retrieval using a textual description. Though the text-based image retrieval can get image semantic information directly and higher retrieval precision, four major difficulties are inherent in this method of image retrieval.

- *Heavy labour and time consumption*

The process of detecting, describing and inputting significant data requires a vast amount of labour and time, especially, when the size of image collections is very large.

- *Visual information scarcity*

Text-based descriptions cannot sufficiently capture the visual content, for example, a description of the semantic content of an image does not include an enumeration of all objects and their characteristics, which may be of interest to the user.

- *Subjectivity*

Different people may have different opinions on the same image. For example, the textual descriptions of visual attributes such as colour, shape and texture vary

greatly among people. Perception subjectivity and annotation imprecision may cause mismatches in later retrieval processes.

- *Language problem*

Language mismatch can occur when the user and the domain expert use the different vocabularies and phrases. In other words, if a user does not specify the right keywords representing his/her desired images, mismatches will occur.

On the other hand, a casual user who has no knowledge of the exact image he is looking for, may just search for the images by sketching or describing the colour of the object, for example, blue sky, green grasses, etc. Possibly, the user provides a sub-image and wants to know the images that include it or are similar to it. Text-based systems are unlikely to find solutions to these queries.

2.2 Content-Based Image Retrieval (CBIR)

In the past twenty years, Content-Based Image Retrieval (CBIR) has been developed to overcome the above difficulties [2-4]. That is, images are indexed by their own visual contents, such as colour, texture and shape. As shown in Figure 2.1, a typical CBIR system can automatically extract visual features from images and store them in a visual feature database in advance. When a user submits a query, pre-defined visual features from the query image are extracted, and then the distance between the feature vector of the query image and the visual feature database is calculated. Finally, a set of images are retrieved and ranked based on the degree of similarity calculated by the feature distance. It is clear that feature extraction and similarity measurements are the two most important parts in content-based image retrieval. Recent CBIR systems have incorporated users' relevance feedback to modify the retrieval process in order to generate more meaningful retrieval results both perceptually and semantically.

Compared with the difficulties of text-based image retrieval described in Section 2.1, CBIR system has the following advantages.

- *Less time and labour intensity*

Most of the visual contents of an image, such as colour, texture and shape, can be extracted and stored by a computer automatically. Visual feature extraction will be described in Section 2.3.1.

- *Objective retrieval results*

The retrieval result is presented by the value of the search/matching functions. Objective retrieval results can be obtained when a suitable similarity measurement is defined. Similarity measurements will be reviewed in Section 2.3.2.

These advantages mean that CBIR systems are applied to many different areas of science and industry, including bio-informatics, crime prevention, geographic information systems and intellectual property. The disadvantages of CBIR are the semantic gap between the low level vision features and high level concepts therefore results in poor retrieval performance of many CBIR systems. How to bridge semantic gap is a big issue to challenge most researchers.

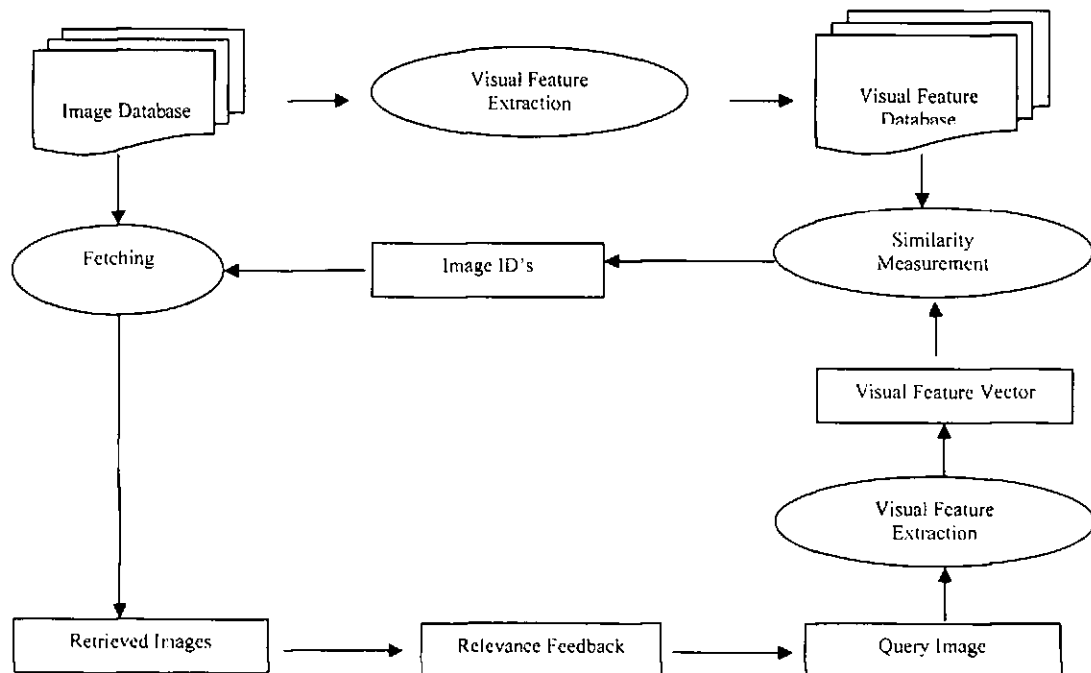


Figure 2.1 Basic framework of a CBIR system

The following figures 2.2 to 2.4 show three samples of image retrieval based on colour, texture and shape respectively.

1) *Colour-based retrieval in natural photographs*

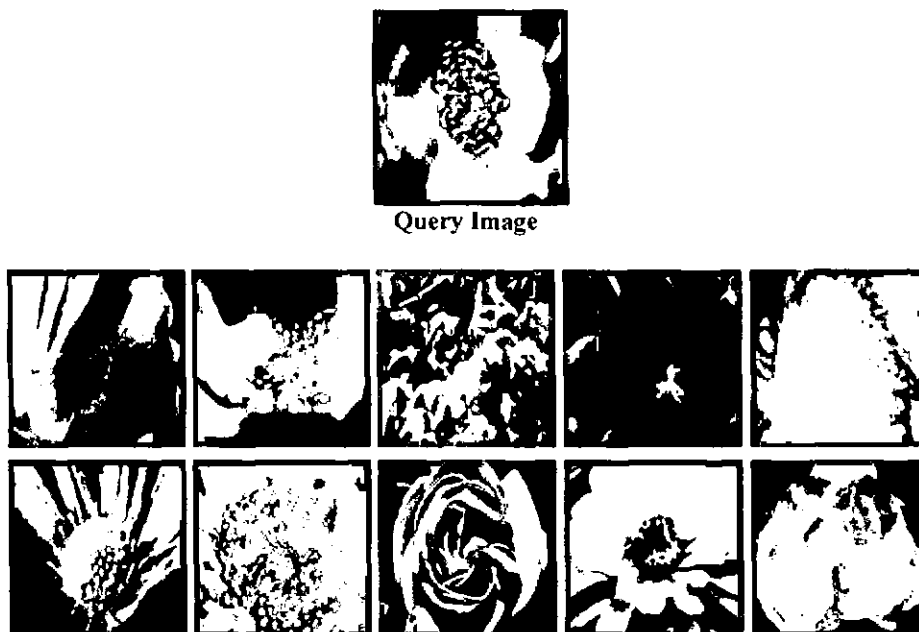


Figure 2.2 Example of colour query

2) *Texture-based retrieval in satellite images databases*

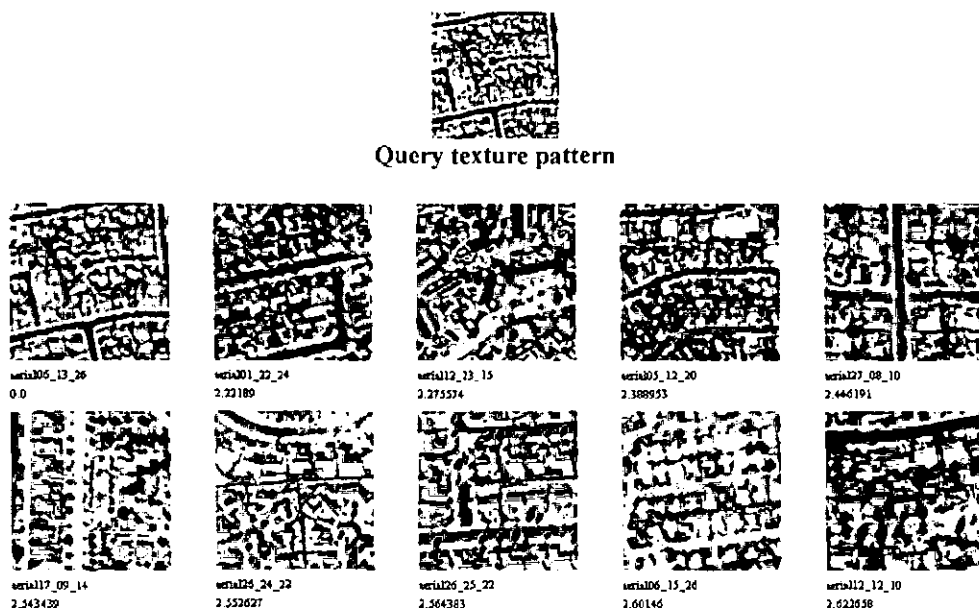


Figure 2.3 Texture query in satellite image databases

3) Shape-based retrieval in trademark image databases

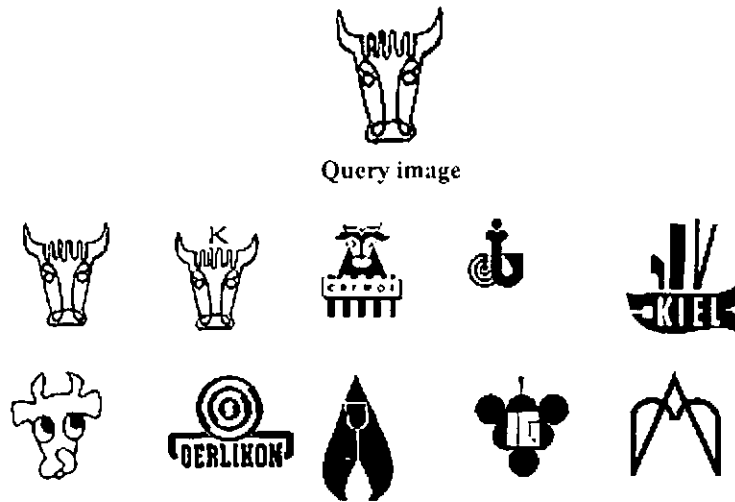


Figure 2.4 Shape query in trademark image databases

2.3 Methods in Content-Based Image Retrieval

Visual feature extraction, similarity measurements and relevance feedback are the most important components in content-based image retrieval, as shown in Figure 2.1. They directly affect the effectiveness of the retrieval. The following sections will review some methods applied in visual feature extraction, similarity measurements and relevance feedback.

2.3.1 Visual Feature Extraction

Visual feature extraction is the basis of content-based image retrieval and is to extract the mathematical representations of the visual contents, which usually include colour, texture and shape. To extract these visual features, many methods of image processing have been utilized as explained below.

2.3.1.1 Colour

Colour is one of the most important visual features in image retrieval, not only from the point of the view of the early stages of the human visual system, but also

from the subconscious reception of the outside-world images by the brain [5]. The typical colour feature extraction consists of three steps.

- 1) Colour space definition
- 2) Colour space quantization
- 3) Colour feature representations

1) Colour space definition

Normally, colour information in digital images is represented by three values Red, Green, and Blue (RGB). RGB colour space is suitable for colour reproduction on computers but not for human perception because:

- Non-intuition, i.e., it is hard to visualise a colour based on the values of R, G, B components, i.e., (23,45 60)
- Non-uniformity, i.e., the differences in two RGB values do not equate to equal differences in colour perception. It is impossible to evaluate the perceived differences between colours based on the distance in RGB space.

Therefore, the first stage is to convert RGB colour space into other colour spaces since most images are represented using RGB when digitised. With respect to subjective colour perception, other colour spaces like HSI, HSV, HSL, CIE_Lab, CIE_Luv and Munsell are more appropriate [6]. In general, they represent colour with three variants based on human perception. Comparing to the RGB colour space, they have:

- Intuition, i.e., user could define the colour easily by indicating the hue (H), saturation (S) and intensity (I , or V , or L) values independently. Hue is the attribute of a colour by which we distinguish red from green, blue from yellow, etc. Saturation is related to colour purity and intensity is corresponding to the brightness of the colour.

- Uniformity, i.e., the equation allows the Euclidian distance between two points in the uniform colour space to predict more accurately the observed difference in colour. This makes colour space quantization and colour similarity measurements easier and more accurate.

According to the advantages discussed above, colour spaces based on human perception, i.e. HSI, HSV, CIELab, etc. are widely applied to represent colour in most CBIR systems [7-12].

2) Colour space quantization

There are up to 256^3 colours when a standard digital camera is used. Colour quantization is used to reduce the size of colour space by partitioning the original colour space into many cells. Colour quantization algorithms have two basic approaches as follows.

- Pre-clustering
- Post-clustering

In the pre-clustering approach, the colour space is divided into a set of rectangular cells. Each colour is determined by its arithmetic mean or another representation for each cell. Uniform and non-uniform quantization, which divides colour space into cube cells and rectangular cells respectively, can be grouped as pre-clustering approaches.

In post-clustering approach, small numbers of cluster centres are selected randomly and each colour is placed in a cluster corresponding to which they are closest. The typical clustering algorithms, such as K-means clustering algorithm [13] and Self-Organising Feature Map (SOFM) [14], can be grouped as post-clustering approaches. By training samples, the quantized colours that are sometimes called codebook or lookup table can represent a colour image better.

3) Colour feature representations

The colour histogram [15] is one of the most used colour representations of an image. The colour histogram counts the percentages of each colour in an image and this is normally applied to represent the global or local colour distribution [16].

Global colour distribution, which is called Global Colour Histogram (GCH), describes the colour distribution of the whole image, ignoring the spatial distribution of the colour.

Local colour distribution, which is called Local Colour Histogram (LCH), describes the colour distribution in the individual cells or regions of an image. It is divided into two basic methods, which are partition-based representations and regional representations.

Partition-based representations describe the colour distribution of each cell of image individually. It decomposes images into a set of fixed cells, such as the quadtree-based colour layout approach [17]. There is no need to explicitly represent spatial properties of the partition cells such as area, shape and spatial location.

Regional representations describe the colour distribution of each image region individually, such as *NeTra* [18], *Blobworld* [8] etc. This exploits the visual contents of the image for segmentation and is necessary to represent at least its colour distribution, size and spatial location. The spatial location of a region can be represented by means of the spatial coordinates of its centre. The shape region can be represented using, for example, a minimum bounding rectangle.

In addition to the colour histogram, several other colour distribution representations have been applied in image retrieval, including colour moments and colour correlograms.

The colour moments [19] are proposed to overcome the quantization effects in the colour histogram. Based on probability theory, colour distribution can be characterised by its moments. The first moment (mean), the second moment (variance) and the third moment (skewness) of each of the three-colour channels are extracted as the colour feature representations.

The colour correlograms [20] combine the colour distribution with spatial layout. This expresses how the spatial correlation of pairs of colour changes with distance. Normally, a correlogram for an image is a table indexed by colour pairs, also called colour co-occurrence matrices, where the d -th entry for position (i,j) specifies the probability of finding a pixel of colour j at a distance d from a pixel of colour i in this image.

In comparison with all the colour representations, the colour histogram is widely applied in most CBIR systems [7-12, 18] with the following advantages.

- Robustness, i.e., invariant to translation, scale, and rotation of image
- Computational simplicity
- Low storage requirements

2.3.1.2 Texture

Texture is an important cue in visual features for analysis of many types of images, such as satellite images and textile images. The “definition” of texture is formulated by different researchers. For example,

“Texture is related to two visual components: Tone and Structure. Tone refers to the intensity of pixels while structure concerns the spatial relationship between pixels. An image texture is described by the number and types of its (tonal) primitives and the spatial organization or layout of its (tonal) primitives.” [21]

“The texture relates mostly to a specific, spatially repetitive (micro) structure of surfaces formed by repeating a particular element or several elements in different relative spatial positions. Generally, the repetition involves local variations of scale, orientation, or other geometric and optical features of the elements.” [22]

“We may regard texture as what constitutes a macroscopic region. Its structure is simply attributed to the repetitive patterns in which elements or primitives are arranged according to a placement rule.” [23]

So far, no one has succeeded in producing a commonly accepted definition of texture. However, most researchers agree that an image of visual texture is spatially homogeneous, and typically contains repeated structures, sometime local variation exists in the repetition.

Image texture is measured as a function of the spatial variation in pixel intensities. The quantifying global properties referred to visual features are defined, such as coarseness, regularity, roughness, granulation etc [23, 24].

In general, three main approaches are used to extract texture features, namely the spatial approach, frequency analysis approach and spatial frequency analysis approach.

1) Spatial approaches, such as Random Field Model, Co-occurrence Matrices and Tamura representations

In random field models, an image is assumed to be a homogeneous 2-D random field. By 2-D decomposition, the image is expressed as the sum of three orthogonal components corresponding to periodicity, directionality and randomness [25].

Co-occurrence matrices, similar to the colour correlograms described in Section 2.3.1.1, are used to represent the grey level spatial dependence of texture. Some meaningful statistics from the matrices, such as moment, entropy, contrast, etc., are extracted as the texture representations [26-28].

Tamura representations [23] are developed based on psychological studies in human visual perception of texture. This is a kind of computational representations of six texture features: coarseness, contrast, directionality, linelikeness, regularity and roughness.

2) Frequency analysis approach, such as Fourier Transform

Fourier transform is applied to transform the image from spatial domain to frequency domain. Normally, the spectrum energy of texture is represented as the texture feature representations [29, 30].

3) Spatial frequency analysis approach, such as Wavelet Transform and Gabor Transform

Wavelet transform and Gabor transform have the ability to capture the presence of dominant information at different scales and orientations for the image. The statistical features (mean and standard deviation) or energy features are extracted from each orientation in each scale as the texture representations respectively [31-35].

2.3.1.3 Shape

Shape is another important clue for object representations. Generally, shape feature extraction consists of the following two steps.

- 1) Shape detection
- 2) Shape feature representations

1) Shape detection

Shape detection is the first step to describe the shape of an object. Edge point is defined as the sharp variation point of the intensity. Based on this definition, edge detection algorithms have two categories. There are traditional methods, such as Edge Operators, and multi-scale edge detection, such as Wavelet Transform Modulus Maxima (WTMM).

Traditional methods, such as the Sobel method, Prewitt method, Zero-cross method, Canny method etc.[36], use edge operator approximation to deviation to find the shape of object. Furthermore, the Canny method [37] defined edge point as local maxima of the gradient of image and this method performs better. All of these methods detect the edge of object just in one scale.

Based on multi-scale analysis of the human visual system and the theory of modulus maxima applied in the Canny method, Wavelet Transform Modulus Maxima (WTMM) is applied to detect the edge of an object in different scales successfully [38]. Thus, shape feature representations in different scales can be extracted after shape detection and the shape matching can be done at different scales.

2) Shape feature representations

In image retrieval, shape feature representations are required to be invariant to translation, rotation and scaling which is also called the rigid transform of object. Mainly, the shape representations, which are invariant to rigid transform, can be divided into three categories. There are Fourier Descriptors, Moment Invariants and Geometric features representations.

Fourier Descriptors use the Fourier transformed edge as the shape feature representations [39]. The first few Fourier descriptors can be used to capture the gross essence of a boundary. Thus, these coefficients carry shape information can be used as the basic shape feature for distinguishing between distinct boundary shapes.

Moment Invariants use region-based moments as the shape feature. From the second-order moments and third-order moments, Hu creates the simple 7 invariant moments [40], which are used for scale, position, and rotation invariant pattern identification [41]. Zernike moments [42] are a set of complex orthogonal moments and invariant to rotation, which has been successfully used in pattern recognition and image analysis [43, 44].

Shape features can be described by some simple geometric representations [45], for example, circularity and rectangularity are mainly applied to represent the object with typical geometric shape. Hole Area Ratio (HAR) is effective in discriminating between symbols that have big holes and symbols that have small holes. Eccentricity is a measure of the elongation of the shape.

Besides the rigid transform that is rotation, translation and scaling transform, the object has the deformation transform. It is said that: "there are no two leaves of the same shape", an object shape will have intrinsic within-class variations. The following section will introduce some models of object deformation.

Object shape can vary. For example, it can incorporate smoothness or elasticity constraints like the shape of balloon and cell, or the shape can be specified using a hand-drawn form. In the 1970s, the concept of deformable templates was introduced and applied to pattern recognition and computer vision. Based on

application, the research about deformable templates can be divided into two classes. These are free-form deformable models and parametric deformable models.

Free-form deformable models can represent any arbitrary shape as long as some regularisation constraint (continuity, smoothness, etc.) is satisfied. In this approach, an energy-minimising contour called an active contour or a “Snake” [46] is controlled by combining it with internal contours energy that enforces smoothness, external constraint force, and image force which attracts the contour to the desired features. It is commonly applied to segment the organs in medical images [47].

Parametric deformable models can encode a specific characteristic shape and its deformation. It is commonly used when some prior information about the object shape is available. There are two ways to parameterise the object shape class and its deformation. This leads to two types of deform templates: analytical deformable templates and prototype-based deformable templates.

In analytical deformable templates, the shape can be expressed by a parametric formula, such as a set of analytical curves (e.g. ellipse), and its deformation can be defined by changing the value of its parameters. This is applied to the deformation of the specific geometrical shape object. For example, Yuille et al. [48] defines the eye and mouth models using circles and parabolic curves, Dubuisson et al. [49] uses a polygonal template to parameterise a vehicle.

In prototype-based deformable templates, the deformable templates are derived from a set of deformation parameters on a prototype. A prototype that describes the ‘most likely’ or ‘average’ shape of a class of objects, can be obtained by a sketch or an example of an object class. Therefore, this is used in image retrieval queried by a shape sketch/example [50, 51] and object tracking in video [52].

In all the models above, the deformable template can alter itself to match the object to a given image. Deformable template matching can be formulated using a Bayesian framework. Within the Bayesian framework an objective function, sometimes called the energy function, is defined. This energy function is related to the degree of template deformation and also the degree of matching between the

deformable template and the object in a given image. A deformable template is matched with a given object in an image when the energy function is minimised.

2.3.2 Similarity Measurements

Generally, a distance function is used to compare the visual features of two images. The distance function affects directly the time spent processing a query and the quality of the retrieval. The better the distance function simulates the similarity of human perception using the visual features, the more effective the CBIR system is at retrieving images relevant to the user's needs. The computational complexity of the distance is an important factor for speed when processing a visual query.

One typical distance function is vector distance function, such as a member of the L_p family of distance. L_p distance is defined as the following.

$$L_p(a, b) = \left(\sum_{i=1}^k |a_i - b_i|^p \right)^{\frac{1}{p}} \quad (2.1)$$

where, $a = \{a_1, a_2, \dots, a_k\}$ and $b = \{b_1, b_2, \dots, b_k\}$ are two k -dimensional vectors. Some well-known members of the L_p family, such as L_1 (City-Block) distance, L_2 (Euclidean) distance, L_∞ (Chebyshev) distance, are widely used to compare the visual features of two images. In the method of vector distance, visual features are first modeled in the vector space, and then the geometric distances are used to compare the visual similarity. The advantage of this method is its simplicity of computation. However, the simple geometric distance may not effectively measure the real difference of human perception.

When considering human perception, various other similarity measures are proposed, for example, histogram quadratic distance [7] which defines a colour cross-correlation matrix, weighted distance which defines the weighting factors based on human perception, and histogram intersection distance [15] which reduces the contribution of unrelated colour by computing the intersection of each colour histogram.

In summary, CBIR technologies strive to create mathematical representations of images derived by a set of rules of the human visual system and to design similarity measurements based on human perception.

2.3.3 Relevance Feedback

Relevance feedback (RF) is a supervised learning technique used to improve the effectiveness of CBIR systems. The main idea is to use positive and negative examples from users to improve system performance. For a given query, the CBIR system first retrieves a list of ranked images according to a predefined similarity measurement of visual features. Then, a user selects a set of positive (relevant) and/or negative (irrelevant) examples from the retrieved images. The system will refine the retrieval results based on the feedback and present a new list of images to the user. Image retrieval based on relevance feedback is repetitive and gradually advancing processes, the interaction between the system and the user enables the retrieval to approach the user's expectation, and finally answers the request.

The aim of relevance feedback is to study from the interaction between retrieval system and user, to discover and capture the user's actual demand, and to modify the retrieval process, thus obtaining a retrieval result which tallies as precise as possible with the user's actual request. The key issue in relevance feedback is how to effectively utilize the information provided from user's feedback to increase the retrieval accuracy. A variety of relevance feedback techniques have been proposed in the last decade. The main algorithms include feature re-weighting, Bayesian target search, Support Vector Machines (SVM) learning and decision trees.

Rui et al. [53] proposed relevance feedback based on the interaction of retrieval approach. Based on a user's feedback, the user's subjective perception was captured by dynamically updating weights for visual features, i.e. colour, texture etc. The experimental results carried on more than 70000 Corel images show that the proposed approach can capture the user's information needs more precisely. This approach of relevance feedback has first been implemented in a Multimedia Analysis and Retrieval System (MARS) [9].

Ishikawa et al. [54] applied the computational method of global optimization to relevance feedback. They formulized a minimization problem on the parameter estimating process. The user can give several examples, and optionally, their 'goodness' scores. Based on the user's information, the system can 'guess' which visual features are important, which correlations are important, and with what weight. Experimental results on real and synthetic databases show this method can estimate the 'hidden' distance function in the user's mind quickly and accurately. The MindReader retrieval system was designed based on this approach.

Cox et al. [55] applied a Bayesian approach to CBIR with relevance feedback. The Bayesian rule was applied to predict the user's actions for refining its answers to converge to a desired target image. This was done via a probability distribution over possible image targets, rather than refining a query. A Bayesian image retrieval system, PicHunter was designed by using Bayes's rule to predict the target image the user wants based on his/her actions. Experimental results show the system performs quite well for a wide spectrum of users tested on a wide variety of target images.

Hong et al. [56] proposed to incorporate Support Vector Machines (SVM) into CBIR with relevant feedback. This approach utilized both positive and negative feedback for image retrieval. SVM was applied to classify the positive and negative images. The SVM learning results were used to update the preference weights for the relevant images. This not only released the users from providing an accurate preference weight for each positive relevant image but also utilized the negative information. Experimental results on Corel images show that the proposed approach offers improvements over the previous approach that uses positive examples only (Rui et al.).

MacArthur et al. [57] applied learned decision trees as a relevance feedback retrieval system. For each retrieval iteration, a Decision Tree (DT) was learned to uncover a common thread between all images marked as relevant. This tree was then used as a model for inferring which of the unseen images the user was most likely to desire. The technique of relevance feedback decision tree was applied in a pre-existing CBIR system for High Resolution Computed Tomography (HRCT) images of the human lung. Experimental results show this approach achieves better retrieval as

measured in off-line experiments and as judged by a radiologist who is a lung specialist.

From the past research, relevance feedback has been shown as an effective scheme to improve the retrieval performance of CBIR and has already been incorporated as a key part when designing a CBIR system.

2.4 Some Samples of CBIR System

Several CBIR systems, both commercial and research, have been proposed, such as *QBIC* [7], *NeTra* [18], *Blobworld* [8], *MARS* [9], *Viper* [10], *Photobook* [25], *VisualSEEK* [11], *CIRES* [12], etc, the comprehensive reviews are in [58] and webpage¹. Most of them support one or more of the following options.

- Query by Example (QBE), i.e., the user specifies a target query image, which can be a normal image, a low resolution scan of an image, or a user sketch using painting tools with graphical interface.
- Query by Features (QBF), i.e., users specify queries by the description of the visual features directly, for example, “retrieve all images that contains 25% red pixels”. This query is usually specified by the use of specialized graphical interface tools.
- Query by Keywords, i.e., content-based queries are often combined with text and keywords at the same time to get powerful retrieval methods for image databases.

Here, we select a few representative systems and highlight their distinctive characteristics.

QBIC^(TM) (Query By Image Content) developed by IBM is the first commercial CBIR system. Its system framework and techniques had a great effect on later image retrieval systems. The *QBIC* system allows queries on large image databases, based on colour, texture, shape, example images/sketch, and keywords. It

is applied in the U. S. Patent and Trademark Office (USPTO) and the State Hermitage Museum in Russia. The online demo² is shown in Figure 2.5.



Figure 2.5 QBIC on-line demn

NeTra is a prototype image retrieval system that was developed in the Alexandria Digital Library (ADL) project. *NeTra* uses colour, texture, shape and spatial location information in the segmented regions to search and retrieve similar regions from an image database. That is, the query image is split into regions and the user can choose which region is utilised, queries can be performed based on colour, location, shape or texture of the chosen regions. It is suitable for retrieving images that contain multiple complex objects. The online demo³ is shown in Figure 2.6.

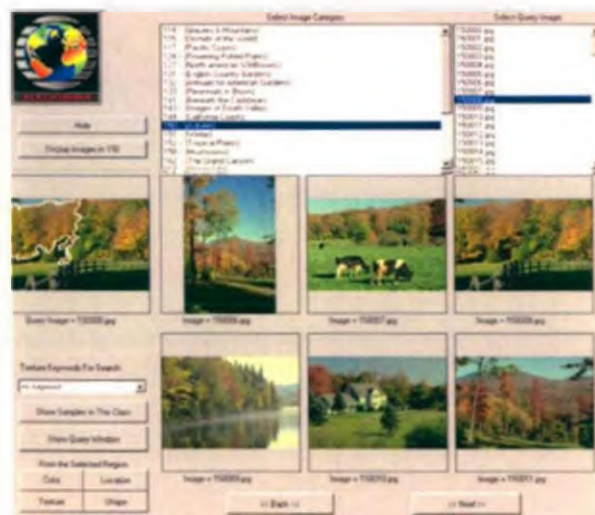


Figure 2.6 NeTra on-line demo

Blobworld was developed by University of California. Similar to *NeTra*, it can segment each image into separate "Blobs" that roughly correspond to objects or parts of objects automatically. It allows query image based on the objects and adjusts the visual feature weights, one example of weight definition shown as below. The online demo⁴ is shown in Figure 2.7.

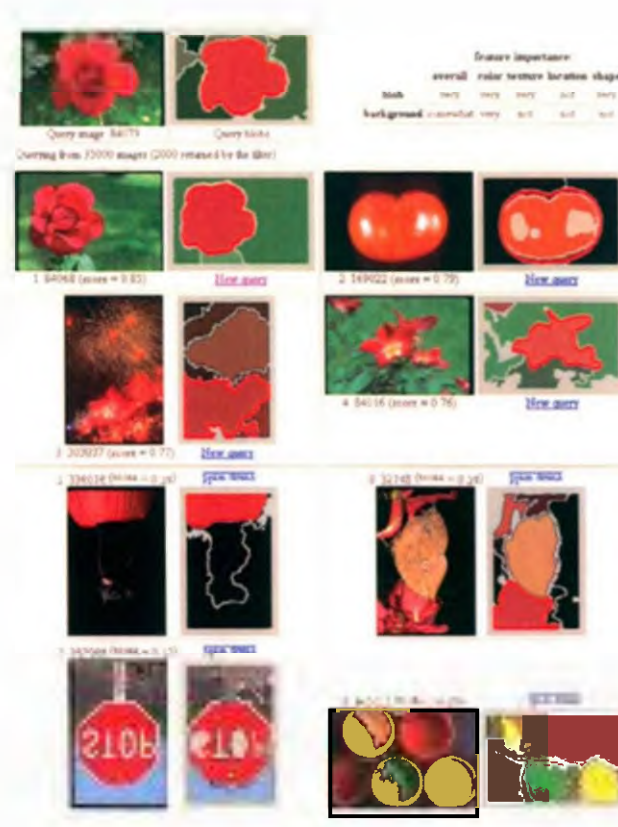


Figure 2.7 Blobworld on-line demo

MARS (Multimedia Analysis and Retrieval System) was developed by the Computer Science Department, University of Illinois at Urbana-Champaign. *MARS* supports queries on a combination of low level features (colour, texture shape) and textual descriptions. The *MARS* team formally proposes a relevance feedback architecture in image retrieval [9, 53]. In *MARS*, the user selects relevant images from previous retrieval results and provides a preference weight for each relevant image. The weights for the low-level features, i.e., colour and texture, etc., are dynamically updated based on the user's feedback. Based on this feedback, the high level concepts implied by the query weights are automatically refined. The online demo⁵ is shown in Figure 2.8.

4. <http://elih.cs.berkeley.edu/photos/blobworld>
5. <http://www.itp.uiuc.edu/~qitian/MARS.html>



Figure 2.8 MARS on-line demo

Table. 2.1 is a summary of techniques in some CBIR systems [8-12, 18, 25, 55].

Table 2.1 Summary of techniques in some CBIR systems

System	Colour				Texture		Shape		Relevance Feedback
	Colour Space	Colour Quantization	Colour Features	Similarity Measure	Texture Features	Similarity Measure	Shape Features	Similarity Measure	
<i>QBIC</i>	CIE Lab, Munsell, RGB, Yiq	256 Colours	Global Histogram	Histogram Quadratic Distance	Tamura Representations	Weighted Euclidean Distance	Moment Invariants, Geometric Features	Weighted Euclidean Distance	
<i>NeTra</i>	RGB	256 Colours (code book)	Region Histogram	Weighted Euclidean Distance	Gabor Transform	L_1 Distance	Fourier Descriptor	L_2 (Euclidean) Distance	
<i>Blobworld</i>	CIE Lab	218 Colours	Region Histogram	Histogram Quadratic Distance	Contrast, Anisotropy	L_2 (Euclidean) Distance	Geometric Features	L_2 (Euclidean) Distance	
<i>MARS</i>	HSV		Global Histogram	Histogram Quadratic Distance	Wavelet, Fourier, Atomic texture features,	Weighted Euclidean Distance	Fourier Descriptor	Weighting Function	Feature re-weighting
<i>PicHunter</i>	HSV, RGB	64	Global Histogram, Colour Correlogram, Colour Coherence vectors	L_2 Distance					Bayes's rule
<i>Viper</i>	HSV	166 Colours	Global, Partition Histogram		Gabor Transform	Weighting Function			Feature re-weighting
<i>Photobook</i>					Random Field	L_2 (Euclidean) Distance	Parametric deformable model	Energy Function	
<i>VisualSEEK</i>	HSV	166 Colours	Region Histogram	Histogram Quadratic Distance	Wavelet Transform	L_2 (Euclidean) Distance			
<i>CIRESE</i>	CIE Lab	15 Colours (coarse) 2520 Colours (finer)	Global Histogram	Histogram Intersection Distance	Gabor Transform	L_2 (Euclidean) Distance			

2.5 MoDA and its Collections

Art design collections from MoDA (Museum of Domestic Design & Architecture) are used for our system. MoDA is part of Middlesex University. It is widely regarded as one of the world's most comprehensive collections of nineteenth and twentieth century decorative arts for the home. Its collections are recognised to be of outstanding national academic importance and are a unique resource for scholar and design professionals. MoDA has an outstanding collection of wallpapers and textiles dating from the 1870s to the 1960s, it comprises around 40,000 designs (for wallpapers, textiles, carpets and other domestic furnishings), 5,000 wallpaper samples and 5,000 textile samples. Some samples are shown in Figure 2.9. Most of them have been digitised and indexed using keywords denoted by the art design experts at MoDA.



Figure 2.9 Some samples from MoDA

Parts of MoDA collections are available on MoDA's online catalogue⁶, which can be searched based on keywords.

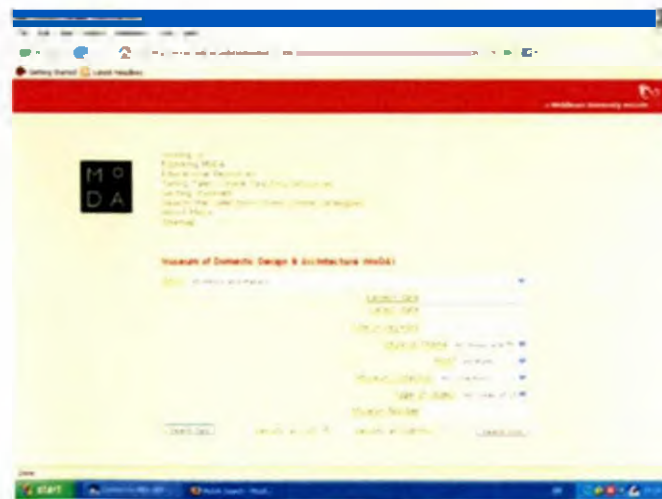


Figure 2.10 On-line search engine based on text in MoDA

6. <http://www.moda.mdx.ac.uk>

However, some clients prefer to retrieve images by visual content, for example, querying similar colourful images, or with similar texture patterns. Therefore, it is necessary to develop a CBIR system for MoDA collections.

2.6 Current Research Work on Wallpaper Images

Current researches on CBIR for wallpaper images are divided into two groups. One focuses on texture. The visual features of wallpaper, which are directionality, regularity and symmetry, are extracted and perform retrieval based on similarity measurements. The other concentrates on symmetry. According to the theory of symmetry groups, the symmetry features are extracted for repeated pattern retrieval.

2.6.1 Texture-Based Wallpaper Retrieval

Wallpaper images typically have visual texture features according to the definition of texture described in Section 2.3.1.2. This normally presents spatially homogeneous areas, contains repeated patterns, or shows geometric structure, as seen in Figure 2.9. It refers to visual texture properties like coarseness, regularity and directionality.

Some research work on texture-based image retrieval for fabric images, such as for textile images, which have similar visual texture features to wallpaper images, i.e. directionality, regularity and symmetry.

Lau et al. [59] proposed a CBIR system called ‘Montage’, which supports CBIR based on the colour histogram, sketch, texture and shape for fashion, textile and clothing images. It uses the co-occurrence matrices as the texture feature representations. The performance for query based on texture shows better results than query based on colour and on sketch for fabric images.

Balmelli et al. [60] first attempted to define the perceptual features for fabric images in the wavelet domain. Three perceptual features: directionality, regularity and symmetry, are extracted from edge and correlation characteristics of the wavelet

subbands in horizontal and vertical direction respectively. The texture feature vector is expressed as follows.

$$\vec{f} = \{D_x, D_y, R_x, R_y, S_x, S_y\} \quad (2.2)$$

where $D_x, D_y, R_x, R_y, S_x, S_y$ represent the features of directionality, regularity and symmetry in horizontal and vertical direction respectively. Bashar et al. [61] further improved these three feature representations and applied the texture feature vector to perform retrieval by similarity measurements for textile (e.g. curtain) images. The experimental results showed that directionality features provide the better retrieval results than regularity and symmetry features.

2.6.2 Symmetry Groups Based Wallpaper Retrieval

Wallpaper groups also called two-dimensional crystallographic groups were discovered and studied in the late 19th century. Fedorov, Schoenflies, and Barlow classify 2D repeated patterns into 17 wallpaper groups [62]. In a 2D repeated pattern, repeated unit is repeated along two linearly independent vectors, producing simultaneously a covering (no gaps) and a packing (no overlaps) of the original image [63]. The two vectors are called translation vectors and these build up lattice structure, seen in Figure 2.11 (c). The 17 wallpaper groups describe patterns extended by two linear independent translational generators. According to the theory of wallpaper groups, there are exactly seventeen different plane symmetry groups, which are characterized by four distinct kinds of planar symmetry, named translation symmetry, rotation symmetry, reflection symmetry and glide reflection symmetry. The following figure shows an example of repeated pattern synthesis. The synthetic image includes rotation and translation symmetries.

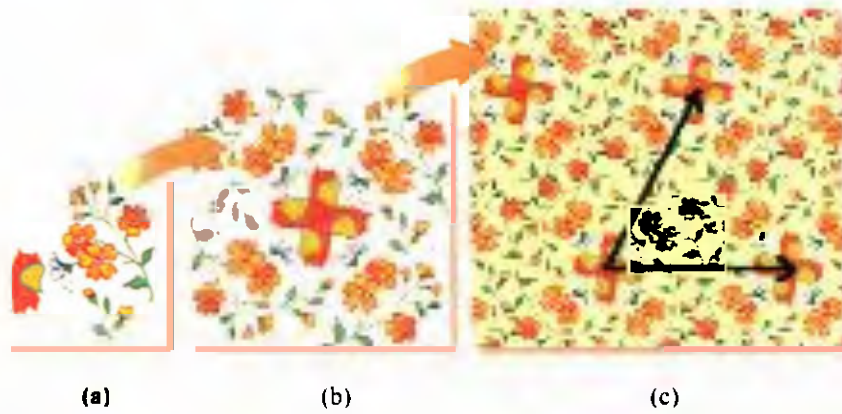


Figure 2.11 Repeated pattern syntheses

According to the symmetry of the wallpaper groups, beautiful patterns can be created by repeating geometric and artistic patterns. Artlandia⁷ is an award-winning software for creating repeated patterns and plug-ins for Adobe Illustrator and Photoshop. In Artlandia, the repeated unit is created first, and then the user can select one of 17 wallpaper groups showing icons in the upper side of Figure 2.12 (a). According to this symmetry of wallpaper groups, repeated patterns can be created automatically. One demo of repeated patterns created by Artlandia is shown in Figure 2.12 (b)

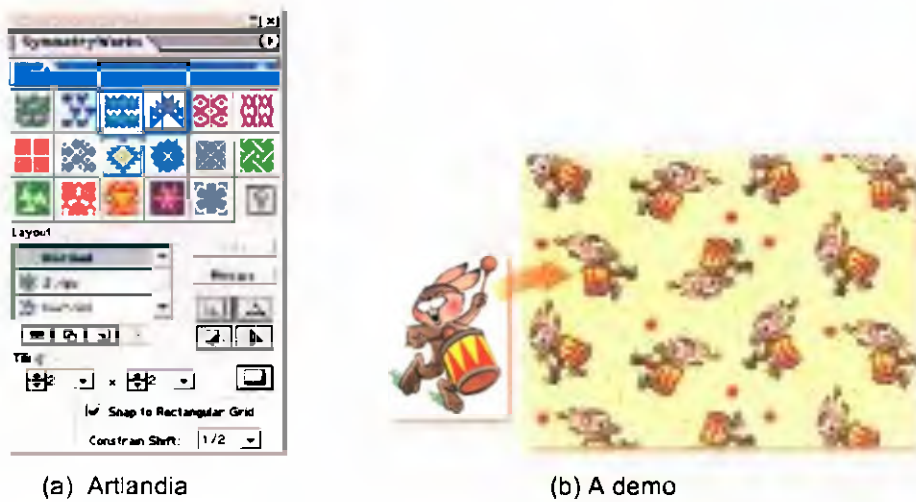


Figure 2.12 Artlandia: graphic design software and one demo

17 wallpaper groups have been studied and applied in texture analysis for decades. A computational model for wallpaper groups' classification of a given 2D repeated patterns has been developed by Yanxi Liu et al. [64-66]. The computational model composes of two parts. One is to find a lattice structure from peaks obtained by

7. <http://www.artlandia.com/>

autocorrelation. The other is to classify the symmetry group of the repeated patterns by computationally verifying the existence of rotation and reflection symmetry. Applications of such a computational model include pattern indexing, texture synthesis, image compression, and gait analysis.

Jingrui He et al. [67] first applied the theory of wallpaper groups to content-based image retrieval. The symmetry features are defined and extracted by using translation vectors for repeated pattern retrieval. By comparing the symmetry features between query image and the images from the database, the images with similar symmetry groups to the query will be retrieved. In comparison to retrieval results with wavelet features in 487 repeated patterns, the symmetry features have a better performance. Their average precision in the top ten is 0.1840 whilst for wavelet is 0.1777.

2.7 The Importance of Human Visual Perception in CBIR for Wallpaper Images

Most current CBIR systems only extract low-level visual features, which are mathematical representations of colour, shape, and texture, whilst users tend to use high-level concepts to retrieve images. The semantic gap between human and CBIR systems therefore results in poor retrieval performance of many CBIR systems. The semantic gap is a big hurdle limiting development of CBIR systems. The ultimate user of an image retrieval system is human, therefore, studying human perception can help to understand the way a user interprets an image and improve performance of CBIR.

In order to establish the link between high-level concepts and low-level features, two research approaches have been developed. One is to incorporate relevance feedback to create the interaction between a system and a user [53-57], as described in Section 2.3.3. Another approach focuses on the study of human perception from psychophysical experiments.

Psychophysics founded by Gustav Theodor Fechner in 1860 is a sub-discipline of psychology dealing with the relationship between physical stimuli and their

subjective correlates [68]. These physical stimuli can be physically measured by human perception, such as vision, hearing, smell, taste, touch etc, for instance, colour varying in luminance, hearing varying in frequency. Therefore, the relationship between observed stimuli and subjective response can be generated by psychophysical experiments. Psychophysical experiments have been widely applied to studies of human senses of perception: hearing, smell, and vision [69-72].

One of the oldest and most successful models in cognitive psychology is Tversky's contrast model of similarity. Tversky [73] provided a general mathematical framework for the perception of similarity. He proposed perceived similarity to be a linear combination or contrast of functions of the common and distinctive features of objects. Data were collected from participants who performed an image description and a similarity judgment task. Structural equation modeling, correlation, and regression analyses confirmed the relationships between perceived features and similarity of objects. The results assist retrieval systems more closely match human similarity judgments.

Biederman [74] proposed a theory of object recognition by components (geons), which are a limited set of basic geometrical shapes. Biederman and his colleagues performed a series of psychophysical experiments to provide support for the role of geons in object representation. The geons were detected on the basis of certain "non accidental" properties of contours in the image, such as colinearity, curvilinearity, symmetry, parallelism and cotermination, and indicated that geons is the fundamental local features of objects.

Psychophysical studies on visual texture perception have been carried out for many years.

Some studies focus on early vision and texture perception [75]. By using textures constructed by repeated placement of micro-patterns or texture elements, early vision of lower-level mechanisms can be studied to discriminate oriented lines.

Other studies concentrate on relating computational texture representations to human perception. For example, Tamura [23, 76] has defined six texture feature

representations through psychophysical studies in human visual perception. Amadasun [77] has defined five properties of texture in terms of spatial changes in intensity according to human visual perception.

For image retrieval, human perception of image similarity is subjective, semantic, and task-dependent. Vision perception varies not only between people, but also in the domain of images. For example, people pay more attention to texture features on satellite images, shape features on trademark images, and colour features on the natural scene images. Psychophysical experiments are the main way to find out the common sense among the population. It is therefore important to know how people perceive specified images and how they perform visual content-based retrieval. However, little work has been done on the study of visual perception in texture-based image retrieval.

In this research, the retrieval objects are the wallpaper images obtained from MoDA collections, which present specified perceptual texture features, named directionality, regularity and coarseness. The aim of this research was to investigate human perception in conducting image retrieval for wallpaper images by psychophysical experiments, leading to development of a human perception oriented content- based image retrieval system for wallpaper images.

3. Methods

This chapter give some basic methods applied to this research, which includes the methods for texture feature representations and for data analysis

In the section on texture feature representations, five computational methods and their texture feature representations were introduced reprehensively. These five models were Grey Level Co-occurrence Matrices (GLCM), Multi-Resolution Simultaneous Auto-Regressive (MRSAR) model, Fourier Transform (FT), Wavelet Transform (WT), and Gabor Transform (GT).

In the data analysis, two methods, which are psychophysical scaling and rank correlation, were applied to analyze the psychophysical experimental data. Psychophysical scaling was applied to scale perceptual events based on the data of rankings obtained from psychophysical experiments. This was used to build the relationship between physical stimuli and their subjective responses. Rank correlation was used to study the relationships between different rankings on the same set of items.

Finally, the Radon transform is introduced and applied to describe the directionality features for wallpaper images in this research.

The following sections will detail the methods applied in this research.

3.1 Computational Texture Features

In computer vision, computational texture features are to employ appropriate mathematical representations to simulate human texture perception in order to facilitate computerised texture processing, such as for image retrieval, classification, segmentation, etc. For texture analysis, three approaches are used to extract texture features, which are spatial analysis, such as Grey Level Co-occurrence Matrices (GLCM), Multi-Resolution Simultaneous Auto-Regressive (MRSAR) model;

frequency analysis, including Fourier Transform (FT); and spatial frequency analysis that includes Wavelet Transform (WT), Gabor Transform (GT). The following sections will detail the above mentioned five computational texture methods and the corresponding texture feature representations.

3.1.1 Grey Level Co-occurrence Matrices (GLCM)

Grey Level Co-occurrence Matrices (GLCM) is one of the earliest methods applied to texture feature analysis. This method was proposed by Haralick [26] in 1973 and has been used to represent the grey level spatial dependence of texture.

GLCM are two dimensional matrices of joint probability of all pairwise combinations of grey levels (i, j) in a size of $M*N$ image $I(p, q)$ separated by a distance d in the direction θ . Mathematically, a co-occurrence matrix $C_{d,\theta}(i, j)$ is defined in Eq.(3.1).

$$C_{d,\theta}(i, j) = \sum_{p=1}^M \sum_{q=1}^N \begin{cases} 1 & \text{if } I(p, q) = i \text{ and } I(p + \Delta x, q + \Delta y) = j \\ 0 & \text{otherwise} \end{cases} \quad (3.1)$$

where

$$\begin{aligned} \Delta x &= d \times \sin(\theta) \\ \Delta y &= d \times \cos(\theta) \end{aligned}$$

A normalised co-occurrence matrix $P_{d,\theta}(i, j)$ is obtained by Eq.(3.2)

$$P_{d,\theta}(i, j) = \frac{C_{d,\theta}(i, j)}{\sum_{i,j=1}^L C_{d,\theta}(i, j)} \quad (3.2)$$

where L is the total number of grey level of an image.

Figure 3.1 (b) and (d) demonstrate the co-occurrence matrices of original images (a) and (c) graphically when $d=3$, $\theta = 0^\circ$ (horizontal direction) respectively.

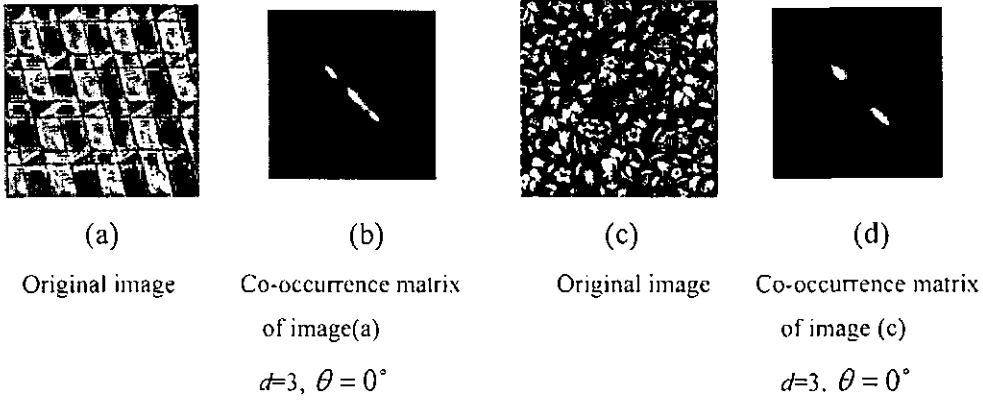


Figure 3.1 Graphical illustration of co-occurrence matrices

Haralick proposed fourteen texture features from the co-occurrence matrices. Four of Haralick's features, which are energy, entropy, contrast and homogeneity, are widely applied to texture representations [27, 78-80]. Energy measures the occurrence of repeated pairs within an image; Entropy measures the randomness of grey-level distribution, Contrast measures the difference in the grey intensity within an image; Homogeneity measures the smoothness of an image. These are formulated in Eqs. (3.3) to (3.6).

$$\text{Energy:} \quad \sum_{i=1}^L \sum_{j=1}^L P_{d,\theta}^2(i, j) \quad (3.3)$$

$$\text{Entropy:} \quad - \sum_{i=1}^L \sum_{j=1}^L P_{d,\theta}(i, j) \log P_{d,\theta}(i, j) \quad (3.4)$$

$$\text{Contrast:} \quad \sum_{i=1}^L \sum_{j=1}^L (i-j)^2 P_{d,\theta}(i, j) \quad (3.5)$$

$$\text{Homogeneity:} \quad \sum_{i=1}^L \sum_{j=1}^L \frac{P_{d,\theta}(i, j)}{1+|i-j|} \quad (3.6)$$

In our experiment, four texture features are computed with four distances of 1, 3, 5, and 7 pixels and with four directions of 0° , 45° , 90° and 135° respectively. We chose four distances to represent four scales, and four directions can be easily calculated from the co-occurrence matrices. So the feature vector includes 4 (measures) * 4 (distances) * 4 (directions) = 64 components, yielding the dimension of the texture feature vector being 64.

3.1.2 Multi-Resolution Simultaneous Auto-Regressive (MRSAR) Model

Multi-Resolution Simultaneous Auto-Regressive (MRSAR) models texture as a stationary random field and use a dense representation with a fixed neighbourhood shape and size. MRSAR model was introduced by Mao and Jain [81] in 1992 and was derived from Simultaneous Auto-Regressive (SAR) model, which is also popular in texture analysis.

The SAR model is a linear regressive model. In the SAR model, the intensity $p(i,j)$ at image position (i,j) is modelled as a linear function of the neighbouring pixels with an additive noise term $\varepsilon(i,j)$, formulated as follows.

$$\begin{aligned}
 p(i,j) = & C_1(p(i-d,j) + p(i+d,j)) + C_2(p(i,j-d) + p(i,j+d)) \\
 & + C_3(p(i-d,j-d) + p(i+d,j+d)) + C_4(p(i+d,j-d) + p(i-d,j+d)) \\
 & + \varepsilon(i,j)
 \end{aligned}$$

(3.7)

where C_1, C_2, C_3 and C_4 as SAR model parameters are a set of weights associated with neighbouring pixels along vertical, horizontal and two diagonal directions respectively, and d determines the resolution of the pixel neighbourhood. Figure 3.2 shows neighbourhood of pixel X when d equals 2, 3, 4 respectively.

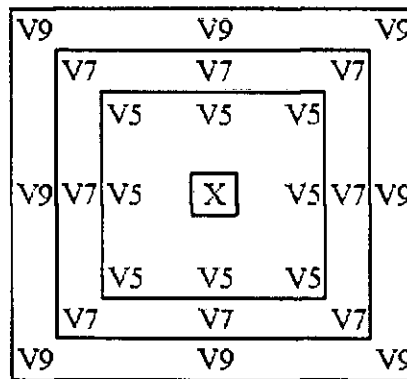


Figure 3.2 Pixel X neighbourhood V5 ($d=2$), V7 ($d=3$), V9 ($d=4$)

The SAR model parameters $\{\bar{C}_i, i = 1, 2, 3, 4\}$ and Least Square Error (LSE) at each pixel (i, j) are estimated using the method of least square fitting with an estimation window centred at (i, j) . This estimation process is repeated for each pixel within an image. Finally, the mean coefficient vector $\{\bar{C}_i, i = 1, 2, 3, 4\}$ and the mean LSE for all pixels of the image are applied to describe texture features. For instance, a higher value of mean LSE represents a finer texture or less coarseness; and a higher coefficient \bar{C}_2 of $p(i, j-d) + p(i, j+d)$ indicates that the texture is horizontally oriented.

The Multi-Resolution SAR (MRSAR) model is applied to describe multi-resolution texture features by defining multiple neighbourhoods with a size of d . In the MRSAR model, 5 features with a mean coefficient vector of $\{\bar{C}_i, i = 1, 2, 3, 4\}$ and mean LSE at each resolution are computed respectively. In our experiment, 3 resolutions, meaning d being 2, 3, 4 respectively, produced a 15(=5*3) dimensional texture feature vector.

3.1.3 Fourier Transform (FT)

The Fourier Transform (FT) is applied to convert an image from spatial domain to the frequency domain. The Fourier analysis provides a mathematical framework for the analysis of images based on the frequency spectrum. Frequency refers to how often an event occurs within a period of time. Texture is often regarded as being related to periodic image patterns or random image patterns. The images with different texture patterns will show different features in the frequency domain. As demonstrated in Figure 3.3, for the image (a) with directional features, its Fourier spectrum (b) shows bright lines perpendicular to the straight lines of the image (a); for the image (c) with random texture features, its Fourier spectrum (d) shows bright spot in the zero frequency.

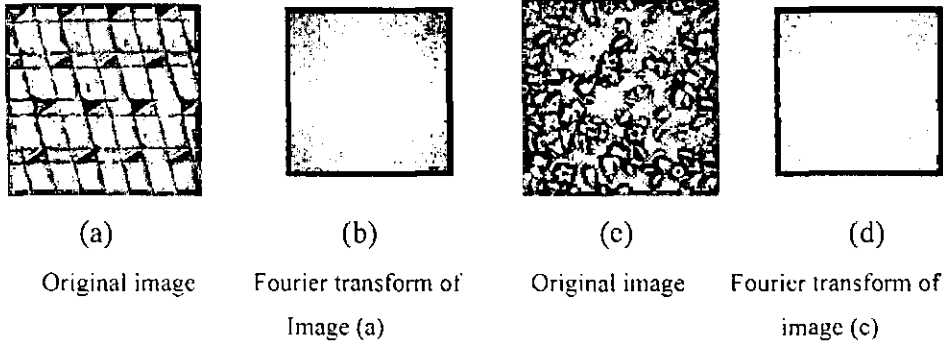


Figure 3.3 Fourier transform of images

The Discrete Fourier Transform (DFT) $F(u, v)$ of an image $f(x, y)$ with the size of $M*N$ is defined as

$$F(u, v) = \frac{1}{M * N} \sum_{x=0}^{M-1} \sum_{y=0}^{N-1} f(x, y) \exp\left(-j2\pi\left(\frac{ux}{M} + \frac{vy}{N}\right)\right) \quad (3.8)$$

$$u = 0, 1, \dots, M-1, \quad v = 0, 1, \dots, N-1$$

where u and v are the discrete spatial frequencies.

A set of statistical measures based on the frequency spectrum, including maximum magnitude, average magnitude, energy of magnitude and variance of magnitude, are extracted as texture descriptors, shown in Eqs. (3.9) to (3.12) [82].

$$\text{Maximum Magnitude:} \quad \max\{|F(u, v)| : (u, v) \neq (0, 0)\} \quad (3.9)$$

$$\text{Average Magnitude:} \quad AM = \sum_{u, v} \frac{|F(u, v)|}{M * N} \quad (3.10)$$

$$\text{Energy of Magnitude:} \quad \sum_{u, v} |F(u, v)|^2 \quad (3.11)$$

$$\text{Variance of Magnitude:} \quad \sum_{u, v} \frac{(|F(u, v)| - AM)^2}{M * N} \quad (3.12)$$

where $|F(u, v)|$ is the amplitude of the frequency spectrum and $M*N$ is the number of frequency components.

3.1.4 Wavelet Transform (WT)

The Wavelet Transform (WT) is applied to transform an image into a representation in both spatial and frequency domain, which is also called spatial frequency analysis or multi-resolution analysis. The Wavelet transform is similar to the multi-scale way by which the human visual system processes an image [83]. It is indicated by psycho-visual studies that an image is decomposed into different frequencies by the human visual system. High frequency of an image is related to the details of the image (e.g. edges) whilst the low frequency corresponds to the blurred image. The Wavelet transform has the ability to capture the presence of dominant information of images in different scales and orientations, and in recent years, is widely applied in texture representations, edge detection and image compression [31-33, 35, 38, 84].

The Continuous Wavelet Transform (CWT) of a one dimensional signal $f(x)$ is expressed as follows

$$W(s, \tau) = \int f(x) \psi_{s,\tau}^*(x) dx \quad (3.13)$$

where * denotes complex conjugation. $\psi(x)$ is a basic Wavelet, the so-called mother Wavelet. The variables of s and τ express scale and translation.

A set of Wavelets $\psi_{s,\tau}(x)$ can be obtained by dilation and translation of the mother Wavelet $\psi(x)$, in Eq. (3.14)

$$\psi_{s,\tau}(x) = \frac{1}{\sqrt{s}} \psi\left(\frac{x-\tau}{s}\right) \quad (3.14)$$

The Discrete Wavelet Transform (DWT) are obtained when $s = 2^n$, $\tau \in Z$.

A fast algorithm of the wavelet transform was proposed by Mallat in 1989 [85]. The 2D Wavelet decomposition of an image involves recursive filtering using

both high-pass (H) and low-pass (L) filters along horizontal and vertical directions, this is followed by a 2 to 1 sub-sampling of each output image, and is expressed in Eq. (3.15). This will generate four Wavelet coefficient images at each scale, i.e., LL_n , LH_n , HL_n and HH_n subbands respectively. LL_n is referred to low resolution of image whilst LH_n , HL_n and HH_n is to detail the image in vertical, horizontal and diagonal directions respectively. The process is then repeated in the lowest frequency subband (LL_n). Figure 3.4 depicts the process of a 2-scale Wavelet transform and Figure 3.5 shows the Wavelet transform of an image in three scales.

$$\begin{aligned}
 LL_n &= [L_x * [L_y * LL_{n-1}] \downarrow_{2,1_y} \downarrow_{2,1_x}] \\
 LH_n &= [L_x * [H_y * LL_{n-1}] \downarrow_{2,1_y} \downarrow_{2,1_x}] \\
 HL_n &= [H_x * [L_y * LL_{n-1}] \downarrow_{2,1_y} \downarrow_{2,1_x}] \\
 HH_n &= [H_x * [H_y * LL_{n-1}] \downarrow_{2,1_y} \downarrow_{2,1_x}]
 \end{aligned}
 \tag{3.15}$$

where $*$ denotes convolution operator, $\downarrow_{2,1_y}$ and $\downarrow_{2,1_x}$ is subsampling along vertical and horizontal directions respectively, and n is the scale level.

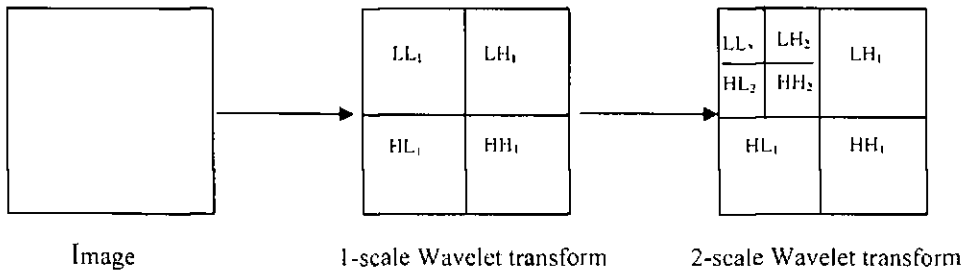
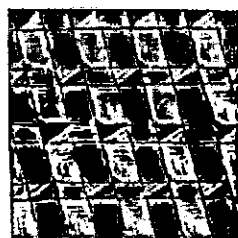
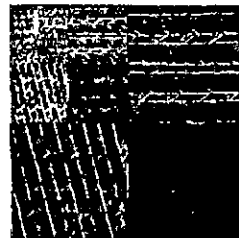


Figure 3.4 Process of 2-scale Wavelet transform of image



(a) Original image



(b) 3-scale wavelet transform of image

Figure 3.5 3-scale Wavelet transform of an image

Finally, the statistical measures (mean μ and standard deviation σ) of the Wavelet coefficients in each subband at each scale are computed as follows.

$$\begin{aligned}\mu_{mn} &= \iint W_{mn}(x, y) dx dy \\ \sigma_{mn} &= \iint (W_{mn}(x, y) - \mu_{mn})^2 dx dy\end{aligned}\quad (3.16)$$

In our experiment, the Haar wavelet was selected from the wavelet family in Matlab [86]. The Haar wavelet is a simplest orthogonal wavelet, compactly supported and symmetric characters and widely applied in multi-resolution feature extraction [87-89]. The Haar wavelet is defined in Eq and its associated high-pass (H) and low-pass (L) filters is shown in Eq. (3.17) and (3.18).

$$\psi(x) = \begin{cases} 1, & x \in [0, 0.5] \\ 0, & x \notin [0, 1] \\ -1, & x \in [0.5, 1] \end{cases}\quad (3.17)$$

$$\begin{aligned}L &= \left[\frac{1}{\sqrt{2}}, \frac{1}{\sqrt{2}} \right] \\ H &= \left[-\frac{1}{\sqrt{2}}, \frac{1}{\sqrt{2}} \right]\end{aligned}\quad (3.18)$$

We chose $s=3$. So there were 20 features, 3 (scales) *3 (subbands in each scale) *2 (measures) +2 (measures in the lowest resolution) =20, derived from a 3-scale Wavelet transform. The dimension of the texture feature vector is 20.

3.1.5 Gabor Transform (GT)

The Gabor Transform (GT) was proposed by Gabor in 1946 [90]. It generates a set of Gabor filters that can be considered as orientation and scale tuneable edge and line (bar) detectors. Using these scale and orientation filters, we can decompose an image into different scales and orientations, which are again similar to the multi-scale

way that the human visual system processes an image [83]. Recently, the Gabor filters are widely applied in the texture analysis [32, 91-94].

The two dimensional Gabor function $g(x, y)$, and its Fourier transform $G(u, v)$, are given in the following equations.

$$g(x, y) = \left(\frac{1}{2\pi\sigma_x\sigma_y} \right) \exp \left[-\frac{1}{2} \left(\frac{x^2}{\sigma_x^2} + \frac{y^2}{\sigma_y^2} \right) + 2\pi j Wx \right] \quad (3.19)$$

$$G(u, v) = \exp \left\{ -\frac{1}{2} \left[\frac{(u - W)^2}{\sigma_u^2} + \frac{v^2}{\sigma_v^2} \right] \right\} \quad (3.20)$$

where $\sigma_u = 1/2\pi\sigma_x$ and $\sigma_v = 1/2\pi\sigma_y$.

A set of self-similar Gabor filters can be generated by appropriate dilation and rotation of $g(x, y)$.

$$g_{mn}(x, y) = a^{-m} g(x', y') \quad a > 1 \quad m, n = \text{integer} \quad (3.21)$$

where

$$x' = a^{-m}(x \cos \theta + y \sin \theta) \quad \text{and} \quad y' = a^{-m}(-x \sin \theta + y \cos \theta) \quad (3.22)$$

$$\theta = \frac{n\pi}{K}$$

$$a = \left(\frac{U_h}{U_l} \right)^{\frac{1}{S-1}}$$

Here, K is the total number of orientations, and a^{-m} is the scale factor that related to the lower centre frequency U_l and upper centre frequency U_h of the region of interest and S is the total number of scale. Therefore, if K, U_l, U_h and S are defined, $K * S$ Gabor filters can be generated by Eq. (3.21). Figure 3.6 visualizes a set of Gabor filters with 4 scales and 6 orientations in each scale. They can be applied to

detect the texture features of an image in 4 scales and 6 orientations at each scale respectively.

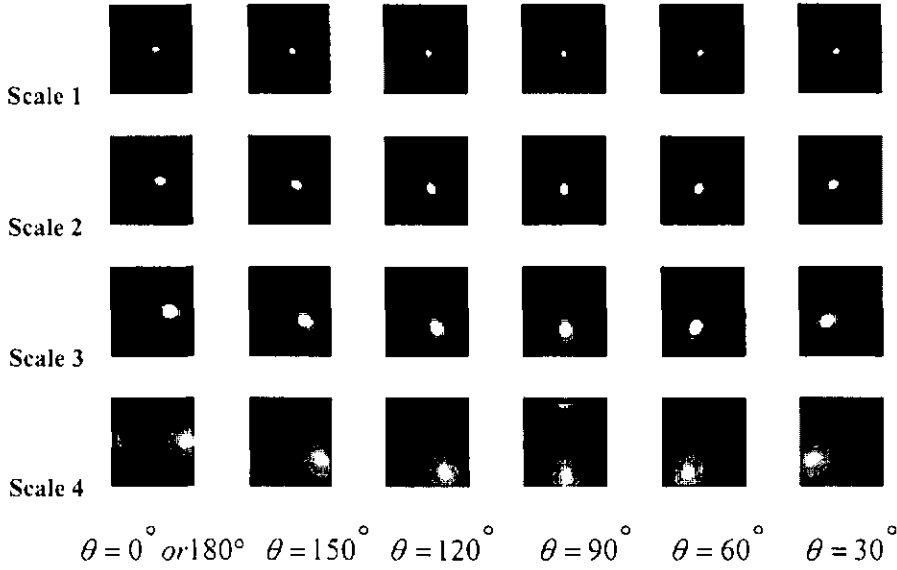


Figure 3.6 Visualization of 24 Gabor filters with 4 scales and 6 orientations in the frequency domain

Given an image $f(x, y)$, its Gabor transform is defined to be the convolution with the Gabor filters in Eq.(3.23)

$$W_{mn}(x, y) = f(x, y) * g_{mn}(x, y) \quad (3.23)$$

$$m \in (1, S), n \in (1, K), m, n = \text{integer}$$

The above function can be described as the following function.

$$W_{mn}(x, y) = F^{-1}(F(x, y) \bullet G_{mn}(x, y)) \quad (3.24)$$

$$m \in (1, S), n \in (1, K), m, n = \text{integer}$$

where $F(x, y)$ and $G_{mn}(x, y)$ are the Fourier transform of $f(x, y)$ and $g_{mn}(x, y)$ respectively, the sign F^{-1} stands for inverse Fourier transform. Figure 3.7 demonstrates the Gabor transform of an image with one Gabor filter ($s=3$ and $\theta = 120^\circ$) by using Eq. (3.24).

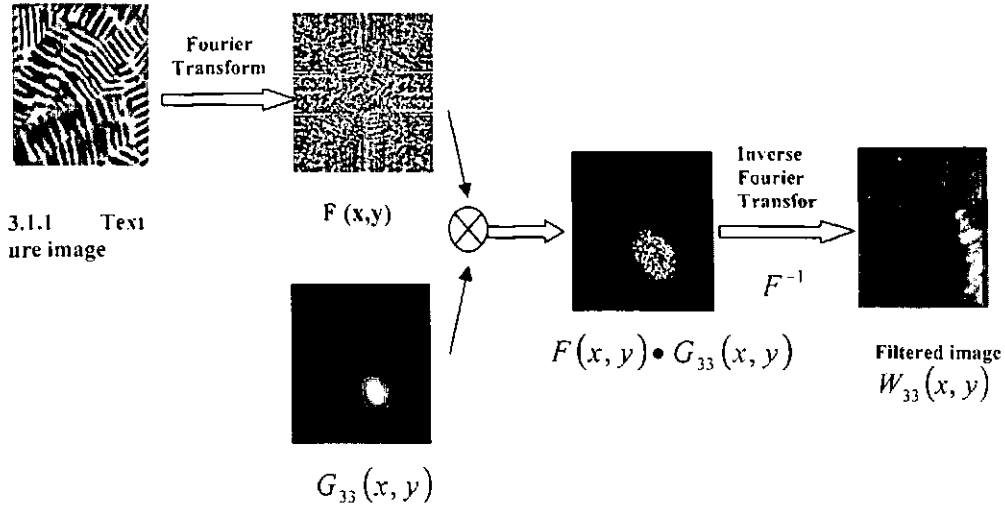


Figure 3.7 Gabor transform of an image with one Gabor filter ($s=3$ and $\theta = 120^\circ$)

After the Gabor transform of an image, the magnitudes of mean μ and standard deviation σ of the Gabor transform coefficients W_{mn} are extracted as the texture feature representations, which are

$$\begin{aligned}\mu_{mn} &= \iint |W_{mn}(x,y)| dx dy \\ \sigma_{mn} &= \iint (|W_{mn}(x,y)| - \mu_{mn})^2 dx dy\end{aligned}\quad (3.25)$$

The texture feature vector of an image can be expressed as

$$\begin{aligned}\vec{f} &= \{\mu_{11}, \sigma_{11}, \mu_{12}, \sigma_{12}, \dots, \mu_{mn}, \sigma_{mn}\} \\ m &\in (1, S), n \in (1, K), m, n = \text{integer}\end{aligned}\quad (3.26)$$

In our experiment, $S=4$ and $K=6$ were chose, so the feature vector included 4 (scales) *6(orientations) *2 (measures) =48 components. Thus, the dimension of Gabor texture feature vector was 48.

3.2 Methods for the Data Analysis

In this section, two methods of data analysis that were used in this PhD study are explained. They are psychophysical scaling and rank correlation, which are used to analyze the psychophysical experimental data. Psychophysical scaling is used to build the relationship between visual texture features and their subjective response. Rank correlation is used to evaluate computational methods by finding relationships between two rankings conducted by subjects and computational methods.

3.2.1 Psychophysical Scaling – Choice Score Method

Psychophysics is a sub-discipline of psychology dealing with the relationship between physical stimuli and their subjective correlates. These physical stimuli can be physically measured by human perception, such as vision, hearing, smell, taste, touch etc, for instance, colour varying in luminance, hearing varying in frequency. Therefore, the relationship between observed stimuli and subjective responses can be generated by psychophysical experiments. Psychophysics is commonly used to produce scales of human perception of various aspects of physical stimuli.

Psychophysical scaling is used to assign numbers to perceptual events based on ranking order data from psychophysical experiments [95]. The following will describe the psychophysical scaling methods obtained from rankings.

3.2.1.1 Obtaining Rankings

In our psychophysical experiment, a total of N subjects were asked to rank order M stimuli with respect to some perceptual attributes. For example: 10 subjects were asked to rank 10 images in order of coarseness (from fineness to coarseness). The rankings were then put into Table 3.1. The entry T_{nm} of Table 3.1 expresses the ranking of the m^{th} image by the n^{th} subject.

Table 3.1 Rankings

Subjects	Ranks Assigned				
	1	2	$M-1$	M
Subject 1					
Subject 2					
·	· · T_{nm} · · ·				
·					
·					
Subject $N-1$					
Subject N					

The data of raw rank orders are in an ordinal scale, which arranges objects in order of magnitude, but does not reveal the differences of magnitude between two objects. An interval scale describing how much difference there is between them was therefore needed.

3.2.1.2 Obtaining Interval Scale — Choice Score Method

The choice score method described by Engen [96] is one of the methods used to obtain interval-scale values from rankings. This converts rankings to choice frequencies first, then normalizes to p values, and finally converts the p values into z scores. The z scores represent the interval scale values for the stimuli, which have equal intervals as a psychological scale on the assumption that the rankings are normally distributed. The following section details the above procedures.

Step 1. Calculate the mean rank (M_r) assigned to each stimulus.

Step 2. Calculate a mean choice score (M_c) for each stimulus by subtracting the mean rank from the number of stimuli (m).

$$M_c = m - M_r \quad (3.27)$$

Step 3. Normalise the mean choice scores (M_c) into p values by dividing them by $(m - 1)$.

$$p = \frac{M_c}{m-1} \quad (3.28)$$

Step 4. Convert the p values into z scores, which is given in a table in Appendix 1.

In this research, the choice score method was applied to obtain psychophysical scaling based on the rankings obtained from psychophysical experiments. Psychophysical scaling was used to build the relationship between visual texture features and their subjective responses.

3.2.2 Rank Correlation – Spearman's Rank Correlation Coefficient

In statistics, rank correlation is the study of relationships between different rankings on the same set of items [97]. It deals with measuring correspondence between two rankings, and assessing the significance of this correspondence.

Spearman's rank correlation coefficient [98], named after Charles Spearman, is one rank correlation method. It can be used to summarise the strength and direction (negative or positive) of a relationship between two variables. The Spearman rank correlation coefficient r_s is defined as

$$r_s = 1 - \frac{6 \sum_{i=1}^n d_i^2}{n^3 - n} \quad (3.29)$$

where d_i is the difference between the ranks assigned to the i th object in two measurements and n is the number of the pairs. This coefficient r_s will always be between 1.0 and -1.0. The value 1.0 (i.e. the two rankings are the same) means a perfect positive correlation whilst -1.0 (i.e., one ranking is the reverse of the other) means a perfect negative correlation. The value 0 means no correlation. The increasing positive or negative values imply increasing positive or negative agreement between two rankings.

To check whether an answer could be the result of a chance, the significance of the relationship was tested as follows.

- 1) Calculate the degrees of freedom. This is the number of pairs n minus 2 ($n-2$).
- 2) Plot result of rank correlation with $n-2$ on the graph in Figure 3.8, with the x axis representing the degrees of freedom and y axis being Spearman's rank correlation coefficient.

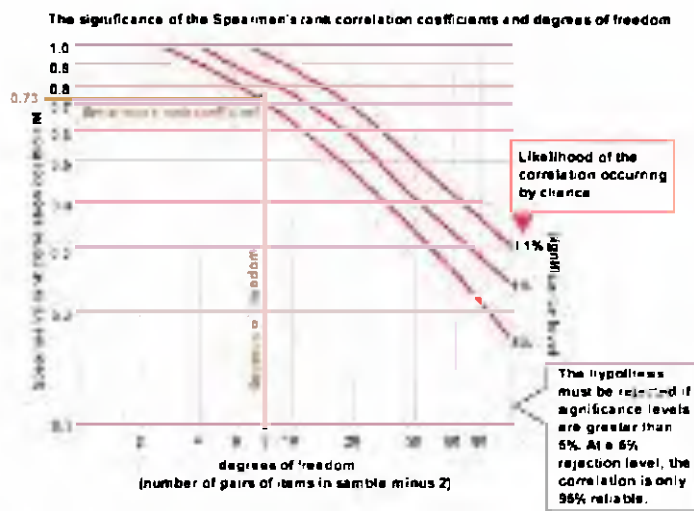


Figure 3.8 Significance of Spearman's rank correlation coefficient

In Figure 3.8, the three red lines from top to bottom show the critical values of Spearman's rank correlation coefficient changed with the degrees of freedom in 0.1%, 1% and 5% significance levels respectively. The significance levels correspond to the probability of the relationship you have found being a chance. If the rank correlation coefficient is smaller than the critical value in the same degree of freedom in significance level 5%, the probability of the relationship being a chance is more than 5%, and then it is a possible result of chance. If the rank correlation coefficient is bigger than the critical value in the same degree of freedom in significance level 5%, but smaller than that in significance level 1%, the probability of the relationship being a chance is between 1% and 5% and the result is significant at the 5% level. For example, in Figure 3.8, when $n=10$, the degree of freedom is $n-2=8$, the critical value 0.73 gives a significance level of slightly less than 5%. If the

rank correlation coefficient with the degree of freedom 8 is smaller than 0.73, that means the probability of the relationship being a chance is more than 5%, and then it is a possible result of chance.

In our research, Spearman's rank correlation coefficient was mainly applied as an assessment method. By measuring the rank correlation coefficient between two rankings carried out by subjects and computational methods, we can evaluate the computational methods. We can also obtain relationships between visual similarity and visual properties (such as regularity, directionality, coarseness etc) by measuring rank correlation coefficient between two rankings conducted by subjects on the experiments of visual similarity and visual properties respectively.

3.3 Radon Transform

The Radon transform [36] is the projection of the intensity values of an image along specified directions. In general, the Radon transform of $f(x, y)$ is the line integral of f parallel to the y axis, as expressed in Eq. (3.30).

$$R_{\theta}(x') = \int_{-\infty}^{\infty} f(x' \cos \theta - y' \sin \theta, x' \sin \theta + y' \cos \theta) dy' \quad (3.30)$$

where

$$\begin{bmatrix} x' \\ y' \end{bmatrix} = \begin{bmatrix} \cos \theta & \sin \theta \\ -\sin \theta & \cos \theta \end{bmatrix} \begin{bmatrix} x \\ y \end{bmatrix} \quad (3.31)$$

According to Eqs. (3.30) and (3.31), Figure 3.9 illustrates the geometry of the Radon transformation.

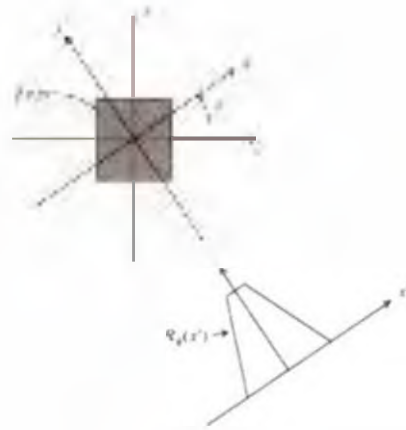


Figure 3.9 Geometry of the Radon transformation

In the field of image processing, the Radon transform is generally applied to detect straight lines. Figure 3.10 shows an original wallpaper image, its edge image and Radon transformation of the edge image. The Radon transform is shown in Figure 3.10 (c), where the horizontal axis expresses the projection angle θ range from 0 to 179 degrees. The vertical axis expresses the corresponding coordinate along x axis. Therefore, the locations of strong peaks in the Radon transform can represent the location of straight lines and direction of these lines in the images. For example, in Figure 3.10 (c), the strong peaks shown as bright points correspond to $\theta \approx 90^\circ$ and $x \approx -170, -140, -40, -10, 90, 120, 220$ respectively, $\theta \approx 16^\circ$ and $x \approx -180, -120, 60, 0, 60, 120, 180$ respectively. The line perpendicular to the angle $\theta \approx 16^\circ$ and located at corresponding x is shown in red on the original image in Figure 3.11. The seven horizontal lines can be detected when $\theta \approx 90^\circ$ and $x \approx -170, -140, -40, -10, 90, 120, 220$ respectively.

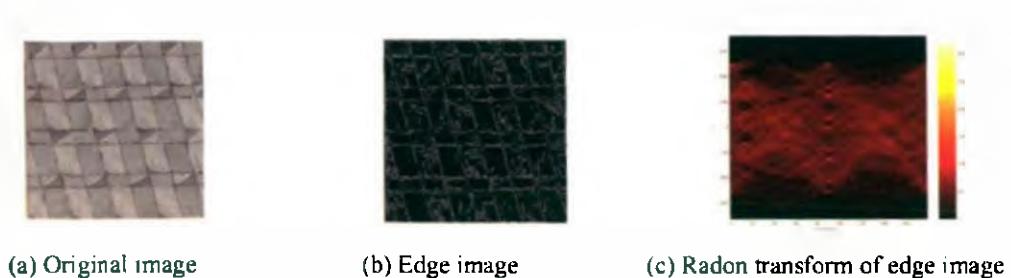


Figure 3.10 Edge image and its Radon transform

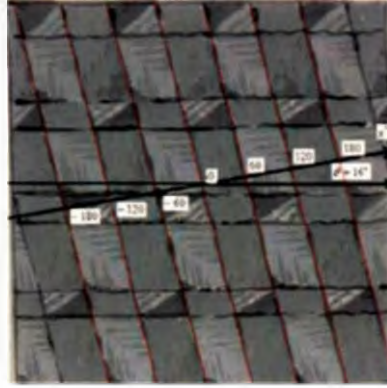


Figure 3.11 Straight line detection (in red) using Radon transform ($\theta \approx 16^\circ$ and $x \approx -180, -120, 60, 0, 60, 120, 180$ respectively)

The Radon transform not only expresses the directionality features, but also describes the spatial property of directionality. This overcomes the drawbacks of directionality representations using the Fourier power spectrum and the direction histogram. Therefore, the Radon transform can represent directionality features more effectively. In this research, we applied the Radon transform to extract the directionality features from wallpaper images.

4. Psychophysical Experiments

The ideal representation of computational texture should be consistent with the response of human visual perception. This is in the consideration that the ultimate user of an image retrieval system is a human being. Therefore, the study of human perception in terms of texture features and similarity measurements are crucial. To do this, psychophysical experiments are employed.

Two psychophysical experiments were conducted in this PhD study to investigate a human's response on perceiving texture features and performing similarity measurements respectively. In the first experiment, subjects were asked to rank sample wallpaper images based on each of the three texture features, i.e., coarseness, regularity and directionality respectively. Psychophysical scaling, which measures the subjects' response to a physical stimulus in a psychophysical experiment, was then obtained from rankings using the choice score method as discussed in Chapter 3. Finally, the relationship between visual texture features and their subjective response was established according to the psychophysical scaling. In the second experiment, sample wallpaper images were ranked based on the order of visual similarity to the query images by subjects. These ranking results can reflect human visual similarity measurements.

Through the two psychophysical experiments, we aimed to evaluate computational texture representations by comparing with human vision perception in texture representations and similarity measurements respectively. We investigated the suitable texture representations for wallpaper images to improve retrieval accuracy, which is in line with human visual perception. The following sections will describe the procedure of two experiments in detail.

4.1 Experiment One: Texture Feature Perception

The purpose of this experiment was to obtain the rankings based on texture features by subjects. These data were then used to establish relationships between

visual texture features and the subjects' response. The experimental method will be explained in detail as follows, sample selection, subject selection, subject training and obtaining rankings.

4.1.1 Experimental Preparation

Before the experiment, test samples and subjects were selected. Sample images needed to represent visual features of wallpapers well. The selection of subjects had to include all possible factors that could affect the results.

4.1.1.1 Sample Selection

Ten wallpaper images were selected from the database of MoDA images and utilised as experimental samples, as shown in Figure.4.1. For the purpose of texture analysis, all of the sample images were converted to grey-level images and cut to the same size of 512*512, removing the margin of images and preparing the texture patterns of wallpaper for comparison.

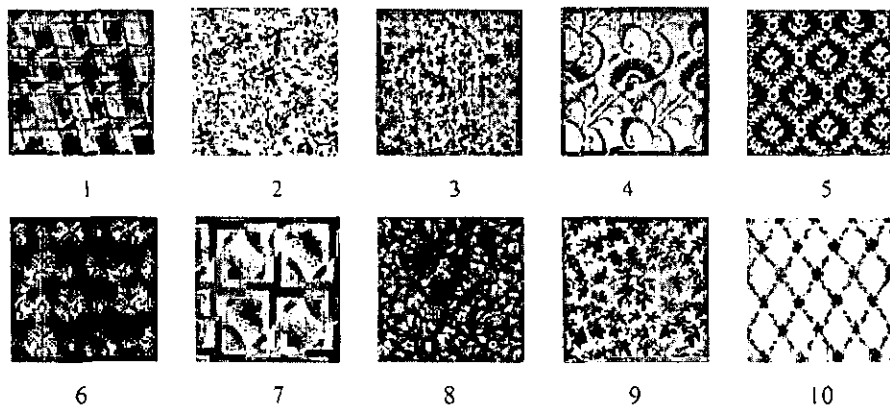


Figure 4.1 Experimental samples

The criterion of selection was that sample images should represent visual texture features of wallpapers, including coarseness, regularity and directionality. We first selected one hundred images from MoDA collections randomly and grouped them based on coarseness, regularity and directionality. Three regular images, shown in Figure.4.1 (4) (5) (6), three directional images (1) (7) (10), and four random texture images (2) (3) (8) (9) were selected from the corresponding group.

4.1.1.2 Subject Selection

Thirteen volunteer observers were employed to take part in the experiments, seven women and six men with ages ranging from 25 to 50 years. Subjects were from different countries. Six were staff and three were PhD students from the School of Computing Science in Middlesex University. Four staff were from the MoDA Museum. Among these observers, three were working in image processing, whilst four of them had some knowledge of wallpaper images.

4.1.2 Experimental Procedure

The experimental procedure started with subject training, that is the basic concept of texture and texture features was explained to subjects. This helped subjects to understand the visual features of texture and the rankings based on texture features effectively. After training, subjects were asked to rank sample images based on each of the texture features: coarseness, regularity and directionality. These rankings were then applied to create psychophysical scaling and to build relationship between visual texture features and their subjective response. Details are given below.

4.1.2.1 Subject Training

Before commencing the experiments, a brief explanation of the basic concepts of texture and texture features were given to observers as shown below.

Texture concerns the intensity of pixels and the spatial relationship between pixels. It refers to global visual properties like coarseness, regularity and directionality [23].

- **Coarseness** — Coarseness versus Fineness

Coarseness has a direct relationship to scale and repetition rates. When two patterns differ only in scale, the magnified one is coarser. For patterns with different structures, the bigger its element size and/or the less its elements are repeated, the coarser it is.

- **Regularity** – Regularity versus Irregularity

Regularity is a fundamental structural property of texture. It is a simple attribute to the repetitive patterns in which elements or primitives are arranged according to a placement rule.

- **Directionality** – Directionality versus Non-directionality

Directionality is a global property. The orientation of the texture does not matter, i.e., two patterns that differ only in orientation should have the same degree of directionality.

Some samples of texture images from the Brodatz database⁹ (standard texture database) shown in Figure 4.2 assisted the subjects to understand the perceptual attributes of texture. Some examples in a ranking based on texture features of coarseness (from fineness to coarseness) in Figure 4.3, regularity (from regularity to irregularity) in Figure 4.4 and directionality (from directionality to non-directionality) in Figure 4.5 were given respectively. When observers fully understood the concepts of texture perceptual attributes, the experiment started.

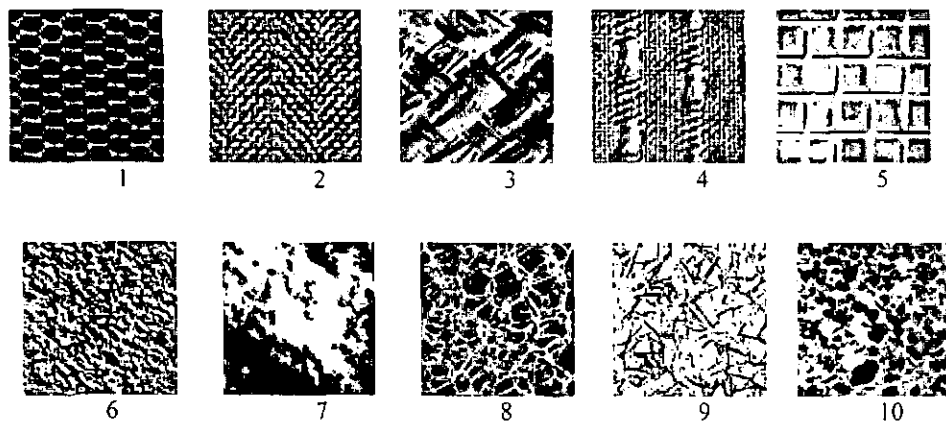
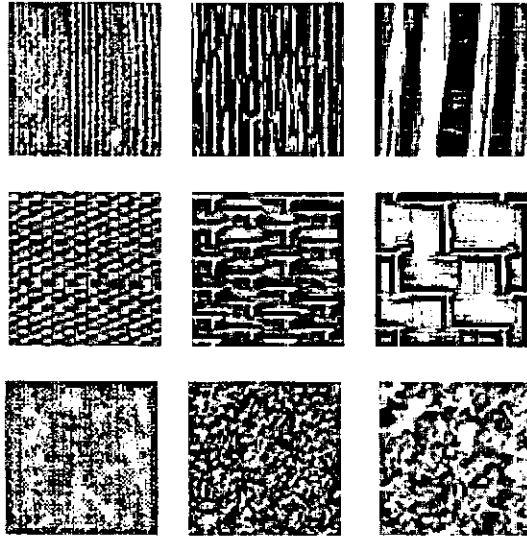
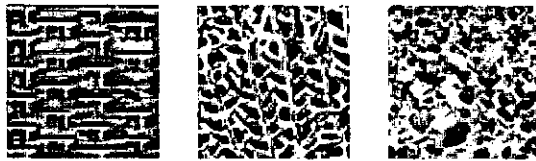


Figure 4.2 Texture images from Brodatz database



Fineness — Coarseness

Figure 4.3 Examples for ranking from fineness to coarseness



Regularity — Irregularity

Figure 4.4 Example for ranking from regularity to irregularity



Directionality — Non-directionality

Figure 4.5 Example for ranking from directionality to non-directionality

4.1.2.2 Obtaining Rankings

After the subject training, ten sample images shown in Figure 4.1 were displayed on the LCD (Liquid Crystal Display) of a 12 inch laptop with layout showing in 2 rows by 5 columns. Each observer was asked to rank the images physically by moving them around in the order of coarseness (from fineness to coarseness), regularity (from regularity to irregularity), directionality (from directionality to non-directionality) respectively. The observers' rankings are shown

in Table 3.1 in Section 3.2.1.1. This was used to obtain interval scale using choice score method introduced in Section 3.2.1.2. The experimental results are shown in Section 5.1.

4.2 Experiment Two: Human Visual Similarity

In this experiment, ten sample images shown in Figure 4.1 were ranked based on visual similarity to each of ten query images by subjects respectively. These ranking results were used to evaluate computational texture methods in visual similarity measurements and to develop a suitable similarity measurement, which is consistent with human visual perception.

Sixteen volunteer observers performed this experiment, eight women and eight men with ages ranging from 25 to 50 years and with different culture backgrounds. Half of the subjects worked in the field of image processing. Each observer was asked to rank the ten sample images based on visual similarity to a query image in terms of texture features.

Each observer's similarity measurements are shown in Table 3.1 of Section 3.2.1.1. This was used to obtain the final rankings using the choice score method introduced in Section 3.2.1.2. The experimental results are shown in Section 5.2.

4.3 Summary

This chapter described two psychophysical experiments. One is to rank sample wallpaper images based on texture features (coarseness, regularity and directionality) respectively by subjects. Another is to rank sample wallpaper images based on visual similarity to a query image from very similar to dissimilar.

Through the two psychophysical experiments, we obtained the results of human visual perception and visual similarity measurements for wallpaper images based on texture features. These results were used to evaluate the computational texture methods by comparing results between computational methods and human

perception in texture representations and similarity measurements. By analyzing the relationship between human visual perception on perceiving similarity and texture features for wallpaper images, we can find out which visual feature plays a more important role in the measurements of visual similarity for wallpaper images, leading to the development of new methods for wallpaper image retrieval. The next chapter will present the results of two psychophysical experiments and the evaluation of five computational methods based on the psychophysical experimental results.

5. Experimental Results and Data Analysis

In this chapter, the results of the two psychophysical experiments based on texture features are shown. By comparing the results between the psychophysical experiments and the computational texture methods, we evaluated five popular computational methods in texture representations and similarity measurements. Finally, an analysis of the relationships between human visual similarity and visual texture features were given in order to find out which visual texture feature played an important role for retrieving wallpaper images.

5.1 Results of Experiment One

In experiment one, we aimed to establish a relationship between visual texture features (coarseness, regularity and directionality) and the subjective response, which can be applied to evaluate the existing computational texture representations. First, ten sample images were ranked by thirteen subjects based on each of three texture features. Then, psychophysical scaling was obtained from these rankings using the choice score method described in Section 3.2.1.2. Finally, relationships between visual texture features and their subjective response were built according to psychophysical scaling. The following will give results of psychophysical experiment one, which included rankings and psychophysical scaling based on coarseness, regularity and directionality respectively.

5.1.1 Rankings

Ten sample images were ranked based on texture features by thirteen subjects. The ranking results from fineness to coarseness, regularity to irregularity, directionality to non-directionality from each subject were obtained respectively. In order to analyze effectively, the ranking for each subject based on coarseness, regularity and directionality are put in Table 3.1 described in Section 3.2.1.1 separately. Finally, the rankings based on coarseness, regularity and directionality are listed in Tables A2.1, A2.2 and A2.3 respectively, as seen in Appendix 2. In Tables

A2.1, A2.2 and A2.3, the entry T_{nm} of table expresses the ranking of the m^{th} image by the n^{th} subject, where the subscription n, m of T_{nm} represents the number of row and column respectively.

In order to represent the visual perception based on averaged data, the raw data were pre-processed to remove some inconsistent data.

5.1.2 Raw Data Analysis and Pre-Processing

In order to achieve a set of consistent averaged data, removing inconsistent data was carried out. First, the coefficient matrix of rank correlation between subjects' ranking was calculated. Then, via analyzing the coefficient matrix, some rankings were removed. Three steps for raw data analysis and pre-processing are detailed as follows.

1) Calculate the coefficient matrix of the rank correlation between subjects' rankings

Based on the rankings shown in Appendix 2, the coefficient matrix of rank correlation between subjects' rankings for each texture feature were calculated respectively by using Eq. (3.29) in Section 3.2.2, here $n=10$. The coefficient matrix of rank correlation for each texture features are shown in Tables A3.1, A3.2 and A3.3 respectively, as seen in Appendix 3. In Tables A3.1, A3.2 and A3.3, the entry T_{nm} of table expresses the coefficient of rank correlation between m^{th} subject and n^{th} subject, where the subscription n, m of T_{nm} represents the number of row and column respectively.

2) Analyze significance of rank correlation between subjects' rankings

To remove the inconsistent rankings with the average results, the significance of rank correlation between subjects' rankings were tested. In Figure 3.8, when $n=10$, the degree of freedom is $n-2=8$, the critical value of rank correlation 0.73 gives a significance level of slightly less than 5%. Therefore, the critical value of rank correlation 0.73 was used as a threshold to remove some inconsistent rankings.

3) Remove inconsistent rankings

By analyzing the coefficient matrix of rank correlation, the rankings that were smaller than 0.73 ($r_s < 0.73$) were removed. Finally, the rankings that were more than 0.73 ($r_s \geq 0.73$) were kept. The removed rankings were highlighted in red in Appendix 3. The final rankings based on coarseness, regularity and directionality are shown in Tables A4.1(a), A4.2(a) and A4.3(a) respectively, and their corresponding coefficient matrix of rank correlation are shown in Tables A4.1(b), A4.2(b) and A4.3(b), given in Appendix 4.

After pre-processing, the raw data of rankings in Tables A4.1 (a), A4.2 (a) and A4.3 (a) were applied to obtain psychophysical scaling based on coarseness, regularity and directionality respectively by using choice score method introduced in Section 3.2.1.2.

5.1.3 Psychophysical Scaling

Based on the rankings after processing, psychophysical scaling was obtained by using choice score method introduced in Section 3.2.1.2. The ranked images based on psychophysical scaling of coarseness, regularity and directionality are shown in Figures 5.1, 5.2 and 5.3 respectively. In Figures 5.1 to 5.3, the sample images are displayed in order from fineness to coarseness, from regularity to irregularity and from directionality to non-directionality separately. The value of psychophysical scaling is shown below each image. The number above each image is the ID number of this image in the ten sample images, as shown in Figure 3.1.

- *Psychophysical Scaling Based on Coarseness*

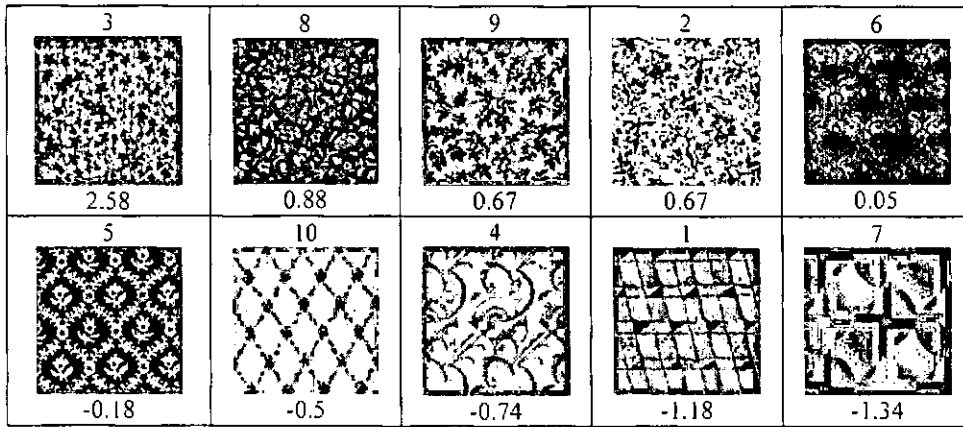


Figure 5.1 Image ranking based on psychophysical scaling of coarseness (from fineness to coarseness)

- *Psychophysical Scaling Based on Regularity*

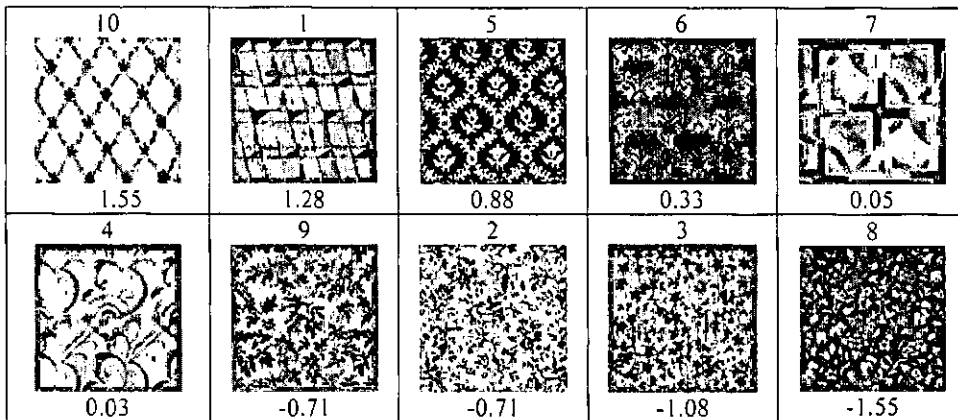


Figure 5.2 Image ranking based on psychophysical scaling of regularity (from regularity to irregularity)

- *Psychophysical Scaling Based on Directionality*

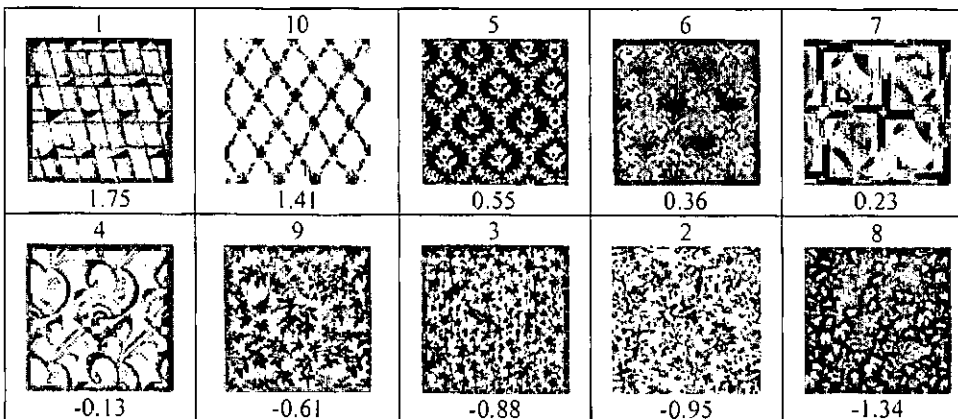


Figure 5.3 Image ranking based on psychophysical scaling of directionality (from directionality to non-directionality)

5.2 Results of Experiment Two

In experiment two, we aimed to get the results of human perception on perceiving similarity of wallpaper images. These data were utilised to evaluate the existing computational texture methods in measuring visual similarity. The procedure was as follows. First, sample images were ranked based on the degree of similarity to a query image estimated by sixteen subjects respectively. Then, psychophysical scaling was calculated from these rankings using choice score method described in Section 3.2.1.2. According to the psychophysical scaling, the final rankings were obtained.

5.2.1 Rankings

The retrieval results of ten query images by sixteen subjects are shown in Table 3.1 in Section 3.2.1.1. Finally, the rankings for ten queries are listed in Tables A5.1-A5.10 separately, as seen in Appendix 5. The entry T_{nm} of table in Appendix 5 again expresses the ranking of the m^{th} image by the n^{th} subject, where the subscription n, m of T_{nm} represents the number of row and column respectively.

Similar to Section 5.1.2, the raw data of rank orders were pre-processed by removing some rankings which were not consistent with major subjects' rankings.

5.2.2 Raw Data Analysis and Pre-Processing

Similar to Section 5.1.2, three steps were applied to pre-process raw data.

1) Calculate the coefficient matrix of the rank correlation between subjects' rankings

Based on the rankings given in Appendix 5, a coefficient matrix of rank correlation between subjects' rankings for each query was calculated respectively by using Eq. (3.29) in Section 3.2.2, here $n=9$. The coefficient matrix of rank correlation for ten queries is shown in Tables A6.1 to A6.10 respectively, given in Appendix 6. In Tables A6.1 to A6.10, again the entry T_{nm} of the tables expresses the coefficient of

rank correlation between m^{th} subject and n^{th} subject, where the subscription n, m of T_{nm} represents the number of row and column respectively.

2) Analyze significance of rank correlation between subjects' rankings

To remove the inconsistent rankings with the average results, the significance of rank correlation between subjects' rankings was tested. In Figure 3.8, where $n=9$, the degree of freedom is $n-2=7$. The value of 0.75 of rank correlation gives a significance level of slightly less than 5%. Therefore, 0.75 was used as a threshold to remove inconsistent rankings.

3) Remove inconsistent rankings

By analyzing the coefficient matrix of rank correlation, the rankings that were smaller than 0.75 ($r_s < 0.75$) were removed. The removed rankings are highlighted in red in Appendix 6 that were removed. The final rankings for ten queries are shown in Tables A7.1(a) to A7.10(a) respectively, and their corresponding coefficient matrix of rank correlation are shown in Tables A7.1(b) to A7.10(b) respectively, given in Appendix 7.

In Appendix 7, after removal of inconsistent rankings, we can see that query 4 in Table A7.4 contains the data only from four subjects out of sixteen subjects, whilst query 6 in Table A7.6 contains the data from only three subjects. Similarly, query 7 in Table A7.7 contains the data from three subjects. The number of subjects with similar rankings is not over 50%, which suggests that most subjects have different opinions of perceiving similarity for these three queries. It was difficult to obtain common rankings from these three queries. Therefore, these three queries were not considered in the following sections of the evaluation of computational texture methods and the studies of human visual perception, which will be discussed in Section 5.3 and Section 5.4 respectively.

After pre-processing, the rankings for the rest seven queries in Tables A7.1 (a) to A7.3 (a), A7.5 (a) and A7.8 (a) to A7.10 (a) were used to obtain final rankings for seven queries by calculating psychophysical scaling.

5.2.3 Psychophysical Scaling

Based on rankings shown in Tables A7.1(a) to A7.3(a), A7.5(a) and A7.8(a) to A7.10(a), psychophysical scaling were obtained by using the choice score method. The ranked images for seven queries are shown in Figures A8.1 to A8.7 respectively, given in Appendix 8. In Figures A8.1 to A8.7, images are displayed in the order from most similar to least similar to each query image. The value of psychophysical scaling is shown below each image.

Through two psychophysical experiments, we obtained results of human visual perception and visual similarity measurements in terms of texture features for wallpaper images. In the following sections, the existing computational methods are evaluated by comparing the results between computational methods and the visual data obtained from these two experiments.

5.3 Comparison between Computational Texture Methods and Human Visual Perception

In this section, five computational texture methods introduced in Section 3.1 are evaluated by comparing the results obtained from each of the two psychophysical experiments respectively. First, the comparison was carried out in terms of texture feature representations. Then, the comparison was conducted in terms of similarity measurements. The approach of rank correlation introduced in Section 3.2.2 was used to indicate the goodness of fit between the data calculated from computational texture methods and perceived by subjects.

5.3.1 Comparison between Computational Texture Representations and Visual Texture Features

In this section, we aim to examine the suitability of five computational texture representations introduced in Section 3.1: Grey Level Co-occurrence Matrices (GLCM), Multi-Resolution Simultaneous Auto-Regressive (MRSAR) model, Fourier Transform (FT), Wavelet Transform (WT) and Gabor Transform (GT).

For the approach of GLCM, texture features were computed with four distances of 1, 3, 5, and 7 pixels and with four directions of $0^\circ, 45^\circ, 90^\circ, 135^\circ$ respectively. So the feature vector included 4 (energy, entropy, contrast and homogeneity) * 4 (distances) * 4 (directions) = 64 components, detailed in Section 3.1.1. Whilst for MRSAR, 3 resolutions (d=2, 3, 4 respectively) were applied, leading to the feature vector with 5(4 regressive parameter and least square error)*3(scales) =15 elements, seen in Section 3.1.2. The texture features calculated from the approach of FT contain a vector with 4 elements, which were Maximum Magnitude, Average Magnitude, Energy of Magnitude and Variance of Magnitude, detailed in Section 3.1.3. As for the method of WT method in Section 3.1.4, the dimension of the feature vector is 20, that was obtained by 3 (scales) *3 (subbands in each scale) *2 (mean and standard deviation) +2 (mean and standard deviation in lowest resolution). The texture features from GT approach took 48 elements in the feature vector, which was calculated by 4 (scales)*6 (orientations) * 2 (mean and standard deviation), seen in Section 3.1.5.

Texture features of ten sample images were calculated by five computational methods respectively. Based on the value of each texture feature, ten sample images were ranked in decreasing order. The ranking results for each of three texture features, i.e., coarseness, regularity, and directionality, for each computational method are shown in Tables A9.1 to A9.5 from column 2 to column 10, listed in Appendix 9. In Tables A9.1 to A9.5, the first row is the ranking based on texture features by subjects and the other rows are the ranks based on each texture feature calculated by five computational methods respectively. The data in the last column in each table represents the coefficient of rank correlation ($|\bar{r}_s|$) between each feature calculated by each method and the data perceived by subjects. We applied the absolute value of the rank correlation, which was in the consideration that both positive and negative rank correlation can reflect the relationship between two variables as seen in Section 3.2.2 in the same way.

Table 5.1 shows the average of rank correlation for each table given in Appendix 9. In Table 5.1, the entry T_{nm} of the table expresses the average rank correlation between rankings of the m^{th} visual texture feature by subjects and ranking

of each texture feature calculated by n^{th} computational method, where the subscription n, m of T_{nm} represents the number of row and column respectively. These averages of rank correlation were applied to evaluate whether the computational texture representations were consistent with the visual feature perception or not. Data analysis and discussion will be detailed in Section 5.3.3.

Table 5.1 The average rank correlation between texture features calculated by computational methods and visual texture features perceived by subjects

$ \bar{r}_s $	<i>GLCM</i>	<i>MRSAR</i>	<i>FT</i>	<i>WT</i>	<i>GT</i>
Coarseness	0.37	0.38	0.41	0.40	0.42
Regularity	0.34	0.62	0.34	0.40	0.39
Directionality	0.33	0.68	0.36	0.42	0.41

In this section, we evaluated the five computational texture methods in terms of texture feature representations. However, when people judge whether two images are similar, they may not consider each texture feature or their combinations. The following section will study the similarity measurements between computational texture methods and subjects.

5.3.2 Comparison Similarity Measurements between Computational Texture Methods and Subjects

In this section, the comparison of similarity measurements obtained by computational methods and subjects were carried out. By using the sample query and sample images, five computational methods, i.e. Grey Level Co-occurrence Matrices (GLCM), Multi-Resolution Simultaneous Auto-Regressive (MRSAR) model, Fourier Transform (FT), Wavelet Transform (WT) and Gabor Transform (GT), again were applied to calculate similarity distances. The ranking of the corresponding computational method for seven queries are given in Tables A10.1 to A10.7 respectively, as shown in Appendix 10. In the Tables A10.1 to A10.7, the first row is the ranking perceived by subjects, whilst the rest of the table is the retrieval performance calculated by five computational methods. The numbers from columns 2 to 10 in Tables A10.1 to A10.7 are the ID numbers of sample images ranking in the

order from the most similar to the least similar to the query images. The last column is the coefficients of rank correlation between computation methods and subjects.

Table 5.2 shows the rank correlation between five computational methods and the human perception for seven query images. The average the rank correlation \bar{r}_s is shown in last row of table.

Table 5.2 Coefficients of rank correlation between computational methods and subjects for seven queries

r_s	<i>GLCM</i>	<i>MRSAR</i>	<i>FT</i>	<i>WT</i>	<i>GT</i>
Query 1	-0.13	0.25	0.05	0.22	0.32
Query 2	0.53	0.6	-0.18	0.35	0.42
Query 3	0.45	0.15	0.48	0.18	0.3
Query 5	-0.7	0.58	0.42	-0.7	-0.7
Query 8	0.45	0.25	0.55	0.18	0.32
Query 9	0.08	0.18	0.4	0.17	0.22
Query 10	0.35	0.53	0.7	0.48	0.33
\bar{r}_s	0.15	0.36	0.35	0.13	0.17

The average the rank correlation was applied to evaluate whether the five computational methods were consistent with human perception on the visual measurements of similarity, which is detailed in the following section.

5.3.3 Data Analysis and Discussion

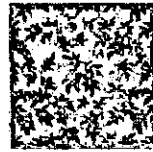
By comparison between computational texture representations and perceived texture features (Experiment one), as shown in Table 5.1, it can be seen that the average rank correlation between ranking results based on each feature of computational methods and ranking results by the subjects based on visual texture features is very low. All rank correlations are less than the significance threshold of 0.73. The value of rank correlation of 0.73 gives a significance level at 5% when the number of comparing pairs n is equal to 10 and the degree of freedom is 8 ($=10-2$), as explained in detail in Section 3.2.2. This suggested that none of the five computational texture methods can represent the texture features in terms of coarseness, regularity and directionality individually very well. For each feature calculated by the five computational methods, as seen in Appendix 9, the rank correlation with coarseness, regularity and directionality are smaller than the

significance threshold of 0.73, implying that most feature elements calculated by the five computational texture methods are not in close correlation with perceived texture features (coarseness, regularity and directionality). According to these results, we can conclude that the five computational texture methods are not consistent with human perception of texture features for wallpaper images in terms of coarseness, regularity and directionality.

As for similarity measurements that are the combination of all the features in each computational method, consistency with human visual similarity is another interesting issue.

By comparison of similarity measured by computational texture methods and subjects (Experiment two), as seen in Table 5.2, again, the average rank correlation for seven query images was very low, for example, 0.15, 0.36, 0.35, 0.13 and 0.17 being the correlations with *GLCM*, *MRSAR*, *FT*, *WT* and *GT* respectively. Even maximum rank correlation 0.7 obtained by *FT* for image query 10 was not over the significance threshold of 0.75, that is the significance level at 5% when the number of comparing pairs n is equal to 9 and the degree of freedoms is 7 ($=9-2$). Judging from the results, we can assume that the five computational texture methods do not simulate human vision very well in terms of performing similarity measurements on wallpaper images, which is in line with our finding that the retrieval results obtained by five computational texture methods are not ideal. This is supported by the following example, which gives the top 5 retrieval results for query image 9 by the subjects and five computational methods respectively. The number below each computational method is the rank correlation between the subjects and the corresponding computational method.

Through the analysis, we can conclude that the five computational texture methods are not consistent with human perception in terms of texture features and visual similarity measurements for wallpaper images. Therefore, the study of the relationship between visual similarity and visual texture features is important to develop suitable retrieval methods for wallpaper images.



Query 9

<i>Subjects</i>					
<i>GLCM</i> ($r_s=0.08$)					
<i>MRSAR</i> ($r_s=0.18$)					
<i>FT</i> ($r_s=0.4$)					
<i>WT</i> ($r_s=0.17$)					
<i>GT</i> ($r_s=0.22$)					

Figure 5.4 Comparing retrieval results between subjects and five computational methods for query 9

5.4 Relationships between Visual Similarity Measurements and Visual Texture Features

In this section, we explore how human perceive similarity based on texture features. Based on the results obtained from our psychophysical experiments one and two, the relationships between visual similarity and texture features can be established. By analyzing this relationship, we found which texture features (coarseness, regularity, and directionality) play a more important role in performing

similarity measurements for wallpaper images, leading to development of new methods to improve retrieval accuracy.

5.4.1 Rank Correlation between Visual Similarity Measurements and Visual Texture Features

Based on the results of experiment one, we obtained rankings based on texture features of coarseness, regularity and directionality respectively by subjects. Whilst from the results of experiment two, we had rankings for seven queries respectively observed by subjects. In both experiments, we adopted the same sample images.

According to the results obtained by subjects, we tried to establish the relationship between visual similarity measurements and visual texture features. First, in order to obtain the rankings for each query image based on coarseness, regularity and directionality individually, we calculated the psychophysical distance between each sample image and the query image based on these three visual features respectively. Then, by calculating the rank correlation between rankings for each query image based on the psychophysical distance of visual texture features and the corresponding ranking for each query based on visual perception, we established the relationship between visual similarity measurements and the visual texture features. The ranking results for seven query images are given in Tables A11.1 to A11.7, as seen in Appendix 11. In Tables A11.1 to A11.7, the first row is the rankings based on perceived similarity measurements for query images and the other rows are the corresponding ranking for query image based on coarseness, regularity and directionality respectively. The numbers from columns 2 to 10 in Tables A11.1 to A11.7 are the ID numbers of ranking images in the order from most similar to least similar to each query image. The last column contains the coefficients of rank correlation between visual similarity measurements and the corresponding visual texture features.

Finally, the rank correlation between perceived visual similarity and the visual texture features for seven queries are listed in Table 5.3. The average rank correlation \bar{r}_s for seven queries is shown in the last column in the table.

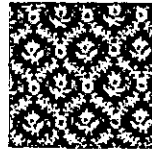
Table 5.3 Coefficients of rank correlation between perceived similarity measurements and visual texture features for seven queries

r_s	Query 1	Query 2	Query 3	Query 5	Query 8	Query 9	Query 10	\bar{r}_s
Coarseness	0.77	0.53	0.87	0.60	0.60	0.37	0.73	0.64
Regularity	0.93	0.73	0.75	0.93	0.77	0.32	0.80	0.75
Directionality	0.92	0.82	0.83	0.73	0.78	0.77	0.82	0.81

The average rank correlation was applied to analyze the relationship between perceived visual similarity and the visual texture features. The data analysis and discussion will be detailed in Section 5.4.2.

5.4.2 Data Analysis and Discussion

In Table 5.3, the average rank correlation between visual similarity measurements and coarseness is 0.64, and regularity is 0.75, and directionality is 0.81. Coefficients of rank correlation between visual similarity measurements and regularity and directionality are over the significance threshold of 0.75 as described in Section 3.2.2. But the rank correlation between visual similarity measurements and coarseness is below the threshold of 0.75. Judging from the results, we can say that the texture features of regularity and directionality play a more important role in perceived visual similarity measurements for wallpaper images. We can also see this result from the following two examples shown in Figures 5.5 and 5.6, which show the top 5 retrieval results for query 5 and query 8 respectively. The number below each texture feature is the rank correlation between rankings of subjects and rankings based on corresponding texture features. In both figures, the ranking results based on regularity and directionality is closer to ranking results based on human visual similarity. It suggests that the texture features of regularity and directionality are very important in image retrieval for these two queries.



Query 5

<i>Subjects</i>					
<i>Coarseness</i> ($r_s=0.60$)					
<i>Regularity</i> ($r_s=0.93$)					
<i>Directionality</i> ($r_s=0.80$)					

Figure 5.5 Comparison between ranking results based on human visual similarity and ranking results based on visual texture feature for query 5



Query 8

<i>Subjects</i>					
<i>Coarseness</i> ($r_s=0.60$)					
<i>Regularity</i> ($r_s=0.77$)					
<i>Directionality</i> ($r_s=0.78$)					

Figure 5.6 Comparison between ranking results based on human visual similarity and ranking results based on visual texture feature for query 8

Through the analysis above, we found that texture features of regularity and directionality play an important role in performing visual similarity measurements for wallpaper images. This provided us with the clue for the development of new methods to improve retrieval accuracy for wallpaper images. Therefore, we considered the texture features of regularity and directionality first in wallpaper image retrieval. The new methods for wallpaper image retrieval will be described in Chapter 6.

5.5 Summary

This chapter presented the results of two psychophysical experiments. Comparison of results across five computational methods and human perception for wallpaper images, we concluded that five computational texture methods are not fully consistent with human perception in terms of texture features and visual similarity. By analyzing the relationship between visual similarity measurements and visual texture features, we found that texture features of regularity and directionality play a more important role in performing visual similarity measurements for wallpaper images than the feature of coarseness.

Therefore, the texture features of regularity and directionality are the main features in performing wallpaper image retrieval. So far, five computational texture methods cannot represent texture features of regularity and directionality individually very well. New methods for wallpaper image retrieval have to be developed, which will form two stages. First, we will classify images based on regularity and directionality respectively. Then, we will perform image retrieval in corresponding classified group of the image database, which will be the content of Chapter 6.

6. Image Retrieval for Wallpaper Images

This chapter describes the approach applied in this research to content-based image retrieval for wallpaper images, and consists of two main parts, which are classification and image retrieval. First, the query image was classified based on regularity and directionality. After classification, image retrieval was performed in the corresponding classes of the image database. An overview of the framework for image retrieval is shown below in Figure 6.1.

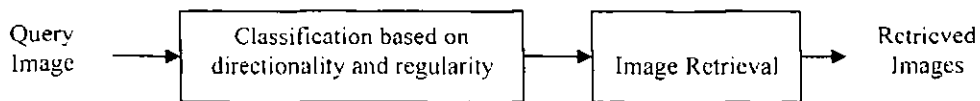


Figure 6.1 An overview of framework for wallpaper image retrieval

Classification based on regularity and directionality is described in Section 6.1. After classification, image retrieval is introduced in Section 6.2. Finally, a content-based image retrieval system for wallpaper images will be presented in Section 6.3.

6.1 Image Classification

According to the analysis of experimental results in Section 5.4, the features of regularity and directionality played a more important role in performing visual similarity for wallpaper images. Psychophysical experiments carried out in this study also show that five existing computational models can not represent perceptual texture features of wallpaper images very well, nor can they perform image retrieval accurately for wallpaper images, as discussed in Section 5.3. In order to retrieve wallpaper images efficiently and effectively, wallpaper images were hence first classified based on directionality and regularity before the retrieval. A schematic diagram shown in Figure 6.2 illustrates the classification tree based on directionality and regularity employed in this study.

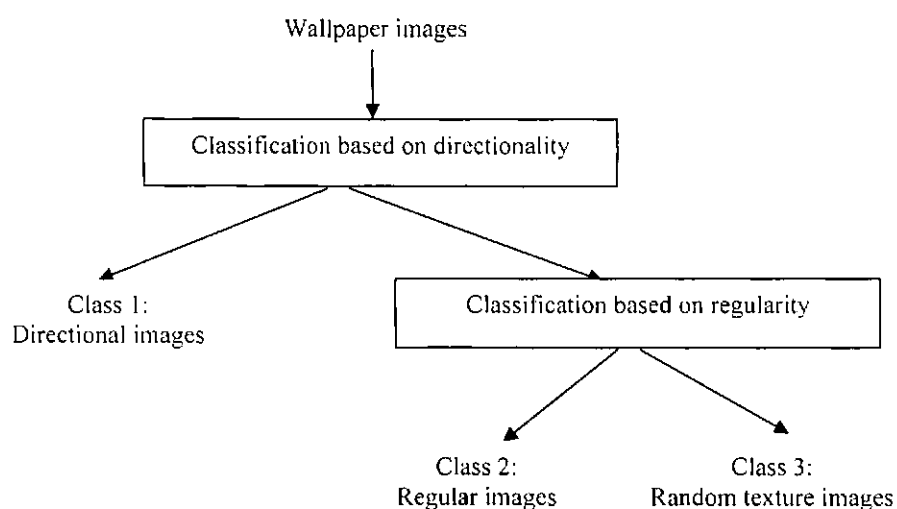


Figure 6.2 Classification tree based on regularity and directionality

After classification, wallpaper images were classified into three groups, which were Class 1: directional images; Class 2: regular images; and Class 3: random texture images. The following section will describe the method of classification based on directionality and regularity respectively in detail.

6.1.1 Classification Based on Directionality

Directionality is a global property over an image, suggesting the orientation of the texture does not matter, i.e., two patterns that are different only in orientations should have the same degree of directionality. Some wallpaper images have strong patterns of geometric structure, for example, images (1) and (2) in Figure 6.3. Therefore, directionality is a very important visual feature embedded in wallpaper images, which is in line with the findings obtained in Section 5.4.

In the field of image processing, the feature of directionality is generally extracted using the Fourier power spectrum, or is obtained by using a direction histogram. Normally, directional images show obvious beams in the Fourier power spectrum or outstanding peaks in the direction histogram, as demonstrated in image (1) in Figure 6.3. However, some wallpaper images with the feature of directionality do not follow this rule. For example, in Figure 6.3, wallpaper image (2) has the feature of directionality similar to that of image (1). But, according to its Fourier

power spectrum and direction histogram, they show features closer to non-directional image (3) than the directional image (1).

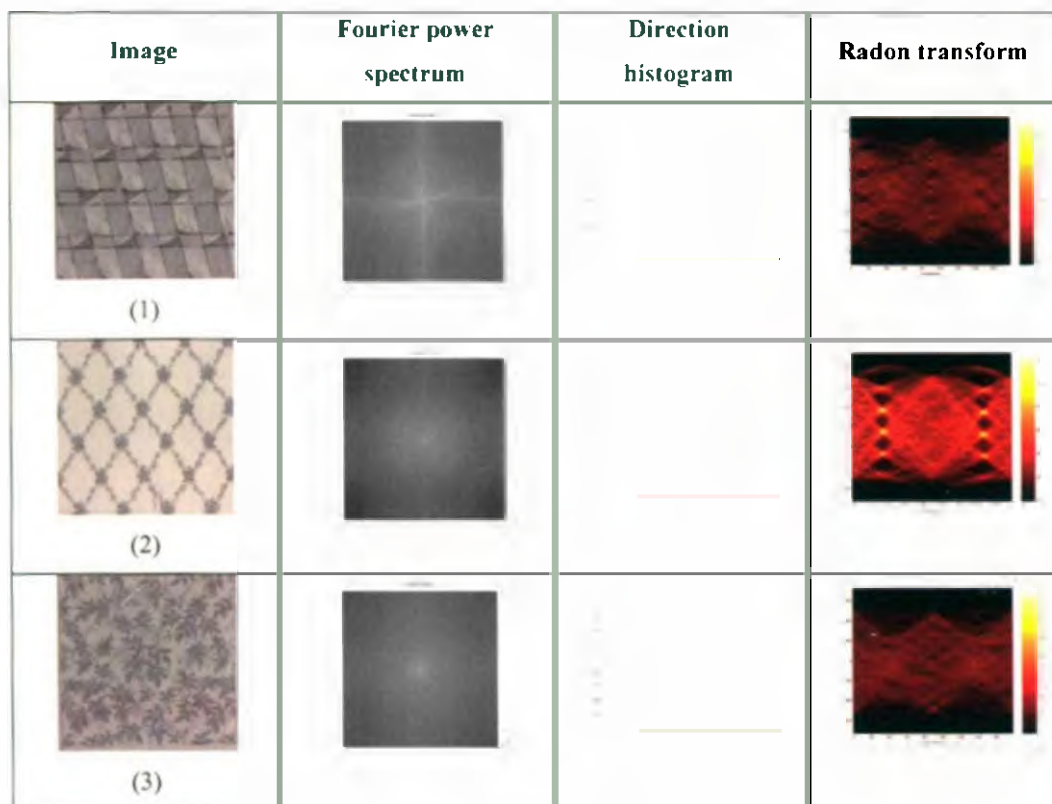


Figure 6.3 Wallpaper images and their Fourier power spectrum, direction histogram and Radon transform

The reason is that the features of directionality extracted from the Fourier power spectrum and the direction histogram are statistic ones, which can not represent the characters of direction in the spatial domain visually. Since directionality is defined as a global property over the given region, we need to consider the spatial distribution of directional lines to represent directionality. Furthermore, the property of directionality shown in wallpaper images are sometimes made of flowers or leaves, some degrees of art effect, such as in image (2) in Figure 6.3. These visible directional lines are difficult to capture in both approaches of Fourier power spectrum and direction histogram.

The Radon transform (in Section 3.3) can overcome these drawbacks by using the Fourier power spectrum and the direction histogram, and can well describe directional lines in a spatial domain. In Figure 6.3, it shows the obvious different

features between the directional image (2) and non-directional (3) in the Radon transform. In this research, we applied the Radon transform to describe the features of directionality for wallpaper images.

Directionality representations were extracted by the Radon transform of edge images. Thresholding were applied to classify images into classes of directionality or non-directionality. Figure 6.4 briefly describes classification based on directionality.

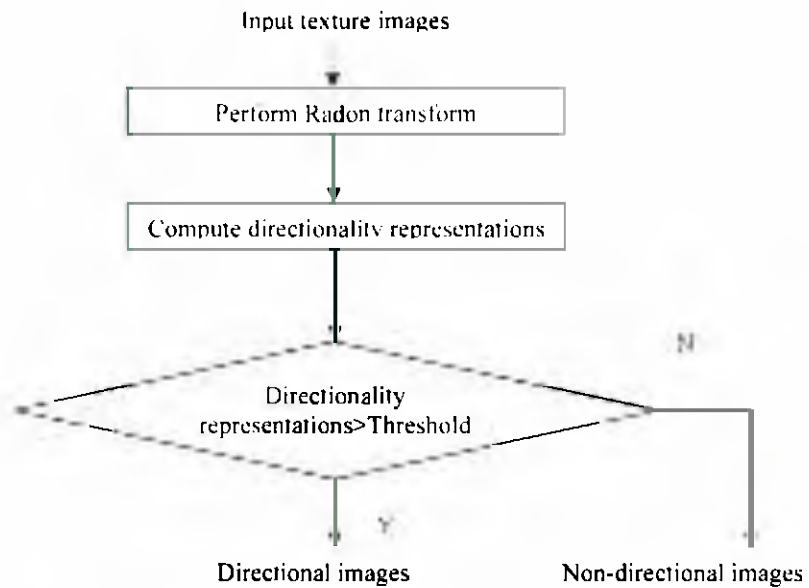


Figure 6.4 Classification based on directionality

The following sections will introduce the directionality representations extracted from the Radon transform, and classification based on directionality using thresholding.

6.1.1.1 Directionality Representations

Since directionality is a global property over a given region, images with strong visual sense of directionality has many specific directional lines scattering over the region of the images. In order to represent this property effectively, we needed to analyze the Radon transform of images in horizontal and vertical direction respectively. We can obtain the angle of the main direction from the horizontal axis and the spatial distribution of directional lines from the vertical axis. Four main steps

were adopted, including obtaining the Radon transform of edge images; projecting the Radon transform in the horizontal axis to decide the main direction of the image by finding the peaks in the projection; projecting the Radon transform of the main direction in vertical axis to obtain the spatial distribution of main directional lines; and representing directionality by the combination of the features shown in both horizontal and vertical axes in the Radon transform. The detailed procedure is described as follows.

- *Obtain the Radon transform of an edge image*

1. Obtain binary edge image by using the Canny filter [37], as shown in Figure 6.5 (h)
2. Perform the Radon transform of the edge image, as demonstrated in Figure 6.5 (c)
3. Threshold the Radon transform. We obtained the possible points that express the straight lines in an image, shown in Figure 6.6 (d). In this research, we set the threshold=10%*size (image), suggesting there is a likely straight line when the total number of edge pixels along a specified direction is over the threshold.

- *Obtain the main direction of an image and the directionality feature $DER_{value_ \theta}$*

1. Project the Radon transform into the vertical direction, we obtained the curve of projection $g(x)$, as shown in Figure 6.6 (e)
2. Obtain the main direction θ of images by computing the local maxima point in $g(x)$. Here, directional lines in image are perpendicular to the projecting axis. Therefore, θ is

$$\theta = \begin{cases} \theta' + \frac{\pi}{2} & \theta' \leq \frac{\pi}{2} \\ \theta' - \frac{\pi}{2} & \theta' > \frac{\pi}{2} \end{cases} \quad (6.1)$$

where θ is an angle of a projecting axis, and its value are given in horizontal axis of Radon transform.

3. Obtain the $DER_{value \theta}$ by normalizing the value of peak in corresponding main direction θ

$$DER_{value \theta} = \frac{P_{\theta}}{\sum g(x)} \quad (6.2)$$

where P_{θ} expresses the value of peak in corresponding main direction θ . The value of $DER_{value \theta}$ is between 0 and 1. The bigger the value of $DER_{value \theta}$, the more likely there is a straight line in the direction θ . As given in Figure 6.6 (e), the value of $DER_{value \theta}$ and the corresponding θ are seen below the curve of $g(x)$.

- *Obtain the spatial distribution of the main directional lines $DER_{position \theta}$*
 1. Project Radon transform into the horizontal direction in each main direction respectively. We obtained the curve $f_{\theta}(x)$ in corresponding orientation, as shown in Figure 6.6 (f).
 2. Compute the χ^2 (Chi-square distribution) statistics for the curve $f_{\theta}(x)$ in different orientations respectively, χ^2 statistics were applied to describe the quality of the match between the distribution of the region and a uniform distribution [99], and is defined as

$$\chi^2 = \sum_{i=1}^m m(p_i - \frac{1}{m})^2$$

where

$$p_i = \sum_{x \in region_i} f_{\theta}(x) / \sum f_{\theta}(x) \quad (6.3)$$

The curve $f_{\theta}(x)$ was evenly divided into m regions in the horizontal direction, p_i is the percentage of value of $f_{\theta}(x)$ in region i over the whole

region. The probability function $\frac{1}{m}$ expresses the uniform distribution over the zones. The smaller the value of χ^2 , the closer to uniform distribution the curve distribution is. When $\chi_{\min}^2 = 0$, the curve shows uniform distribution. When the value of $f_{\theta}(x)$ is put together in one region, χ^2 has a maximum value $\chi_{\max}^2 = m - 1$, which is obtained by setting one $p_i = 1$ and the other $p_i = 0$. Finally, the spatial distribution of specified directional lines $DER_{\text{position}_{\theta}}$ is defined by normalizing χ_{θ}^2 between 0 and 1 using Eq. (6.4).

$$DER_{\text{position}_{\theta}} = 1 - \frac{\chi_{\theta}^2}{\chi_{\max}^2 - \chi_{\theta}^2} \quad (6.4)$$

Value of $DER_{\text{position}_{\theta}}$ is between 0 and 1, i.e., the bigger the value of $DER_{\text{position}_{\theta}}$ is, the closer to uniform distribution the directional line distribution is. In Figure 6.6 (f), the value of $DER_{\text{position}_{\theta}}$ is shown below the corresponding figure.

Finally, directionality representations in a specified direction θ expressed as DER_{θ} multiplied two features obtained in horizontal direction analysis $DER_{\text{value}_{\theta}}$ and vertical direction analysis $DER_{\text{position}_{\theta}}$ in the Radon transform together as shown in Eq. (6.5)

$$DER_{\theta} = DER_{\text{value}_{\theta}} \cdot DER_{\text{position}_{\theta}} \quad (6.5)$$

Generally, an image with strong directionality patterns should have many specified directional lines scattered over the regions of the image. Therefore, they should have a bigger value in $DER_{\text{value}_{\theta}}$, $DER_{\text{position}_{\theta}}$ and DER_{θ} as well. Considering classification based on directionality, we used the maximum value of DER_{θ} as the directionality representations and defined as follows.

$$DER = \text{Max}(DER_{\theta}) \quad (6.6)$$

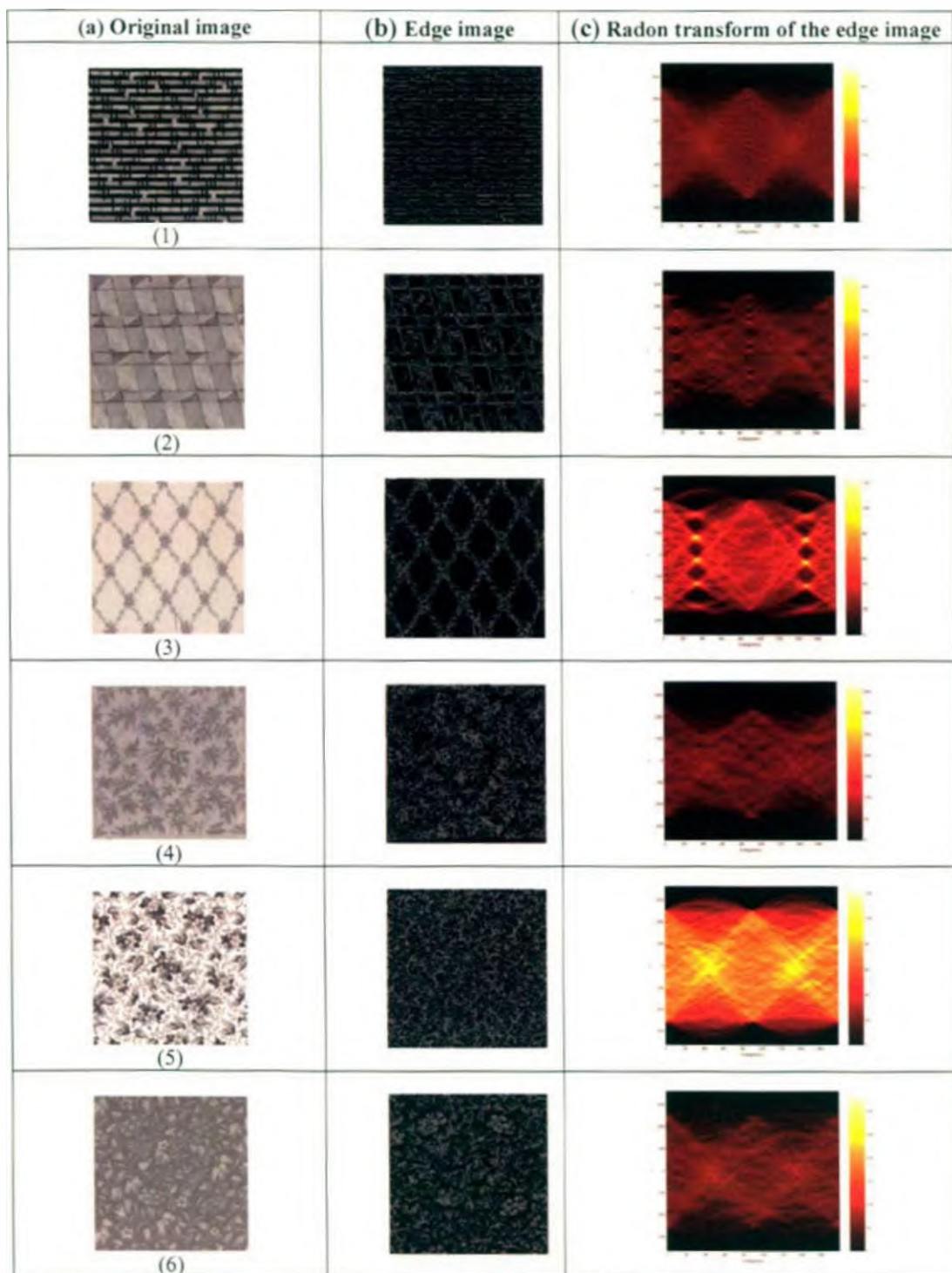
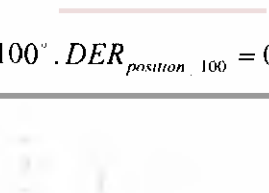
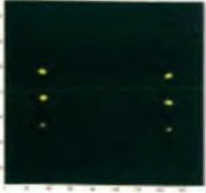


Figure 6.5 Radon transform of the edge images

(d) Radon transform after thresholding	(e) Projection (d) in vertical direction	(f) Projection of Radon transform in horizontal direction
	 <p>$\theta = 0^\circ . DER_{value_0} = 0.8032$</p>	 <p>$\theta = 0^\circ . DER_{position_0} = 0.9959$</p>
	 <p>$\theta_1 = 100^\circ . DER_{value_{100}} = 0.2859$ $\theta_2 = 0^\circ . DER_{value_0} = 0.2290$ $\theta_3 = 50^\circ . DER_{value_0} = 0.1100$</p>	 <p>$\theta_1 = 100^\circ . DER_{position_{100}} = 0.9575$</p> <hr/> <p>$\theta_2 = 0^\circ . DER_{position_0} = 0.9757$</p> <hr/> <p>$\theta_2 = 50^\circ . DER_{position_{50}} = 0.5575$</p>
	 <p>$\theta_1 = 120^\circ . DER_{value_{120}} = 0.5177$ $\theta_1 = 50^\circ . DER_{value_{50}} = 0.3630$</p>	 <p>$\theta_1 = 120^\circ . DER_{position_{120}} = 0.7788$</p>

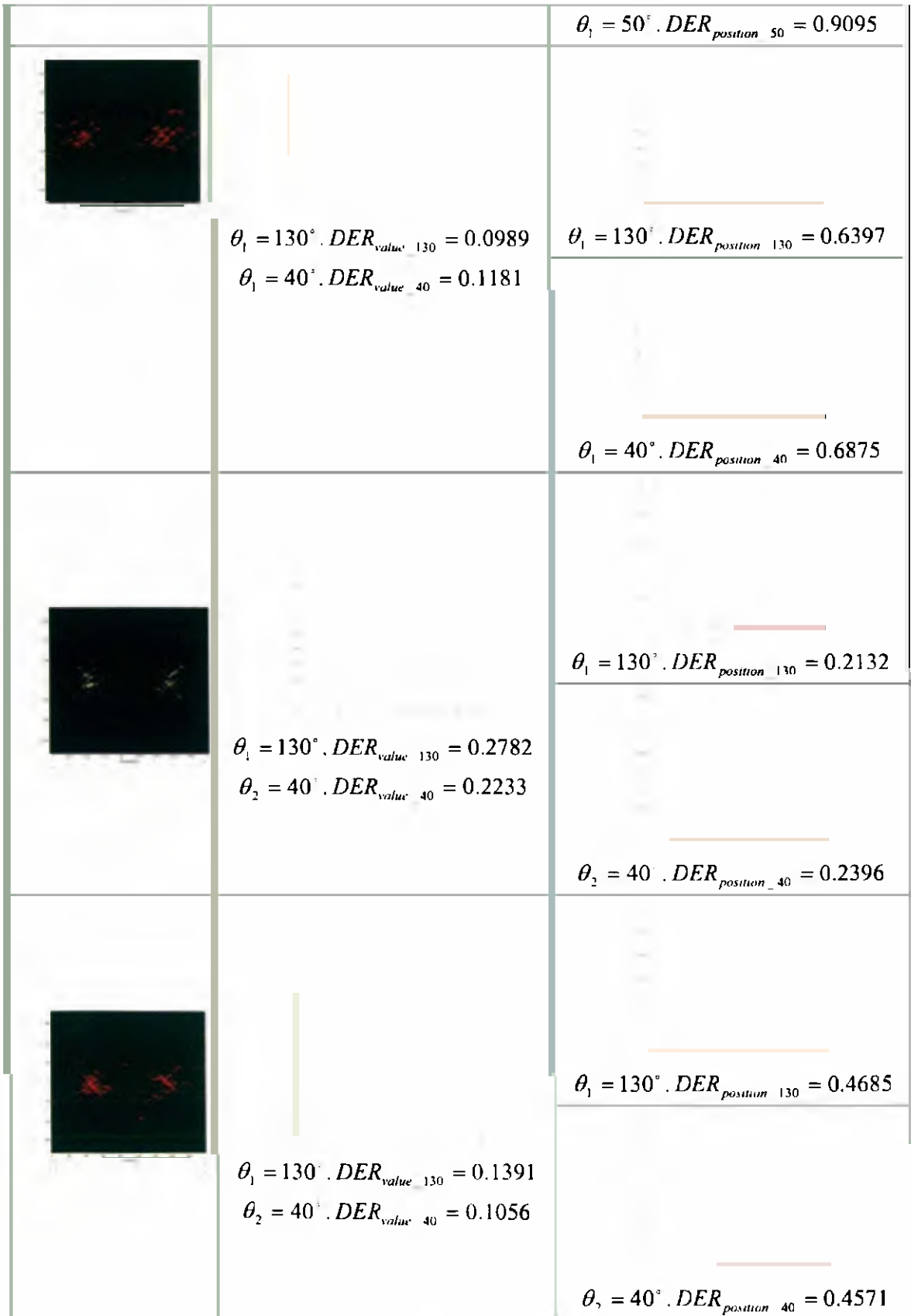


Figure 6.6 Directionality representations in Radon transform

Table 6.1 gives the directionality features DER of images ((1)—(6)) shown in Figure 6.5 (a).

Table 6.1 Directionality features of images

Image	(1)	(2)	(3)	(4)	(5)	(6)
DER	0.7999	0.2737	0.4032	0.0812	0.0593	0.0652

Table 6.1 shows that images ((1) to (3) in Figure 6.5 (a)) with characteristics of directionality have bigger values of DER than images ((4) to (6) with less directionality). Therefore, a threshold for DER were applied to classify images into the class of directionality or non-directionality.

6.1.1.2 Classification Based on Directionality

Twenty directional images and twenty non-directional images were chosen by subjects from MoDA database. Their DER were depicted in Figure 6.7. The horizontal axis represents the sample image numbers and the vertical axis represents DER (\star) expresses directional samples and (\diamond) represents non-directional samples.

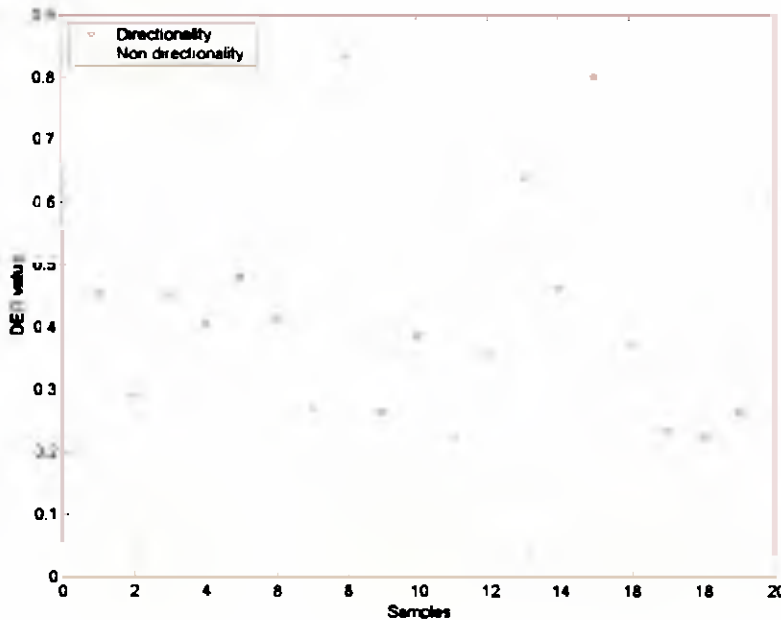


Figure 6.7 Directionality features of 40 training sample images

From the Figure 6.7, it can be seen that the majority of the *DER* values of directional images (★) are bigger than 0.18. However, the majority of the *DER* values of non-directional images (⊙) are smaller than 0.18. Therefore, a *DER* value 0.18 was used as a threshold to distinguish directional images from non-directional images.

In summary, directional and non-directional images were classified by a threshold of $DER = 0.18$, i.e., if $DER > 0.18$ the image was labelled with directionality, otherwise non-directionality. The classification results based on directionality are shown in Section 7.1.1.

6.1.2 Classification Based on Regularity

Regularity is a fundamental structural property of texture. It is simply attributed to the structure of repetitive or periodic patterns. The more regular the periodicity, the stronger the structure is. Generally, wallpaper images have strong texture structure, such as periodic patterns. Therefore, regularity is a very important visual feature for describing wallpaper images. This finding was also proved in Section 5.4.

In image processing, the periodic or repetitive patterns were captured by computing the correlation between the intensity values in rows or columns of an image. The curve of the Correlation Coefficient with periodic patterns shows periodic peak, whilst the curve of the Correlation Coefficient for an irregular image tends to be flat. Regularity representations were therefore extracted from the correlation coefficient. Thresholding was applied again to classify images into regularity and irregularity. Figure 6.8 briefly describes the procedure of classification based on regularity.

In following sections, we will introduce the regularity representations extracted from correlation coefficients, and classification based on regularity using thresholding.

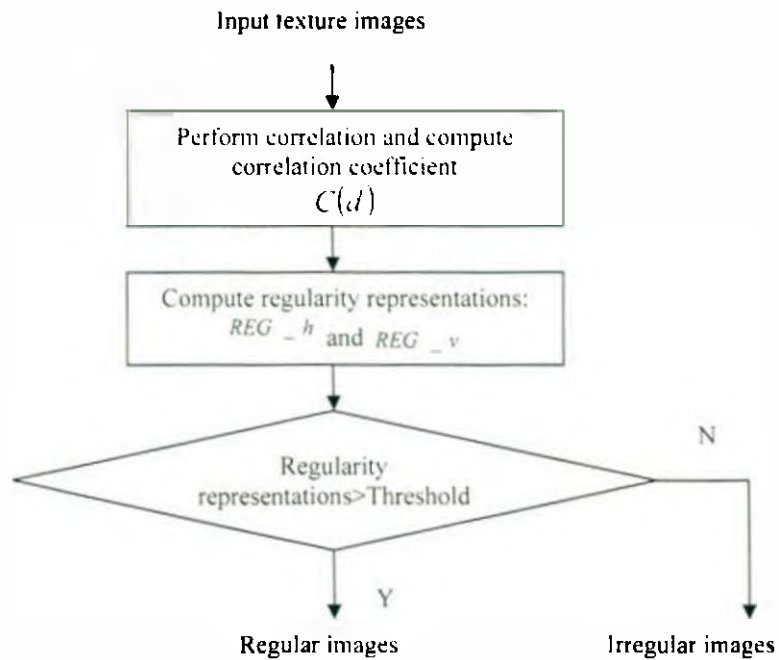


Figure 6.8 Classification based on regularity

6.1.2.1 Regularity Representations

Correlation is widely used in finding repeated patterns of images in the field of image processing [60, 61, 64].

The normalized correlation $c(i, j)$ between the rows (or columns) of an image is formulated as

$$c(i, j) = \frac{E(d_i, d_j) - E(d_i)E(d_j)}{\sigma(d_i)\sigma(d_j)} \quad (6.7)$$

where d_i and d_j are the intensity values within the rows (or columns) i and j respectively. $E(\bullet)$ is the expected value and $\sigma(\bullet)$ is the standard deviation.

In order to analyze easily, $C(d)$ was introduced to describe the correlation between the rows (columns) in a distance d .

$$C(d) = \frac{1}{N-d} \sum_{i=1}^{N-d} c(i, j+d)$$

$$d = 1, 2, 3, \dots, N-1 \quad (6.8)$$

where N is the number of rows (columns). Therefore, we analyzed regularity in one dimension of $C(d)$ instead of two dimensions of $c(i, j)$.

Figure 6.9 visualizes the correlation coefficient matrix $c(i, j)$ and $C(d)$ of images in horizontal (column) and vertical (row) direction respectively. According to Eq. (6.8), $C(d)$ was obtained by projecting correlation coefficient matrix $c(i, j)$ in the direction with 45° .

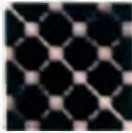
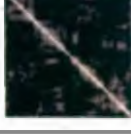
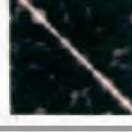
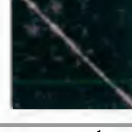
Original image	Horizontal(column) direction		Vertical(row) direction	
	Correlation coefficient matrix $c(i, j)$	$C(d)$ (Project of $c(i, j)$ in $\theta = 45^\circ$)	Correlation coefficient matrix $c(i, j)$	$C(d)$ (Project of $c(i, j)$ in $\theta = 45^\circ$)
				
				
				
				
				
				

Figure 6.9 Visualizing the correlation coefficient matrix $c(i, j)$, $C(d)$ of images in horizontal and vertical direction

From Figure 6.9, $C(d)$ curves of images with repeated patterns (images (1) to (3)) show periodic peaks, while $C(d)$ curves of images without repeated patterns (images (4) to (6)) tend to be flat. Therefore, the features of $C(d)$ were used to represent the characters of regularity.

In order to describe the periodic features of wallpaper images, two measures of REG_{value} and $REG_{position}$ were derived from $C(d)$. REG_{value} was the contrast of $C(d)$ and is applied to describe the amplitude of the curve whilst $REG_{position}$ was used to describe the relative position of peaks that decide whether a curve showed periodic properties or not. These two measures expressed the characteristics of $C(d)$, i.e., periodic peaks for regular images or a flat curve for irregular images.

REG_{value} is the contrast of $C(d)$ and defined as

$$REG_{value} = \frac{1}{M} \sum_{i=1}^M p_value(i) - \frac{1}{N} \sum_{j=1}^N v_value(j) \quad (6.9)$$

where $p_value(i)$ and $v_value(j)$ are magnitudes of peaks and valleys in $C(d)$, M is the number of peaks and N is the number of valleys.

$REG_{position}$ is defined as

$$REG_{position} = 1 - \frac{\sigma_{p_position}}{\mu_{p_position}} \quad (6.10)$$

where $\mu_{p_position}$ is the average of distances among the peaks in $C(d)$, $\sigma_{p_position}$ is the standard deviation of distances among the peaks in $C(d)$.

$C(d)$ with periodic peaks has bigger values of REG_{value} and $REG_{position}$, whereas $C(d)$ with a flat curve has smaller values of REG_{value} and $REG_{position}$.

Finally, the regularity representation REG was defined as a multiplication of the two measures shown in Eq. (6.13).

$$REG = |REG_{value} \cdot REG_{position}| \quad (6.11)$$

The following table gives the regularity features REG_h and REG_v of images ((1) to (6) given in Figure 6.9) in horizontal and vertical direction respectively.

Table 6.2 Regularity features of images

Image	Horizontal(column) direction			Vertical(row) direction		
	REG_{value_h}	$REG_{position_h}$	REG_h	REG_{value_v}	$REG_{position_v}$	REG_v
(1)	0.8693	0.9883	0.8591	0.7320	0.9964	0.7293
(2)	0.4151	0.8908	0.3698	0.7977	0.9943	0.7932
(3)	1.0093	0.9965	1.0057	0.7609	0.9501	0.7229
(4)	0.1840	0.8861	0.1630	0.1830	0.6239	0.1142
(5)	0.2056	0.4424	0.0910	0.1822	0.3262	0.0594
(6)	0.0943	0.7535	0.0710	0.0569	0.8452	0.0481

Table 6.2 shows that regular images ((1), (2) and (3) in Figure 6.9) with periodic peaks of $C(d)$ have a bigger REG value (REG_h or REG_v) than irregular images ((4), (5) and (6) in Figure 6.9) with flat curve of $C(d)$. Therefore, thresholding for REG was applied to classify an image into either the regularity or irregularity class.

6.1.2.2 Classification Based on Regularity

Twenty regular images and twenty irregular images were chosen from the MoDA database. Twenty regular images were selected with regularity features both in horizontal and vertical direction. Their values of REG_h and REG_v are shown in Figure 6.10. The horizontal axis represents the sample image numbers and the vertical axis represents REG value. (★) expresses regularity samples and (●) represents irregularity samples.

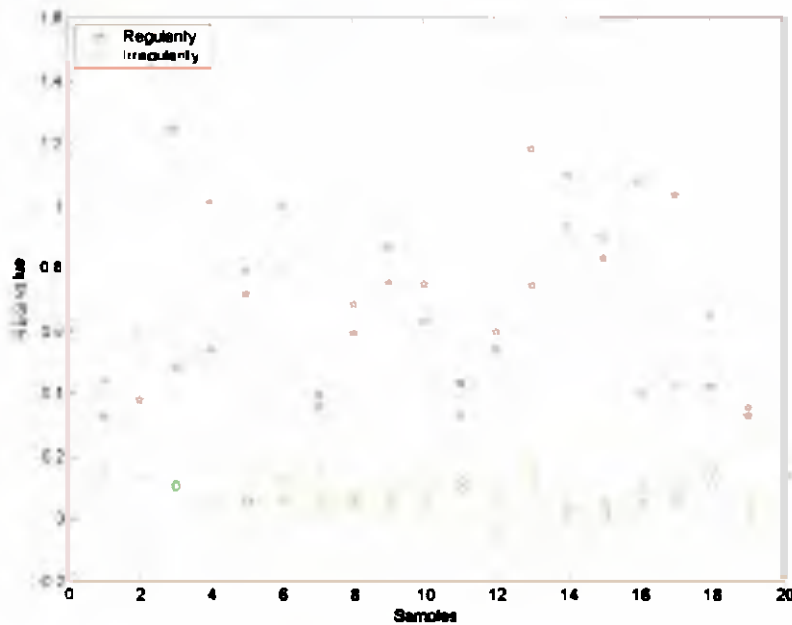


Figure 6.10 Regularity features of 40 (training sample images)

From the Figure 6.10, it can be seen that the majority of the REG values of regular images (\star) are bigger than 0.23. Whereas, the majority of the REG values of irregular images (\diamond) are smaller than 0.23. Therefore, a REG value 0.23 was used as threshold to distinguish regular images from irregular ones.

In summary, regular and irregular images were classified by a threshold of $REG = 0.23$, i.e., if $REG_h > 0.23$ or $REG_v > 0.23$, the image was labelled with regularity, otherwise irregularity. The classification results based on regularity are shown in Section 7.1.2.

6.1.3 Classification Based on Directionality and Regularity

After introducing classification based on directionality and regularity respectively, we combined these two methods to classify wallpaper images.

According to the results of our psychophysical experiments in Table 5.3, the average of rank correlation between visual similarity measurements and regularity is 0.75, and directionality is 0.81. Therefore, the directionality character plays a slightly

more important role in visual similarity measurements than regularity and this is taken into account first in the classification.

Therefore, the wallpaper images were classified into directional images or non-directional images first. Then, these non-directional images were further classified based on regularity into sub-class of either regular or random texture images. Figure 6.11 describes the procedure of classification based on directionality and regularity. After classification, images were classified into three groups: Class 1: directional images; Class 2: regular images; and Class 3: random texture images. The classification results based on directionality and regularity will be shown in Section 7.1.3.

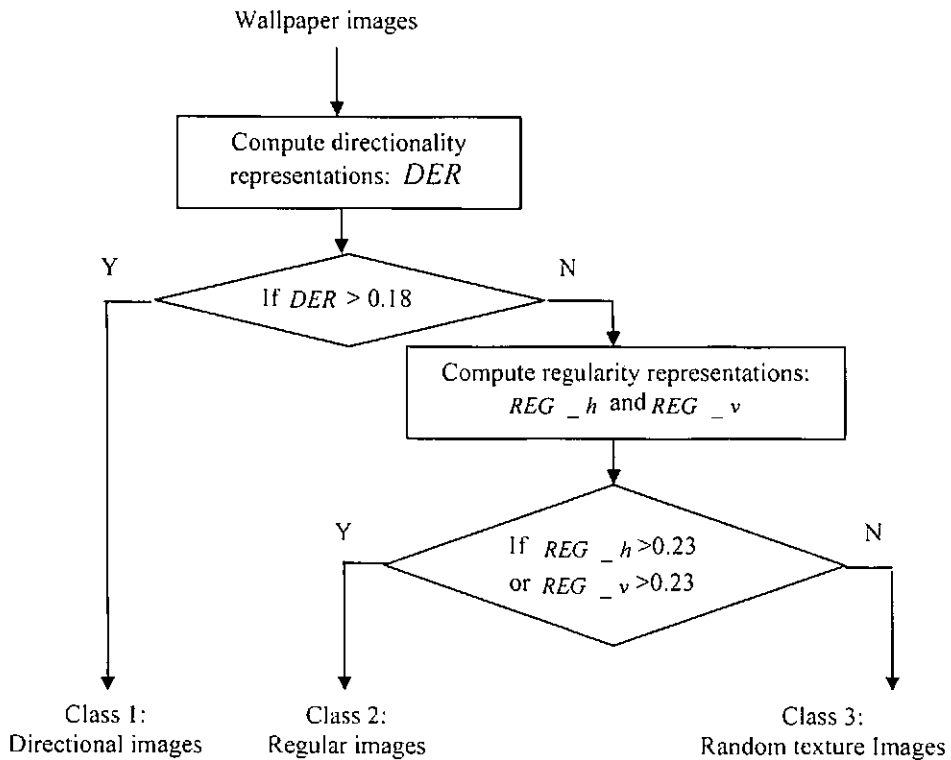


Figure 6.11 Flow of classification based on directionality and regularity

6.2 Image Retrieval

After classification, the image retrieval was performed in each specified class by calculating similarity measurements between feature vectors of a query image and the images in that class.

Query image was classified based on regularity and directionality. Then, similar texture images were retrieved in the same classified group as the query image by using five computational methods. The following retrieval results were performed in other class groups. The path for the category index is described as follows.

If query=directionality, then index path= directional images → regular images
→ random texture images.

If query=regularity, then index path= regular images → directional images
→ random texture images.

If query=random, then index path= random texture images → regular images
→directional images

The above index path was set based on the relationship between three different classes.

According to the rankings based on coarseness, regularity and directionality, obtained in Section 5.1, we calculated the coefficients of the rank correlation between three texture features. We put rankings based on coarseness, regularity and directionality shown in Figures 5.1, 5.2 and 5.3 in Table 6.3 and coefficients of rank correlation between texture features were calculated and shown in Table 6.4.

Table 6.3 Rankings based on coarseness, regularity, and directionality

Texture Feature	Rankings									
Coarseness	3	8	9	2	6	5	10	4	1	7
Regularity	10	1	5	6	7	4	9	2	3	8
Directionality	1	10	5	6	7	4	9	3	2	8

Table 6.4 Coefficients of the rank correlation between texture features

r_s	Coarseness	Regularity	Directionality
Coarseness	1	0.72	0.71
Regularity	0.72	1	0.98
Directionality	0.71	0.98	1

Judging from the rank correlation r_s between different texture features, we can see the coefficients of rank correlation between regularity and directionality is 0.98. It is higher than that between regularity and coarseness and between directionality and coarseness. This suggests there is a stronger correlation between directionality and regularity. This can help us to set the index path between three different classes. This

is why the class of regularity and directionality in the indexing path are followed by each other.

The retrieval results by using five computational methods will be shown in Section 7.2, whereas the comparison between retrieval results before and after classification is discussed in Section 7.2.

6.3 A Content-Based Image Retrieval System for Wallpaper Images

In this research, a preliminary content-based image retrieval system for wallpaper images was developed with the diagram shown in Figure 6.12.

This system includes two main parts, which are image database processing and image retrieval. Image database processing inside the dashed lines contains two procedures. One is to classify the image database into three classes: directional, regular and random images. The other is to extract the texture features of images by using each of five computational methods respectively. Finally it yields the three sub-databases of texture features, which is the texture feature database of class 1, texture feature database of class 2 and texture feature database of class 3. These three sub-databases of texture features were obtained and stored in the archives in advance.

When a user submits a query, the query image was classified based on directionality and regularity first. At the same time, the texture feature vectors of the query image were extracted using one computational texture method selected by the user. According to the classification result, the system set the category index detailed in Section 6.2. This category index determined the ranking of three classes in the retrieval results. Then image retrieval was performed by calculating the similarity measurements between the feature vectors of the query image and the corresponding texture features in the three sub-databases. Finally, a set of images were retrieved and ranked based on the degree of similarity calculated by the similarity measurements. By recalling the image database, the retrieved images were displayed on screen.

A graphical user interface to display the retrieval results and classification results for wallpaper images is shown in Figure 7.16.

6.4 Summary

In this chapter, the methodology of content-based image retrieval for wallpaper images was developed. First, a query image was classified based on regularity and directionality. After classification, image retrieval was performed in the corresponding classes of the image database.

Classification based on directionality and regularity was introduced respectively. Directionality features of images were extracted from the Radon transform of edge images. Regularity features were extracted from the correlation of images. After training images, thresholds for directionality and regularity features were obtained and applied to classify images into directionality and non-directionality, regularity and irregularity respectively. Finally, according to the psychophysical results, the classification tree based on directionality and regularity was built. After classification, images were classified into three classes, which are directional, regular and random textures.

After classification, image retrieval was performed in each specified class by using one of five computational methods. According to the psychophysical results, the category index for image retrieval was built.

Finally, a prototype of a content-based image retrieval system for wallpaper images was developed and diagrammed in Figure 6.12.

Chapter 7 will give the results of classification and the results of image retrieval after classification. A graphical user interface of a retrieval system is presented as well.

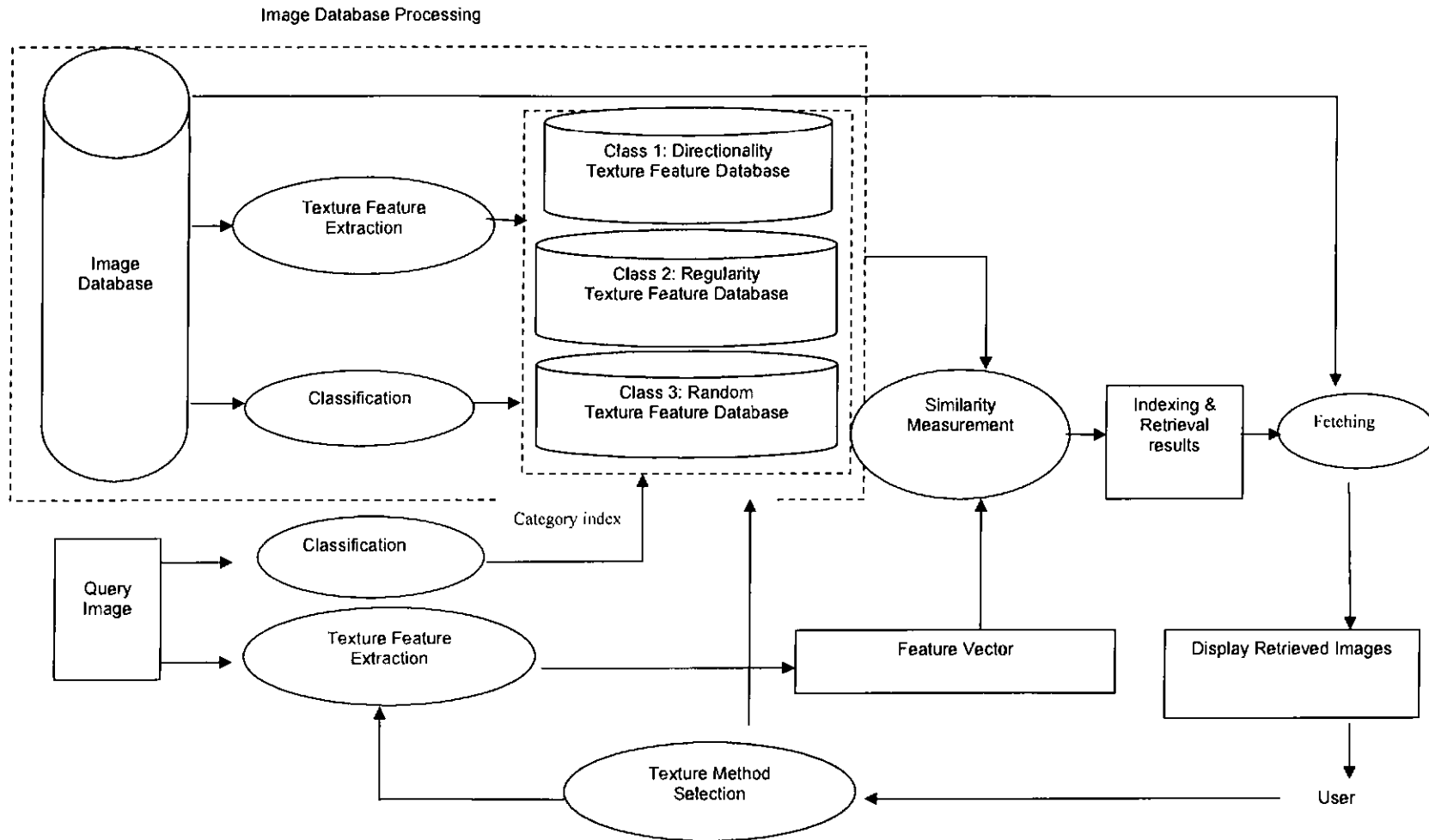


Figure 6.12 Diagram for content-based image retrieval system for wallpaper images

7. Results of Classification and Retrieval

In this chapter, we present the results for classification based on directionality and regularity representatively, and classification results based on both directionality and regularity. Then, image retrieval results after classification by five computational texture methods are shown. A comparison between retrieval results before and after classification is carried out to test the effectiveness of classification. A graphical user interface for image retrieval is presented.

7.1 Results for Classification

In this section, we present the results of the classification. Two image sets are applied. One is ten sample images shown in Figure 4.1, which ranking results based on directionality and regularity has been obtained by psychophysical experiments, seen in Section 5.1.3. The other includes one hundred testing images from MoDA image database, seen in Appendix 13.

The performance of classification is estimated using False Positive (Type I errors), False Negative (Type II errors), True Positive and True Negative values [100-102]. In Table 7.1, classification of a positive data as negative is considered as False Positive and classification of negative data as positive is considered False Negative. True Positive and True Negative are the cases where the positive is classified as positive and negative classified as negative respectively.

Table 7.1 True Positive, False Positive, False Negative and True Negative

	Positive	Negative
Positive	True Positive	False Positive
Negative	False Negative	True Negative

The False Positive Rate, False Negative Rate, Sensitivity, Specificity and Accuracy were applied to evaluate the classification results in this research. Sensitivity and Specificity are the proportions of positive data classified as positive, negative data classified as negative respectively. Accuracy is the global representation of classifier performance. They are defined as the following relation.

$$\text{False Positive Rate} = \text{False Positive} / (\text{False Positive} + \text{True Negative}) \quad (7.1)$$

$$\text{False Negative Rate} = \text{False Negative} / (\text{True Positive} + \text{False Negative}) \quad (7.2)$$

$$\text{Sensitivity} = \text{True Positive} / (\text{True Positive} + \text{False Negative}) \quad (7.3)$$

$$\text{Specificity} = \text{True Negative} / (\text{False Positive} + \text{True Negative}) \quad (7.4)$$

$$\text{Accuracy} = (\text{True Positive} + \text{True Negative}) / (\text{True Positive} + \text{False Positive} + \text{False Negative} + \text{True Negative}) \quad (7.5)$$

In the following sections, we show the results based on directionality and regularity respectively first. Then, the final classification results combining regularity and directionality are presented.

7.1.1 Classification Based on Directionality

Directionality features of images were presented by using the Radon transform of edge images. *DER* was obtained by analyzing the Radon transform of edge images in horizontal and vertical direction. A threshold of *DER* was set to classify images into directionality and non-directionality. According to the preliminary study on training images in Section 6.1.1.2, wallpaper images were classified into directionality and non-directionality by a threshold of $DER = 0.18$. For test images, if the value of $DER > 0.18$, the image was labelled as having the property of directionality, otherwise, non-directionality.

7.1.1.1 Results

The following gives the results of classification based on directionality from two sets of image data, which are ten sample images and one hundred images from MoDA collection respectively.

1) Classification results based on directionality for ten sample images

Figure 7.1 shows the ranking results for ten sample images from directionality to non-directionality by subjects, obtained in Section 5.1.3. Figure 7.2 shows classification results based on directionality for the ten sample images. The classified

directional images are shown in Figure 7.2(a) and the classified non-directional images shown in Figure 7.2(b). *DER* values of each image are shown below the image.

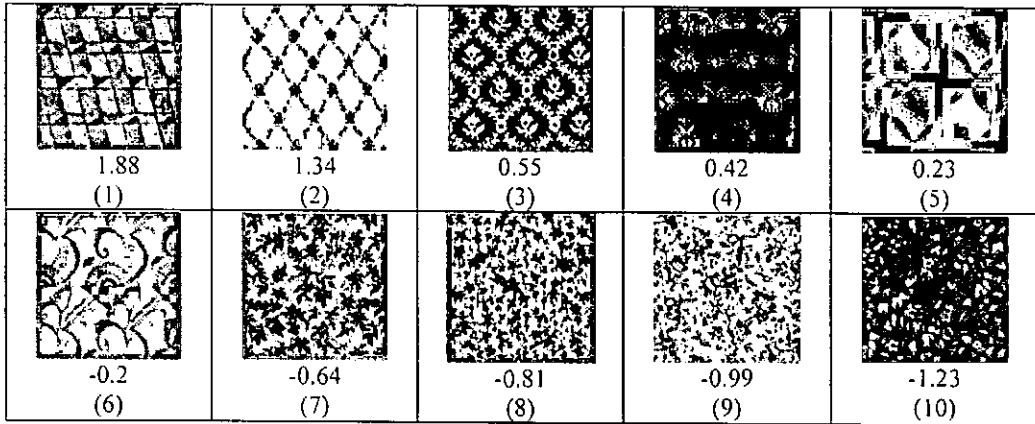
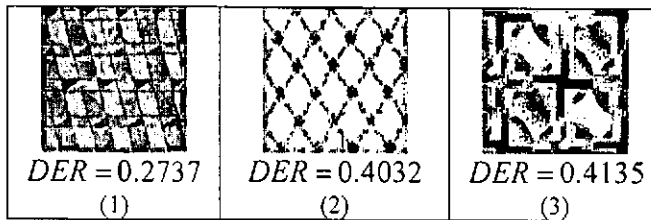
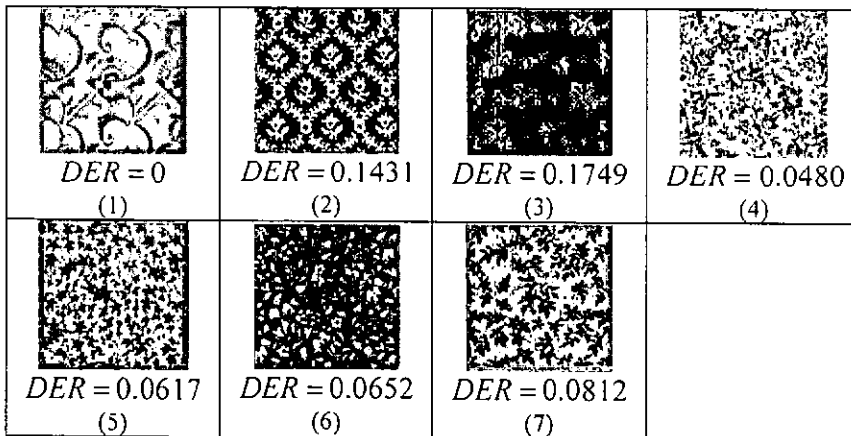


Figure 7.1 Ranking from directionality to non-directionality by subjects



(a) Class 1: Directionality



(b) Class 2: Non-Directionality

Figure 7.2 Classification based on directionality for ten sample images

Compared to the ranking results by subjects, the top two images were classified into the class of directionality by the classification method, and the last four images were classified into the class of non-directionality, which was consistent with the subjects' ranking results

2) *Classification results based on directionality for one hundred test images*

One hundred wallpaper images shown in Appendix 13 were used to test the classification method based on directionality. These images include 33 directional images and 67 non-directional images as categorized by subjects. The False Positive, False Negative, True Positive and True Negative values for 100 test images are shown as in Table 7.2. False Positive and False Negative are the errors where the directional image is classified as non-directionality and non-direction image classified as directionality respectively. True Positive and True Negative are the cases where the directional image is classified as directionality and non-direction image classified as non-directionality respectively.

Table 7.2 Classification results based on directionality for 100 test images

	Directionality	Non-directionality
Directionality	True Positive =28	False Positive =5
Non-directionality	False Negative =5	True Negative =62

The False Positive Rate, False Negative Rate, Sensitivity, Specificity and Accuracy were calculated using Eqs (7.1) to (7.5).

$$\text{False Positive Rate} = 5 / (5+62) = 7.5\%$$

$$\text{False Negative Rate} = 5 / (5+28) = 15.2\%$$

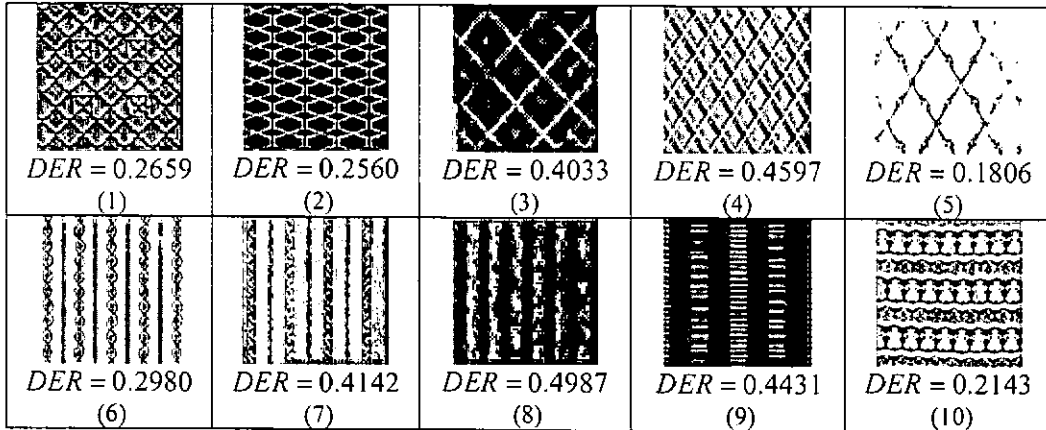
$$\text{Sensitivity} = 28 / (5+28) = 84.8\%$$

$$\text{Specificity} = 62 / (5+62) = 92.5\%$$

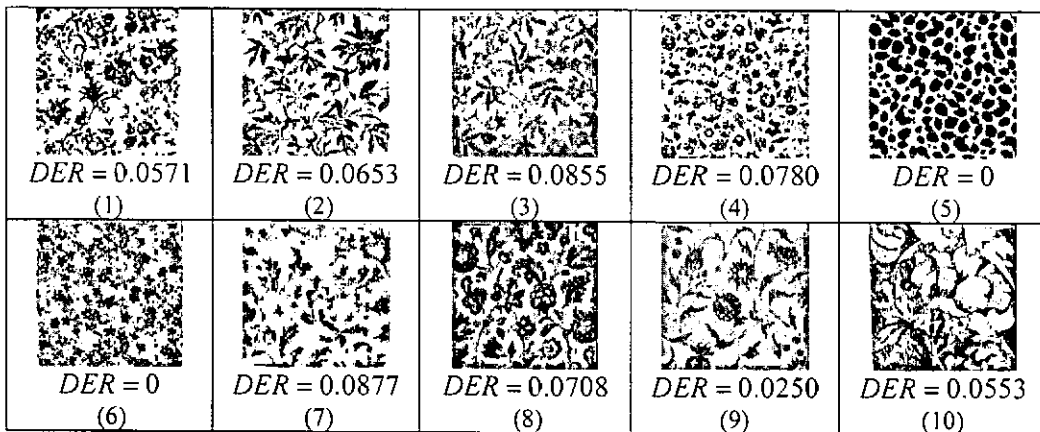
$$\text{Accuracy} = (28+62) / (28+5+5+62) = 90\%$$

The classification results show 7.5% error for classifying directional images as non-directionality and 15.2% for classifying non-directional images as directionality, 84.8% accurate classification for directionality and 92.5% accurate classification for non-directionality. The global classification accuracy is 90%.

Figure 7.3 shows some examples of correctly classified directional textures and non-directional textures. The misclassified textures are shown in Figure 7.4. *DER* values of each images are shown below the figure.

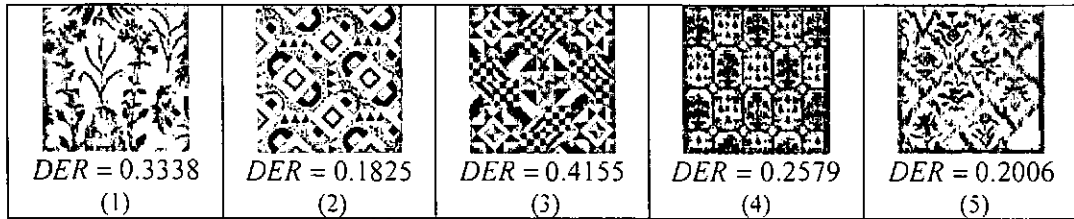


(a) Correctly classified directional textures

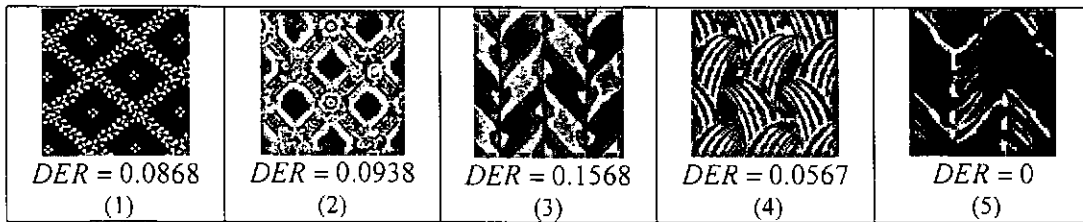


(b) Correctly classified non-directional textures

Figure 7.3 Some correctly classified directional textures and non-directional textures and their directionality representations



(a) Misclassified non-directional textures



(b) Misclassified directional textures

Figure 7.4 Misclassified textures and their directionality representations

7.1.1.2 Analysis

Figure 7.4(a) shows misclassified non-directional textures. For images (2), (3), (4), and (5) in Figure 7.4(a) have repeated geometric structures like rectangle and diamond. Their directional lines were captured by the Radon transform. According to the human visual perception, these images are more like regular images than directional images due to content in the geometric structures. Therefore, these images were classified as non-directional images by subjects instead of directional images. For image (1), the vertical plant branches were captured by the Radon transform. Due to the visual interruption such as leaves and the random distribution of directional elements, these images were classified as random images instead by subjects.

Figure 7.4(b) shows misclassified directional textures. For images (3), (4) and (5) in Figure 7.4(b), they were classified into directional images by subjects due to the existing obvious bi-directional line segments crossing with each other. Therefore, these directionality features were not captured by the Radon transform easily. For images (1) and (2), there are only two directional lines in each direction, not covering whole image region. Therefore, the value of spatial distribution of directional lines

$DER_{position_theta}$ is small. It leads to a small DER . The description of $DER_{position_theta}$ and DER is in Section 6.1.1.1.

Although there are some misclassifications, we still have 90% accuracy for classification based on directionality in the 100 testing images. Some examples of correctly classified images are shown in Figure 7.3. For the 10 sample images, the classified images mostly match the ranking based on directionality by subjects, as seen in Figure 7.2.

From the analysis above we can see that this classification method classified images into directionality and non-directionality effectively. It is more suitable for those directional images that have many directional lines scattered over the whole image region.

7.1.2 Classification Based on Regularity

Regularity features of images were presented by calculating the correlation coefficients of the images. As described in Section 6.1.2, regularity representation REG was extracted from correlation coefficients of an image. A threshold of REG was set to classify images into regularity and irregularity. According to a preliminary study on training images in Section 6.1.2.2, regular and irregular images were classified by a threshold of $REG = 0.23$. For test images, if $REG_h > 0.23$ or $REG_v > 0.23$, the image was labelled as regularity, otherwise, irregularity.

7.1.2.1 Results

The following will give two classification results based on regularity, which again are for ten sample images and one hundred images from the MoDA collection.

1) Classification results based on regularity for ten sample images

Figure 7.5 shows the ranking results by subjects for ten sample images from regularity to irregularity, obtained in Section 5.1. Figure 7.6 shows classification

results based on regularity for the ten sample images. The classified regular images are shown in Figure 7.6(a) and in Figure 7.6(b) for irregular images. The values of REG_h and REG_v for each image are given under the image.

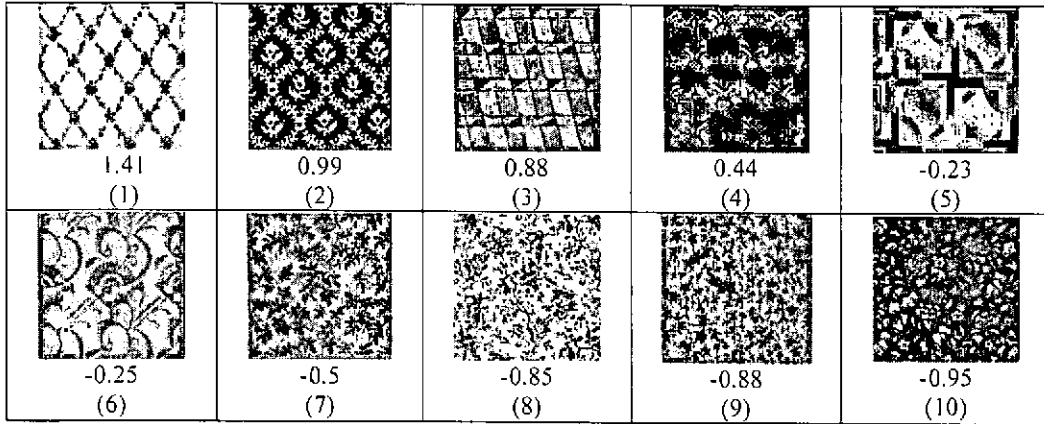
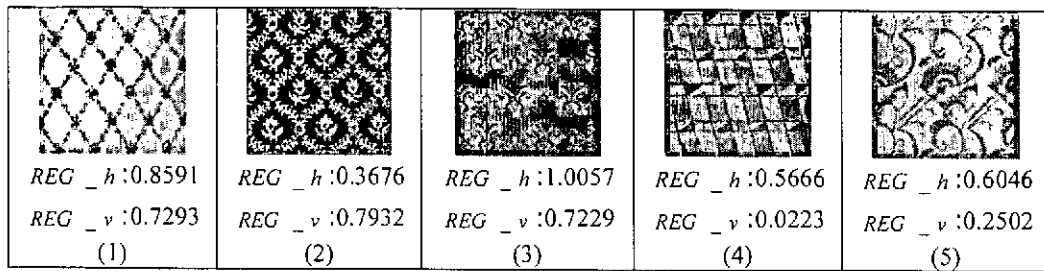
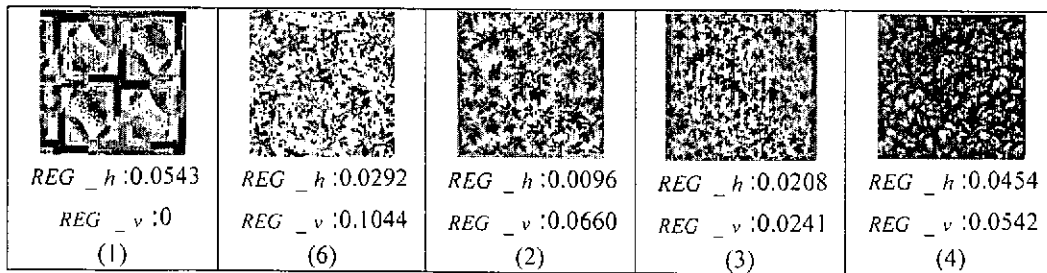


Figure 7.5 Ranking from regularity to irregularity by subjects



(a) class 1: Regularity



(b) Class 2: Irregularity

Figure 7.6 Classification based on regularity for ten samples images

In comparison with the ranking results done by the subjects, the top four images were classified into the class of regularity, and the last four images were classified into the class of irregularity, which was very consistent with human

perception. The image ranked in the 5th position was classified as irregular, because we could not find periodic features by correlation, though it looks regular.

2) *Classification results based on regularity for one hundred test images*

One hundred wallpaper images shown in Appendix 13 were used as test samples, which include 59 regular and 41 irregular images. The False Positive, False Negative, True Positive and True Negative values for 100 test images are shown as in Table 7.3. False Positive and False Negative are the errors where the regular image is classified as irregularity and irregular image classified as regularity respectively. True Positive and True Negative are the cases where the regular image is classified as regularity and irregular image classified as irregularity respectively.

Table 7.3 Classification results based on regularity for 100 test images

	Regularity	Irregularity
Regularity	True Positive =53	False Positive =6
Irregularity	False Negative =6	True Negative =35

The False Positive Rate, False Negative Rate, Sensitivity, Specificity and Accuracy were calculated using Eqs (7.1) to (7.5).

$$\text{False Positive Rate} = 6 / (6+35) = 14.6\%$$

$$\text{False Negative Rate} = 6 / (6+53) = 10.2\%$$

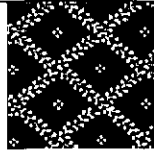
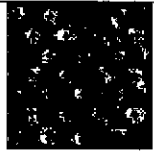
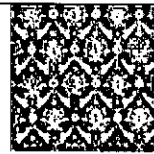
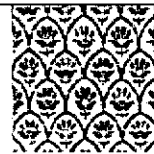
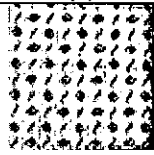
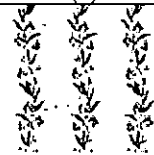
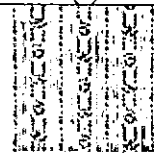
$$\text{Sensitivity} = 53 / (6+53) = 89.8\%$$

$$\text{Specificity} = 35 / (6+35) = 85.4\%$$

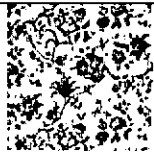
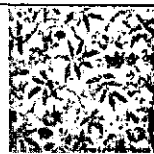
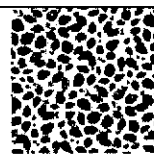
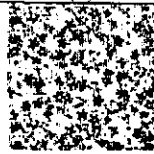
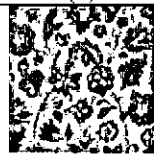
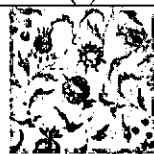
$$\text{Accuracy} = (53+35) / (53+6+6+35) = 88\%$$

The classification results show 14.6% error for classifying regular images as irregularity and 10.2% for classifying irregular images as regularity, 89.8% accurate classification for regularity and 85.4% accurate classification for irregularity. The global classification accuracy is 88%.

Figure 7.7 shows some examples of correctly classified regularity and irregularity. The misclassified textures are shown in Figure 7.8. The values of REG_h and REG_v of each image are shown under each image.

 $REG_h:0.6631$ $REG_v:0.5586$ (1)	 $REG_h:0.8197$ $REG_v:0.5849$ (2)	 $REG_h:0.8436$ $REG_v:0.7266$ (3)	 $REG_h:0.7094$ $REG_v:0.7587$ (4)	 $REG_h:0.6944$ $REG_v:0.6216$ (5)
 $REG_h:0.2780$ $REG_v:0.3604$ (6)	 $REG_h:0.2743$ $REG_v:0.4320$ (7)	 $REG_h:0.3507$ $REG_v:0.3866$ (8)	 $REG_h:0.8468$ $REG_v:0.1623$ (9)	 $REG_h:0.1278$ $REG_v:0.4189$ (10)

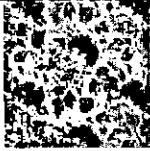
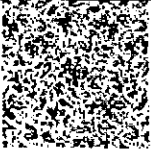
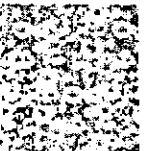
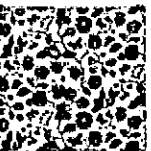
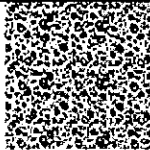
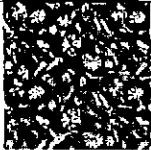
(a) Correctly classified regular textures

 $REG_h:0.0685$ $REG_v:0.0813$ (1)	 $REG_h:0.0710$ $REG_v:0.0481$ (2)	 $REG_h:0.0715$ $REG_v:0.0341$ (3)	 $REG_h:0.0506$ $REG_v:0.0573$ (4)	 $REG_h:0.1629$ $REG_v:0.1119$ (5)
 $REG_h:0.0886$ $REG_v:0$ (6)	 $REG_h:0.0842$ $REG_v:0.1241$ (7)	 $REG_h:0.2156$ $REG_v:0.1213$ (8)	 $REG_h:0.1072$ $REG_v:0.1263$ (9)	 $REG_h:0$ $REG_v:0.1809$ (10)

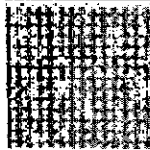
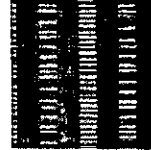
(b) Correctly classified irregular textures

(c)

Figure 7.7 Some correctly classified regular textures and irregular textures and their REG values in horizontal and vertical direction respectively

 $REG_h: 0$ $REG_v: 0.7544$ (1)	 $REG_h: 0.6161$ $REG_v: 0.0830$ (2)	 $REG_h: 0.8011$ $REG_v: 0.0257$ (3)	 $REG_h: 0.1165$ $REG_v: 0.6389$ (4)
 $REG_h: 0.2926$ $REG_v: 0.7433$ (5)	 $REG_h: 0.7069$ $REG_v: 0.4088$ (6)		

(a) Misclassified irregular textures

 $REG_h: 0.1443$ $REG_v: 0.0547$ (1)	 $REG_h: 0.1746$ $REG_v: 0.0623$ (2)	 $REG_h: 0.1766$ $REG_v: 0.1103$ (3)	 $REG_h: 0.1157$ $REG_v: 0.0824$ (4)
 $REG_h: 0.1286$ $REG_v: 0.0468$ (5)	 $REG_h: 0.0543$ $REG_v: 0$ (6)		

(b) Misclassified regular textures

Figure 7.8 Misclassified textures and their *REG* values in horizontal and vertical direction

7.1.2.2 Analysis

Figure 7.8(a) shows misclassified irregular textures. These classification errors are mainly caused by one reason. For all of images in Figure 7.8(a), they really have repeated patterns and their regularity features can be obviously presented by correlation coefficients. But due to the boundary between repeated patterns is not clear, these repeated patterns are not easy to be detected by the subjects. Therefore, these images are normally classified into irregular images by subjects.

Figure 7.8(b) shows misclassified regular textures. These classification errors could be caused by the following reason: for all images in Figure 7.8(b) have repeated patterns according to human visual perception, but when you see them in detail, you could find differences in repeated patterns. Therefore these regular features to human perception could not be captured by correlation. This might be why they were misclassified into irregularity.

Although there are a few misclassifications, there still is 88% accuracy for classification based on regularity in the 100 testing images. For 10 sample images, the classified images mostly match the ranking results perceived by subjects, as seen in Figure 7.6.

From the analysis above, we can see that this classification method can classify images into regularity and irregularity effectively. It is considered more suitable for those regular images with repeated patterns being absolutely repeated in horizontal or vertical direction and repeated patterns having an obvious boundary as well as having at least two repeated cycles.

7.1.3 Classification Based on Directionality and Regularity

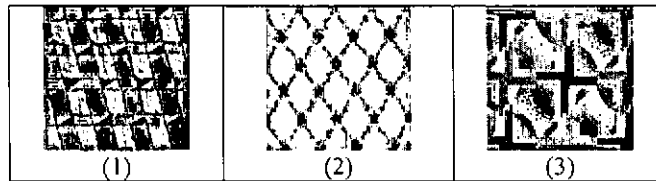
Wallpaper images were classified based on directionality first. The images were classified into directional images and non-directional images. Then, we classified non-directional images based on regularity. Finally, non-directional images were classified into regular images and random texture images. Figure 5.14 gives the flow of classification based on directionality and regularity.

7.1.3.1 Results

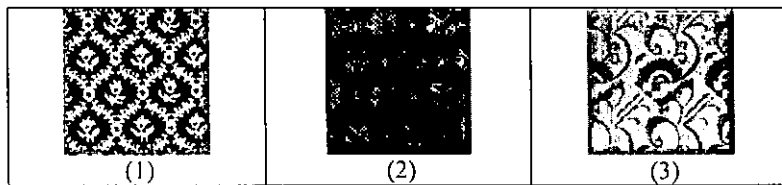
The following sections will give two classification results based on both directionality and regularity, working on sample images with numbers of ten and one hundred respectively.

1) *Classification results based on directionality and regularity for ten sample images*

Figure 7.9 shows the classification results based on directionality and regularity for the ten sample images. The classified directional images are shown in Figure 7.9(a), the classified regular images shown in Figure 7.9(b) and the random texture images shown in Figure 7.9(c).



(a) Class 1: Directional images



(b) Class 2: Regular images



(c) Class 3: Random texture images

Figure 7.9 Classification based on directionality and regularity for ten sample images

2) *Classification results based on directionality and regularity for one hundred test images*

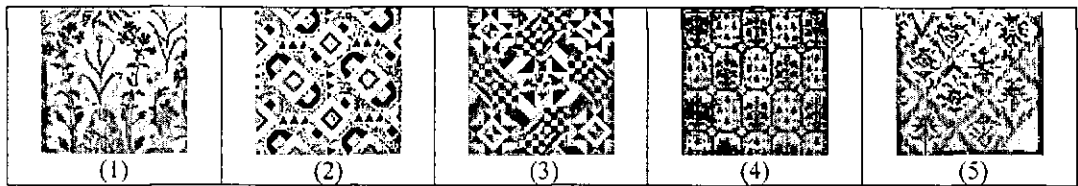
One hundred wallpaper images shown in Appendix 13 were used to test the classification method based on directionality and regularity. We considered directionality first. The images were classified into directional images and non-directional images. Then, we considered regularity in non-directional images. Finally, non-directional images were classified regular images and random texture images.

Therefore, 100 images include 33 directional images and the rest images include 26 regular images and 41 random texture images. The False Positive, False Negative, True Positive and True Negative values for each class were obtained against all other classes, detailed in Section 7.1. The False Positive Rate, False Negative Rate, Sensitivity, Specificity and Accuracy for three classes were calculated using Eqs (7.1) to (7.5) respectively, as shown in Table 7.4.

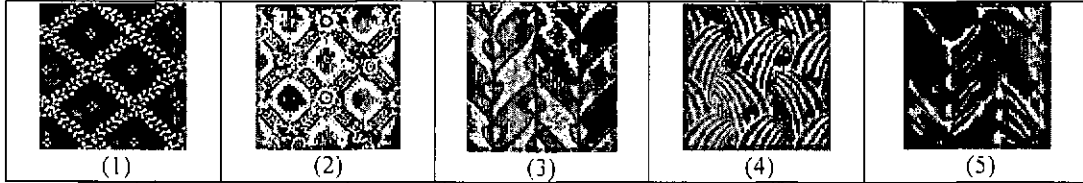
Table 7.4 Classification results based on directionality and regularity for 100 images

Classes	False Positive Rate	False Negative Rate	Sensitivity	Specificity	Accuracy
Directionality	7.5%	15.2%	84.8%	92.5%	90%
Regularity	8.1%	23.1%	76.9%	91.9%	88%
Random	11.9%	17.1%	82.9%	88.1%	86%

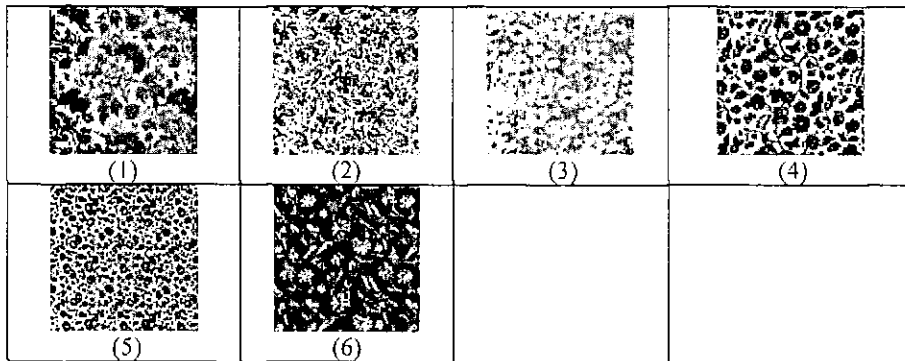
The following figure gives some samples of misclassification.



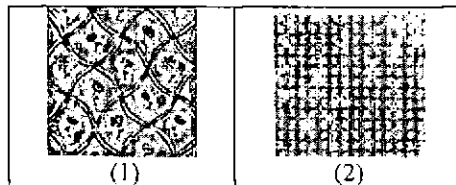
(a) Misclassified non-directional textures into directional textures



(b) Misclassified directional textures into non-directional textures



(c) Misclassified random textures into regular textures



(d) Misclassified regular textures into random textures

Figure 7.10 Misclassified textures

7.1.3.2 Analysis

In Figure 7.10(b), the directional textures misclassified into non-directional textures were classified to regularity. In Figure 7.8(b), misclassified images (1), (4), (5) and (6) were classified into directional textures first. Therefore, the regular textures misclassified into random texture have only two images left, shown in Figure 7.10(d). As seen in Figure 7.10, there were six images (4 in directionality group and 2 in random group) that were misclassified into directionality or random from the regular textures, and seven images (1 in directionality group and 6 in regularity group) misclassified into directionality or regularity from the random textures. The reason for misclassification was explained in Section 7.1.1.2 and 7.1.2.2. Therefore, there are 90% accuracy for the class of directionality, 88% for the class of regularity, and 86% for the class of random textures.

After classification, the image retrieval was performed in specified class by calculating similarity between feature vectors of a query image and the images in the specified class. The retrieval results will be presented in Section 7.2.

7.2 Results for Image Retrieval after Classification

In this section, we present the retrieval results after classification by using five computational methods. Two sets of test samples were applied to evaluate the retrieval results by using five computational texture methods after classification. One test set consists of seven queries in ten sample images. The ranking results in terms of similarity to the query image perceived by subjects were obtained in Section 5.2.3. The other test set contains nine queries in a set of 100 images from the MoDA image collections. For each query, similar images ranked by subjects were obtained, given in Appendix 15. These ranking results were applied to evaluate the retrieval results performed by each of the five computational texture methods respectively. In order to test the effectiveness of image retrieval after classification, the comparison between retrieval results before and after classification is presented as follows.

7.2.1 Results

Two retrieval results are given in this section for the data sets of seven queries in ten sample images and of nine queries in one hundred images.

1) Retrieval results for seven queries in ten sample images

The ranking results of the corresponding computational method for seven queries are given in Appendix 12, Tables A12.1 to A12.7 respectively. In Tables A12.1-A12.7, the first row is the ranking done by the subjects and is obtained in Section 5.2.3. The other rows are retrieval results after classification calculated by five computational methods respectively. The numbers from columns 2 to 10 in Tables A12.1-A12.7 are the label of ranking images in the order from most similar to less similar to query images. The last column is the coefficients of rank correlation between computation methods and subjects.

Finally, the rank correlation between five computational methods and subjects for seven queries are listed in Table 7.5. The average of the rank correlation for seven queries were calculated and shown in the last row of the table. These average values of rank correlation \bar{r}_s were employed to evaluate the retrieval results by five computational methods after classification.

Table 7.5 Coefficients of rank correlation between subjects and computational methods for image retrieval after classification

r_s	GLCM	MRSAR	FT	WT	GT
Query 1	0.78	0.72	0.78	0.72	0.72
Query 2	0.95	0.85	0.93	0.90	0.90
Query 3	0.98	0.95	0.95	0.98	0.95
Query 5	0.73	0.82	0.82	0.72	0.73
Query 8	1.00	0.93	0.98	0.98	0.97
Query 9	0.98	0.93	0.95	0.98	0.97
Query 10	0.83	0.88	1.00	0.83	0.88
Average r_s	0.89	0.87	0.91	0.87	0.87

In order to evaluate the performance of image retrieval after classification effectively, the comparison between retrieval results before classification and after classification are presented in Table 7.6. In Table 7.6, the second column is the average of rank correlation \bar{r}_s of retrieval results before classification, which is

obtained in Section 5.3.2. The average of rank correlation \bar{r}_s of retrieval results after classification are given in the third column. The improvement by comparing \bar{r}_s after classification with \bar{r}_s before classification are calculated and given in the last column. The average values for five computational texture methods are shown in last row.

Table 7.6 Comparison of retrieval results before and after classification by using five computational texture methods

Computational texture methods	\bar{r}_s before classification	\bar{r}_s after classification	Improved
<i>GLCM</i>	0.15	0.89	0.74
<i>MRSAR</i>	0.36	0.87	0.51
<i>FT</i>	0.35	0.91	0.56
<i>WT</i>	0.13	0.87	0.74
<i>GT</i>	0.17	0.87	0.70
Average	0.23	0.88	0.65

2) *Retrieval results for the dataset with nine queries in one hundred images*

In order to evaluate CBIR efficiently, the second test was carried out using nine queries in one hundred sample images as presented in Appendix 13. The nine queries images were selected from MoDA collections, which include three directional images as shown in Figure 7.11 (images (3),(4) and (9)), three regularity images as shown in Figure 7.11 (images (1),(6) and (8)), and three random texture images as shown in Figure 7.11(images (2), (5) and (7)).

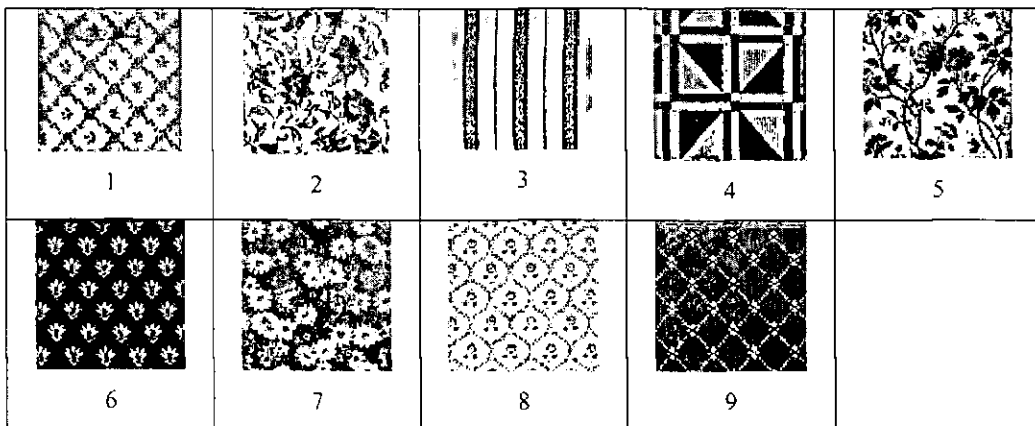


Figure 7.11 Nine query images selected from MnDA collections

Thirteen volunteer observers were asked to get top nine ranking from one hundred testing images based on visual similarity to each query image. The rankings

are listed in Appendix 14. In Tables A14.1-A14.9, the entry T_{nm} of table expresses the ID number of images in 100 image database ranked in the m^{th} position by the n^{th} subject, where the subscription n, m of T_{nm} represents the number of row and column respectively.

Due to the ranking results obtained top ten ranking results from one hundred images, while the choice score method as described in Section 3.2.1 is only suitable to analyze ranking results for all sample images, i.e. obtaining ten ranking images from ten samples, therefore the choice score method is not suitable for obtaining final retrieval results in this experiment. A statistics method of accumulated histogram was applied to obtain the final ranking results by subjects, which is to comprehensively consider the frequency of each image i ranking in top M by N subjects and the ranking position for each image. The formula is expressed as follows.

$$AH_i = \sum_{r=1}^M Hist_r \quad (7.6)$$

where $Hist_r$ is the frequency of each image ranking in top r by N subjects. In this experiment, M was set to 10 suggesting to get top 10 ranking results and N represents 13 subjects. The final top ten ranking results for each query were obtained in the decreased order of AH_i values, as showed in Appendix 15. In Tables A15.1-A15.9, images are displayed in order of visual similarity from most similar to least similar to each query image. The number above the image is the ID number of the image in the 100 image dataset, and the corresponding accumulated histogram is showed below each image.

These retrieval results for nine queries in one hundred wallpaper images by subjects were used to evaluate retrieval results in CBIR system for wallpaper images.

Traditional evaluation methods for image retrieval, which are precision-recall and mean average precision [103], were applied to evaluate the retrieval results after classification by five computational methods. The following contents give the

definition of precision, recall and mean average precision, and the corresponding results for nine queries done by five computational methods respectively.

With respect to a given query, the images can be partitioned into four sets, in terms of relevant or not, retrieved or not, shown as in Table 7.7.

Table 7.7 Four sets for retrieving images

	Relevant	Irrelevant
Retrieved	A	B
Not Retrieved	C	D

Precision is defined as a fraction of retrieved images that are relevant to the user's information needed, and formulated as

$$Precision = \frac{A}{A \cup B} \quad (7.7)$$

Recall is defined as a fraction of relevant images retrieved, and expressed as

$$Recall = \frac{A}{A \cup C} \quad (7.8)$$

Precision-recall graphs are applied to show the retrieval performance at each point in the ranking. The horizontal axis expresses recall and vertical axis expresses the corresponding precision at standard recall points 10%, 20%, ..., 100%.

Average Precision (AP) is applied to measure the effectiveness of a ranked list for a single query, and defined as

$$Average\ Precision\ (AP) = \frac{1}{N_r} \sum_{i=1}^{N_r} P_i \quad (7.9)$$

where N_r is the total number of relevant images in a dataset, P_i is the precision when retrieve the i^{th} relevant image.

After all queries are done, the mean of all average precisions (MAP) is calculated. Mean Average Precision (MAP) is the overall performance measured and defined as

$$\text{Mean Average Precision (MAP)} = \frac{1}{M} \sum_{i=1}^M AP_i \quad (7.10)$$

where M is the total number of the queries, and AP_i is the average precision for the i^{th} query.

In this study, we obtained the ranking results of top ten for nine queries ranked by subjects, as shown in Appendix 15. The ranked images for each query were assumed to be relevant to the corresponding query in the sample size of 100 image database. Based on this information, the following contents will give the results of precision-recall graphs, Average Precision (AP) and Mean Average Precision (MAP) for the retrieval results after classification and before classification together with the comparison results before and after classification.

- **Retrieval results after classification**

The precision-recall graphs for nine queries after classification are shown in Figures A16.1 (b) – A16.9 (b) of Appendix 16 respectively. The curve with (-*-) expresses precision-recall by using the method of *GLCM*, (-o-) for *MRSAR*, (-x-) for *FT*, (-□-) for *WT*, and (-◇-) for *GT*. The Average Precision (AP) of each query were calculated by using Eq.(7.9) and shown in Figure 7.12. In Figure 7.12, the horizontal axis expresses the number of nine queries and vertical axis expresses their corresponding average precision.

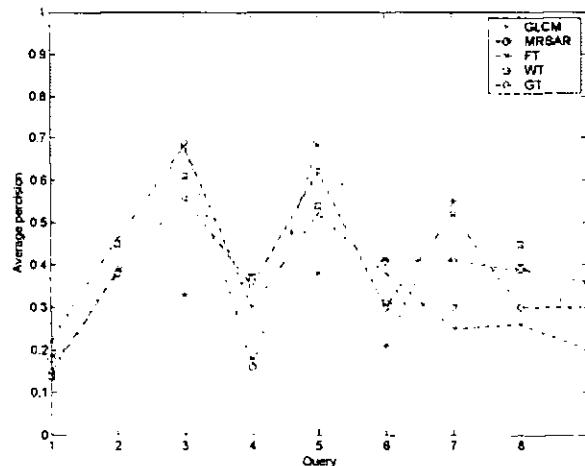


Figure 7.12 Average precision for nine queries after classification

The average precision for nine queries are listed in Table 7.8, Mean Average Precisions (MAP) was calculated by using Eq.(7.10) and shown in the last row in Table 7.8.

Table 7.8 Average precision and mean average precision for nine queries after classification

Average Precision (AP)	GLCM	MRSAR	FT	WT	GT
Query 1	0.13	0.18	0.22	0.14	0.15
Query 2	0.39	0.38	0.46	0.45	0.38
Query 3	0.33	0.69	0.68	0.61	0.56
Query 4	0.18	0.16	0.30	0.37	0.35
Query5	0.38	0.69	0.52	0.54	0.62
Query 6	0.21	0.41	0.38	0.31	0.30
Query 7	0.55	0.41	0.25	0.30	0.52
Query 8	0.40	0.39	0.26	0.45	0.30
Query 9	0.26	0.36	0.20	0.23	0.30
Mean Average Precision(MAP)	0.31	0.41	0.36	0.38	0.39

- *Retrieval results before classification*

Similarly, the precision-recall graphs for nine queries before classification are shown in Figures A16.1 (a) – A16.9 (a) of Appendix 16 respectively. The Average Precision (AP) of each query were calculated by using Eq.(7.9) and shown in Figure 7.13. After obtaining the average precision for nine queries, the Mean Average Precisions (MAP) was calculated by using Eq.(7.10) and shown in the last row in Table 7.9.

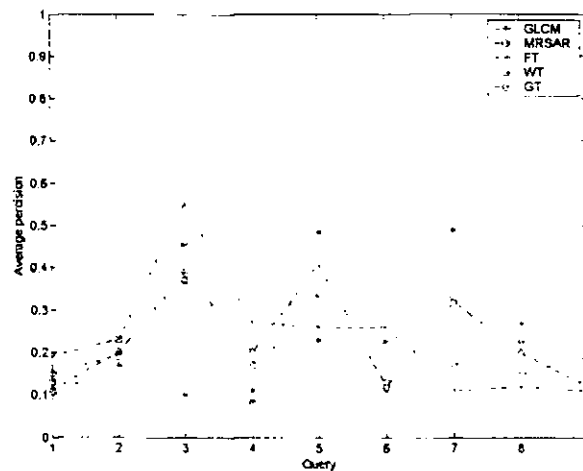


Figure 7.13 Average precision for nine queries before classification

Table 7.9 Average precision and mean average precision for nine queries before classification

Average Precision (AP)	<i>GLCM</i>	<i>MRSAR</i>	<i>FT</i>	<i>WT</i>	<i>GT</i>
Query 1	0.10	0.15	0.19	0.13	0.11
Query 2	0.17	0.19	0.23	0.23	0.20
Query 3	0.10	0.46	0.55	0.37	0.39
Query 4	0.11	0.08	0.27	0.17	0.20
Query 5	0.23	0.49	0.26	0.34	0.41
Query 6	0.11	0.22	0.26	0.13	0.12
Query 7	0.49	0.33	0.11	0.17	0.32
Query 8	0.27	0.15	0.12	0.23	0.20
Query 9	0.17	0.19	0.11	0.13	0.12
Mean Average Precision(MAP)	0.19	0.25	0.23	0.21	0.23

- **Comparison retrieval results before and after classification**

In order to further evaluate the effectiveness of image retrieval after classification, the comparison between retrieval results before and after classification is fulfilled in Table 7.10. In Table 7.10, the second column is the Mean Average Precision (MAP) of retrieval results before classification, whilst the Mean Average Precision (MAP) of retrieval results after classification are shown in the third column. The last column shows the improvement by comparing MAP after with before classification. The average values for five computational texture methods are shown in the last row.

Table 7.10 Comparison retrieval results before and after classification by using five computational texture methods for nine queries in dataset of one hundred images

Computational texture methods	MAP before classification	MAP after classification	Improved
<i>GLCM</i>	0.19	0.31	0.12
<i>MRSAR</i>	0.25	0.41	0.16
<i>FT</i>	0.23	0.36	0.13
<i>WT</i>	0.21	0.38	0.17
<i>GT</i>	0.23	0.39	0.16
Average	0.22	0.37	0.15

The following figures show two examples. One is comparison retrieval results before and after classification by using *GLCM* for query 3, shown in Figure 7.14. The other is comparison retrieval results before and after classification by *WT* for query 7, shown in Figure 7.15. Figures 7.14(a) and 7.15 (a) are the ranking results done by subjects, whilst Figures 7.14(b) and 7.15 (b) are the retrieval results before

classification. Figures 7.14(c) and 7.15 (c) show the retrieval results after classification.

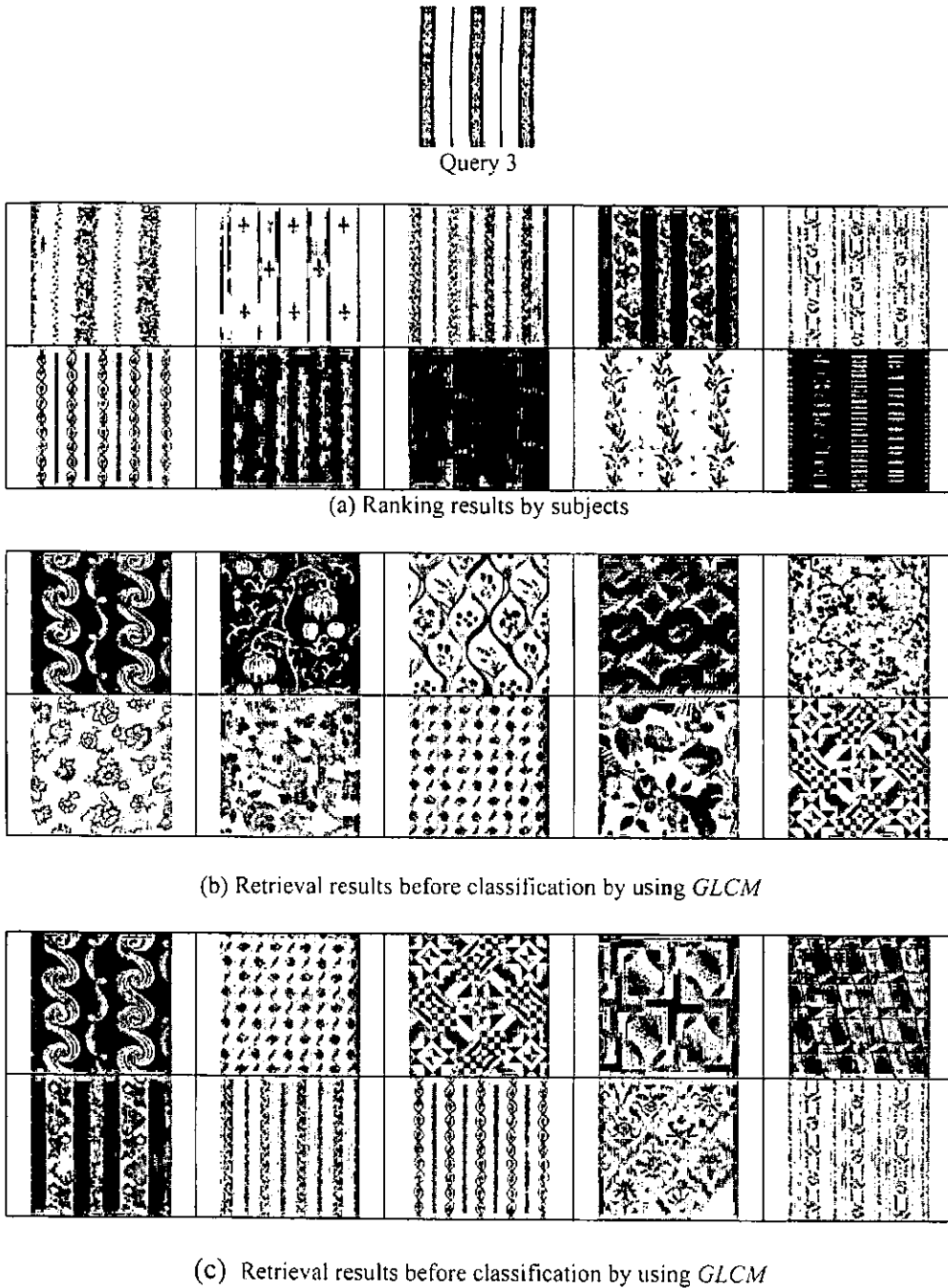
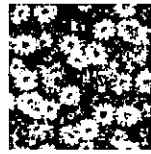
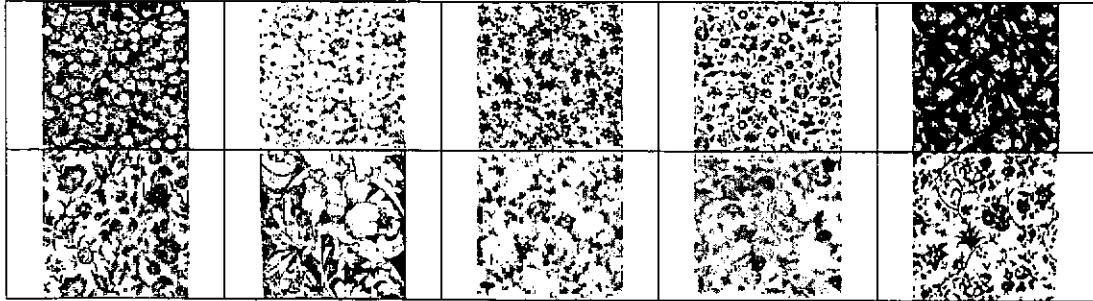


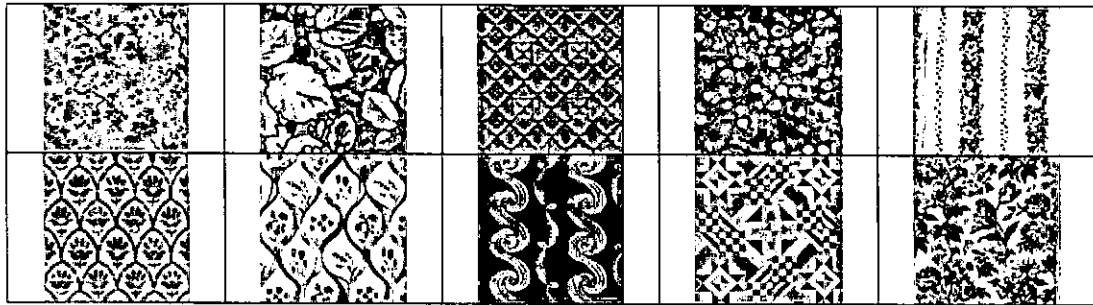
Figure 7.14 Comparison retrieval results before and after classification by GLCM for query 3



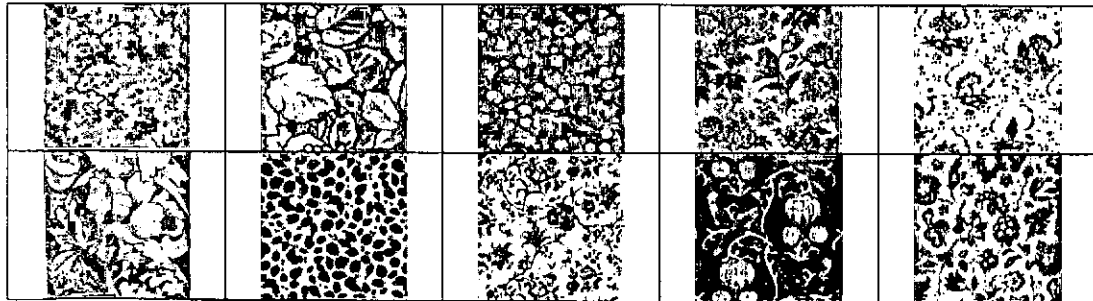
Query 7



(a) Ranking results by subjects



(b) Retrieval results before classification using WT



(c) Retrieval results after classification by using WT

Figure 7.15 Comparison retrieval results before and after classification by WT for query 7

- *Query time*

Table.7.11 shows the average query time for nine queries in one hundred images using five texture methods respectively. All methods run in Matlab 6.5 with CPU of Inter Pentium M 1.4GHz and 1GB RAM. The second column is the average

query time for five methods before classification, whilst the average query time after classification is shown in the third column.

Table 7.11 Query time

Computational texture methods	Time for retrieval before classification (Seconds)	Time for retrieval after classification (Seconds)
<i>GLCM</i>	4.3	3.5
<i>MRSAR</i>	22.1	21.4
<i>FT</i>	2.8	2.1
<i>WT</i>	2.3	1.8
<i>GT</i>	26.8	26.0

7.2.1 Analysis

Based on the retrieval results shown above, the analysis and evaluation in terms of visual similarity by subjects form two parts. One is to evaluate the performance of image retrieval after and before classification; second is to investigate the goodness of five computational texture methods in performing image retrieval after classification.

- *Image retrieval after classification*

Considering the seven queries in the dataset of ten sample images, the average rank correlation with subjects' ranking results for all five methods is 0.88, as seen in Table 7.6, whilst the retrieved results before classification is only 0.23, demonstrating a big improvement when comparing with the retrieved results before classification.

For the image dataset with nine queries and one hundred samples, the average of Mean Average Precision (MAP) for all five methods is 0.37, as shown in Table 7.10. Since the retrieval results before classification is 0.22, 0.15 improvement was achieved. According to the visual evaluation, the retrieval results after classification have better match than before classification, as illustrated for the two examples shown in Figure 7.14 and Figure 7.15. The reason could be that the retrieved images ranked in front belong to the same class as the query, therefore the visual match of images retrieved after classification are better than that before classification, even if the average MAP for retrieval after classification only has 0.37.

According to the Table 7.11, the average query time after classification is quicker than before classification. Since similarity measurement was performed in the corresponding class group instead of whole image dataset. The methods of *MRSAR* and *GT* take long time (over 20s) to extract the features of query image.

- *Evaluation of five computational texture methods*

According to average r_s and MAP for all queries in Tables 7.5 and 7.8, it is difficult to conclude which computational method is better, due to the fact that the values for each method are similar. Based on the values of r_s and AP for individual query, it is also hard to decide which method is suitable for what type of query image. This is because that these five texture methods can not represent texture features (directionality, regularity and coarseness) for wallpaper images well, as proved in Section 5.3.1. Therefore, all methods can not perform image retrieval ideally in the way human perception performs.

We can conclude that retrieval for wallpaper images after classification has better performance than retrieval before classification. By using five texture methods, we couldn't get ideal retrieval results after classification though some improvement had been seen than before classification. Therefore, a new way to represent texture features for wallpaper images is required in the future.

7.3 A GUI for Wallpaper Images

The following interface was developed to perform Content-Based Image Retrieval (CBIR) for wallpaper images using MATLAB [36].



Figure 7.16 Interface of content-based image retrieval for wallpaper images

The system is running according to the following steps.

- **Query Creation**

An image is selected to be a query from the list of images shown in the left area. This list is obtained from the MoDA collection. The query image is shown in the upper middle area. In the future, a query image can also be created by scanning or a sketch.

- **Classification results**

When the “Classification” button is pressed, the class of the query image is shown in right of ‘Classification Result’. All the images belonging to the same class as the query image are shown in the upper right area. When the button “Prev 5” or “Next 5” is pressed, these images will be shown on the screen in a group of 5 images each time. When the ‘Output’ button is clicked, the classification results will be saved into a file in terms of image names.

- *Retrieval results*

When the computational texture method from 'Retrieval Method' in the bottom middle area is selected, the corresponding results is shown at the bottom right area retrieved using this method. Again, when the button "Prev 5" or "Next 5" is clicked, the previous or next 5 similar images are shown. All the similar image numbers will be saved into a file once the "Output" button is clicked.

Using the interface shown in Figure 7.16, users can get the image retrieval results calculated using each of five texture models and the classification results of a query image, whereby the images from the same class from a database are also shown on the screen for users to browse.

7.4 Summary

In this chapter, we presented the results of image classification and image retrieval. The results of psychophysical experiments obtained in Chapter 5 served as benchmarks for evaluation of each methodology.

In order to evaluate the classification methods for directionality and regularity, we examined classification based on directionality and regularity respectively in a dataset with one hundred samples of wallpaper images, as seen in Table 7.2 and 7.3. The classification results combining both features are shown in Table 7.4. On the other hand, for the dataset with ten sample images, their rank results based on directionality and regularity perceived by subjects were obtained from psychophysical experiments. In principle, the classification results for this dataset match the ranking results ordered by subjects.

For image retrieval, we presented the retrieval results by using five computational texture methods for the two datasets, i.e., seven queries with ten sample images and nine queries with one hundred images. According to the data analysis and visual effect, we concluded that image retrieval for wallpapers after classification performed better than before classification. As for the five texture methods, they did not retrieve images matching human perception, even after

classification, although an improvement was achieved with the classification. It was therefore concluded that a new texture representation model for wallpaper images needs to be developed in the future in order to match the retrieval results similar to human perception.

8. Conclusions and Future Work

This Chapter will draw together conclusions from my research. The contributions to knowledge are presented and the possible directions for future work are also discussed.

8.1 Conclusions

The aims of this research were two fold. One aim was to investigate human perception in conducting image retrieval, and another was to evaluate the performance of five existing texture models in performing Content-Based Image Retrieval (CBIR) in comparison with human perception. These five models have been widely applied in retrieving texture feature of images. MoDA wallpaper images were employed in the research, of which most of images can be categorised as having texture-like patterns. Therefore, texture structure is the main content to be studied in this research, leading to the development of a perception-driven CBIR system for MoDA collections.

Two psychophysical experiments were designed and conducted. The first one was to study a human's response in perceiving each individual component of a texture feature, i.e., coarseness, regularity and directionality. The second experiment was to investigate the way in which a subject sees similarity of two images in terms of texture patterns. A statistic method for scoring was introduced to rank subjects' data when ranking images in terms of coarseness, regularity and directionality respectively, and when ordering images in terms of similarity to the query image. The results showed that visual components of regularity and directionality played a more important role in perceiving similar images than coarseness, with rank correlation being 0.75, 0.81, and 0.64 respectively. Since 0.75 is the threshold of significance, regularity and directionality are the main texture features to be studied in the remaining work.

Five computational models of texture representations were studied based on the two psychophysical experiments conducted above. They are Grey Level Co-occurrence Matrix (GLCM), Multi-Resolution Simultaneous Auto-Regressive

(MRSAR) model, Fourier Transform (FT), Wavelet Transform (WT) and Gabor Transform (GT). Texture feature vectors are computed using these five models and are compared with subjects' data. It was found that none of these models was consistent with the subjects' data, with mean coefficients of rank correlation being 0.15, 0.36, 0.35, 0.13 and 0.17 for GLCM, MRSAR, FT, WT, and GT respectively. It was therefore decided to introduce classification before applying any of these models in performing CBIR for MoDA images.

According to the results of psychophysical experiments, users focused on directionality and regularity when perceiving a texture rather than coarseness. Classification was then carried out on directionality first (Class 1). Then, the remaining non-directional data were further classified into groups of with regular (Class 2) and random texture patterns (Class 3). Image retrieval was conducted in the classified group where a query image falls into. In comparison with the subjects' data, the accuracy for classifying directionality, regularity, and random textures were 90%, 88% and 86% respectively. After classification, the retrieval performance of the five models in terms of Mean Average Precision (MAP) were 0.31, 0.41, 0.36, 0.38 and 0.39 for GLCM, MRSAR, FT, WT, and GT respectively, whereas MAP are 0.19, 0.25, 0.23, 0.21, and 0.23 respectively before the classification, implying some degrees of improvement. Although the improvement is not huge, every model's performance was improved. It is therefore concluded that classification is necessary when using any of these five models to take part in CBIR for the MoDA collection. In order to match human perception, new models are needed to represent texture features.

8.2 Contributions

This dissertation presents the approach of human perception oriented Content-Based Image Retrieval (CBIR) for wallpaper images. This research contributes to knowledge in the following ways:

- *To CBIR*
 - Paving some way for future application of CBIR based on human visual perception. Via the psychophysical experiments, we can study human visual perception for images. The experimental results can be applied to evaluate the computational method of visual features and choose the better visual feature representations for image collection. Through analyzing the experimental results, we can learn which visual features perform the more important role in visual similarity to help us weight the visual features to match the human visual perception.
 - Evaluating the performances of five popular computational methods in texture representations and similarity measurements in relation to human perception for wallpaper images. Though the limited parameters were selected in each method, we provided the evaluation method based on human perception via comparing the rank correlation between computational methods and human perception.
 - Improving the retrieval performance for wallpaper images based on human visual perception, as seen in Table 7.10.
- *To classification*
 - Applying Radon transform to represent the feature of directionality to classify images. Radon transform presents not only the statistical distribution but also spatial distribution of directional lines. This overcomes the drawbacks of traditional statistical descriptions of directionality and better represents the directionality for wallpaper images, as seen in Section 6.1.1.
 - Defining a regularity representation from correlation sequence to classify images based on regularity in Eq. (6.11). Through considering the magnitudes (in Eq. (6.9)) and positions (in Eq. (6.10)) of the peaks in correlation sequence, we can easily distinguish the regularity with periodic peaks and irregularity with flat curve.

- Designing classification trees based on human visual perception in Figure 6.11. The directionality character is first take into account for classification, since this plays a slightly more important role in visual similarity for wallpaper images than regularity, as proved in Table 5.3 and Section 6.1.3.
- *To MoDA images*
 - Providing a CBIR system to enhance their current text-based image retrieval system and classifying the image database based on directionality and regularity automatically.
 - Better understanding of relationship between visual texture features and visual similarity for wallpaper collections, that is the directionality and regularity play a more important role than coarseness in visual similarity. Comparing to regularity, the directionality is slight important, as proved in Table 5.3.

8.3 Future Work

In this study, all the findings obtained from psychophysical experiments were based on a limited dataset, i.e., ten and one-hundred sample images for testing visual feature perception and visual similarity, which is in the consideration that subjects might get tired if more images are included. In the future, tests should replicate this study with large sample sizes to confirm, verify or contradict the findings. When doing similarity experiments, for some queries, only a few subjects (25%) had similar views, whilst the majority of subjects ranked images in different ways. These queries were removed in order to make the experimental results reflect the common sense of human perception. Further experiments are needed using similar query images. A larger subject team is also needed to do those experiments.

Although in general, none of those five models shows consistent retrieval results with that by subjects. Some models do perform better for some individual components of texture feature than the others. Future work should include

combinations of some or all of these to form a better representation of texture consistent with human perception.

In this dissertation the scope of the study is limited to texture feature analysis for wallpaper images. Colour is the other important feature to represent the wallpaper images. In the future, the original colour images should be utilised and a colour representation should be formulated simulating human colour perception. Finally, based on human visual perception, a CBIR system combining colour and texture features should be developed.

In this research, we focused on CBIR for wallpaper images. In the future, the method of CBIR based on human visual perception could be extended to the retrieval of other types of images.

References

1. B.E. Prasad, A. Gupta, H.D. Toong, and S.E. Madnick, "*A Microcomputer-Based Image Database Management System*". IEEE Transactions on Industrial Electronics, 1987. **34**(1): p. 83-88.
2. A.W.M. Smeulders, M. Worring, S. Santini, A. Gupta, and R. Jain, "*Content-Based Image Retrieval at the End of the Early Years*". IEEE Transactions on Pattern Analysis and Machine Intelligence, 2000. **22**(12): p. 1349-1380.
3. Y. Rui, T.S. Huang, and S.F. Chang, "*Image Retrieval: Current Technique, Promising Directions, and Open Issues*". Journal of Visual Communication and Image Representation, 1999. **10**: p. 39-62.
4. A. Halawani, A. Teynor, L. Setia, G. Brunner, and H. Burkhardt, "*Fundamentals and Applications of Image Retrieval: An Overview*". Datenbank-Spektrum, 2006. **18**: p. 14-23.
5. J.R. Ohm, F. Bunjamin, W. Liebsch, B. Makai, K. Müller, A. Smolic, and D. Zier, "*A Set of Visual Feature Descriptors and their Combination in a low-level Description Scheme*". Proceeding Signal Processing Image Communications, EURASIP, 2000: p. 157-179.
6. S.J. Sangwine and R.E. Horne, "*The Colour Image Processing Handbook*". 1998: Chapman & Hall.
7. W. Niblack, R. Barber, W. Equitz, E. Glasman, D. Petkovic, P. Yanker, C. Faloutsos, and G. Taubin, "*The QBIC project: Querying Image by Content Using Colour, Texture and Shape*". Proceeding of Storage and Retrieval for Image and Video Databases, 1987. **1908**: p. 173-178.
8. C. Carson, S. Belongie, H. Greenspan, and J. Malik, "*Region-based Image Querying*". Proceeding of IEEE workshop on Content Based Access of Image and Video Libraries, 1997: p. 42-49.
9. Y. Rui, T.S. Huang, and S. Mehrotra, "*Content-based Image Retrieval with Relevance Feedback in MARS*". Proceeding of IEEE International Conference on Image Prococessing, 1997. **2**: p. 815-818.

10. D.M. Squire, W. Müller, and H. Müller, "*Relevance Feedback and Term Weighting Schemes for Content-based Image Retrieval*". Proceeding of International Conference On Visual Information Systems, 1999.p. 549--556.
11. J.R. Smith and S.F. Chang, "*Visualseek: A Fully Automated Content-based Image Query System*". Proceeding of ACM Multimedia, 1996: p. 87-98.
12. Q. Iqbal and J.K. Aggarwal, "*CIRES: A System for Content-based Retrieval in Digital Image Libraries*". International Conference on Control, Automation, Robotics and Vision, 2002. 1(1): p. 205-210.
13. O. Verevka and J.W. Buchanan, "*Local K-means Algorithm for Color Image Quantization*". Proceeding of Graphics Interface, 1995: p. 128-135.
14. S. Albayrak, "*A Comparison of 1D and 2D Self-organizing Feature Map Algorithm on Color Image Quantization*". Proceedings of International Conference on Neural Information Processing, 2002: p. 1291-1294.
15. M.J. Swain and D.H. Ballard, "*Colour Indexing*". Journal of Computer Vision, 1991. 7(1): p. 11-32.
16. R.O. Stehling, M.A. Nascimento, and A.X. Falcao, "*Technique for Color-Based Image Retrieval*". Technical Report TR 01-16, 2001.
17. F.G.B.D. Natale and F.Granelli, "*Structure-Based Image Retrieval Using a Structure Color Descriptor*". Proceeding of International Workshop of Content-Based Multimedia Indexing, 2001.
18. W.Y. Ma and B.S. Manjunath, "*Netra: A Toolbox for Navigating Large Image Databases*". IEEE Proceeding of Image Processing, 1997. 1: p. 568-571.
19. M. Strickner and M. Orengo, "*Similarity of Color Images*". Proceeding on Storage and Retrieval for Image and Video Databases, 1995: p. 381-392.
20. J. Huang, S.R. Kumar, M. Mitra, W.J. Zhu, and R. Zabih, "*Image Indexing Using Color Correlograms*". IEEE Proceeding on Computer Vision and Pattern Recognition, 1997: p. 762-768.
21. R.M. Haralick, "*Statistical and Structural Approaches to Texture*". Proceeding of IEEE workshop on Content Based Access of Image and Video Libraries, 1979. 67(5): p. 786-804.
22. S.W. Zucker and K. Kant, "*Multiple-level Representations for Texture Discrimination*". Proceeding of the IEEE Conference on Pattern Recognition and Image Processing, 1981: p. 609-614.

23. H. Tamura, S. Mori, and T. Yamawaki, "*Texture Features Corresponding to Visual perception*". IEEE Transactions on Systems, Man, and Cybernetics SMC-3, 1978. 6(4): p. 460-473.
24. W. Richards and A. Polit, "*Texture Matching*". Kybernetik, 1974. 16: p. 155-162.
25. A. Pentland, R. Picard, and S. Sclaroff, "*Photobook: Content-based Manipulation of Image Databases*". Journal of Computer Vision, 1996. 18(3): p. 233-254.
26. R.M. Haralick, K. Shanmugam, and I. Dinstein, "*Textural Features for Image Classification*". IEEE Transactions on Systems, Man, and Cybernetics, 1973. 3(6): p. 610-621.
27. C.C. Gotlieb and H.E. Kreyszig, "*Texture Descriptors Based on Co-occurrence Matrix*". Computer Vision, Graphics, and Image Processing, 1990. 51(1): p. 70-86.
28. M.Partio, B.Cramariuc, and M.Gabbouj, "*An Ordinal Co-occurrence Matrix Framework for Texture Retrieval*". Journal on Image and Video Processing, 2007. 2007(1): p. 1-1.
29. D.C. He and L.Wang, "*Texture Features based on Texture Spectrum*". Pattern Recognition, 1991. 24(5): p. 391-399.
30. F. Zhou, J.F.Feng, and Q.Y. Shi, "*Texture Feature Based on Local Fourier Transform*". Proceeding of International Conference on Image Processing, 2001: p. 610-613.
31. S. Livens, P. Scheunders, G.V.d. Wouwer, and D.V. Dyck, "*Wavelets for texture analysis, an overview*". Proceeding of IEEE International Conference on Image Processing and Applications, 1997: p. 581-585.
32. B.S. Manjunath and W.Y. Ma, "*Texture Feature for Browsing and Retrieval of Image Data*". IEEE Transactions on Pattern Analysis and Machine Intelligence, 1996. 18(8): p. 837-842.
33. S. Boraha, E.L. Hinesa, and M. Bhuyanb, "*Wavelet Transform Based Image Texture Analysis for Size Estimation Applied to The Sorting of Tea Granules*". Journal of Food Engineering, 2007: p. 629-639.
34. S.E. Grigorescu, N. Petkov, and P. Kruizinga, "*A Comparative Study of Filter Based Texture Operators Using Mahalanobis Distance*". Proceeding of IEEE International Conference on Pattern Recognition, 2000. 3: p. 885-888.

35. S. Arivazhagan and L. Ganesan, "*Texture Classification Using Wavelet Transform*". Journal of Pattern Recognition Letters, 2003. **24**(9-10): p. 1513-1521.
36. T. Mathworks, "*Image Processing Toolbox for Use with Matlab*". 1997: p. 19-25.
37. J. Canny, "*A Computational Approach to Edge Detection*". IEEE Transactions on Pattern Analysis and Machine Intelligence, 1986. **8**(6): p. 679-698.
38. F.A. Cheikh, A. Quddus, and M. Gabbouj, "*Multi-level Shape Recognition based on Wavelet-Transform Modulus Maxima*". Proceeding of the Southwest Symposium on Image Analysis and Interpretation, 2000: p. 8-12.
39. E. Persoon and K.S. Fu, "*Shape Discrimination Using Fourier Descriptors*". IEEE Transactions on Systems, Man and Cybernetics, 1986. **8**(3): p. 388-397.
40. M.K. Hu, "*Visual Pattern Recognition by Moment Invariant*". IEEE Transactions on Information theory, 1962. **8**: p. 179-187.
41. J.S. Noh and K.H. Rhee, "*Palmprint Identification Algorithm Using Hu Invariant Moments*". Lecture Notes in Computer Science, 2005: p. 91-94.
42. A. Khotanzad and Y.H. Hong, "*Invariant Image Recognition by Zernike Moments*". IEEE Transactions on Pattern Analysis and Machine Intelligence, 1990. **12**(5): p. 489 - 497.
43. W. Kim and Y. Kim, "*A region-based shape descriptor using Zernike moments*". Signal Processing: Image Communications of the ACM, 2000. **16**: p. 95-102.
44. H.Hse and A.R.Ncwton, "*Robust Sketched Symbol Recognition using Zernike Moments*". Proceeding of International Conference on Pattern recognition, 2004: p. 367-370.
45. A. Soffer and H. Samet, "*Negative Shape Feature for Image Databases Consisting of Geographic Symbols*". Proceeding of International Workshop of Visual Form, 1997: p. 569--581.
46. M. Kass, A.Witkin, and D.Terzopoulos, "*Snakes: Active Contour Models*". Journal of Computer Vision, 1988. **1**(14): p. 321-331.
47. C. Xu, D.L. Pham, and J.L. Prince, "*Medical Image Segmentation Using Deformable Models*". SPIE Handbook on Medical Imaging, 2000. **3**: p. 129-174.

48. A.L. Yuille, P.W. Hullinan, and D.S. Cohen, "*Feature Extraction From Faces Using Deformable Templates*". *Journal of Computer Vision and Pattern Recognition*, 1989. **8**(2): p. 104-109.
49. M.P. Dubuisson-Jolly, S. Lakshmanan, and A.K. Jain, "*Vehicle Segmentation Using Deformable Templates*". *IEEE Transactions of Pattern Analysis and Machine Intelligence*, 1996. **18**(3): p. 293-308.
50. A.K. Jain and A.Vailaya, "*Shape -Based Retrieval: A Case Study with Trademark Image Database*". *Journal of Pattern Recognition*, 1998. **31**(9): p. 1369-1390.
51. A.K. Jain, Y. Zhong, and S. Lakshmanan, "*Object Matching using Deformable Templates*". *IEEE Transactions of Pattern Analysis and Machine Intelligence*, 1996. **18**(3): p. 267-277.
52. Y. Zhong, A. K.Jain, and M.P. Dubuisson-Jolly, "*Object Tracking Using Deformable Templates*". *IEEE Transactions of Pattern Analysis and Machine Intelligence*, 2000. **22**(5): p. 544-549.
53. Y. Rui, T.S. Huang, M. Ortega, and S. Mehrotra, "*Relevance Feedback: A Power Tool for Interactive Content-based Image Retrieval*". *IEEE Transactions on Circuits and Systems for Video Technology*, 1998. **8**(5): p. 644-655.
54. Ishikawa, Subramanya, and Faloutsos, "*MindReader: Querying Databases through Multiple Examples*". *Proceeding of the 24th Very Large Data Bases (VLDB) Conference*, 1998: p. 433--438.
55. I.J. Cox, L. Miller, P. Minka, V. Papatomas, and P. Yianilos, "*The Bayesian Image Retrieval System, PicHunter: Theory, Implementation and Psychophysical Experiments*". *IEEE Transactions on Image Processing*, 2000. **9**(1): p. 20-37.
56. P. Hong, Q. Tian, and T.S. Huang, "*Incorporate Support Vector Machines to Content-based Image Retrieval with Relevant Feedback*". *IEEE International Conference on Image Processing*, 2000: p. 750-753.
57. S.D. MacArthur, C.E. Brodley, and C.-R. Shyu, "*Relevance Feedback Decision Trees in Content-Based Image Retrieval*". *Proceeding of IEEE Workshop on Content-based Access of Image and Video Libraries.*, 2000: p. 68-72.

58. R.C. Veltkamp and M. Tanase, "*A Survey of Content-Based Image Retrieval Systems* ", Content-based Image and Video Retrieval by O.Marques & B.Furht(Eds), 2002.p.47-101.
59. T.K. Lau and I. King, "*Montage : An Image Database for the Fashion, Textile, and Clothing Industry in Hong Kong*". Lecture Notes in Computer Science, 1998. **I**: p. 410-417.
60. L. Balumelli and A. Mojsilovic, "*Wavelet Domain Feature for Texture Description, Classification and Replicability Analysis*". Proceeding of IEEE International Conference on Image Processing, 1999. **4**: p. 440-444.
61. M.K. Basher, N. Ohnishi, T. Matsumoto, Y. Takeuchi, H. Kudo, and K. Agusa, "*Image Retrieval by Pattern Categorization using Wavelet Domain perceptual Feature with LVQ Neural network*". Pattern Recognition Letters, 2005. **26**: p. 2315-2335.
62. E.S. Fedorov, "*Symmetry in the Plane*". In Zapiski Imperatorskogo S. Peterburgskogo Mineralogicheskogo Obshchestva, 1891. **2**(28): p. 345-390.
63. Y. Liu and R.T. Collins, "*Frieze and Wallpaper Symmetry Groups Classification under Affine and Perspective Distortion*". Technical Report CMU-PI-TR-98-37, 1998.
64. Y. Liu, R.T. Collins, and Y.H. Tsing, "*A Computational Model for Periodic Pattern Perception Based on Frieze and Wallpaper Groups*". IEEE Transactions on Pattern Analysis and Machine Intelligence, 2004. **26**(3): p. 354-371.
65. Y. Liu and R.T. Collins, "*A Computational Model for Repeated Pattern Using Frieze and Wallpaper Groups*". Proceeding of Conference on Computer Vision and Pattern Recognition Conference., 2000: p. 537 - 544.
66. H.C. Lin, L.L. Wang, and S.N. Yang, "*Extracting Periodicity of a Regular Texture based on Autocorrelation Functions*". Pattern Recognition Letters, 1997. **18**(5): p. 433-443.
67. J.He, M. Li, H.J. Zhang, H.H. Tong, and C.S. Zhang, "*Automatic Peak Number Detection in Image Symmetry Analysis*". Lecture Notes in Computer Science, 2004. **3333**(Oct.): p. 111-118.
68. G. Gescheider, "*Psychophysics: the Fundamentals*". 3rd, Lawrence Erlbaum Associates, ix, 1997.

69. E.A. Day, R.S. Berns, L.A. Taplin, and F.H. Imai, "*A Psychophysical Experiment Evaluating the Color Accuracy of Several Multispectral Image Capture Techniques*". Proceeding of IS&T PICS Conference, IS&T, Springfield, 2003: p. 199-204.
70. J.J. DiGiovanni, P.B. Nelson, and R.S. Schlauch, "*A Psychophysical Evaluation of Spectral Enhancement*". Journal of Speech, Language, and Hearing Research, 2005. **48**(5): p. 1121-1135.
71. T. Engen and C.O. Lindström, "*Psychophysical Scales of the Odor Intensity of Aryl Acetate*". Journal of Psychology, 1963: p. 23-28.
72. V. Bruce, P.R. Green, and M.A. Georgeson, "*Visual Perception*". Visual perception, 3rd, Psychology Press, 1996.
73. A. Tversky, "*Features of similarity*". Journal of Psychological Reviews, 1977. **84**(4): p. 327-352.
74. I. Biederman, "*Recognition-by-Components: A Theory of Human Image Understanding*". Journal of Psychological Review, 1987. **94**(2): p. 115-147.
75. J.R. Bergen and E.H. Adelson, "*Early Vision and Texture Perception*". Nature, 1998. **333**: p. 363-364.
76. H. Tamura, S. Mori, and T. Yamawaki, "*Psychological and Computational Measurement of Basic Textural Features and Their Comparison*". Proceeding of 3rd International Conference on Pattern Recognition, 1976: p. 273-277.
77. M. Amadasun and R. King, "*Textural features corresponding to textural properties*". IEEE Transactions on Circuits and Systems for Video Technology,, 1998. **19**(5): p. 1264-1274.
78. F. Mendoza, P. Dejmek, and J.M. Aguilera, "*Colour and Image Texture Analysis in Classification of Commercial Potato Chips*". Journal of Food Research International, 2007. **40**(2007): p. 1146-1154.
79. B. Liu and S.C. Liew, "*Texture Retrieval using Grey-level Co-occurrence Matrix for Ikonos Panchromatic Images of Earthquake in Java 2006*". Proceeding of IEEE International Geoscience and Remote Sensing Symposium, 2007: p. 23-27.
80. M. Partio, B. Cramariuc, M.Gabbouj, and A. Visa, "*Rock Texture Retrieval using Gray Level Co-occurrence Matrix*". Proceeding of NOrdic Signal Processing Symposim, 2002: p. 308-311.

81. J. Mao and A.K. Jain, "*Texture Classification and Segmentation using Multiresolution Simultaneous Autoregressive Models*". Journal of Pattern Recognition, 1992. **25**(2): p. 173-188.
82. M.F. Augusteijn, L.E. Clemens, and K.A. Shaw, "*Performance Evaluation of Texture Measures for Ground Cover Identification in Satellite Images by Means of a Neural Network Classifier*". IEEE Transactions on Geoscience and Remote Sensing, 1995. **33**(3): p. 616-626.
83. J.G. Daugman, "*An Information-theoretic View of Analogue Representation in Striate Cortex*". Journal of Computational Neuroscience, 1993: p. 403-424.
84. S.P. Nanavati and P.K. Panigrahi, "*Wavelets: Applications to image compression-I*". Journal of Resonance, 2005. **10**(2): p. 52-61.
85. S. Mallat, "*A Theory for Multiresolution Signal Decomposition: the Wavelet Representation*". IEEE Transactions on Pattern Analysis and Machine Intelligence, 1989. **11**(7): p. 674-693.
86. T. Mathworks, "*Wavelet Toolbox*". 2000.
87. C.E. Jacobs, A. Finkelstein, and D.H. Salesin, "*Fast Multiresolution Image Querying*". ACM Proceeding of Special Interest Group on GRAPHics and Interactive Techniques, 1995: p. 277-286.
88. A. Busch and W.W. Boles, "*Texture Classification Using Multiple Wavelet Analysis*". Proceeding of Digital Image Computing Techniques and Applications, 2002.
89. P. S. Hiremath, S. Shivashankar, and J. Pujari, "*Wavelet Based Features For Color Texture Classification with Application to CBIR*". Journal of Computer Science and Network Security, 2006. **6**(9): p. 124-133.
90. D. Gabor, "*Theory of Communication*". JIEE, 1946. **93**(3): p. 429-459.
91. P. Wu, B.S. Manjunanth, S.D. Newsam, and H.D. Shin, "*A Texture Descriptor for Image Retrieval and Browsing*". Proceeding of IEEE Workshop on Content-based Access of Image and Video Libraries., 1999: p. 3-7.
92. C.S. Sastry, M. Ravindranath, A.K. Pujari, and B.L. Deekshatulu, "*A modified Gabor function for content based image retrieval*".
93. V. Castelli and L. Bergman, "*Image Databases – Search and Retrieval of Digital Imagery*". John Wiley & Sons, Inc., 2002.

94. R. Manthalkar, P.K. Biswas, and B.N. Chatterji, "*Rotation Invariant Texture Classification using Even Symmetric Gabor Filters*". *Journal of Pattern Recognition Letters*, 2003. **24**(12): p. 2061–2068.
95. W.S. Torgerson, "*Theory and Methods of Scaling*". 1958, New York: J. Wiley & Sons, Inc.
96. T. Engen, "*Psychophysics: II. Scaling Methods*", ed. W.S.s.E.P. In J. W. Kling and L. A. Riggs (Eds.). 1971, New York.
97. M.G. Kendall, "*Rank correlation methods*". Griffin, 1962.
98. C. Spearman and A.J. Psychol, "*The proof and measurement of association between two things*". *Am J Psychol*, 1904: p. 72-101.
99. R.L. Plackett, "*Karl Pearson and the Chi-Squared Test*". *International Statistical Review*, 1983. **51**(1): p. 59–72.
100. S.C. Manoharan, M. Veezhinathan, and S. Ramakrishnan, "*Comparison of Two ANN Methods for Classification of Spirometer Data*". *Journal of Measurement Science Review*, 2008. **8**(2): p. 53-57.
101. H.F. Kaiser, "*Directional Statistical Decisions*". *Journal of Psychological Review*, 1960. **67**(3): p. 160-167.
102. D.G. Altman and J.M. Bland, "*Diagnostic tests 1: sensitivity and specificity*". *BMJ*, 1994. **308**(6943): p. 1552.
103. R.B. Yates and B.R. Neto, "*Modern Information Retrieval*". ACM Press, Addison-Wesley, 1999.

Appendix 1: p-z Conversation Table

In Table A1, the p values change from 0.01 to 0.995, the corresponding z values are show the below row.

Table A1: p-z conversation table ¹⁰

		p - z values									
p	0.01	0.02	0.03	0.04	0.05	0.06	0.07	0.08	0.09	0.1	
z	-2.33	-2.05	-1.88	-1.75	-1.64	-1.55	-1.48	1.41	-1.34	-1.28	
p	0.11	0.12	0.13	0.14	0.15	0.16	0.17	0.18	0.19	0.02	
z	-1.23	-1.18	-1.13	-1.08	-1.04	-0.99	-0.95	-0.92	-0.88	-0.84	
p	0.21	0.22	0.23	0.24	0.25	0.26	0.27	0.28	0.29	0.3	
z	-0.81	-0.77	-0.74	-0.71	-0.67	-0.64	-0.61	-0.58	-0.55	-0.52	
p	0.31	0.32	0.33	0.34	0.35	0.36	0.37	0.38	0.39	0.4	
z	-0.5	-0.47	-0.44	-0.41	-0.39	-0.36	-0.33	-0.31	-0.28	-0.25	
p	0.41	0.42	0.43	0.44	0.45	0.46	0.47	0.48	0.49	0.5	
z	-0.23	-0.2	-0.18	-0.15	-0.13	-0.1	-0.08	-0.05	-0.03	0	
p	0.51	0.52	0.53	0.54	0.55	0.56	0.57	0.58	0.59	0.6	
z	0.03	0.05	0.08	0.1	0.13	0.15	0.18	0.2	0.23	0.25	
p	0.61	0.62	0.63	0.64	0.65	0.66	0.67	0.68	0.69	0.7	
z	0.28	0.31	0.33	0.36	0.39	0.41	0.44	0.47	0.5	0.52	
p	0.71	0.72	0.73	0.74	0.75	0.76	0.77	0.78	0.79	0.8	
z	0.55	0.58	0.61	0.64	0.67	0.71	0.74	0.77	0.81	0.84	
p	0.81	0.82	0.83	0.84	0.85	0.86	0.87	0.88	0.89	0.9	
z	0.88	0.92	0.95	0.99	1.04	1.08	1.13	1.18	1.23	1.28	
p	0.91	0.92	0.93	0.94	0.95	0.96	0.97	0.98	0.99	0.995	
z	1.34	1.41	1.48	1.55	1.64	1.75	1.88	2.05	2.33	2.58	

Appendix 2: Rankings Based on Texture Features

Contents:

Table A2.1: Rankings based on coarseness

Table A2.2: Rankings based on regularity

Table A2.3: Rankings based on directionality

In Tables A2.1, A2.2 and A2.3, the entry T_{nm} of table expresses the ranking of the m^{th} image by the n^{th} subject, where the subscription n, m of T_{nm} represents the number of row and column respectively.

Table A2.1 Rankings based on coarseness

Subjects	Ranks Assigned for Coarseness									
	1	2	3	4	5	6	7	8	9	10
Subject 1	9	6	3	8	1	5	10	7	4	2
Subject 2	9	5	2	1	10	8	6	7	4	3
Subject 3	8	2	1	9	6	4	6	3	5	10
Subject 4	9	4	1	8	6	7	10	2	3	5
Subject 5	6	2	1	9	6	5	10	4	3	8
Subject 6	10	6	3	2	8	1	9	4	5	7
Subject 7	9	3	1	8	5	7	10	2	4	6
Subject 8	1	8	2	7	3	9	6	10	5	4
Subject 9	10	2	1	7	6	5	9	3	4	8
Subject 10	10	4	1	6	7	5	9	2	3	8
Subject 11	9	4	1	8	6	5	10	3	2	7
Subject 12	10	4	1	8	7	5	9	2	3	6
Subject 13	9	4	1	8	6	5	10	3	2	7

Table A2.2 Rankings based on regularity

Subjects	Ranks Assigned for Regularity									
	1	2	3	4	5	6	7	8	9	10
Subject 1	8	4	9	10	2	5	3	7	6	1
Subject 2	2	10	7	9	1	4	8	5	6	3
Subject 3	3	8	9	5	2	4	7	10	6	1
Subject 4	1	9	7	5	3	4	10	8	6	2
Subject 5	6	7	10	4	3	1	5	8	9	2
Subject 6	2	7	9	5	3	4	6	10	8	1
Subject 7	2	5	9	7	3	4	10	8	6	1
Subject 8	1	7	8	6	3	5	4	10	9	2
Subject 9	3	9	7	5	2	6	4	10	8	1
Subject 10	2	7	10	6	3	4	5	8	9	1
Subject 11	1	10	8	5	4	3	6	9	7	2
Subject 12	1	7	10	6	2	4	5	9	8	3
Subject 13	3	7	5	10	1	4	9	8	6	2

Table A2.3 Rankings based on directionality

Subjects	Ranks Assigned for Directionality									
	1	2	3	4	5	6	7	8	9	10
Subject 1	1	10	6	8	3	4	5	9	7	2
Subject 2	1	9	6	10	4	2	5	7	8	3
Subject 3	2	6	9	8	5	4	3	10	7	1
Subject 4	1	9	10	5	2	4	6	8	7	3
Subject 5	2	9	7	6	3	4	5	10	8	1
Subject 6	2	8	10	6	4	5	3	9	7	1
Subject 7	2	7	9	6	4	3	5	10	8	1
Subject 8	1	10	8	4	3	6	5	9	7	2
Subject 9	1	9	7	5	4	6	3	10	8	2
Subject 10	1	7	8	6	3	4	5	9	10	2
Subject 11	1	8	7	5	3	4	6	9	10	2
Subject 12	1	10	8	5	6	3	4	9	7	2
Subject 13	1	9	10	7	3	4	6	8	5	2

Appendix 3: Coefficient Matrix of Rank Correlation between Subjects' Rankings Based on Texture Features

Contents:

Table A3.1 Coefficient matrix of rank correlation between subjects' rankings based on coarseness

Table A3.2 Coefficient matrix of rank correlation between subjects' rankings based on regularity

Table A3.3 Coefficient matrix of rank correlation between subjects' rankings based on directionality

In Tables A3.1 to A3.3, the entry T_{nm} of table expresses the coefficient of rank correlation between m^{th} subject and n^{th} subject, where the subscription n, m of T_{nm} represents the number of row and column respectively.

Table A3.1 Coefficient matrix of rank correlation between subjects' rankings based on coarseness

r_s	1	2	3	4	5	6	7	8	9	10	11	12	13
1	1.00	0.04	0.11	0.56	0.38	0.16	0.55	0.27	0.39	0.32	0.53	0.47	0.53
2	0.04	1.00	-0.06	0.31	0.02	0.44	0.21	-0.03	0.26	0.36	0.22	0.31	0.22
3	0.11	-0.06	1.00	0.63	0.81	0.36	0.71	-0.28	0.86	0.77	0.75	0.75	0.75
4	0.56	0.31	0.63	1.00	0.81	0.41	0.98	-0.09	0.87	0.88	0.94	0.95	0.94
5	0.38	0.02	0.81	0.81	1.00	0.32	0.85	-0.00	0.86	0.79	0.90	0.81	0.90
6	0.16	0.44	0.36	0.41	0.32	1.00	0.38	-0.54	0.59	0.70	0.54	0.58	0.54
7	0.55	0.21	0.71	0.98	0.85	0.38	1.00	-0.12	0.92	0.88	0.93	0.93	0.93
8	0.27	-0.03	-0.28	-0.09	-0.00	-0.54	-0.12	1.00	-0.32	-0.36	-0.15	-0.28	-0.15
9	0.39	0.26	0.86	0.87	0.86	0.59	0.92	-0.32	1.00	0.95	0.93	0.93	0.93
10	0.32	0.36	0.77	0.88	0.79	0.70	0.88	-0.36	0.95	1.00	0.94	0.95	0.94
11	0.53	0.22	0.75	0.94	0.90	0.54	0.93	-0.15	0.93	0.94	1.00	0.96	1.00
12	0.47	0.31	0.75	0.95	0.81	0.58	0.93	-0.28	0.93	0.95	0.96	1.00	0.96
13	0.53	0.22	0.75	0.94	0.90	0.54	0.93	-0.15	0.93	0.94	1.00	0.96	1.00

Table A3.2 Coefficient matrix of rank correlation between subjects' rankings based on regularity

r_s	1	2	3	4	5	6	7	8	9	10	11	12	13
1	1.00	0.32	0.44	0.05	0.50	0.43	0.41	0.42	0.43	0.53	0.19	0.44	0.45
2	0.32	1.00	0.66	0.78	0.39	0.58	0.67	0.54	0.56	0.62	0.70	0.65	0.84
3	0.44	0.66	1.00	0.85	0.76	0.95	0.83	0.83	0.87	0.87	0.89	0.88	0.68
4	0.05	0.78	0.85	1.00	0.50	0.79	0.84	0.66	0.67	0.70	0.87	0.72	0.75
5	0.50	0.39	0.76	0.50	1.00	0.79	0.55	0.67	0.66	0.82	0.70	0.75	0.35
6	0.43	0.58	0.95	0.79	0.79	1.00	0.81	0.94	0.89	0.95	0.90	0.94	0.61
7	0.41	0.67	0.83	0.84	0.55	0.81	1.00	0.65	0.55	0.76	0.68	0.75	0.78
8	0.42	0.54	0.83	0.66	0.67	0.94	0.65	1.00	0.92	0.93	0.85	0.94	0.56
9	0.43	0.56	0.87	0.67	0.66	0.89	0.55	0.92	1.00	0.84	0.84	0.83	0.56
10	0.53	0.62	0.87	0.70	0.82	0.95	0.76	0.93	0.84	1.00	0.85	0.95	0.56
11	0.19	0.70	0.89	0.87	0.70	0.90	0.68	0.85	0.84	0.85	1.00	0.87	0.59
12	0.44	0.65	0.88	0.72	0.75	0.94	0.75	0.94	0.83	0.95	0.87	1.00	0.59
13	0.45	0.84	0.68	0.75	0.35	0.61	0.78	0.56	0.56	0.56	0.59	0.59	1.00

Table A3.3 Coefficient matrix of rank correlation between subjects' rankings based on directionality

r_s	1	2	3	4	5	6	7	8	9	10	11	12	13
1	1.00	0.90	0.78	0.82	0.94	0.81	0.83	0.85	0.87	0.84	0.85	0.85	0.85
2	0.90	1.00	0.72	0.68	0.78	0.66	0.73	0.61	0.66	0.77	0.75	0.75	0.75
3	0.78	0.72	1.00	0.72	0.84	0.93	0.93	0.71	0.82	0.84	0.75	0.81	0.79
4	0.82	0.68	0.72	1.00	0.87	0.87	0.87	0.92	0.81	0.87	0.87	0.83	0.94
5	0.94	0.78	0.84	0.87	1.00	0.89	0.94	0.92	0.93	0.93	0.94	0.89	0.84
6	0.81	0.66	0.93	0.87	0.89	1.00	0.93	0.88	0.90	0.87	0.81	0.88	0.88
7	0.83	0.73	0.93	0.87	0.94	0.93	1.00	0.83	0.85	0.94	0.90	0.88	0.85
8	0.85	0.61	0.71	0.92	0.92	0.88	0.83	1.00	0.94	0.84	0.88	0.88	0.85
9	0.87	0.66	0.82	0.81	0.93	0.90	0.85	0.94	1.00	0.88	0.88	0.89	0.76
10	0.84	0.77	0.84	0.87	0.93	0.87	0.94	0.84	0.88	1.00	0.98	0.82	0.78
11	0.85	0.75	0.75	0.87	0.94	0.81	0.90	0.88	0.88	0.98	1.00	0.83	0.76
12	0.85	0.75	0.81	0.83	0.89	0.88	0.88	0.88	0.89	0.82	0.83	1.00	0.83
13	0.85	0.75	0.79	0.94	0.84	0.88	0.85	0.85	0.76	0.78	0.76	0.83	1.00

Appendix 4: Rankings Based on Texture Features after Pre-processing

Contents:

Table A4.1 Coefficient matrix of rank correlation between subjects' rankings based on coarseness

Table A4.2 Coefficient matrix of rank correlation between subjects' rankings based on regularity

Table A4.3 Coefficient matrix of rank correlation between subjects' rankings based on directionality

In Tables A4.1(a), A4.2(a) and A4.3(a), the entry T_{nm} of table expresses the ranking of the m^{th} image by the n^{th} subject, where the subscription n, m of T_{nm} represents the number of row and column respectively.

In Tables A4.1 (b), A4.2 (b) and A4.3 (b), the entry T_{nm} of table expresses the coefficient of rank correlation between m^{th} subject and n^{th} subject, where the subscription n, m of T_{nm} represents the number of row and column respectively.

Table A4.1 Rankings and corresponding coefficient matrix based on coarseness

Subjects	Ranks Assigned for Coarseness									
	1	2	3	4	5	6	7	8	9	10
Subject 3	8	2	1	9	6	4	6	3	5	10
Subject 4	9	4	1	8	6	7	10	2	3	5
Subject 5	6	2	1	9	6	5	10	4	3	8
Subject 7	9	3	1	8	5	7	10	2	4	6
Subject 9	10	2	1	7	6	5	9	3	4	8
Subject 10	10	4	1	6	7	5	9	2	3	8
Subject 11	9	4	1	8	6	5	10	3	2	7
Subject 12	10	4	1	8	7	5	9	2	3	6
Subject 13	9	4	1	8	6	5	10	3	2	7

(a) Rankings based on coarseness

r_s	3	4	5	7	9	10	11	12	13
3	1.00	0.63	0.81	0.71	0.86	0.77	0.75	0.75	0.75
4	0.63	1.00	0.81	0.98	0.87	0.88	0.94	0.95	0.94
5	0.81	0.81	1.00	0.85	0.86	0.79	0.90	0.81	0.90
7	0.71	0.98	0.85	1.00	0.92	0.88	0.93	0.93	0.93
9	0.86	0.87	0.86	0.92	1.00	0.95	0.93	0.93	0.93
10	0.77	0.88	0.79	0.88	0.95	1.00	0.94	0.95	0.94
11	0.75	0.94	0.90	0.93	0.93	0.94	1.00	0.96	1.00
12	0.75	0.95	0.81	0.93	0.93	0.95	0.96	1.00	0.96
13	0.75	0.94	0.90	0.93	0.93	0.94	1.00	0.96	1.00

(b) Coefficient matrix of rank correlation between subjects' rankings

Table A4.2 After pre-processing, rankings and corresponding coefficient matrix based on regularity

Subjects	Ranks Assigned for Regularity									
	1	2	3	4	5	6	7	8	9	10
Subject 3	3	8	9	5	2	4	7	10	6	1
Subject 6	2	7	9	5	3	4	6	10	8	1
Subject 8	1	7	8	6	3	5	4	10	9	2
Subject 9	3	9	7	5	2	6	4	10	8	1
Subject 10	2	7	10	6	3	4	5	8	9	1
Subject 11	1	10	8	5	4	3	6	9	7	2
Subject 12	1	7	10	6	2	4	5	9	8	3

(a) Rankings based on regularity

r_s	3	6	8	9	10	11	12
3	1.00	0.95	0.83	0.87	0.87	0.89	0.88
6	0.95	1.00	0.94	0.89	0.95	0.90	0.94
8	0.83	0.94	1.00	0.92	0.93	0.85	0.94
9	0.87	0.89	0.92	1.00	0.84	0.84	0.83
10	0.87	0.95	0.93	0.84	1.00	0.85	0.95
11	0.89	0.90	0.85	0.84	0.85	1.00	0.87
12	0.88	0.94	0.94	0.83	0.95	0.87	1.00

(b) Coefficient matrix of rank correlation between subjects' rankings

Table A4.3 After pre-processing, rankings and corresponding coefficient matrix based on directionality

Subjects	Ranks Assigned for Directionality									
	1	2	3	4	5	6	7	8	9	10
Subject 1	1	10	6	8	3	4	5	9	7	2
Subject 3	2	6	9	8	5	4	3	10	7	1
Subject 4	1	9	10	5	2	4	6	8	7	3
Subject 5	2	9	7	6	3	4	5	10	8	1
Subject 6	2	8	10	6	4	5	3	9	7	1
Subject 7	2	7	9	6	4	3	5	10	8	1
Subject 8	1	10	8	4	3	6	5	9	7	2
Subject 9	1	9	7	5	4	6	3	10	8	2
Subject 10	1	7	8	6	3	4	5	9	10	2
Subject 11	1	8	7	5	3	4	6	9	10	2
Subject 12	1	10	8	5	6	3	4	9	7	2
Subject 13	1	9	10	7	3	4	6	8	5	2

(a) Rankings based on directionality

r_s	1	3	4	5	6	7	8	9	10	11	12	13
1	1.00	0.78	0.82	0.94	0.81	0.83	0.85	0.87	0.84	0.85	0.85	0.85
3	0.78	1.00	0.72	0.84	0.93	0.93	0.71	0.82	0.84	0.75	0.81	0.79
4	0.82	0.72	1.00	0.87	0.87	0.87	0.92	0.81	0.87	0.87	0.83	0.94
5	0.94	0.84	0.87	1.00	0.89	0.94	0.92	0.93	0.93	0.94	0.89	0.84
6	0.81	0.93	0.87	0.89	1.00	0.93	0.88	0.90	0.87	0.81	0.88	0.88
7	0.83	0.93	0.87	0.94	0.93	1.00	0.83	0.85	0.94	0.90	0.88	0.85
8	0.85	0.71	0.92	0.92	0.88	0.83	1.00	0.94	0.84	0.88	0.88	0.85
9	0.87	0.82	0.81	0.93	0.90	0.85	0.94	1.00	0.88	0.88	0.89	0.76
10	0.84	0.84	0.87	0.93	0.87	0.94	0.84	0.88	1.00	0.98	0.82	0.78
11	0.85	0.75	0.87	0.94	0.81	0.90	0.88	0.88	0.98	1.00	0.83	0.76
12	0.85	0.81	0.83	0.89	0.88	0.88	0.88	0.89	0.82	0.83	1.00	0.83
13	0.85	0.79	0.94	0.84	0.88	0.85	0.85	0.76	0.78	0.76	0.83	1.00

(b) Coefficient matrix of rank correlation between subjects' rankings

Appendix 5: Rankings for Ten Queries

Contents:

- Table A5.1 Rankings for query 1
- Table A5.2 Rankings for query 2
- Table A5.3 Rankings for query 3
- Table A5.4 Rankings for query 4
- Table A5.5 Rankings for query 5
- Table A5.6 Rankings for query 6
- Table A5.7 Rankings for query 7
- Table A5.8 Rankings for query 8
- Table A5.9 Rankings for query 9
- Table A5.10 Rankings for query 10

In Tables A5.1- A5.10, The entry T_{nm} of table expresses the ranking of the m^{th} image by the n^{th} subject, where the subscription n, m of T_{nm} represents the number of row and column respectively.

Table A5.1 Rankings for query 1

Subjects	Ranks Assigned for Query 1								
	2	3	4	5	6	7	8	9	10
Subject 1	6	8	5	1	3	4	9	7	2
Subject 2	6	9	5	2	3	1	8	7	4
Subject 3	6	8	5	3	4	1	9	7	2
Subject 4	7	4	8	9	6	1	5	3	2
Subject 5	7	6	5	2	4	3	9	8	1
Subject 6	6	8	5	2	7	3	9	4	1
Subject 7	4	9	7	1	3	8	6	5	2
Subject 8	9	8	5	2	3	4	7	6	1
Subject 9	6	7	5	2	4	3	8	9	1
Subject 10	8	9	5	3	6	2	4	7	1
Subject 11	9	6	5	3	2	1	7	8	4
Subject 12	5	9	7	1	3	4	8	6	2
Subject 13	2	9	5	3	4	6	8	1	7
Subject 14	7	9	6	2	1	3	8	5	4
Subject 15	3	7	5	8	9	4	2	1	6
Subject 16	4	5	7	3	8	2	9	6	1

Table A5.2 Rankings for query 2

Subjects	Ranks Assigned for Query 2								
	1	3	4	5	6	7	8	9	10
Subject 1	9	2	6	5	4	8	3	1	7
Subject 2	9	2	4	5	6	8	3	1	7
Subject 3	9	2	6	4	3	8	5	1	7
Subject 4	7	3	6	8	4	5	2	1	9
Subject 5	8	3	4	7	5	6	2	1	9
Subject 6	9	2	5	4	3	7	6	1	8
Subject 7	7	6	5	1	2	9	4	3	8
Subject 8	9	3	7	5	4	6	2	1	8
Subject 9	9	3	5	6	4	7	1	2	8
Subject 10	7	2	6	5	4	9	3	1	8
Subject 11	9	3	6	5	4	8	2	1	7
Subject 12	7	6	4	1	2	9	5	3	8
Subject 13	7	9	6	2	3	5	4	1	8
Subject 14	8	7	6	5	2	4	3	1	9
Subject 15	7	9	6	8	3	1	2	5	4
Subject 16	9	2	6	4	5	8	3	1	7

Table A5.3 Rankings for query 3

Subjects	Ranks Assigned for Query 3								
	1	2	4	5	6	7	8	9	10
Subject 1	5	3	8	9	4	6	1	2	7
Subject 2	9	3	6	5	4	7	1	2	8
Subject 3	8	2	5	7	3	9	4	1	6
Subject 4	6	3	8	5	4	7	1	2	9
Subject 5	8	3	6	5	4	7	2	1	9
Subject 6	9	2	4	3	5	6	8	1	7
Subject 7	8	3	6	5	4	7	2	1	9
Subject 8	8	2	6	5	4	7	3	1	9
Subject 9	8	2	9	4	5	6	3	1	7
Subject 10	10	1	6	5	4	8	2	3	7
Subject 11	8	3	7	5	6	9	2	1	4
Subject 12	8	3	6	5	4	7	2	1	9
Subject 13	8	5	7	6	3	4	1	2	9
Subject 14	5	7	3	4	6	8	1	2	9
Subject 15	9	3	2	6	5	1	4	8	7
Subject 16	8	1	6	5	4	7	2	3	9

Table A5.4 Rankings for query 4

Subjects	Ranks Assigned for Query 4									
	1	2	3	5	6	7	8	9	10	
Subject 1	6	4	8	3	2	1	9	5	7	
Subject 2	8	2	4	7	6	1	5	3	9	
Subject 3	3	6	8	5	4	2	9	7	1	
Subject 4	6	3	5	9	4	2	7	1	8	
Subject 5	4	9	8	3	2	5	7	6	1	
Subject 6	9	2	8	4	5	7	6	1	3	
Subject 7	8	4	7	2	3	1	5	6	9	
Subject 8	9	3	4	8	6	2	5	1	7	
Subject 9	2	6	9	3	4	1	9	8	5	
Subject 10	3	8	7	9	4	1	5	6	2	
Subject 11	9	6	7	4	3	2	5	8	1	
Subject 12	8	4	7	2	3	1	6	5	9	
Subject 13	3	8	9	1	2	5	6	7	4	
Subject 14	8	3	4	7	5	1	6	2	9	
Subject 15	9	1	8	3	4	5	6	2	7	
Subject 16	3	8	9	4	5	1	6	7	2	

Table A5.5 Rankings for query 5

Subjects	Ranks Assigned for Query 5									
	1	2	3	4	6	7	8	9	10	
Subject 1	4	3	7	6	1	8	9	2	5	
Subject 2	2	7	9	5	1	3	8	6	4	
Subject 3	7	4	2	8	1	6	9	3	5	
Subject 4	3	5	7	8	1	6	4	2	9	
Subject 5	3	8	9	4	1	5	6	7	2	
Subject 6	9	2	5	6	1	7	8	2	4	
Subject 7	2	4	9	6	1	5	8	7	3	
Subject 8	8	5	4	6	1	7	3	2	9	
Subject 9	3	6	9	5	1	4	7	8	2	
Subject 10	5	3	8	4	1	9	6	7	2	
Subject 11	2	9	7	5	1	4	6	8	3	
Subject 12	4	2	9	6	1	5	8	7	3	
Subject 13	2	7	9	3	1	6	8	5	4	
Subject 14	2	8	9	5	1	7	6	4	3	
Subject 15	5	1	7	3	4	8	9	6	2	
Subject 16	4	6	7	5	1	3	9	8	2	

Table A5.6 Rankings for query 6

Subjects	Ranks Assigned for Query 6									
	1	2	3	4	5	7	8	9	10	
Subject 1	2	3	6	5	1	7	9	4	8	
Subject 2	2	4	6	8	1	7	5	3	9	
Subject 3	8	3	5	6	1	7	9	4	2	
Subject 4	4	7	6	8	1	5	2	3	9	
Subject 5	3	8	9	4	1	5	6	7	2	
Subject 6	8	2	6	5	1	4	9	3	6	
Subject 7	2	3	9	5	1	6	8	7	4	
Subject 8	7	6	4	5	1	8	2	3	9	
Subject 9	3	6	9	5	1	4	7	8	2	
Subject 10	9	6	7	3	1	8	4	5	2	
Subject 11	8	4	7	2	1	9	6	5	3	
Subject 12	2	3	9	5	1	6	7	8	4	
Subject 13	1	6	8	4	2	3	9	7	5	
Subject 14	1	3	8	6	2	9	7	5	4	
Subject 15	6	2	4	5	3	8	9	7	1	
Subject 16	4	5	6	7	1	3	8	9	2	

Table A5.7 Rankings for query 7

Subjects	Ranks Assigned for Query 7									
	1	2	3	4	5	6	8	9	10	
Subject 1	2	4	6	1	8	7	9	5	3	
Subject 2	1	6	8	2	4	3	9	5	7	
Subject 3	5	6	8	1	4	3	9	7	2	
Subject 4	2	4	5	3	9	6	7	1	8	
Subject 5	1	9	6	2	5	4	8	7	3	
Subject 6	8	6	7	2	3	5	9	4	1	
Subject 7	6	4	8	1	3	2	9	5	7	
Subject 8	5	6	7	3	2	1	8	9	4	
Subject 9	1	9	6	3	4	5	8	7	2	
Subject 10	4	8	7	1	5	6	9	3	2	
Subject 11	3	8	7	2	4	5	9	6	1	
Subject 12	6	4	8	1	3	2	9	5	7	
Subject 13	6	2	8	3	4	1	7	5	9	
Subject 14	1	5	8	3	2	4	9	7	6	
Subject 15	5	6	3	4	2	7	1	8	9	
Subject 16	2	8	7	1	4	5	6	9	3	

Table A5.8 Rankings for query 8

Subjects	Ranks Assigned for Query 8									
	1	2	3	4	5	6	7	9	10	
Subject 1	6	4	1	7	2	5	8	3	9	
Subject 2	8	3	1	9	6	4	7	2	5	
Subject 3	6	3	1	8	5	4	7	2	9	
Subject 4	5	3	1	7	9	4	6	2	8	
Subject 5	8	2	3	6	5	4	7	1	9	
Subject 6	8	1	2	6	5	4	7	3	9	
Subject 7	7	3	2	6	4	5	8	1	9	
Subject 8	9	2	3	6	4	5	8	1	7	
Subject 9	6	2	3	7	5	4	9	1	8	
Subject 10	5	2	4	8	6	3	9	1	7	
Subject 11	8	4	1	6	5	3	9	2	7	
Subject 12	7	3	2	6	4	5	8	1	9	
Subject 13	7	3	1	8	6	4	5	2	9	
Subject 14	8	3	1	5	7	4	6	2	9	
Subject 15	7	5	2	4	3	9	6	1	8	
Subject 16	9	3	1	8	4	5	7	2	6	

Table A5.9 Rankings for query 9

Subjects	Ranks Assigned for Query 9									
	1	2	3	4	5	6	7	8	10	
Subject 1	8	1	2	5	6	4	7	3	9	
Subject 2	9	2	1	6	5	3	8	4	7	
Subject 3	7	2	1	6	5	3	8	4	9	
Subject 4	4	3	1	7	9	5	6	2	8	
Subject 5	7	3	1	4	8	5	6	2	9	
Subject 6	7	1	2	4	5	3	6	9	8	
Subject 7	8	3	2	6	5	4	7	1	9	
Subject 8	8	1	2	6	4	5	7	3	9	
Subject 9	5	3	1	4	7	6	9	2	8	
Subject 10	6	1	4	2	8	7	5	3	9	
Subject 11	8	4	2	3	6	5	9	1	7	
Subject 12	8	3	2	6	5	4	7	1	9	
Subject 13	7	3	1	8	5	4	6	2	9	
Subject 14	7	3	1	5	7	4	6	2	9	
Subject 15	9	4	2	6	5	7	8	3	1	
Subject 16	9	3	2	7	5	4	8	1	6	

Table A5.10 Rankings for query 10

Subjects	Ranks Assigned for Query 10								
	1	2	3	4	5	6	7	8	9
Subject 1	1	4	8	2	5	6	3	9	7
Subject 2	2	6	7	9	1	3	4	8	5
Subject 3	2	6	8	3	4	5	1	9	7
Subject 4	2	4	7	3	8	5	1	9	6
Subject 5	2	7	6	3	4	5	1	9	8
Subject 6	2	4	8	6	1	7	3	9	5
Subject 7	1	4	9	6	2	3	5	7	8
Subject 8	3	6	8	5	1	2	4	9	7
Subject 9	2	8	7	1	4	5	3	9	6
Subject 10	1	8	6	2	3	4	5	9	7
Subject 11	3	6	8	2	4	5	1	9	7
Subject 12	1	6	9	4	5	3	2	7	8
Subject 13	1	8	9	4	5	3	2	7	6
Subject 14	3	7	9	5	1	2	4	8	6
Subject 15	3	6	9	4	2	5	1	7	8
Subject 16	4	7	6	5	1	2	3	8	9

Appendix 6: Coefficient Matrix of Rank Correlation between Subjects' Rankings for Ten Queries

Contents:

- Table A6.1 Coefficients matrix of rank correlation between subjects' rankings for query 1
- Table A6.2 Coefficients matrix of rank correlation between subjects' rankings for query 2
- Table A6.3 Coefficients matrix of rank correlation between subjects' rankings for query 3
- Table A6.4 Coefficients matrix of rank correlation between subjects' rankings for query 4
- Table A6.5 Coefficients matrix of rank correlation between subjects' rankings for query 5
- Table A6.6 Coefficients matrix of rank correlation between subjects' rankings for query 6
- Table A6.7 Coefficients matrix of rank correlation between subjects' rankings for query 7
- Table A6.8 Coefficients matrix of rank correlation between subjects' rankings for query 8
- Table A6.9 Coefficients matrix of rank correlation between subjects' rankings for query 9
- Table A6.10 Coefficients matrix of rank correlation between subjects' rankings for query 10

In Tables A6.1 to A6.10, the entry T_{nm} of table expresses the coefficient of ranking between m^{th} subject and n^{th} subject, where the subscription n, m of T_{nm} represents the number of row and column respectively.

Table A6.1 Coefficients matrix of rank correlation between subjects' rankings for query 1

C	1	2	3	4	5	6	7	8	9	10	11	12	13	14	15	16
1	1.00	0.87	0.88	-0.17	0.92	0.77	0.68	0.87	0.92	0.60	0.70	0.93	0.27	0.85	-0.63	0.57
2	0.87	1.00	0.93	-0.02	0.78	0.67	0.42	0.75	0.82	0.67	0.82	0.83	0.27	0.88	-0.42	0.48
3	0.88	0.93	1.00	0.18	0.90	0.80	0.37	0.78	0.90	0.70	0.78	0.82	0.13	0.78	-0.42	0.70
4	-0.17	-0.02	0.18	1.00	0.07	0.18	-0.35	0.08	-0.02	0.25	0.15	-0.08	-0.35	-0.03	0.32	0.35
5	0.92	0.78	0.90	0.07	1.00	0.75	0.43	0.85	0.97	0.65	0.78	0.78	-0.08	0.68	-0.68	0.70
6	0.77	0.67	0.80	0.18	0.75	1.00	0.48	0.72	0.70	0.65	0.40	0.75	0.32	0.58	-0.12	0.80
7	0.68	0.42	0.37	-0.35	0.43	0.48	1.00	0.58	0.50	0.35	0.12	0.82	0.48	0.60	-0.32	0.23
8	0.87	0.75	0.78	0.08	0.85	0.72	0.58	1.00	0.82	0.78	0.77	0.80	0.02	0.82	-0.53	0.41
9	0.92	0.82	0.90	-0.02	0.97	0.70	0.50	0.82	1.00	0.72	0.75	0.82	-0.08	0.67	-0.63	0.67
10	0.60	0.67	0.70	0.25	0.65	0.65	0.35	0.78	0.72	1.00	0.62	0.60	-0.20	0.52	-0.10	0.45
11	0.70	0.82	0.78	0.15	0.78	0.40	0.12	0.77	0.75	0.62	1.00	0.57	-0.22	0.75	-0.65	0.30
12	0.93	0.83	0.82	-0.08	0.78	0.75	0.82	0.80	0.82	0.60	0.57	1.00	0.40	0.87	-0.45	0.57
13	0.27	0.27	0.13	-0.35	-0.08	0.32	0.48	0.02	-0.08	-0.20	-0.22	0.40	1.00	0.42	0.20	0.02
14	0.85	0.88	0.78	-0.03	0.68	0.58	0.60	0.82	0.67	0.52	0.75	0.87	0.42	1.00	-0.48	0.27
15	-0.63	-0.42	-0.42	0.32	-0.68	-0.12	-0.32	-0.53	-0.63	-0.10	-0.65	-0.45	0.20	-0.48	1.00	-0.15
16	0.57	0.48	0.70	0.35	0.70	0.80	0.23	0.40	0.67	0.45	0.30	0.57	0.02	0.27	-0.15	1.00

Table A6.2 Coefficients matrix of rank correlation between subjects' rankings for query 2

r_i	1	2	3	4	5	6	7	8	9	10	11	12	13	14	15	16
1	1.00	0.93	0.95	0.77	0.83	0.88	0.60	0.93	0.92	0.95	0.98	0.55	0.38	0.58	-0.15	0.98
2	0.93	1.00	0.85	0.70	0.87	0.82	0.50	0.83	0.88	0.88	0.92	0.48	0.28	0.45	-0.25	0.95
3	0.95	0.85	1.00	0.63	0.70	0.97	0.68	0.85	0.78	0.90	0.90	0.67	0.43	0.57	-0.27	0.93
4	0.77	0.70	0.63	1.00	0.93	0.63	0.27	0.87	0.87	0.77	0.78	0.20	0.35	0.73	0.22	0.70
5	0.83	0.87	0.70	0.93	1.00	0.72	0.38	0.87	0.93	0.82	0.85	0.35	0.37	0.68	0.07	0.80
6	0.88	0.82	0.97	0.63	0.72	1.00	0.65	0.80	0.73	0.83	0.82	0.67	0.45	0.60	-0.28	0.87
7	0.60	0.50	0.68	0.27	0.38	0.65	1.00	0.55	0.53	0.65	0.63	0.48	0.73	0.58	-0.23	0.62
8	0.93	0.83	0.85	0.87	0.87	0.80	0.55	1.00	0.93	0.87	0.95	0.47	0.53	0.77	0.10	0.92
9	0.92	0.88	0.78	0.87	0.93	0.73	0.53	0.93	1.00	0.87	0.95	0.47	0.40	0.68	0.10	0.88
10	0.95	0.88	0.90	0.77	0.82	0.83	0.65	0.87	0.87	1.00	0.93	0.60	0.37	0.53	-0.30	0.93
11	0.98	0.92	0.90	0.78	0.85	0.82	0.63	0.95	0.95	0.93	1.00	0.57	0.47	0.65	-0.03	0.97
12	0.55	0.48	0.67	0.20	0.35	0.67	0.98	0.47	0.47	0.60	0.57	1.00	0.70	0.53	-0.30	0.57
13	0.38	0.28	0.43	0.35	0.37	0.45	0.73	0.53	0.40	0.37	0.47	0.70	1.00	0.55	0.27	0.40
14	0.58	0.45	0.57	0.73	0.68	0.60	0.58	0.77	0.68	0.53	0.65	0.53	0.85	1.00	0.45	0.53
15	-0.15	-0.25	-0.27	0.22	0.07	-0.28	-0.25	0.10	0.10	-0.30	-0.03	-0.30	0.27	0.45	1.00	-0.23
16	0.98	0.95	0.93	0.70	0.80	0.87	0.62	0.92	0.88	0.93	0.97	0.57	0.40	0.53	0.23	1.00

Table A6.3 Coefficients matrix of rank correlation between subjects' rankings for query 3

r_i	1	2	3	4	5	6	7	8	9	10	11	12	13	14	15	16
1	1.00	0.68	0.63	0.82	0.70	0	0.70	0.67	0.65	0.58	0.58	0.70	0.73	0.35	-0.10	0.67
2	0.68	1.00	0.78	0.88	0.97	0.48	0.97	0.93	0.83	0.93	0.77	0.97	0.85	0.60	0.17	0.93
3	0.63	0.78	1.00	0.65	0.80	0.60	0.80	0.83	0.67	0.84	0.78	0.80	0.52	0.37	-0.08	0.77
4	0.82	0.88	0.65	1.00	0.92	0.28	0.92	0.88	0.85	0.76	0.67	0.92	0.83	0.60	-0.10	0.88
5	0.70	0.97	0.80	0.92	1.00	0.57	1.00	0.98	0.85	0.87	0.72	1.00	0.85	0.65	0.07	0.93
6	0	0.48	0.60	0.28	0.57	1.00	0.57	0.67	0.57	0.58	0.42	0.57	0.25	0.15	0.13	0.53
7	0.70	0.97	0.80	0.92	1.00	0.57	1.00	0.98	0.85	0.87	0.72	1.00	0.85	0.65	0.07	0.93
8	0.67	0.93	0.83	0.88	0.98	0.67	0.98	1.00	0.87	0.89	0.70	0.98	0.78	0.55	0.08	0.95
9	0.65	0.83	0.67	0.85	0.85	0.57	0.85	0.87	1.00	0.81	0.78	0.85	0.72	0.30	-0.08	0.82
10	0.58	0.93	0.84	0.76	0.87	0.58	0.87	0.89	0.81	1.00	0.79	0.87	0.65	0.37	0.22	0.93
11	0.58	0.77	0.78	0.67	0.72	0.42	0.72	0.70	0.78	0.79	1.00	0.72	0.45	0.42	-0.28	0.65
12	0.70	0.97	0.80	0.92	1.00	0.57	1.00	0.98	0.85	0.87	0.72	1.00	0.85	0.65	0.07	0.93
13	0.73	0.85	0.52	0.83	0.85	0.25	0.85	0.78	0.72	0.65	0.45	0.85	1.00	0.52	0.23	0.75
14	0.35	0.60	0.37	0.60	0.65	0.15	0.65	0.55	0.30	0.37	0.42	0.65	0.52	1.00	-0.13	0.48
15	-0.10	0.17	0.08	-0.10	0.07	0.13	0.07	0.55	0.08	0.22	-0.28	0.07	0.23	-0.13	1.00	0.23
16	0.67	0.93	0.77	0.88	0.93	0.53	0.93	0.95	0.82	0.93	0.65	0.93	0.75	0.48	0.23	1.00

Table A6.4 Coefficients matrix of rank correlation between subjects' rankings for query 4

r_i	1	2	3	4	5	6	7	8	9	10	11	12	13	14	15	16
1	1.00	0.33	0.48	0.40	0.28	0.17	0.77	0.17	0.72	0.10	0.35	0.83	0.43	0.43	0.53	0.38
2	0.33	1.00	-0.35	0.80	-0.72	0.13	0.53	0.90	-0.17	-0.13	-0.12	0.57	-0.63	0.97	0.50	-0.35
3	0.48	-0.35	1.00	-0.10	0.73	-0.07	-0.02	-0.35	0.82	0.67	0.53	0.02	0.57	-0.28	-0.20	0.85
4	0.40	0.80	-0.10	1.00	-0.43	0.20	0.25	0.83	-0.06	0.13	-0.25	0.35	-0.50	0.88	0.42	-0.25
5	0.28	-0.72	0.73	-0.43	1.00	0.02	-0.07	-0.60	0.56	0.47	0.55	-0.05	0.85	-0.25	-0.22	0.73
6	0.17	0.13	-0.07	0.20	0.02	1.00	0.07	0.37	-0.26	-0.35	0.17	0.15	-0.10	0.17	0.80	-0.22
7	0.77	0.53	-0.02	0.25	-0.07	0.07	1.00	0.28	0.38	-0.17	0.35	0.98	0.25	0.53	0.58	0.13
8	0.17	0.90	-0.35	0.83	-0.60	0.37	0.28	1.00	-0.38	-0.05	-0.07	0.35	-0.72	0.92	0.50	-0.38
9	0.72	-0.17	0.82	-0.06	0.56	-0.26	0.85	-0.38	1.00	0.44	0.34	0.40	0.70	-0.12	-0.06	0.81
10	0.10	-0.13	0.67	0.13	0.47	-0.35	-0.17	-0.05	0.44	1.00	0.40	-0.18	0.22	-0.08	-0.50	0.73
11	0.35	-0.12	0.53	-0.25	0.55	0.17	0.35	-0.07	0.34	0.40	1.00	0.30	0.38	-0.12	0.08	0.57
12	0.83	0.57	0.02	0.35	-0.05	0.15	0.98	0.35	0.40	-0.18	0.30	1.00	0.23	0.60	0.65	0.12
13	0.43	-0.63	0.57	-0.50	0.85	-0.10	0.25	-0.72	0.70	0.22	0.38	0.23	1.00	-0.55	-0.07	0.68
14	0.43	0.97	-0.28	0.88	-0.58	0.17	0.53	0.92	-0.12	-0.08	-0.12	0.60	-0.55	1.00	0.52	-0.32
15	0.53	0.50	-0.20	0.42	-0.22	0.80	0.58	0.50	-0.06	-0.50	0.08	0.65	-0.07	0.52	1.00	-0.28
16	0.38	-0.35	0.85	0.25	0.73	-0.22	0.13	-0.38	0.81	0.73	0.57	0.12	0.68	-0.32	-0.28	1.00

Table A6.5 Coefficients matrix of rank correlation between subjects' rankings for query 5

r_i	1	2	3	4	5	6	7	8	9	10	11	12	13	14	15	16
1	1.00	0.43	0.63	0.55	0.28	0.74	0.60	0.32	0.33	0.58	0.12	0.63	0.60	0.57	0.60	0.33
2	0.43	1.00	0.07	0.30	0.87	0.02	0.87	-0.23	0.90	0.40	0.85	0.70	0.88	0.78	0.23	0.85
3	0.63	0.07	1.00	0.30	-0.10	0.80	0.17	0.47	0	0.17	-0.05	0.27	0.05	0.05	0.22	0.25
4	0.55	0.30	0.30	1.00	0.10	0.24	0.27	0.67	0.07	0.07	0.12	0.20	0.30	0.43	-0.23	-0.08
5	0.28	0.87	-0.10	0.10	1.00	-0.03	0.78	-0.25	0.93	0.62	0.92	0.62	0.87	0.87	0.28	0.80
6	0.74	0.02	0.80	0.24	-0.03	1.00	0.21	0.51	0.05	0.46	-0.22	0.43	0.13	0.11	0.51	0.18
7	0.60	0.87	0.17	0.27	0.78	0.21	1.00	-0.27	0.92	0.70	0.70	0.93	0.80	0.72	0.57	0.65
8	0.32	-0.23	0.47	0.67	-0.25	0.51	-0.27	1.00	-0.35	0	-0.27	-0.17	-0.12	0	-0.28	0.37
9	0.33	0.90	0	0.07	0.93	0.05	0.92	-0.35	1.00	0.65	0.87	0.82	0.80	0.73	0.42	0.92
10	0.58	0.40	0.17	0.07	0.62	0.46	0.70	0	0.65	1.00	0.38	0.77	0.60	0.58	0.78	0.52
11	0.12	0.85	-0.05	0.12	0.92	-0.22	0.70	-0.27	0.87	0.38	1.00	0.47	0.75	0.75	0.03	0.80
12	0.63	0.70	0.27	0.20	0.62	0.43	0.93	-0.17	0.82	0.77	0.47	1.00	0.63	0.52	0.70	0.77
13	0.60	0.88	0.05	0.30	0.87	0.13	0.80	-0.12	0.80	0.60	0.75	0.63	1.00	0.90	0.43	0.70
14	0.57	0.78	0.05	0.43	0.87	0.11	0.74	0	0.73	0.58	0.75	0.52	0.90	1.00	0.25	0.55
15	0.60	0.23	0.22	-0.23	0.28	0.51	0.57	-0.28	0.42	0.78	0.47	0.70	0.43	0.25	1.00	0.43
16	0.33	0.85	0.25	-0.08	0.80	0.18	0.83	-0.37	0.92	0.52	0.80	0.77	0.70	0.55	0.43	1.00

Table A6.6 Coefficients matrix of rank correlation between subjects' rankings for query 6

r_i	1	2	3	4	5	6	7	8	9	10	11	12	13	14	15	16
1	1.00	0.77	0.38	0.30	0.22	0.56	0.70	0.25	0.30	-0.05	0.28	0.62	0.58	0.73	0.30	0.25
2	0.77	1.00	0.10	0.78	0.07	0.29	0.42	0.57	0.08	-0.12	0.02	0.38	0.25	0.60	-0.12	0.03
3	0.38	0.10	1.00	-0.17	0.23	0.75	0.43	0.07	0.33	0.58	0.70	0.35	0.12	0.40	0.82	0.47
4	0.30	0.78	-0.17	1.00	0.10	0.07	0.03	0.73	0	0.02	-0.12	0.05	0.03	0.13	-0.53	-0.08
5	0.22	0.07	0.23	0.10	1.00	0.03	0.70	-0.13	0.93	0.48	0.42	0.72	0.73	0.50	0.22	0.67
6	0.56	0.29	0.75	0.07	0.03	1.00	0.39	0.19	0.19	0.29	0.48	0.29	0.24	0.21	0.41	0.29
7	0.70	0.42	0.43	0.03	0.70	0.39	1.00	-0.17	0.83	0.22	0.43	0.98	0.80	0.85	0.50	0.68
8	0.25	0.57	0.07	0.73	-0.13	0.19	-0.17	1.00	-0.30	0.38	0.33	-0.15	-0.33	0.02	-0.25	-0.37
9	0.30	0.08	0.33	0	0.93	0.19	0.83	-0.30	1.00	0.35	0.35	0.85	0.82	0.55	0.37	0.88
10	-0.05	-0.12	0.58	0.02	0.48	0.29	0.22	0.38	0.35	1.00	0.90	0.23	-0.08	0.18	0.40	0.17
11	0.28	0.02	0.70	-0.12	0.42	0.48	0.43	0.33	0.35	0.90	1.00	0.42	0.07	0.42	0.60	0.17
12	0.62	0.38	0.35	0.05	0.72	0.29	0.98	-0.15	0.85	0.23	0.42	1.00	0.77	0.82	0.47	0.70
13	0.58	0.25	0.12	0.03	0.73	0.24	0.80	-0.33	0.82	-0.08	0.07	0.77	1.00	0.52	0.17	0.68
14	0.73	0.60	0.40	0.13	0.50	0.21	0.85	0.02	0.55	0.18	0.42	0.82	0.52	1.00	0.48	0.37
15	0.30	-0.12	0.82	-0.53	0.22	0.41	0.50	-0.25	0.37	0.40	0.60	0.47	0.17	0.48	1.00	0.53
16	0.25	0.03	0.47	-0.08	0.67	0.29	0.68	-0.37	0.85	0.17	0.17	0.70	0.68	0.37	0.53	1.00

Table A6.7 Coefficients matrix of rank correlation between subjects' rankings for query 7

r_i	1	2	3	4	5	6	7	8	9	10	11	12	13	14	15	16
1	1.00	0.52	0.55	0.57	0.58	0.37	0.28	0.10	0.53	0.70	0.63	0.28	0	0.43	-0.47	0.48
2	0.52	1.00	0.62	0.42	0.70	0.23	0.73	0.57	0.60	0.55	0.58	0.73	0.55	0.90	-0.18	0.57
3	0.55	0.62	1.00	-0.13	0.72	0.78	0.70	0.82	0.68	0.73	0.87	0.70	0.32	0.65	-0.40	0.73
4	0.57	0.42	-0.13	1.00	0.68	-0.20	0.15	-0.43	-0.05	0.27	-0.05	0.15	0.20	0.10	-0.28	-0.17
5	0.58	0.70	0.72	0.08	1.00	0.35	0.30	0.58	0.97	0.72	0.88	0.30	-0.08	0.67	-0.18	0.88
6	0.37	0.23	0.78	-0.20	0.35	1.00	0.53	0.48	0.40	0.77	0.72	0.53	0.10	0.27	-0.48	0.33
7	0.28	0.73	0.70	0.15	0.30	0.53	1.00	0.68	0.18	0.42	0.38	1.00	0.85	0.67	-0.18	0.30
8	0.10	0.57	0.82	-0.43	0.58	0.48	0.68	1.00	0.55	0.30	0.60	0.68	0.47	0.70	-0.07	0.65
9	0.53	0.60	0.68	-0.05	0.97	0.40	0.18	0.55	1.00	0.72	0.92	0.18	0.73	0.65	-0.18	0.87
10	0.70	0.55	0.73	0.27	0.72	0.77	0.42	0.30	0.72	1.00	0.88	0.42	-0.07	0.43	-0.48	0.57
11	0.63	0.58	0.87	-0.05	0.88	0.72	0.38	0.60	0.92	0.88	1.00	0.38	-0.10	0.62	-0.40	0.80
12	0.28	0.73	0.70	0.15	0.30	0.53	1.00	0.68	0.18	0.42	0.38	1.00	0.85	0.67	0.18	0.30
13	0	0.55	0.32	0.20	-0.08	0.10	0.85	0.47	-0.23	-0.07	-0.10	0.85	1.00	0.47	-0.07	-0.05
14	0.43	0.90	0.65	0.10	0.67	0.27	0.67	0.70	0.65	0.43	0.62	0.67	0.47	1.00	-0.05	0.65
15	-0.47	-0.18	-0.40	-0.28	-0.18	-0.48	-0.18	-0.07	-0.18	-0.48	-0.40	-0.18	-0.07	-0.05	1.00	0.10
16	0.48	0.57	0.73	-0.17	0.88	0.33	0.30	0.65	0.87	0.57	0.80	0.30	-0.05	0.65	0.10	1.00

Table A6.8 Coefficients matrix of rank correlation between subjects' rankings for query 8

r_s	1	2	3	4	5	6	7	8	9	10	11	12	13	14	15	16
1	1.00	0.63	0.88	0.52	0.77	0.78	0.90	0.75	0.80	0.63	0.80	0.90	0.85	0.67	0.68	0.78
2	0.63	1.00	0.82	0.73	0.73	0.75	0.72	0.78	0.77	0.75	0.83	0.72	0.82	0.72	0.37	0.93
3	0.88	0.82	1.00	0.83	0.88	0.88	0.92	0.78	0.90	0.82	0.85	0.92	0.95	0.85	0.55	0.83
4	0.52	0.73	0.83	1.00	0.72	0.72	0.68	0.55	0.73	0.73	0.68	0.68	0.87	0.85	0.33	0.60
5	0.77	0.73	0.88	0.72	1.00	0.95	0.95	0.93	0.92	0.80	0.85	0.95	0.87	0.90	0.62	0.82
6	0.78	0.73	0.88	0.72	0.95	1.00	0.90	0.88	0.87	0.73	0.83	0.90	0.87	0.90	0.53	0.82
7	0.90	0.72	0.92	0.68	0.95	0.90	1.00	0.92	0.93	0.78	0.85	1.00	0.83	0.85	0.75	0.83
8	0.75	0.78	0.78	0.55	0.93	0.88	0.92	1.00	0.88	0.75	0.87	0.92	0.73	0.78	0.67	0.90
9	0.80	0.77	0.90	0.73	0.92	0.87	0.93	0.88	1.00	0.95	0.87	0.93	0.78	0.77	0.52	0.78
10	0.63	0.75	0.82	0.73	0.80	0.73	0.78	0.75	0.95	1.00	0.77	0.78	0.70	0.63	0.27	0.67
11	0.80	0.83	0.85	0.68	0.85	0.83	0.88	0.87	0.87	0.77	1.00	0.88	0.77	0.83	0.52	0.87
12	0.90	0.72	0.92	0.68	0.95	0.90	1.00	0.92	0.93	0.78	0.88	1.00	0.85	0.75	0.83	
13	0.75	0.82	0.95	0.87	0.87	0.87	0.82	0.73	0.78	0.70	0.77	0.83	1.00	0.90	0.52	0.82
14	0.67	0.72	0.85	0.85	0.90	0.90	0.85	0.78	0.77	0.63	0.83	0.85	0.90	1.00	0.58	0.75
15	0.68	0.37	0.55	0.32	0.62	0.53	0.75	0.67	0.52	0.27	0.52	0.75	0.52	0.58	1.00	0.60
16	0.78	0.93	0.83	0.60	0.82	0.82	0.83	0.90	0.78	0.67	0.87	0.83	0.82	0.75	0.60	1.00

Table A6.9 Coefficients matrix of rank correlation between subjects' rankings for query 9

r	1	2	3	4	5	6	7	8	9	10	11	12	13	14	15	16
1	1.00	0.90	0.93	0.68	0.88	0.65	0.92	0.95	0.78	0.72	0.78	0.92	0.85	0.92	0.28	0.80
2	0.90	1.00	0.93	0.67	0.72	0.67	0.85	0.88	0.67	0.38	0.75	0.85	0.82	0.80	0.52	0.88
3	0.93	0.93	1.00	0.67	0.78	0.70	0.88	0.92	0.77	0.48	0.72	0.88	0.88	0.87	0.25	0.78
4	0.68	0.67	0.67	1.00	0.83	0.23	0.68	0.58	0.80	0.58	0.55	0.68	0.77	0.84	0.15	0.57
5	0.88	0.72	0.78	0.83	1.00	0.43	0.85	0.77	0.87	0.80	0.82	0.85	0.78	0.98	0.23	0.68
6	0.65	0.67	0.70	0.23	0.43	1.00	0.37	0.60	0.33	0.40	0.25	0.37	0.40	0.47	-0.02	0.55
7	0.92	0.85	0.88	0.68	0.85	0.37	1.00	0.92	0.77	0.55	0.83	1.00	0.93	0.92	0.33	0.90
8	0.95	0.88	0.92	0.58	0.77	0.60	0.92	1.00	0.72	0.60	0.72	0.92	0.88	0.84	0.33	0.82
9	0.78	0.67	0.77	0.80	0.87	0.33	0.77	0.72	1.00	0.68	0.87	0.77	0.68	0.84	0.35	0.67
10	0.72	0.38	0.48	0.58	0.80	0.40	0.55	0.60	0.68	1.00	0.58	0.55	0.42	0.70	0	0.32
11	0.78	0.75	0.72	0.55	0.82	0.25	0.83	0.72	0.87	0.58	1.00	0.83	0.63	0.80	0.53	0.82
12	0.92	0.85	0.88	0.68	0.85	0.37	1.00	0.92	0.77	0.55	0.83	1.00	0.93	0.92	0.33	0.90
13	0.85	0.82	0.88	0.77	0.78	0.40	0.93	0.88	0.68	0.42	0.63	0.93	1.00	0.89	0.27	0.83
14	0.92	0.80	0.87	0.84	0.98	0.47	0.92	0.84	0.84	0.70	0.80	0.92	0.89	1.00	0.23	0.77
15	0.28	0.52	0.25	0.15	0.23	-0.02	0.33	0.33	0.35	0	0.53	0.33	0.27	0.23	1.00	0.67
16	0.80	0.88	0.78	0.57	0.68	0.25	0.90	0.82	0.67	0.32	0.82	0.90	0.83	0.77	0.67	1.00

Table A6.10 Coefficients matrix of rank correlation between subjects' rankings for query 10

r_s	1	2	3	4	5	6	7	8	9	10	11	12	13	14	15	16
1	1.00	0.28	0.90	0.85	0.82	0.68	0.63	0.58	0.82	0.73	0.88	0.80	0.70	0.52	0.73	0.43
2	0.28	1.00	0.47	0.13	0.42	0.73	0.75	0.80	0.30	0.45	0.35	0.50	0.53	0.80	0.55	0.67
3	0.90	0.47	1.00	0.82	0.95	0.72	0.63	0.73	0.88	0.77	0.98	0.88	0.85	0.70	0.90	0.67
4	0.85	0.13	0.82	1.00	0.75	0.43	0.35	0.35	0.67	0.48	0.80	0.73	0.67	0.28	0.55	0.25
5	0.82	0.42	0.95	0.75	1.00	0.60	0.53	0.68	0.88	0.82	0.93	0.82	0.78	0.62	0.83	0.73
6	0.68	0.73	0.72	0.43	0.60	1.00	0.70	0.70	0.53	0.52	0.65	0.53	0.50	0.67	0.73	0.50
7	0.63	0.75	0.63	0.35	0.53	0.70	1.00	0.85	0.45	0.60	0.55	0.78	0.65	0.82	0.73	0.70
8	0.58	0.80	0.73	0.35	0.68	0.70	0.85	1.00	0.65	0.75	0.70	0.73	0.70	0.97	0.78	0.90
9	0.82	0.30	0.88	0.67	0.88	0.53	0.45	0.65	1.00	0.92	0.90	0.73	0.80	0.65	0.72	0.58
10	0.73	0.45	0.77	0.48	0.82	0.52	0.60	0.75	0.92	1.00	0.75	0.70	0.73	0.72	0.63	0.70
11	0.88	0.35	0.98	0.67	0.93	0.65	0.55	0.70	0.90	0.75	1.00	0.83	0.83	0.67	0.80	0.65
12	0.80	0.50	0.88	0.73	0.82	0.53	0.78	0.73	0.73	0.70	0.83	1.00	0.93	0.73	0.85	0.67
13	0.70	0.53	0.85	0.67	0.78	0.50	0.65	0.70	0.80	0.73	0.80	0.93	1.00	0.77	0.78	0.60
14	0.52	0.80	0.70	0.28	0.62	0.67	0.62	0.97	0.65	0.72	0.67	0.73	0.77	1.00	0.78	0.83
15	0.73	0.55	0.90	0.55	0.83	0.73	0.73	0.78	0.72	0.63	0.88	0.85	0.78	0.78	1.00	0.77
16	0.43	0.67	0.67	0.25	0.73	0.50	0.70	0.90	0.58	0.73	0.65	0.67	0.60	0.83	0.77	1.00

Appendix 7: Rankings after Pre-processing for Ten Queries

Contents:

- Table A7.1 After pre-processing, rankings and corresponding coefficient matrix for query 1
- Table A7.1 After pre-processing, rankings and corresponding coefficient matrix for query 1
- Table A7.2 After pre-processing, rankings and corresponding coefficient matrix for query 2
- Table A7.3 After pre-processing, rankings and corresponding coefficient matrix for query 3
- Table A7.4 After pre-processing, rankings and corresponding coefficient matrix for query 4
- Table A7.5 After pre-processing, rankings and corresponding coefficient matrix for query 5
- Table A7.6 After pre-processing, rankings and corresponding coefficient matrix for query 6
- Table A7.7 After pre-processing, rankings and corresponding coefficient matrix for query 7
- Table A7.8 After pre-processing, rankings and corresponding coefficient matrix for query 8
- Table A7.9 After pre-processing, rankings and corresponding coefficient matrix for query 9
- Table A7.10 After pre-processing, rankings and corresponding coefficient matrix for query 10

In Tables A7.1(a) to A7.10(a), the entry T_{nm} of table expresses the ranking order of the m^{th} image by the n^{th} subject, where the subscription n, m of T_{nm} represents the number of row and column respectively.

In Tables A7.1(b)-A7.10(b), the entry T_{nm} of table expresses the coefficient of ranking order between m^{th} subject and n^{th} subject, where the subscription n, m of T_{nm} represents the number of row and column respectively.

Table A7.1 After pre-processing, raw data of ranking order and corresponding coefficient matrix for query 1

Subjects	Ranks Assigned for Query 1								
	2	3	4	5	6	7	8	9	10
Subject 1	6	8	5	1	3	4	9	7	2
Subject 2	6	9	5	2	3	1	8	7	4
Subject 3	6	8	5	3	4	1	9	7	2
Subject 5	7	6	5	2	4	3	9	8	1
Subject 8	9	8	5	2	3	4	7	6	1
Subject 9	6	7	5	2	4	3	8	9	1
Subject 11	9	6	5	3	2	1	7	8	4
Subject 12	5	9	7	1	3	4	8	6	2
Subject 14	7	9	6	2	1	3	8	5	4

(a) Rankings for query 1

r_i	1	2	3	5	8	9	11	12	14
1	1.00	0.87	0.88	0.92	0.87	0.92	0.70	0.93	0.85
2	0.87	1.00	0.93	0.78	0.75	0.82	0.82	0.83	0.88
3	0.88	0.93	1.00	0.90	0.78	0.90	0.78	0.82	0.78
5	0.92	0.78	0.90	1.00	0.85	0.97	0.78	0.78	0.68
8	0.87	0.75	0.78	0.85	1.00	0.82	0.77	0.80	0.82
9	0.92	0.82	0.90	0.97	0.82	1.00	0.75	0.82	0.67
11	0.70	0.82	0.78	0.78	0.77	0.75	1.00	0.57	0.75
12	0.93	0.83	0.82	0.78	0.80	0.82	0.57	1.00	0.87
14	0.85	0.88	0.78	0.68	0.82	0.67	0.75	0.87	1.00

(b) Coefficients matrix of rank correlation between subjects' rankings for query 1

Table A7.2 After pre-processing, rankings and corresponding coefficient matrix for query 2

Subjects	Ranks Assigned for Query 2								
	1	3	4	5	6	7	8	9	10
Subject 1	9	2	6	5	4	8	3	1	7
Subject 2	9	2	4	5	6	8	3	1	7
Subject 3	9	2	6	4	3	8	5	1	7
Subject 5	8	3	4	7	5	6	2	1	9
Subject 6	9	2	5	4	3	7	6	1	8
Subject 8	9	3	7	5	4	6	2	1	8
Subject 9	9	3	5	6	4	7	1	2	8
Subject 10	7	2	6	5	4	9	3	1	8
Subject 11	9	3	6	5	4	8	2	1	7
Subject 16	9	2	6	4	5	8	3	1	7

(a) Rankings for query 2

r_i	1	2	3	5	6	8	9	10	11	16
1	1.00	0.93	0.95	0.83	0.88	0.93	0.92	0.95	0.98	0.98
2	0.93	1.00	0.85	0.87	0.82	0.83	0.88	0.88	0.92	0.95
3	0.95	0.85	1.00	0.70	0.97	0.85	0.78	0.90	0.90	0.93
5	0.83	0.87	0.70	1.00	0.72	0.87	0.93	0.82	0.85	0.80
6	0.88	0.82	0.97	0.72	1.00	0.80	0.73	0.83	0.82	0.87
8	0.93	0.83	0.85	0.87	0.80	1.00	0.93	0.87	0.95	0.92
9	0.92	0.88	0.78	0.93	0.73	0.93	1.00	0.87	0.95	0.88
10	0.95	0.88	0.90	0.82	0.83	0.87	0.87	1.00	0.93	0.93
11	0.98	0.92	0.90	0.85	0.82	0.95	0.95	0.93	1.00	0.97
16	0.98	0.95	0.93	0.80	0.87	0.92	0.88	0.93	0.97	1.00

(b) Coefficients of rank correlation between subjects' rankings for query 2

Table A7.3 After pre-processing, rankings and corresponding coefficient matrix for query 3

Subjects	Ranks Assigned for Query 3									
	1	2	4	5	6	7	8	9	10	
Subject 2	9	3	6	5	4	7	1	2	8	
Subject 4	6	3	8	5	4	7	1	2	9	
Subject 5	8	3	6	5	4	7	2	1	9	
Subject 7	8	3	6	5	4	7	2	1	9	
Subject 8	8	2	6	5	4	7	3	1	9	
Subject 9	8	2	9	4	5	6	3	1	7	
Subject 10	10	1	6	5	4	8	2	3	7	
Subject 12	8	3	6	5	4	7	2	1	9	
Subject 13	8	5	7	6	3	4	1	2	9	
Subject 16	8	1	6	5	4	7	2	3	9	

(a) Rankings for query 3

r_s	2	4	5	7	8	9	10	12	13	16
2	1.00	0.88	0.97	0.97	0.93	0.83	0.93	0.97	0.85	0.93
4	0.88	1.00	0.92	0.92	0.88	0.85	0.76	0.92	0.83	0.88
5	0.97	0.92	1.00	1.00	0.98	0.85	0.87	1.00	0.85	0.93
7	0.97	0.92	1.00	1.00	0.98	0.85	0.87	1.00	0.85	0.93
8	0.93	0.88	0.98	0.98	1.00	0.87	0.89	0.98	0.78	0.95
9	0.83	0.85	0.85	0.85	0.87	1.00	0.81	0.85	0.72	0.82
10	0.93	0.76	0.87	0.87	0.89	0.81	1.00	0.87	0.65	0.93
12	0.97	0.92	1.00	1.00	0.98	0.85	0.87	1.00	0.85	0.93
13	0.85	0.83	0.85	0.85	0.78	0.72	0.65	0.85	1.00	0.75
16	0.93	0.88	0.93	0.93	0.95	0.82	0.93	0.93	0.75	1.00

(b) Coefficients of rank correlation between subjects' rankings for query 3

Table A7.4 After pre-processing, rankings and corresponding coefficient matrix for query 4

Subjects	Ranks Assigned for Query 4									
	1	2	3	5	6	7	8	9	10	
Subject 2	8	2	4	7	6	1	5	3	9	
Subject 4	6	3	5	9	4	2	7	1	8	
Subject 8	9	3	4	8	6	2	5	1	7	
Subject 14	8	3	4	7	5	1	6	2	9	

(a) Rankings for query 4

r_s	2	4	8	14
2	1.00	0.80	0.90	0.97
4	0.80	1.00	0.83	0.88
8	0.90	0.83	1.00	0.92
14	0.97	0.88	0.92	1.00

(b) Coefficients of rank correlation between subjects' rankings for query 4

Table A7.5 After pre-processing, rankings and corresponding coefficient matrix for query 5

Subjects	Ranks Assigned for Query 5								
	1	2	3	4	6	7	8	9	10
Subject 2	2	7	9	5	1	3	8	6	4
Subject 5	3	8	9	4	1	5	6	7	2
Subject 7	2	4	9	6	1	5	8	7	3
Subject 9	3	6	9	5	1	4	7	8	2
Subject 11	2	9	7	5	1	4	6	8	3
Subject 13	2	7	9	3	1	6	8	5	4
Subject 14	2	8	9	5	1	7	6	4	3
Subject 16	4	6	7	5	1	3	9	8	2

(a) Rankings for query 5

r_i	2	5	7	9	11	13	14	16
2	1.00	0.87	0.87	0.90	0.85	0.88	0.78	0.85
5	0.87	1.00	0.78	0.93	0.92	0.87	0.87	0.80
7	0.87	0.78	1.00	0.92	0.70	0.80	0.72	0.83
9	0.90	0.93	0.92	1.00	0.87	0.80	0.73	0.92
11	0.85	0.92	0.70	0.87	1.00	0.75	0.75	0.80
13	0.88	0.87	0.80	0.80	0.75	1.00	0.90	0.70
14	0.78	0.87	0.74	0.73	0.75	0.90	1.00	0.55
16	0.85	0.80	0.83	0.92	0.80	0.70	0.55	1.00

(b) Coefficients of rank correlation between subjects' rankings for query 5

Table A7.6 After pre-processing, rankings and corresponding coefficient matrix for query 6

Subjects	Ranks Assigned for Query 6								
	1	2	3	4	5	7	8	9	10
Subject 7	2	3	9	5	1	6	8	7	4
Subject 12	2	3	9	5	1	6	7	8	4
Subject 14	1	3	8	6	2	9	7	5	4

(a) Rankings for query 6

r_i	7	12	14
7	1.00	0.98	0.85
12	0.98	1.00	0.82
14	0.85	0.82	1.00

(b) Coefficients of rank correlation between subjects' rankings for query 6

Table A7.7 After pre-processing, rankings and corresponding coefficient matrix for query 7

Subjects	Ranks Assigned for Query 7									
	1	2	3	4	5	6	8	9	10	
Subject 5	1	9	6	2	5	4	8	7	3	
Subject 9	1	9	6	3	4	5	8	7	2	
Subject 11	3	8	7	2	4	5	9	6	1	

(a) Rankings for query 7

r_s	5	9	11
5	1.00	0.97	0.88
9	0.97	1.00	0.92
11	0.88	0.92	1.00

(b) Coefficients of rank correlation between subjects' rankings for query 7

Table A7.8 After pre-processing, rankings and corresponding coefficient matrix for query 8

Subjects	Ranks Assigned for Query 8									
	1	2	3	4	5	6	7	9	10	
Subject 1	6	4	1	7	2	5	8	3	9	
Subject 3	6	3	1	8	5	4	7	2	9	
Subject 5	8	2	3	6	5	4	7	1	9	
Subject 6	8	1	2	6	5	4	7	3	9	
Subject 7	7	3	2	6	4	5	8	1	9	
Subject 8	9	2	3	6	4	5	8	1	7	
Subject 9	6	2	3	7	5	4	9	1	8	
Subject 11	8	4	1	6	5	3	9	2	7	
Subject 12	7	3	2	6	4	5	8	1	9	
Subject 13	7	3	1	8	6	4	5	2	9	
Subject 14	8	3	1	5	7	4	6	2	9	
Subject 16	9	3	1	8	4	5	7	2	6	

(a) Rankings for query 8

r_s	1	3	5	6	7	8	9	11	12	13	14	16
1	1.00	0.88	0.77	0.78	0.90	0.75	0.80	0.80	0.90	0.75	0.67	0.78
3	0.88	1.00	0.88	0.88	0.92	0.78	0.90	0.85	0.92	0.95	0.85	0.83
5	0.77	0.88	1.00	0.95	0.95	0.93	0.92	0.85	0.95	0.87	0.90	0.82
6	0.78	0.88	0.95	1.00	0.90	0.88	0.87	0.83	0.90	0.87	0.90	0.82
7	0.90	0.92	0.95	0.90	1.00	0.92	0.93	0.88	1.00	0.83	0.85	0.83
8	0.75	0.78	0.93	0.88	0.92	1.00	0.88	0.87	0.92	0.73	0.78	0.90
9	0.80	0.90	0.92	0.87	0.93	0.88	1.00	0.87	0.93	0.78	0.77	0.78
11	0.80	0.85	0.85	0.83	0.88	0.87	0.87	1.00	0.88	0.77	0.83	0.87
12	0.90	0.92	0.95	0.90	1.00	0.92	0.93	0.88	1.00	0.83	0.85	0.83
13	0.75	0.95	0.87	0.87	0.83	0.73	0.78	0.77	0.83	1.00	0.90	0.82
14	0.67	0.85	0.90	0.90	0.85	0.78	0.77	0.83	0.85	0.90	1.00	0.75
16	0.78	0.83	0.82	0.82	0.83	0.90	0.78	0.87	0.83	0.82	0.75	1.00

(b) Coefficients of rank correlation between subjects' rankings for query 8

Table A7.9 After pre-processing, rankings and corresponding coefficient matrix for query 9

Subjects	Ranks Assigned for Query 9									
	1	2	3	4	5	6	7	8	10	
Subject 1	8	1	2	5	6	4	7	3	9	
Subject 2	9	2	1	6	5	3	8	4	7	
Subject 3	7	2	1	6	5	3	8	4	9	
Subject 5	7	3	1	4	8	5	6	2	9	
Subject 7	8	3	2	6	5	4	7	1	9	
Subject 8	8	1	2	6	4	5	7	3	9	
Subject 11	8	4	2	3	6	5	9	1	7	
Subject 12	8	3	2	6	5	4	7	1	9	
Subject 13	7	3	1	8	5	4	6	2	9	
Subject 14	7	3	1	5	7	4	6	2	9	
Subject 16	9	3	2	7	5	4	8	1	6	

(a) Rankings for query 9

r_i	1	2	3	5	7	8	11	12	13	14	16
1	1.00	0.90	0.93	0.88	0.92	0.95	0.78	0.92	0.85	0.92	0.80
2	0.90	1.00	0.93	0.72	0.85	0.88	0.75	0.85	0.82	0.80	0.88
3	0.93	0.93	1.00	0.78	0.88	0.92	0.72	0.88	0.88	0.87	0.78
5	0.88	0.72	0.78	1.00	0.85	0.77	0.82	0.85	0.78	0.98	0.68
7	0.92	0.85	0.88	0.85	1.00	0.92	0.83	1.00	0.93	0.92	0.90
8	0.95	0.88	0.92	0.77	0.92	1.00	0.72	0.92	0.88	0.84	0.82
11	0.78	0.75	0.72	0.82	0.83	0.72	1.00	0.83	0.63	0.80	0.82
12	0.92	0.85	0.88	0.85	1.00	0.92	0.83	1.00	0.93	0.92	0.90
13	0.85	0.82	0.88	0.78	0.93	0.88	0.63	0.93	1.00	0.89	0.83
14	0.92	0.80	0.87	0.98	0.92	0.84	0.80	0.92	0.89	1.00	0.77
16	0.80	0.88	0.78	0.68	0.90	0.82	0.82	0.90	0.83	0.77	1.00

(b) Coefficients of rank correlation between subjects' rankings for query 9

Table A7.10 After pre-processing, rankings and corresponding coefficient matrix for query 10

Subjects	Ranks Assigned for Query 10								
	1	2	3	4	5	6	7	8	9
Subject 1	1	4	8	2	5	6	3	9	7
Subject 3	2	6	8	3	4	5	1	9	7
Subject 5	2	7	6	3	4	5	1	9	8
Subject 9	2	8	7	1	4	5	3	9	6
Subject 10	1	8	6	2	3	4	5	9	7
Subject 11	3	6	8	2	4	5	1	9	7
Subject 12	1	6	9	4	5	3	2	7	8
Subject 13	1	8	9	4	5	3	2	7	6
Subject 15	3	6	9	4	2	5	1	7	8

(a) Rankings for query 10

r_s	1	3	5	9	10	11	12	13	15
1	1.00	0.90	0.82	0.82	0.73	0.88	0.80	0.70	0.73
3	0.90	1.00	0.95	0.88	0.77	0.98	0.88	0.85	0.90
5	0.82	0.95	1.00	0.88	0.82	0.93	0.82	0.78	0.83
9	0.82	0.88	0.88	1.00	0.92	0.90	0.73	0.80	0.72
10	0.73	0.77	0.82	0.92	1.00	0.75	0.70	0.73	0.63
11	0.88	0.98	0.93	0.90	0.75	1.00	0.83	0.80	0.88
12	0.80	0.88	0.82	0.73	0.70	0.83	1.00	0.93	0.85
13	0.70	0.85	0.78	0.80	0.73	0.80	0.93	1.00	0.78
15	0.73	0.90	0.83	0.72	0.63	0.88	0.85	0.78	1.00

(b) Coefficients of rank correlation between subjects' rankings for query 10

Appendix 8: Image Rankings for Seven Queries by Subjects

Contents:

- Figure A8.1 Image rankings for query 1 by subjects
- Figure A8.2 Image rankings for query 2 by subjects
- Figure A8.3 Image rankings for query 3 by subjects
- Figure A8.4 Image rankings for query 5 by subjects
- Figure A8.5 Image rankings for query 8 by subjects
- Figure A8.6 Image rankings for query 9 by subjects
- Figure A8.7 Image rankings for query 10 by subjects

In Figures A8.1-A8.7, images are displayed in order of visual similarity from most similar to least similar to each query image. The value of psychophysical scaling is shown below each image.

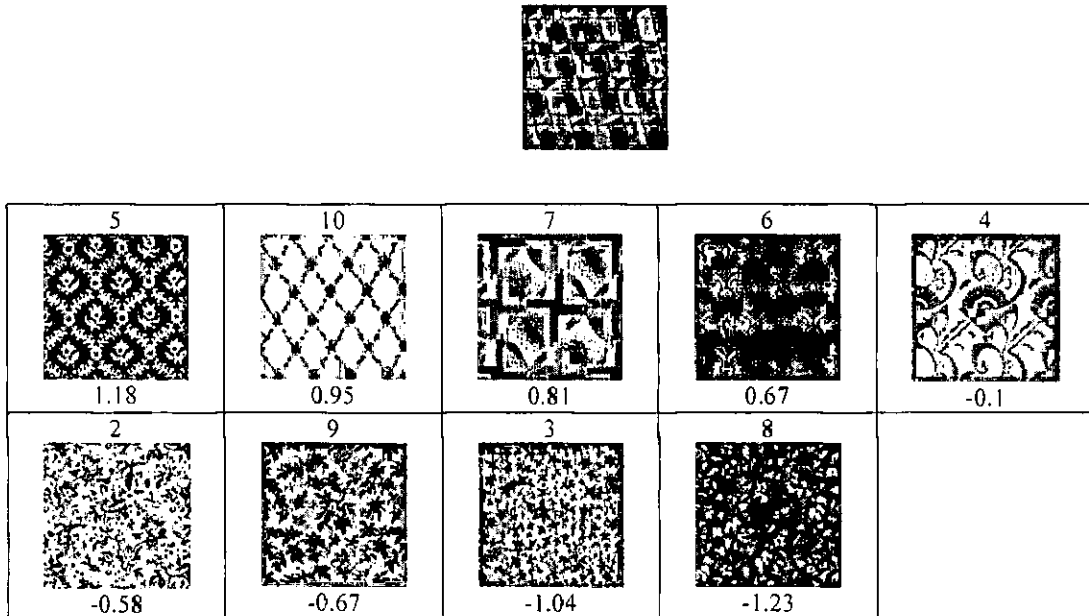


Figure A8.1 Image rankings for query 1 by subjects

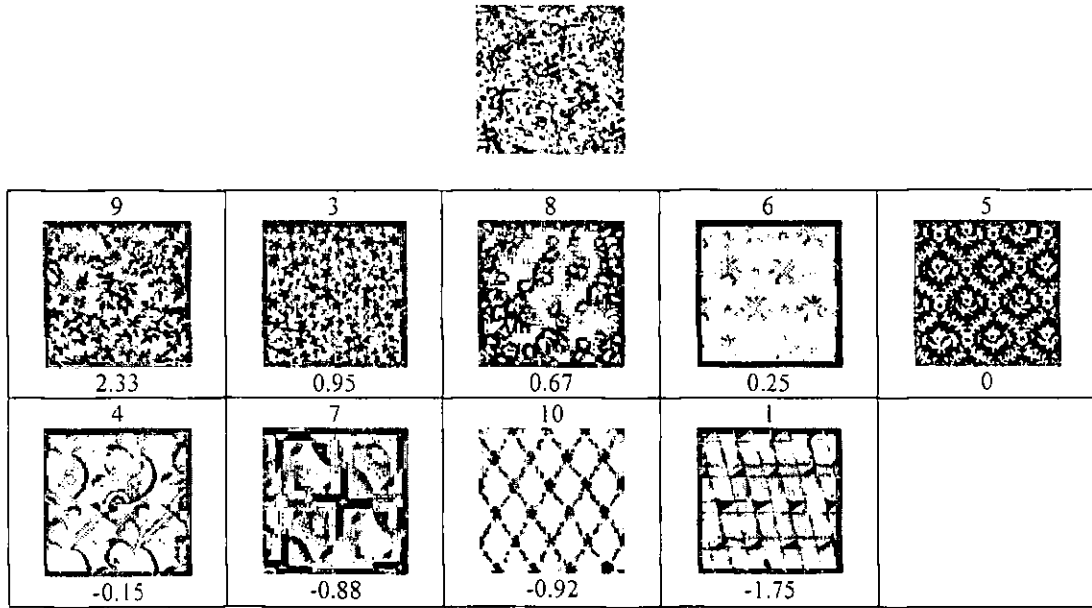


Figure A8.2 Image rankings for query 2 by subjects

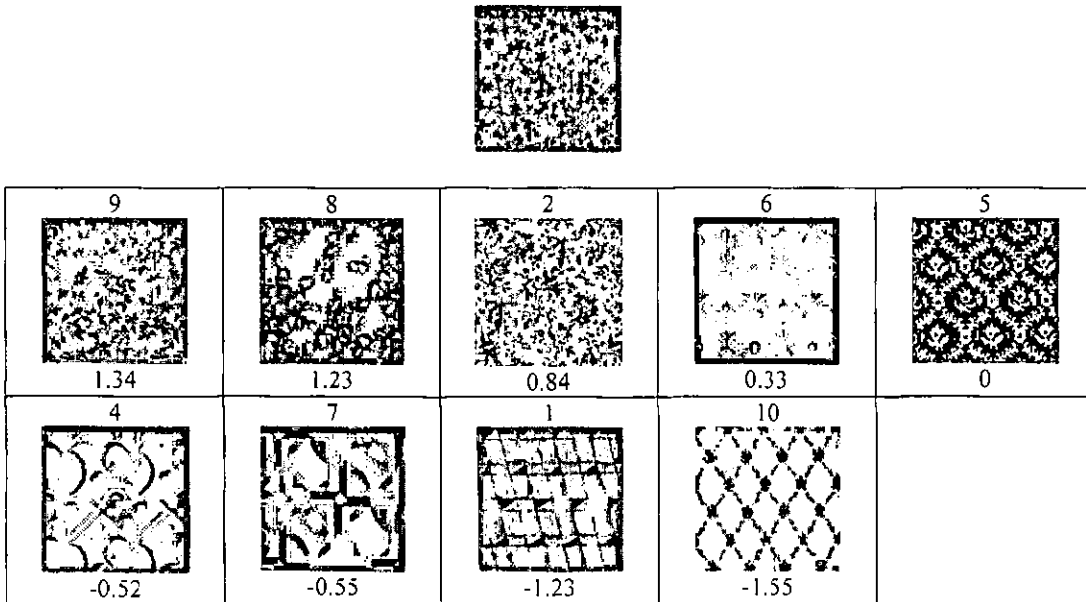


Figure A8.3 Image rankings for query 3 by subjects

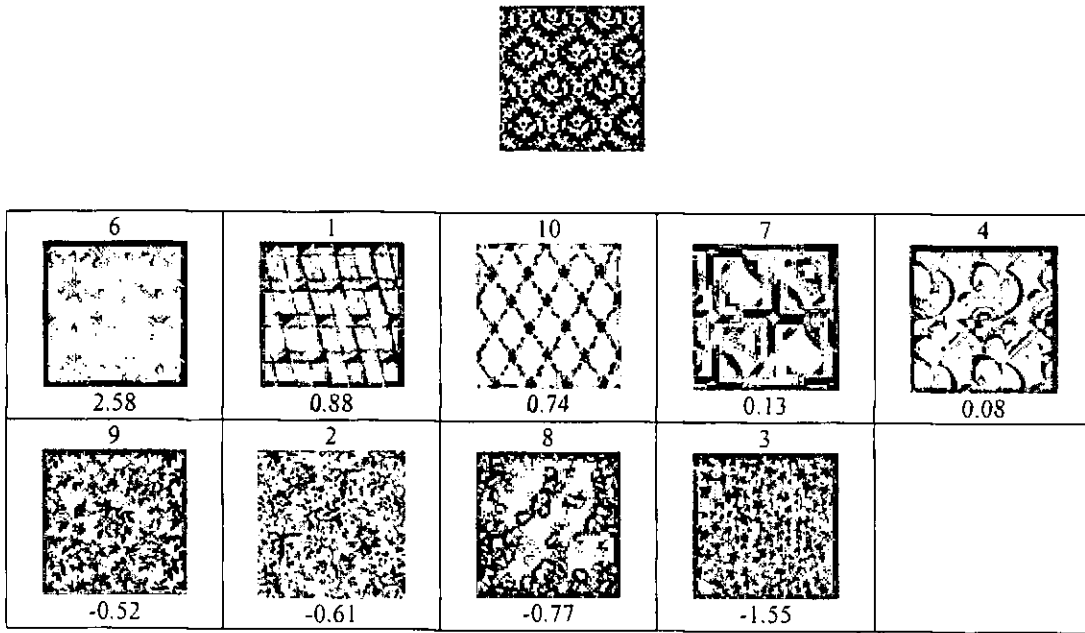


Figure A8.4 Image rankings for query 5 by subjects

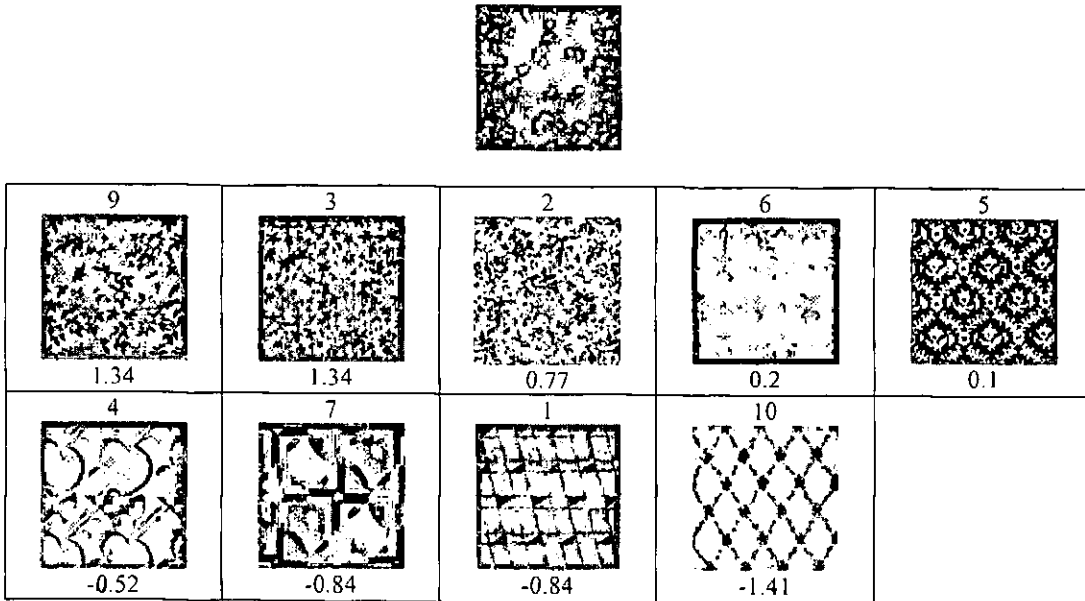


Figure A8.5 Image rankings for query 8 by subjects

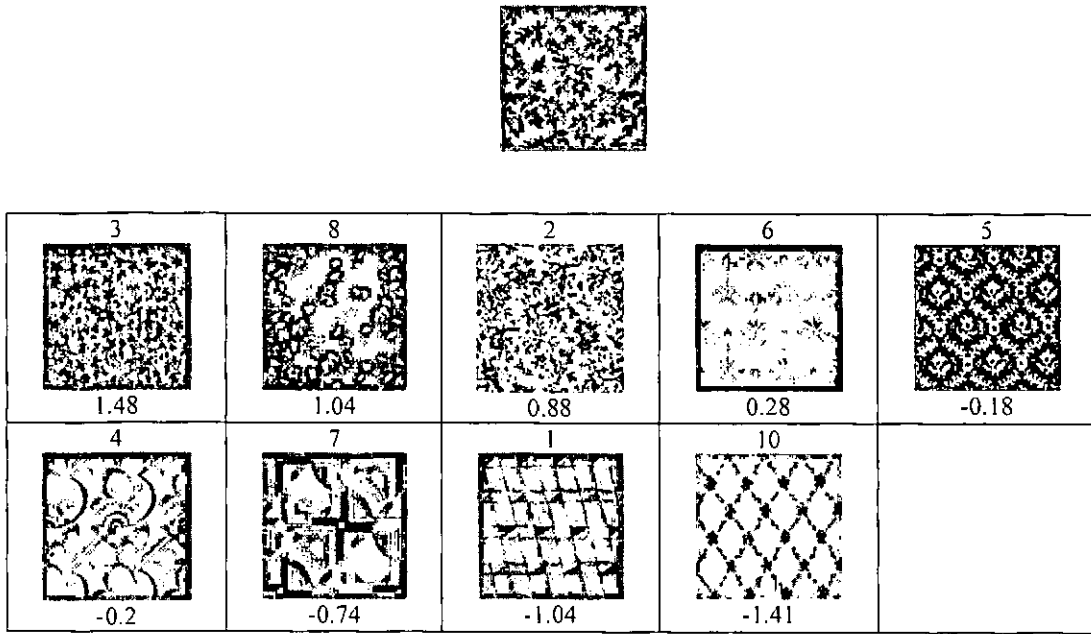


Figure A8.6 Image rankings for query 9 by subjects

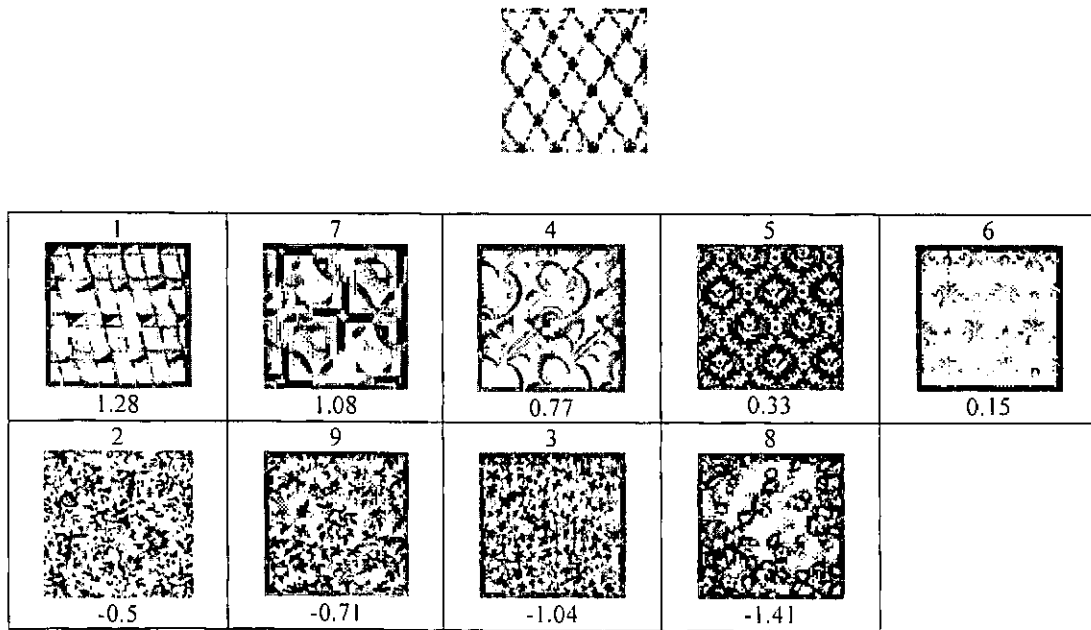


Figure A8.7 Image rankings for query 10 by subjects

Appendix 9: Comparison between Computational Texture Representations and Visual Texture Features

Contents:

- Table A9.1 Comparison between texture features of GLCM with visual feature perception
- Table A9.2 Comparison between texture features of MRSAR with visual feature perceptinn
- Table A9.3 Comparison between texture features of FT with visual feature perception
- Table A9.4 Comparison between texture features of WT with visual feature perception
- Table A9.5 Comparison between texture features of GT with visual feature perception

In Tables A9.1-A9.5, the first row is the ranking based on texture features ranking by subjects and the other rows are rankings based on each texture feature calculated by five computational methods respectively. The data in the last column in each table represents the coefficient of rank correlation ($|r_s|$) between each feature calculated by each method and the data perceived by subjects

Table A9.1 Comparisonn between texture features of GLCM with visual feature perception

Subjects	3	8	9	2	6	5	10	4	1	7	$ r_s $
f_1	10	4	6	8	9	1	7	3	5	2	0.19
f_2	2	5	8	3	7	9	1	10	6	4	0.43
f_3	2	5	3	7	9	1	8	6	10	4	0.27
f_4	4	10	6	1	7	9	8	3	5	2	0.55
f_5	10	4	6	9	8	1	7	3	5	2	0.2
f_6	2	5	8	3	7	9	1	10	6	4	0.43
f_7	2	5	3	7	9	8	1	6	10	4	0.36
f_8	4	10	6	1	7	9	8	3	5	2	0.55
f_9	10	4	6	8	9	1	7	3	5	2	0.19
f_{10}	2	5	3	8	7	9	1	6	10	4	0.47
f_{11}	2	5	3	7	9	1	8	6	10	4	0.27
f_{12}	4	10	6	1	7	9	8	3	5	2	0.55
f_{13}	10	4	6	9	8	1	7	3	5	2	0.2
f_{14}	2	5	3	8	7	9	6	10	1	4	0.54
f_{15}	2	5	3	7	9	8	1	6	10	4	0.36
f_{16}	4	10	1	6	7	9	8	3	5	2	0.6
f_{17}	10	4	6	8	9	1	7	3	5	2	0.19
f_{18}	2	5	3	8	7	9	1	10	6	4	0.44
f_{19}	2	5	3	1	7	9	8	6	10	4	0.21
f_{20}	4	10	7	1	6	9	8	3	5	2	0.67
f_{21}	10	4	6	8	9	1	7	3	5	2	0.19

f_{22}	2	5	8	3	9	7	1	10	6	4	0.52
f_{23}	2	5	3	9	1	7	8	6	10	4	0.37
f_{24}	4	10	7	1	6	9	8	3	5	2	0.67
f_{25}	10	4	8	6	9	7	1	3	5	2	0.16
f_{26}	2	5	3	8	7	9	1	10	6	4	0.44
f_{27}	2	5	3	1	7	9	8	6	10	4	0.21
f_{28}	4	10	7	1	6	9	8	3	5	2	0.67
f_{29}	10	4	6	8	9	1	7	3	5	2	0.19
f_{30}	2	5	3	8	7	9	10	1	6	4	0.47
f_{31}	2	5	3	7	1	9	8	6	10	4	0.2
f_{32}	4	10	1	7	9	6	8	3	5	2	0.64
f_{33}	10	4	8	6	9	7	1	3	5	2	0.16
f_{34}	2	5	3	8	7	9	1	10	6	4	0.44
f_{35}	2	5	1	3	7	9	8	6	10	4	0.12
f_{36}	4	10	7	6	1	8	9	3	5	2	0.61
f_{37}	10	4	8	6	9	7	1	3	5	2	0.16
f_{38}	2	5	8	3	9	7	1	10	6	4	0.52
f_{39}	2	5	3	1	9	7	8	6	10	4	0.3
f_{40}	4	10	7	1	6	9	8	3	5	2	0.67
f_{41}	10	4	8	6	9	3	7	1	5	2	0.04
f_{42}	2	5	3	8	7	9	1	10	6	4	0.44
f_{43}	2	5	1	3	7	9	8	6	10	4	0.12
f_{44}	4	10	7	6	1	8	9	3	5	2	0.61
f_{45}	10	4	6	8	9	1	7	3	5	2	0.19
f_{46}	2	5	3	8	7	9	1	10	6	4	0.44
f_{47}	2	5	3	1	7	9	8	6	10	4	0.21
f_{48}	4	10	7	1	9	6	8	3	5	2	0.65
f_{49}	10	4	8	6	9	1	3	7	5	2	0.04
f_{50}	2	5	3	8	7	9	1	10	6	4	0.44
f_{51}	2	5	1	3	7	9	8	6	10	4	0.12
f_{52}	4	10	7	6	1	8	9	3	5	2	0.61
f_{53}	10	4	8	6	9	7	1	3	5	2	0.16
f_{54}	2	5	8	3	9	7	1	6	10	4	0.54
f_{55}	2	5	3	1	9	7	8	6	10	4	0.3
f_{56}	4	10	7	1	6	8	9	3	5	2	0.66
f_{57}	10	4	8	6	9	3	1	7	5	2	0.05
f_{58}	2	5	3	8	7	9	1	10	6	4	0.44
f_{59}	2	5	1	7	3	9	8	6	10	4	0.01
f_{60}	4	10	7	6	1	8	9	3	5	2	0.61
f_{61}	10	4	6	8	9	1	7	3	5	2	0.19
f_{62}	2	5	3	8	7	9	1	10	6	4	0.44
f_{63}	2	5	3	1	7	9	8	6	10	4	0.21
f_{64}	4	10	7	1	6	9	8	3	5	2	0.67

(a) Comparison between texture features of GLCM and visual feature of coarseness

Subjects	10	1	5	6	7	4	9	2	3	8	$ r_c $
f_1	10	4	6	8	9	1	7	3	5	2	0.28
f_2	2	5	8	3	7	9	1	10	6	4	0.45

f_3	2	5	3	7	9	1	8	6	10	4	0.28
f_4	4	10	6	1	7	9	8	3	5	2	0.5
f_5	10	4	6	9	8	1	7	3	5	2	0.32
f_6	2	5	8	3	7	9	1	10	6	4	0.45
f_7	2	5	3	7	9	8	1	6	10	4	0.38
f_8	4	10	6	1	7	9	8	3	5	2	0.5
f_9	10	4	6	8	9	1	7	3	5	2	0.28
f_{10}	2	5	3	8	7	9	1	6	10	4	0.48
f_{11}	2	5	3	7	9	1	8	6	10	4	0.28
f_{12}	4	10	6	1	7	9	8	3	5	2	0.5
f_{13}	10	4	6	9	8	1	7	3	5	2	0.32
f_{14}	2	5	3	8	7	9	6	10	1	4	0.49
f_{15}	2	5	3	7	9	8	1	6	10	4	0.38
f_{16}	4	10	1	6	7	9	8	3	5	2	0.53
f_{17}	10	4	6	8	9	1	7	3	5	2	0.28
f_{18}	2	5	3	8	7	9	1	10	6	4	0.44
f_{19}	2	5	3	1	7	9	8	6	10	4	0.19
f_{20}	4	10	7	1	6	9	8	3	5	2	0.48
f_{21}	10	4	6	8	9	1	7	3	5	2	0.28
f_{22}	2	5	8	3	9	7	1	10	6	4	0.48
f_{23}	2	5	3	9	1	7	8	6	10	4	0.27
f_{24}	4	10	7	1	6	9	8	3	5	2	0.48
f_{25}	10	4	8	6	9	7	1	3	5	2	0.18
f_{26}	2	5	3	8	7	9	1	10	6	4	0.44
f_{27}	2	5	3	1	7	9	8	6	10	4	0.19
f_{28}	4	10	7	1	6	9	8	3	5	2	0.48
f_{29}	10	4	6	8	9	1	7	3	5	2	0.28
f_{30}	2	5	3	8	7	9	10	1	6	4	0.43
f_{31}	2	5	3	7	1	9	8	6	10	4	0.22
f_{32}	4	10	1	7	9	6	8	3	5	2	0.48
f_{33}	10	4	8	6	9	7	1	3	5	2	0.18
f_{34}	2	5	3	8	7	9	1	10	6	4	0.44
f_{35}	2	5	1	3	7	9	8	6	10	4	0.1
f_{36}	4	10	7	6	1	8	9	3	5	2	0.42
f_{37}	10	4	8	6	9	7	1	3	5	2	0.18
f_{38}	2	5	8	3	9	7	1	10	6	4	0.48
f_{39}	2	5	3	1	9	7	8	6	10	4	0.21
f_{40}	4	10	7	1	6	9	8	3	5	2	0.48
f_{41}	10	4	8	6	9	3	7	1	5	2	0.04
f_{42}	2	5	3	8	7	9	1	10	6	4	0.44
f_{43}	2	5	1	3	7	9	8	6	10	4	0.1
f_{44}	4	10	7	6	1	8	9	3	5	2	0.42
f_{45}	10	4	6	8	9	1	7	3	5	2	0.28
f_{46}	2	5	3	8	7	9	1	10	6	4	0.44
f_{47}	2	5	3	1	7	9	8	6	10	4	0.19
f_{48}	4	10	7	1	9	6	8	3	5	2	0.44
f_{49}	10	4	8	6	9	1	3	7	5	2	0.16
f_{50}	2	5	3	8	7	9	1	10	6	4	0.44
f_{51}	2	5	1	3	7	9	8	6	10	4	0.1
f_{52}	4	10	7	6	1	8	9	3	5	2	0.42

f_{53}	10	4	8	6	9	7	1	3	5	2	0.18
f_{54}	2	5	8	3	9	7	1	6	10	4	0.52
f_{55}	2	5	3	1	9	7	8	6	10	4	0.21
f_{56}	4	10	7	1	6	8	9	3	5	2	0.44
f_{57}	10	4	8	6	9	3	1	7	5	2	0.08
f_{58}	2	5	3	8	7	9	1	10	6	4	0.44
f_{59}	2	5	1	7	3	9	8	6	10	4	0.05
f_{60}	4	10	7	6	1	8	9	3	5	2	0.42
f_{61}	10	4	6	8	9	1	7	3	5	2	0.28
f_{62}	2	5	3	8	7	9	1	10	6	4	0.44
f_{63}	2	5	3	1	7	9	8	6	10	4	0.19
f_{64}	4	10	7	1	6	9	8	3	5	2	0.48

(b) Comparison between texture features of GLCM and visual feature of regularity

Subjects	1	10	5	6	7	4	9	3	2	8	$ r_i $
f_1	10	4	6	8	9	1	7	3	5	2	0.25
f_2	2	5	8	3	7	9	1	10	6	4	0.48
f_3	2	5	3	7	9	1	8	6	10	4	0.27
f_4	4	10	6	1	7	9	8	3	5	2	0.5
f_5	10	4	6	9	8	1	7	3	5	2	0.28
f_6	2	5	8	3	7	9	1	10	6	4	0.48
f_7	2	5	3	7	9	8	1	6	10	4	0.38
f_8	4	10	6	1	7	9	8	3	5	2	0.5
f_9	10	4	6	8	9	1	7	3	5	2	0.25
f_{10}	2	5	3	8	7	9	1	6	10	4	0.48
f_{11}	2	5	3	7	9	1	8	6	10	4	0.27
f_{12}	4	10	6	1	7	9	8	3	5	2	0.5
f_{13}	10	4	6	9	8	1	7	3	5	2	0.28
f_{14}	2	5	3	8	7	9	6	10	1	4	0.53
f_{15}	2	5	3	7	9	8	1	6	10	4	0.38
f_{16}	4	10	1	6	7	9	8	3	5	2	0.54
f_{17}	10	4	6	8	9	1	7	3	5	2	0.25
f_{18}	2	5	3	8	7	9	1	10	6	4	0.45
f_{19}	2	5	3	1	7	9	8	6	10	4	0.15
f_{20}	4	10	7	1	6	9	8	3	5	2	0.48
f_{21}	10	4	6	8	9	1	7	3	5	2	0.25
f_{22}	2	5	8	3	9	7	1	10	6	4	0.5
f_{23}	2	5	3	9	1	7	8	6	10	4	0.25
f_{24}	4	10	7	1	6	9	8	3	5	2	0.48
f_{25}	10	4	8	6	9	7	1	3	5	2	0.13
f_{26}	2	5	3	8	7	9	1	10	6	4	0.45
f_{27}	2	5	3	1	7	9	8	6	10	4	0.15
f_{28}	4	10	7	1	6	9	8	3	5	2	0.48
f_{29}	10	4	6	8	9	1	7	3	5	2	0.25
f_{30}	2	5	3	8	7	9	10	1	6	4	0.47
f_{31}	2	5	3	7	1	9	8	6	10	4	0.2
f_{32}	4	10	1	7	9	6	8	3	5	2	0.49
f_{33}	10	4	8	6	9	7	1	3	5	2	0.13

f_{34}	2	5	3	8	7	9	1	10	6	4	0.45
f_{35}	2	5	1	3	7	9	8	6	10	4	0.07
f_{36}	4	10	7	6	1	8	9	3	5	2	0.41
f_{37}	10	4	8	6	9	7	1	3	5	2	0.13
f_{38}	2	5	8	3	9	7	1	10	6	4	0.5
f_{39}	2	5	3	1	9	7	8	6	10	4	0.18
f_{40}	4	10	7	1	6	9	8	3	5	2	0.48
f_{41}	10	4	8	6	9	3	7	1	5	2	0.01
f_{42}	2	5	3	8	7	9	1	10	6	4	0.45
f_{43}	2	5	1	3	7	9	8	6	10	4	0.07
f_{44}	4	10	7	6	1	8	9	3	5	2	0.41
f_{45}	10	4	6	8	9	1	7	3	5	2	0.25
f_{46}	2	5	3	8	7	9	1	10	6	4	0.45
f_{47}	2	5	3	1	7	9	8	6	10	4	0.15
f_{48}	4	10	7	1	9	6	8	3	5	2	0.44
f_{49}	10	4	8	6	9	1	3	7	5	2	0.14
f_{50}	2	5	3	8	7	9	1	10	6	4	0.45
f_{51}	2	5	1	3	7	9	8	6	10	4	0.07
f_{52}	4	10	7	6	1	8	9	3	5	2	0.41
f_{53}	10	4	8	6	9	7	1	3	5	2	0.13
f_{54}	2	5	8	3	9	7	1	6	10	4	0.53
f_{55}	2	5	3	1	9	7	8	6	10	4	0.18
f_{56}	4	10	7	1	6	8	9	3	5	2	0.44
f_{57}	10	4	8	6	9	3	1	7	5	2	0.05
f_{58}	2	5	3	8	7	9	1	10	6	4	0.45
f_{59}	2	5	1	7	3	9	8	6	10	4	0.03
f_{60}	4	10	7	6	1	8	9	3	5	2	0.41
f_{61}	10	4	6	8	9	1	7	3	5	2	0.25
f_{62}	2	5	3	8	7	9	1	10	6	4	0.45
f_{63}	2	5	3	1	7	9	8	6	10	4	0.15
f_{64}	4	10	7	1	6	9	8	3	5	2	0.48

(c) Comparison between texture features of GLCM and visual feature of directionality

Table A9.2 Comparison between texture features of MRSAR with visual feature perception

Subjects	3	8	9	2	6	5	10	4	1	7	$ r_s $
f_1	6	5	10	1	4	3	9	7	8	2	0.28
f_2	6	5	1	10	9	4	8	3	7	2	0.19
f_3	2	8	7	3	9	4	1	10	5	6	0.31
f_4	2	8	7	3	4	9	10	1	5	6	0.27
f_5	2	3	5	8	9	7	10	1	4	6	0.58
f_6	6	5	10	1	3	4	7	9	8	2	0.28
f_7	6	5	1	9	4	8	7	10	2	3	0.27
f_8	2	8	3	9	7	10	4	1	5	6	0.54
f_9	2	8	3	4	7	9	10	5	1	6	0.44

f_{10}	2	5	3	8	9	7	10	1	6	4	0.55
f_{11}	6	1	10	3	5	7	4	9	8	2	0.32
f_{12}	1	6	5	9	4	7	8	2	3	10	0.35
f_{13}	2	8	10	9	3	7	4	5	1	6	0.47
f_{14}	2	8	4	10	3	7	9	5	1	6	0.27
f_{15}	2	5	3	8	9	7	10	1	6	4	0.55

(a) Comparison between texture features of MRSAR and visual feature of coarseness

Subjects	10	1	5	6	7	4	9	2	3	8	$ r_s $
f_1	6	5	10	1	4	3	9	7	8	2	0.75
f_2	6	5	1	10	9	4	8	3	7	2	0.67
f_3	2	8	7	3	9	4	1	10	5	6	0.77
f_4	2	8	7	3	4	9	10	1	5	6	0.75
f_5	2	3	5	8	9	7	10	1	4	6	0.55
f_6	6	5	10	1	3	4	7	9	8	2	0.73
f_7	6	5	1	9	4	8	7	10	2	3	0.44
f_8	2	8	3	9	7	10	4	1	5	6	0.77
f_9	2	8	3	4	7	9	10	5	1	6	0.82
f_{10}	2	5	3	8	9	7	10	1	6	4	0.45
f_{11}	6	1	10	3	5	7	4	9	8	2	0.7
f_{12}	1	6	5	9	4	7	8	2	3	10	0.36
f_{13}	2	8	10	9	3	7	4	5	1	6	0.54
f_{14}	2	8	4	10	3	7	9	5	1	6	0.56
f_{15}	2	5	3	8	9	7	10	1	6	4	0.45

(b) Comparison between texture features of MRSAR and visual feature of regularity

Subjects	1	10	5	6	7	4	9	3	2	8	$ r_s $
f_1	6	5	10	1	4	3	9	7	8	2	0.78
f_2	6	5	1	10	9	4	8	3	7	2	0.71
f_3	2	8	7	3	9	4	1	10	5	6	0.79
f_4	2	8	7	3	4	9	10	1	5	6	0.79
f_5	2	3	5	8	9	7	10	1	4	6	0.58
f_6	6	5	10	1	3	4	7	9	8	2	0.78
f_7	6	5	1	9	4	8	7	10	2	3	0.49
f_8	2	8	3	9	7	10	4	1	5	6	0.82
f_9	2	8	3	4	7	9	10	5	1	6	0.87
f_{10}	2	5	3	8	9	7	10	1	6	4	0.49
f_{11}	6	1	10	3	5	7	4	9	8	2	0.78
f_{12}	1	6	5	9	4	7	8	2	3	10	0.45
f_{13}	2	8	10	9	3	7	4	5	1	6	0.66
f_{14}	2	8	4	10	3	7	9	5	1	6	0.67
f_{15}	2	5	3	8	9	7	10	1	6	4	0.49

(c) Comparison between texture features of MRSAR and visual feature of directionality

Table A9.3 Comparison between texture features of FT with visual feature perception

Subjects	3	8	9	2	6	5	10	4	1	7	$ r_s $
f_1	2	5	8	3	7	9	10	1	6	4	0.45
f_2	10	2	4	7	9	3	1	8	5	6	0.24
f_3	10	2	4	7	9	3	1	8	5	6	0.24
f_4	5	10	1	7	2	6	4	9	8	3	0.70

(a) Comparison between texture features of FT and visual feature of coarseness

Subjects	10	1	5	6	7	4	9	2	3	8	$ r_s $
f_1	2	5	8	3	7	9	10	1	6	4	0.44
f_2	10	2	4	7	9	3	1	8	5	6	0.03
f_3	10	2	4	7	9	3	1	8	5	6	0.03
f_4	5	10	1	7	2	6	4	9	8	3	0.85

(b) Comparison between texture features of FT and visual feature of regularity

Subjects	1	10	5	6	7	4	9	3	2	8	$ r_s $
f_1	2	5	8	3	7	9	10	1	6	4	0.49
f_2	10	2	4	7	9	3	1	8	5	6	0.09
f_3	10	2	4	7	9	3	1	8	5	6	0.09
f_4	5	10	1	7	2	6	4	9	8	3	0.78

(c) Comparison between texture features of FT and visual feature of directionality

Table A9.4 Comparison between texture features of WT with visual feature perception

Subjects	3	8	9	2	6	5	10	4	1	7	$ r_s $
f_1	10	2	4	7	9	3	1	8	5	6	0.24
f_2	5	2	7	10	1	9	8	3	6	4	0.25
f_3	2	5	9	8	3	1	7	6	10	4	0.52
f_4	5	2	1	7	8	9	3	10	6	4	0.07
f_5	2	5	3	8	9	7	1	6	10	4	0.55
f_6	5	2	7	1	3	8	10	9	6	4	0.09
f_7	2	5	3	8	9	6	7	10	1	4	0.68
f_8	2	5	7	8	3	9	10	6	1	4	0.30
f_9	2	5	8	3	9	1	7	6	10	4	0.55
f_{10}	2	5	1	8	7	9	3	10	6	4	0.05
f_{11}	2	5	3	8	9	7	6	1	10	4	0.60
f_{12}	2	5	8	3	7	9	1	10	6	4	0.43
f_{13}	2	5	3	8	9	7	10	1	6	4	0.55
f_{14}	2	8	5	3	7	9	10	1	4	6	0.47
f_{15}	2	5	3	8	9	7	1	6	10	4	0.55
f_{16}	2	5	8	7	9	3	1	10	6	4	0.30
f_{17}	2	5	3	8	9	7	6	1	10	4	0.60

f_{18}	2	5	3	7	8	9	10	6	1	4	0.42
f_{19}	2	8	3	5	7	9	4	10	1	6	0.53
f_{20}	2	7	8	3	5	9	4	10	1	6	0.27

(a) Comparison between texture features of WT and visual feature of coarseness

Subjects	10	1	5	6	7	4	9	2	3	8	$ r_s $
f_1	10	2	4	7	9	3	1	8	5	6	0.03
f_2	5	2	7	10	1	9	8	3	6	4	0.31
f_3	2	5	9	8	3	1	7	6	10	4	0.42
f_4	5	2	1	7	8	9	3	10	6	4	0.02
f_5	2	5	3	8	9	7	1	6	10	4	0.5
f_6	5	2	7	1	3	8	10	9	6	4	0.04
f_7	2	5	3	8	9	6	7	10	1	4	0.5
f_8	2	5	7	8	3	9	10	6	1	4	0.36
f_9	2	5	8	3	9	1	7	6	10	4	0.48
f_{10}	2	5	1	8	7	9	3	10	6	4	0.1
f_{11}	2	5	3	8	9	7	6	1	10	4	0.53
f_{12}	2	5	8	3	7	9	1	10	6	4	0.45
f_{13}	2	5	3	8	9	7	10	1	6	4	0.45
f_{14}	2	8	5	3	7	9	10	1	4	6	0.55
f_{15}	2	5	3	8	9	7	1	6	10	4	0.5
f_{16}	2	5	8	7	9	3	1	10	6	4	0.38
f_{17}	2	5	3	8	9	7	6	1	10	4	0.53
f_{18}	2	5	3	7	8	9	10	6	1	4	0.39
f_{19}	2	8	3	5	7	9	4	10	1	6	0.73
f_{20}	2	7	8	3	5	9	4	10	1	6	0.65

(b) Comparison between texture features of WT and visual feature of regularity

Subjects	1	10	5	6	7	4	9	3	2	8	$ r_s $
f_1	10	2	4	7	9	3	1	8	5	6	0.09
f_2	5	2	7	10	1	9	8	3	6	4	0.22
f_3	2	5	9	8	3	1	7	6	10	4	0.43
f_4	5	2	1	7	8	9	3	10	6	4	0.02
f_5	2	5	3	8	9	7	1	6	10	4	0.5
f_6	5	2	7	1	3	8	10	9	6	4	0.04
f_7	2	5	3	8	9	6	7	10	1	4	0.54
f_8	2	5	7	8	3	9	10	6	1	4	0.43
f_9	2	5	8	3	9	1	7	6	10	4	0.48
f_{10}	2	5	1	8	7	9	3	10	6	4	0.12
f_{11}	2	5	3	8	9	7	6	1	10	4	0.54
f_{12}	2	5	8	3	7	9	1	10	6	4	0.48
f_{13}	2	5	3	8	9	7	10	1	6	4	0.49
f_{14}	2	8	5	3	7	9	10	1	4	6	0.6
f_{15}	2	5	3	8	9	7	1	6	10	4	0.5
f_{16}	2	5	8	7	9	3	1	10	6	4	0.43
f_{17}	2	5	3	8	9	7	6	1	10	4	0.54
f_{18}	2	5	3	7	8	9	10	6	1	4	0.44

f_{19}	2	8	3	5	7	9	4	10	1	6	0.77
f_{20}	2	7	8	3	5	9	4	10	1	6	0.7

(c) Comparison between texture features of WT and visual feature of directionality

Table A9.5 Comparison between texture features of GT with visual feature perception

Subjects	3	8	9	2	6	5	10	4	1	7	$ r_s $
f_1	5	2	3	7	8	9	1	6	10	4	0.35
f_2	5	2	3	8	9	6	10	4	7	1	0.73
f_3	5	2	3	8	9	6	1	4	10	7	0.70
f_4	5	2	1	8	9	7	3	6	10	4	0.14
f_5	5	2	8	3	9	6	7	10	1	4	0.65
f_6	2	5	3	8	9	1	6	10	7	4	0.66
f_7	2	5	3	7	8	1	9	6	10	4	0.30
f_8	5	2	3	8	9	7	6	10	4	1	0.61
f_9	5	2	8	3	9	7	6	1	10	4	0.56
f_{10}	2	5	1	8	9	7	3	6	10	4	0.16
f_{11}	2	5	3	9	8	7	6	10	1	4	0.61
f_{12}	2	5	3	8	9	1	7	6	10	4	0.56
f_{13}	2	3	5	8	7	9	1	10	6	4	0.50
f_{14}	2	5	3	8	9	7	10	6	1	4	0.60
f_{15}	2	5	8	3	9	7	10	1	4	6	0.50
f_{16}	2	5	8	9	3	1	7	10	6	4	0.50
f_{17}	2	5	3	8	9	7	10	1	6	4	0.55
f_{18}	2	5	3	8	9	7	10	1	6	4	0.55
f_{19}	2	5	3	6	7	8	9	1	10	4	0.42
f_{20}	2	5	8	3	7	9	10	4	1	6	0.43
f_{21}	2	8	3	5	9	7	1	4	10	6	0.58
f_{22}	2	5	3	8	7	9	6	1	10	4	0.52
f_{23}	2	3	8	5	9	7	1	4	10	6	0.59
f_{24}	2	5	3	8	7	9	1	10	6	4	0.44
f_{25}	7	2	5	1	6	8	3	9	10	4	0.24
f_{26}	5	2	10	8	3	9	4	6	7	1	0.48
f_{27}	2	5	6	1	8	9	3	4	10	7	0.32
f_{28}	5	1	7	2	9	8	3	6	10	4	0.19
f_{29}	5	2	6	8	9	3	4	10	7	1	0.58
f_{30}	5	2	10	8	1	3	9	7	6	4	0.21
f_{31}	2	5	7	1	3	6	8	10	9	4	0.10
f_{32}	5	2	7	8	10	3	6	9	4	1	0.14
f_{33}	5	2	7	8	1	9	6	10	4	3	0.18
f_{34}	1	2	5	7	9	8	10	3	4	6	0.26
f_{35}	2	5	7	9	8	6	10	3	4	1	0.18
f_{36}	2	5	7	1	10	8	3	6	9	4	0.24
f_{37}	2	3	8	7	1	9	5	10	6	4	0.43
f_{38}	2	5	8	10	3	9	7	6	4	1	0.52
f_{39}	2	8	9	3	5	7	10	1	4	6	0.62
f_{40}	2	1	9	8	7	3	5	10	4	6	0.15

f_{41}	2	8	9	3	5	7	10	1	4	6	0.62
f_{42}	2	5	8	3	10	9	7	1	6	4	0.53
f_{43}	2	5	7	3	8	6	9	1	4	10	0.27
f_{44}	2	8	7	3	5	9	10	4	6	1	0.43
f_{45}	2	8	7	3	9	5	4	10	1	6	0.41
f_{46}	2	5	7	1	9	8	3	6	4	10	0.05
f_{47}	2	7	8	3	9	5	10	4	1	6	0.32
f_{48}	2	8	7	5	3	9	10	4	1	6	0.32

(a) Comparison between texture features of GT and visual feature of coarseness

Subjects	10	1	5	6	7	4	9	2	3	8	$ r_s $
f_1	5	2	3	7	8	9	1	6	10	4	0.36
f_2	5	2	3	8	9	6	10	4	7	1	0.45
f_3	5	2	3	8	9	6	1	4	10	7	0.44
f_4	5	2	1	8	9	7	3	6	10	4	0.1
f_5	5	2	8	3	9	6	7	10	1	4	0.45
f_6	2	5	3	8	9	1	6	10	7	4	0.41
f_7	2	5	3	7	8	1	9	6	10	4	0.36
f_8	5	2	3	8	9	7	6	10	4	1	0.5
f_9	5	2	8	3	9	7	6	1	10	4	0.48
f_{10}	2	5	1	8	9	7	3	6	10	4	0.16
f_{11}	2	5	3	9	8	7	6	10	1	4	0.48
f_{12}	2	5	3	8	9	1	7	6	10	4	0.47
f_{13}	2	3	5	8	7	9	1	10	6	4	0.52
f_{14}	2	5	3	8	9	7	10	6	1	4	0.48
f_{15}	2	5	8	3	9	7	10	1	4	6	0.49
f_{16}	2	5	8	9	3	1	7	10	6	4	0.42
f_{17}	2	5	3	8	9	7	10	1	6	4	0.45
f_{18}	2	5	3	8	9	7	10	1	6	4	0.45
f_{19}	2	5	3	6	7	8	9	1	10	4	0.32
f_{20}	2	5	8	3	7	9	10	4	1	6	0.52
f_{21}	2	8	3	5	9	7	1	4	10	6	0.72
f_{22}	2	5	3	8	7	9	6	1	10	4	0.5
f_{23}	2	3	8	5	9	7	1	4	10	6	0.71
f_{24}	2	5	3	8	7	9	1	10	6	4	0.44
f_{25}	7	2	5	1	6	8	3	9	10	4	0.04
f_{26}	5	2	10	8	3	9	4	6	7	1	0.18
f_{27}	2	5	6	1	8	9	3	4	10	7	0.08
f_{28}	5	1	7	2	9	8	3	6	10	4	0.13
f_{29}	5	2	6	8	9	3	4	10	7	1	0.33
f_{30}	5	2	10	8	1	3	9	7	6	4	0.1
f_{31}	2	5	7	1	3	6	8	10	9	4	0.05
f_{32}	5	2	7	8	10	3	6	9	4	1	0.14
f_{33}	5	2	7	8	1	9	6	10	4	3	0.04
f_{34}	1	2	5	7	9	8	10	3	4	6	0.15
f_{35}	2	5	7	9	8	6	10	3	4	1	0.22
f_{36}	2	5	7	1	10	8	3	6	9	4	0.21
f_{37}	2	3	8	7	1	9	5	10	6	4	0.6

f_{38}	2	5	8	10	3	9	7	6	4	1	0.32
f_{39}	2	8	9	3	5	7	10	1	4	6	0.67
f_{40}	2	1	9	8	7	3	5	10	4	6	0.33
f_{41}	2	8	9	3	5	7	10	1	4	6	0.67
f_{42}	2	5	8	3	10	9	7	1	6	4	0.35
f_{43}	2	5	7	3	8	6	9	1	4	10	0.42
f_{44}	2	8	7	3	5	9	10	4	6	1	0.67
f_{45}	2	8	7	3	9	5	4	10	1	6	0.76
f_{46}	2	5	7	1	9	8	3	6	4	10	0.14
f_{47}	2	7	8	3	9	5	10	4	1	6	0.64
f_{48}	2	8	7	5	3	9	10	4	1	6	0.58

(b) Comparison between texture features of GT and visual feature of regularity

Subjects	1	10	5	6	7	4	9	3	2	8	$ r_s $
f_1	5	2	3	7	8	9	1	6	10	4	0.35
f_2	5	2	3	8	9	6	10	4	7	1	0.5
f_3	5	2	3	8	9	6	1	4	10	7	0.43
f_4	5	2	1	8	9	7	3	6	10	4	0.09
f_5	5	2	8	3	9	6	7	10	1	4	0.49
f_6	2	5	3	8	9	1	6	10	7	4	0.41
f_7	2	5	3	7	8	1	9	6	10	4	0.35
f_8	5	2	3	8	9	7	6	10	4	1	0.54
f_9	5	2	8	3	9	7	6	1	10	4	0.49
f_{10}	2	5	1	8	9	7	3	6	10	4	0.16
f_{11}	2	5	3	9	8	7	6	10	1	4	0.52
f_{12}	2	5	3	8	9	1	7	6	10	4	0.45
f_{13}	2	3	5	8	7	9	1	10	6	4	0.52
f_{14}	2	5	3	8	9	7	10	6	1	4	0.53
f_{15}	2	5	8	3	9	7	10	1	4	6	0.54
f_{16}	2	5	8	9	3	1	7	10	6	4	0.44
f_{17}	2	5	3	8	9	7	10	1	6	4	0.49
f_{18}	2	5	3	8	9	7	10	1	6	4	0.49
f_{19}	2	5	3	6	7	8	9	1	10	4	0.33
f_{20}	2	5	8	3	7	9	10	4	1	6	0.58
f_{21}	2	8	3	5	9	7	1	4	10	6	0.72
f_{22}	2	5	3	8	7	9	6	1	10	4	0.52
f_{23}	2	3	8	5	9	7	1	4	10	6	0.7
f_{24}	2	5	3	8	7	9	1	10	6	4	0.45
f_{25}	7	2	5	1	6	8	3	9	10	4	0.04
f_{26}	5	2	10	8	3	9	4	6	7	1	0.3
f_{27}	2	5	6	1	8	9	3	4	10	7	0.09
f_{28}	5	1	7	2	9	8	3	6	10	4	0.18
f_{29}	5	2	6	8	9	3	4	10	7	1	0.41
f_{30}	5	2	10	8	1	3	9	7	6	4	0.03
f_{31}	2	5	7	1	3	6	8	10	9	4	0.05
f_{32}	5	2	7	8	10	3	6	9	4	1	0.25
f_{33}	5	2	7	8	1	9	6	10	4	3	0.02
f_{34}	1	2	5	7	9	8	10	3	4	6	0.15

f_{35}	2	5	7	9	8	6	10	3	4	1	0.35
f_{36}	2	5	7	1	10	8	3	6	9	4	0.15
f_{37}	2	3	8	7	1	9	5	10	6	4	0.58
f_{38}	2	5	8	10	3	9	7	6	4	1	0.44
f_{39}	2	8	9	3	5	7	10	1	4	6	0.72
f_{40}	2	1	9	8	7	3	5	10	4	6	0.32
f_{41}	2	8	9	3	5	7	10	1	4	6	0.72
f_{42}	2	5	8	3	10	9	7	1	6	4	0.42
f_{43}	2	5	7	3	8	6	9	1	4	10	0.43
f_{44}	2	8	7	3	5	9	10	4	6	1	0.75
f_{45}	2	8	7	3	9	5	4	10	1	6	0.81
f_{46}	2	5	7	1	9	8	3	6	4	10	0.14
f_{47}	2	7	8	3	9	5	10	4	1	6	0.7
f_{48}	2	8	7	5	3	9	10	4	1	6	0.65

(c) Comparison between texture features of GT and visual feature of directionality

Appendix 10: Comparison Similarity Measurements between Computational Texture Methods and Subjects

Contents:

Table A10.1 Comparison between computational methods and subjects in similarity measurements for query 1

Table A10.2 Comparison between computational methods and subjects in similarity measurements for query 2

Table A10.3 Comparison between computational methods and subjects in similarity measurements for query 3

Table A10.4 Comparison between computational methods and subjects in similarity measurements for query 5

Table A10.5 Comparison between computational methods and subjects in similarity measurements for query 8

Table A10.6 Comparison between computational methods and subjects in similarity measurements for query 9

Table A10.7 Comparison between computational methods and subjects in similarity measurements for query 10

In Tables A10.1-A10.7, the first row is the ranking done by subjects and the other rows are retrieval results calculating by five computational methods. The numbers from column 2 to 10 in Tables A10.1-A10.7 are the ID numbers of ranking images in the order from most similar to least similar to each query image. The last column is the coefficients of rank correlation between computation methods and subjects.

Table A10.1 Comparison between computational methods and subjects in similarity measurements for query 1

Subjects	5	10	7	6	4	2	9	3	8	r_s
<i>GLCM</i>	7	9	6	3	8	5	4	10	2	-0.13
<i>MRSAR</i>	10	4	6	9	7	3	8	5	2	0.25
<i>FT</i>	9	7	6	5	3	8	4	10	2	0.05
<i>WT</i>	6	10	7	9	8	4	3	5	2	0.22
<i>GT</i>	6	10	7	4	9	8	3	5	2	0.32

Table A10.2 Comparison between computational methods and subjects in similarity measurements for query 2

Subjects	9	3	8	6	5	4	7	10	1	r_s
<i>GLCM</i>	5	3	9	7	8	1	6	4	10	0.53
<i>MRSAR</i>	8	3	9	7	4	5	1	10	6	0.60
<i>FT</i>	7	4	10	9	3	8	1	5	6	-0.18
<i>WT</i>	5	8	3	7	9	1	10	6	4	0.35
<i>GT</i>	5	8	3	7	9	1	6	10	4	0.42

Table A10.3 Comparison between computational methods and subjects in similarity measurements for query 3

Subjects	9	8	2	6	5	4	7	1	10	r_s
<i>GLCM</i>	9	7	8	1	5	6	2	4	10	0.45
<i>MRSAR</i>	9	8	7	1	10	4	6	5	2	0.15
<i>FT</i>	9	8	7	4	1	6	5	2	10	0.48
<i>WT</i>	8	9	7	1	10	6	5	4	2	0.18
<i>GT</i>	8	9	7	6	10	1	4	5	2	0.30

Table A10.4 Comparison between computational methods and subjects in similarity measurements for query 5

Subjects	6	1	10	7	4	9	2	8	3	r_s
<i>GLCM</i>	3	2	9	7	8	1	6	4	10	-0.70
<i>MRSAR</i>	10	1	6	9	3	4	8	7	2	0.58
<i>FT</i>	6	1	8	7	3	9	10	4	2	0.42
<i>WT</i>	8	3	9	7	2	1	6	10	4	-0.70
<i>GT</i>	8	2	3	7	9	1	6	10	4	-0.70

Table A10.5 Comparison between computational methods and subjects in similarity measurements for query 8

Subjects	9	3	2	6	5	4	7	1	10	r_s
<i>GLCM</i>	9	7	6	3	1	5	4	2	10	0.45
<i>MRSAR</i>	3	9	7	4	1	10	6	2	5	0.25
<i>FT</i>	3	9	7	6	1	5	4	2	10	0.55
<i>WT</i>	3	9	7	1	10	6	5	4	2	0.18
<i>GT</i>	3	9	7	6	10	1	5	4	2	0.32

Table A10.6 Comparison between computational methods and subjects in similarity measurements for query 9

Subjects	3	8	2	6	5	4	7	1	10	r_s
<i>GLCM</i>	7	1	8	3	6	5	4	2	10	0.08
<i>MRSAR</i>	8	3	7	1	4	10	6	5	2	0.18
<i>FT</i>	3	7	8	4	1	6	5	2	10	0.40
<i>WT</i>	8	3	7	1	10	6	4	5	2	0.17
<i>GT</i>	8	3	7	10	6	1	4	5	2	0.22

Table A10.7 Comparison between computational methods and subjects in similarity measurements for query 10

Subjects	1	7	4	5	6	2	9	3	8	r_s
<i>GLCM</i>	4	6	1	8	7	9	3	5	2	0.35
<i>MRSAR</i>	1	4	6	9	7	3	8	5	2	0.53
<i>FT</i>	4	1	7	2	9	3	5	6	8	0.70
<i>WT</i>	6	4	1	7	9	3	8	5	2	0.48
<i>GT</i>	4	6	9	1	7	3	8	5	2	0.33

Appendix 11: Rank Correlation between Visual Similarity Measurements and Visual Texture Features

Contents:

Table A11.1 Rank correlation between visual similarity measurements and visual texture feature for query 1

Table A11.2 Rank correlation between visual similarity measurements and visual texture feature for query 2

Table A11.3 Rank correlation between visual similarity measurements and visual texture feature for query 3

Table A11.4 Rank correlation between visual similarity measurements and visual texture feature for query 5

Table A11.5 Rank correlation between visual similarity measurements and visual texture feature for query 8

Table A11.6 Rank correlation between visual similarity measurements and visual texture feature for query 9

Table A11.7 Rank correlation between visual similarity measurements and visual texture feature for query 10

In Table A11.1-A11.7, the first row is the ranking based on human similarity measurements for query images and the other rows are the corresponding rankings for query image based on coarseness, regularity and directionality respectively. The numbers from column 2 to 10 in Table A11.1-A11.7 are the ID numbers of ranking images in order from most similar to less similar for query images. The last column is the coefficients of rank correlation between visual similarity measurements and the corresponding visual texture feature.

Table A11.1 Rank correlation between visual similarity measurements and visual texture feature for query 1

Subjects	5	10	7	6	4	2	9	3	8	r_s
Coarseness	7	4	5	10	6	2	8	9	3	0.77
Regularity	5	6	10	7	4	9	2	3	8	0.93
Directionality	10	5	6	7	4	9	3	2	8	0.92

Table A11.2 Rank correlation between visual similarity measurements and visual texture feature for query 2

Subjects	9	3	8	6	5	4	7	10	1	r_s
Coarseness	9	8	6	5	10	4	1	3	7	0.53
Regularity	3	8	9	4	7	6	1	5	10	0.73
Directionality	3	8	9	4	7	6	5	10	1	0.82

Table A11.3 Rank correlation between visual similarity measurements and visual texture feature for query 3

Subjects	9	8	2	6	5	4	7	1	10	r_s
Coarseness	8	9	2	6	5	10	4	1	7	0.87
Regularity	2	8	9	4	7	6	1	5	10	0.75
Directionality	9	2	8	4	7	6	5	10	1	0.83

Table A11.4 Rank correlation between visual similarity measurements and visual texture feature for query 5

Subjects	6	1	10	7	4	9	2	8	3	r_s
Coarseness	6	10	4	2	9	1	8	7	3	0.60
Regularity	1	10	6	7	4	9	2	3	8	0.93
Directionality	6	7	4	10	9	1	3	2	8	0.73

Table A11.5 Rank correlation between visual similarity measurements and visual texture feature for query 8

Subjects	9	3	2	6	5	4	7	1	10	r_s
Coarseness	9	2	6	5	10	4	3	1	7	0.60
Regularity	3	2	9	4	7	6	1	5	10	0.77
Directionality	2	3	9	4	7	6	5	10	1	0.78

Table A11.6 Rank correlation between visual similarity measurements and visual texture feature for query 9

Subjects	3	8	2	6	5	4	7	1	10	r_s
Coarseness	2	8	6	5	10	4	1	3	7	0.37
Regularity	4	7	2	3	8	6	1	5	10	0.32
Directionality	3	2	4	8	7	6	5	10	1	0.77

Table A11.7 Rank correlation between visual similarity measurements and visual texture feature for query 10

Subjects	1	7	4	5	6	2	9	3	8	r_s
Coarseness	4	5	6	1	7	2	9	8	3	0.73
Regularity	5	1	6	7	4	9	2	3	8	0.80
Directionality	1	5	6	7	4	9	3	2	8	0.82

Appendix 12: Comparison between Subjects and Computational Texture Methods for Image Retrieval after Classification

Contents:

Table A12.1 Comparison between computational methods and subjects in similarity measurements for query 1 after classification

Table A12.2 Comparison between computational methods and subjects in similarity measurements for query 2 after classification

Table A12.3 Comparison between computational methods and subjects in similarity measurements for query 3 after classification

Table A12.4 Comparison between computational methods and subjects in similarity measurements for query 5 after classification

Table A12.5 Comparison between computational methods and subjects in similarity measurements for query 8 after classification

Table A12.6 Comparison between computational methods and subjects in similarity measurements for query 9 after classification

Table A12.7 Comparison between computational methods and subjects in similarity measurements for query 10 after classification

In Tables A12.1-A12.7, the first row is the ranking done by subjects and the other rows are retrieval results calculating by five computational methods after classification. The numbers from column 2 to 10 in Tables A12.1-A12.7 are the ID numbers of ranking images in order from most similar to less similar for query images. The last column is the coefficients of rank correlation between computation methods and subjects.

Table A12.1 Comparison between computational methods and subjects in similarity measurements for query 1 after classification

Subjects	5	10	7	6	4	2	9	3	8	r_s
<i>GLCM</i>	7	10	6	5	4	9	3	8	2	0.78
<i>MRSAR</i>	10	7	4	6	5	9	3	8	2	0.72
<i>FT</i>	7	10	6	5	4	9	3	8	2	0.78
<i>WT</i>	10	7	6	4	5	9	8	3	2	0.72
<i>GT</i>	10	7	6	4	5	9	8	3	2	0.72

Table A12.2 Comparison between computational methods and subjects in similarity measurements for query 2 after classification

Subjects	9	3	8	6	5	4	7	10	1	r_s
<i>GLCM</i>	3	9	8	5	6	4	7	1	10	0.95
<i>MRSAR</i>	8	3	9	4	5	6	7	1	10	0.85
<i>FT</i>	9	3	8	4	5	6	7	10	1	0.93
<i>WT</i>	8	3	9	5	6	4	7	1	10	0.90
<i>GT</i>	8	3	9	5	6	4	7	1	10	0.90

Table A12.3 Comparison between computational methods and subjects in similarity measurements for query 3 after classification

Subjects	9	8	2	6	5	4	7	1	10	r_s
<i>GLCM</i>	9	8	2	5	6	4	7	1	10	0.98
<i>MRSAR</i>	9	8	2	4	6	5	7	1	10	0.95
<i>FT</i>	9	8	2	4	6	5	7	1	10	0.95
<i>WT</i>	8	9	2	6	5	4	7	1	10	0.98
<i>GT</i>	8	9	2	6	4	5	7	10	1	0.95

Table A12.4 Comparison between computational methods and subjects in similarity measurements for query 5 after classification

Subjects	6	1	10	7	4	9	2	8	3	r_s
<i>GLCM</i>	6	4	7	1	10	3	2	9	8	0.73
<i>MRSAR</i>	6	4	10	1	7	9	3	8	2	0.82
<i>FT</i>	6	4	1	7	10	9	3	8	2	0.82
<i>WT</i>	6	4	7	1	10	8	3	9	2	0.72
<i>GT</i>	6	4	7	1	10	8	2	3	9	0.73

Table A12.5 Comparison between computational methods and subjects in similarity measurements for query 8 after classification

Subjects	9	3	2	6	5	4	7	1	10	r_s
<i>GLCM</i>	9	3	2	6	5	4	7	1	10	1.00
<i>MRSAR</i>	3	9	2	4	6	5	7	1	10	0.93
<i>FT</i>	3	9	2	6	5	4	7	1	10	0.98
<i>WT</i>	3	9	2	6	5	4	7	1	10	0.98
<i>GT</i>	3	9	2	6	5	4	7	10	1	0.97

Table A12.6 Comparison between computational methods and subjects in similarity measurements for query 9 after classification

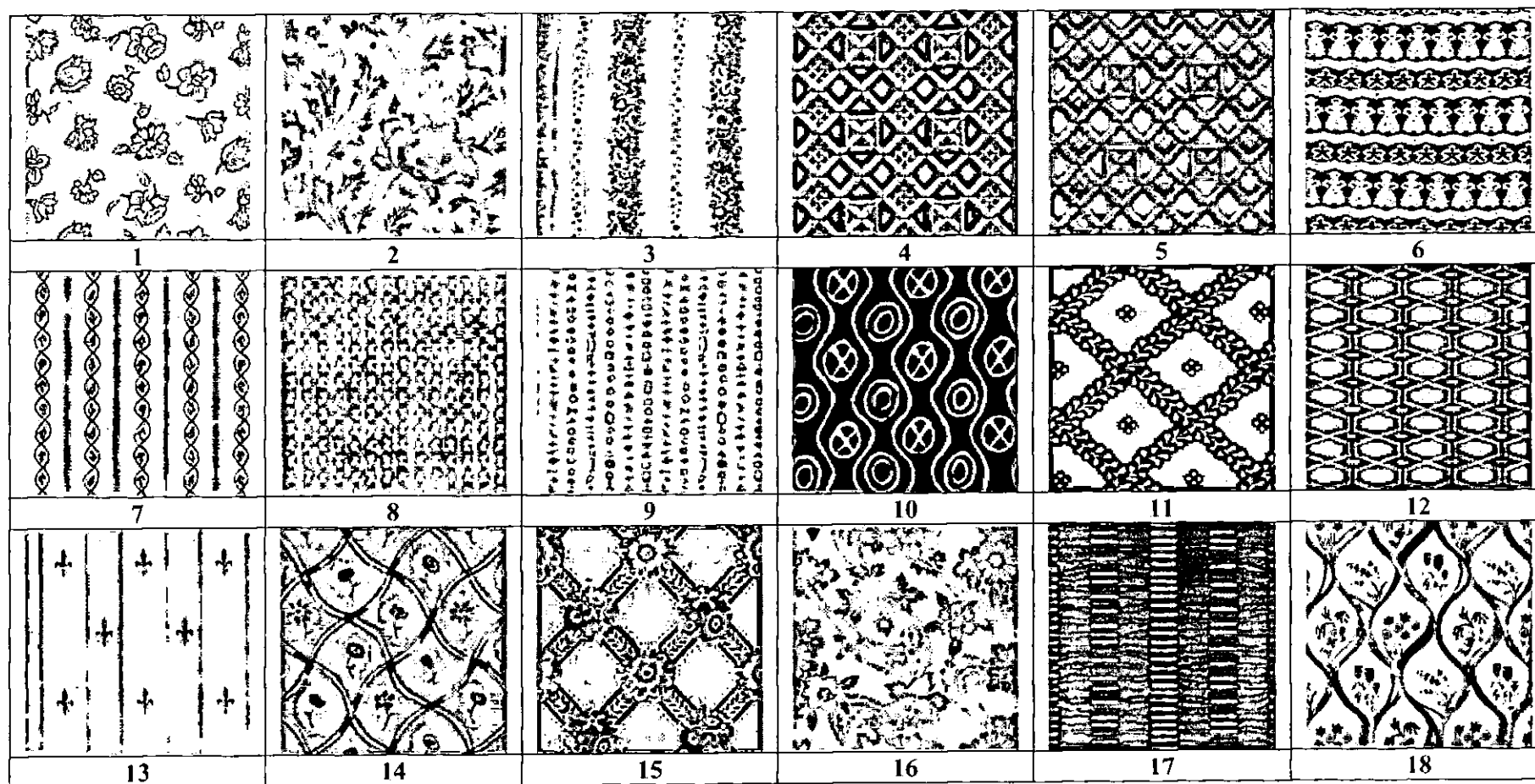
Subjects	3	8	2	6	5	4	7	1	10	r_s
<i>GLCM</i>	8	3	2	6	5	4	7	1	10	0.98
<i>MRSAR</i>	8	3	2	4	6	5	7	1	10	0.93
<i>FT</i>	3	8	2	4	6	5	7	1	10	0.95
<i>WT</i>	8	3	2	6	5	4	7	1	10	0.98
<i>GT</i>	8	3	2	6	5	4	7	10	1	0.97

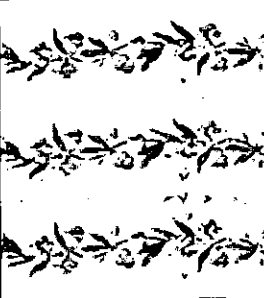
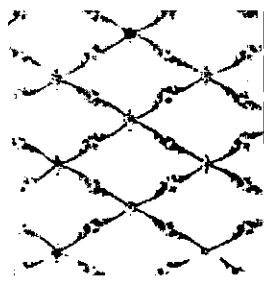
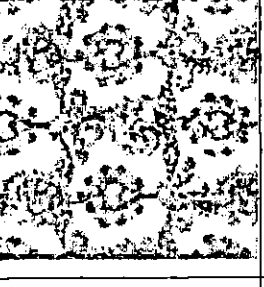
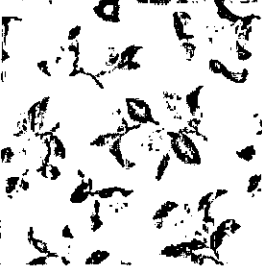
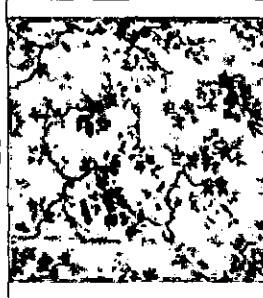
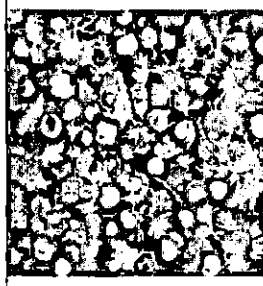
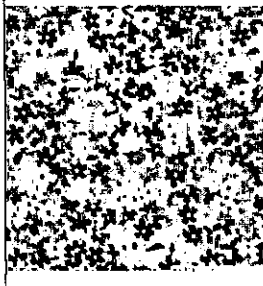
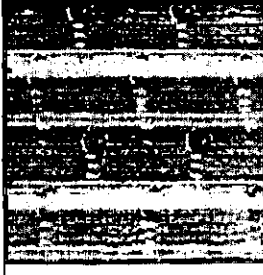
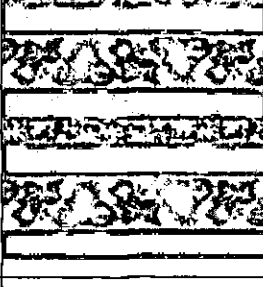
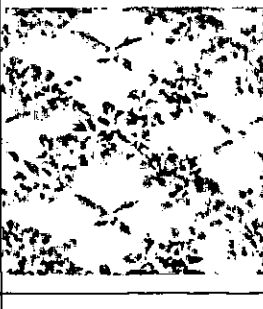
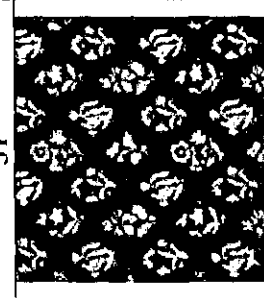
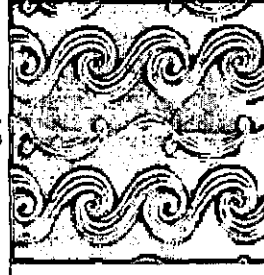
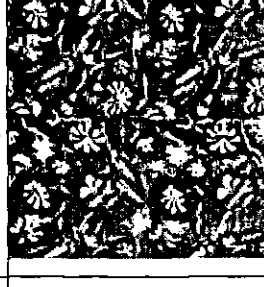
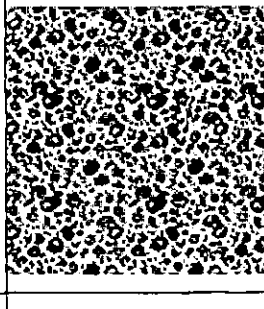
Table A12.7 Comparison between computational methods and subjects in similarity measurements for query 10 after classification

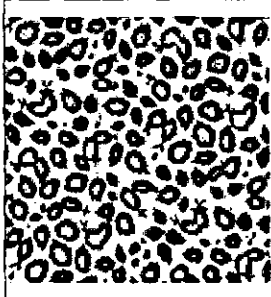
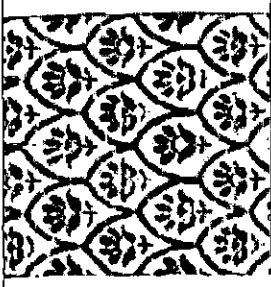
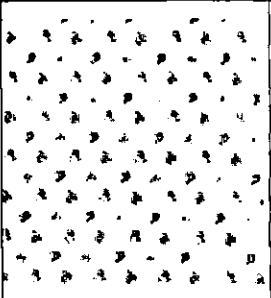
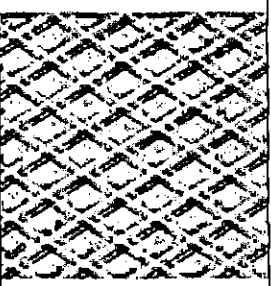
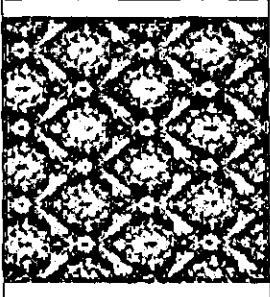
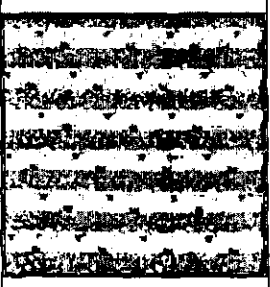
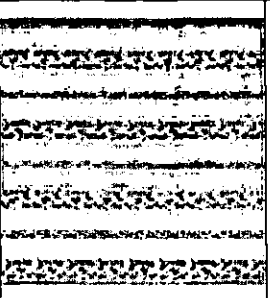
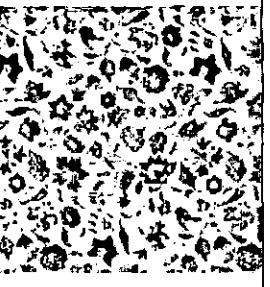
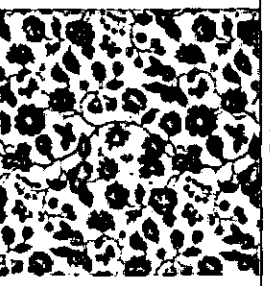
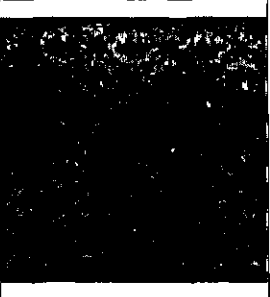
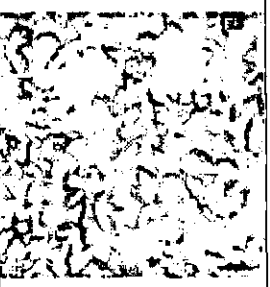
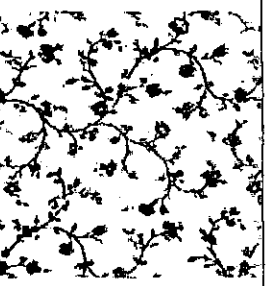
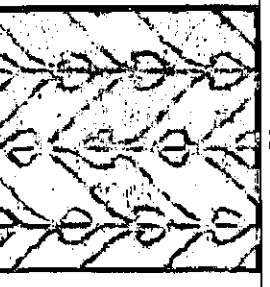
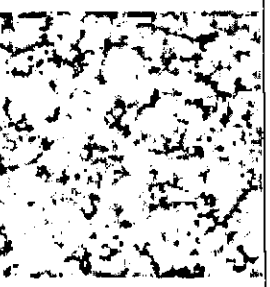
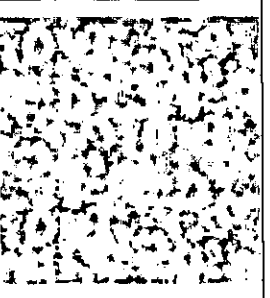
Subjects	1	7	4	5	6	2	9	3	8	r_s
<i>GLCM</i>	1	7	4	6	5	8	9	3	2	0.83
<i>MRSAR</i>	1	7	4	6	5	9	3	8	2	0.88
<i>FT</i>	1	7	4	5	6	2	9	3	8	1.00
<i>WT</i>	1	7	6	5	4	9	3	8	2	0.83
<i>GT</i>	1	7	4	6	5	9	3	8	2	0.88

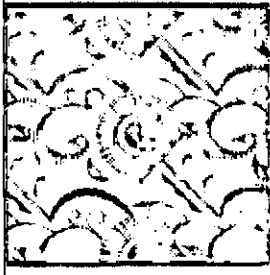
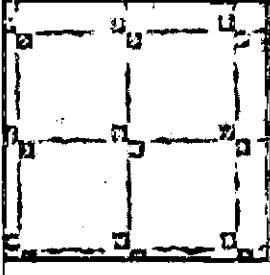
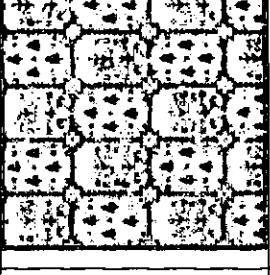
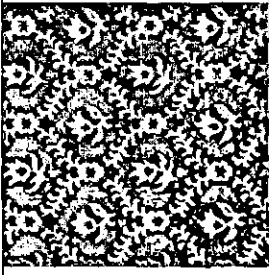
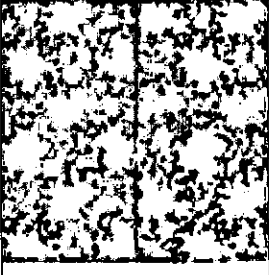
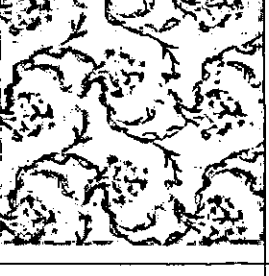
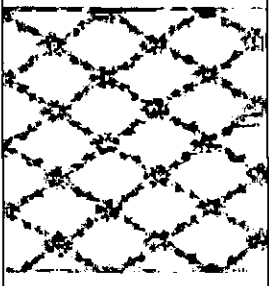
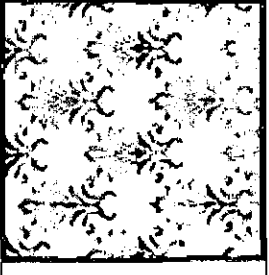
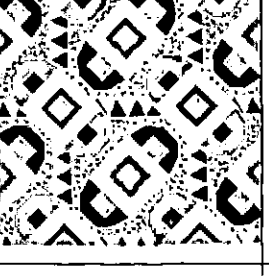
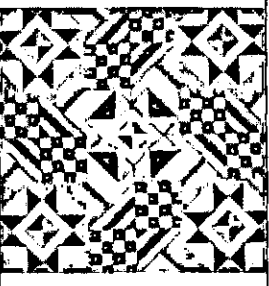
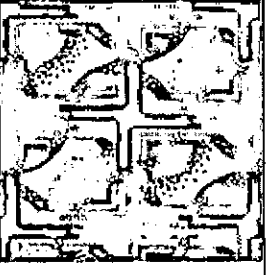
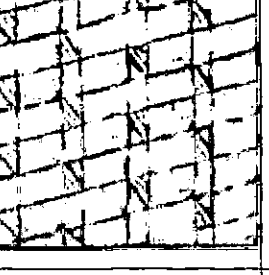
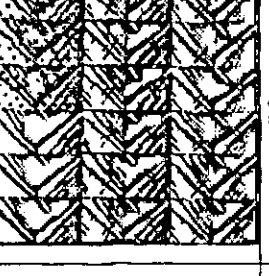
Appendix 13: One Hundred Test Wallpaper Images

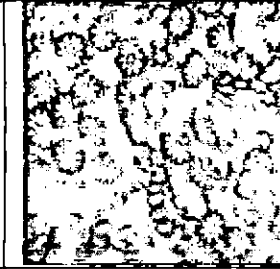
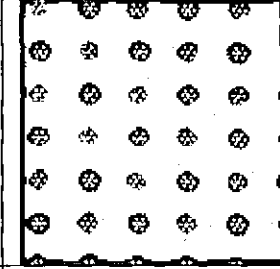
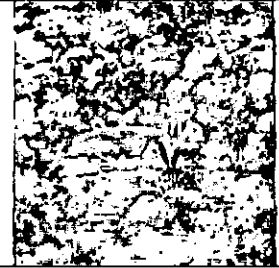
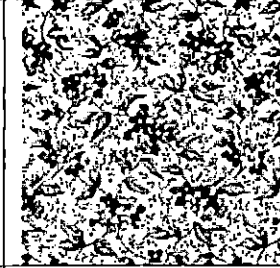
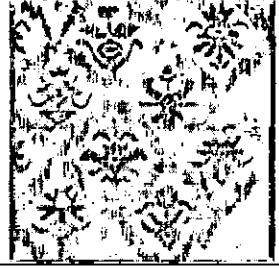
For the purpose of texture analysis, the sample images are converted to grey-level images and normalized to the same size of 512×512 pixels. The number below each image is the ID number of the image in the 100 image dataset.



					
43	44	45	46	47	48
					
49	50	51	52	53	54
					
55	56	57	58	59	60
					
61	62	63	64	65	66

					
91	92	93	94	95	96
					
97	98	99	100		

Appendix 14: Rankings for Nine Queries in One Hundred Images by Subjects

Contents:

- Table A14.1 Rankings for query 1
- Table A14.2 Rankings for query 2
- Table A14.3 Rankings for query 3
- Table A14.4 Rankings for query 4
- Table A14.5 Rankings for query 5
- Table A14.6 Rankings for query 6
- Table A14.7 Rankings for query 7
- Table A14.8 Rankings for query 8
- Table A14.9 Rankings for query 9

In Tables A14.1-A14.9, the entry T_{nm} of table expresses the ID number of images in 100 image dataset ranked in the m^{th} position by the n^{th} subject, where the subscription n, m of T_{nm} represents the number of row and column respectively.

Table A14.1 Rankings for query 1

Subjects	Ranking results								
Subject 1	79	100	36	20	49	78	57	18	11
Subject 2	14	18	74	11	79	46	5	4	20
Subject 3	79	49	20	36	57	18	14	74	44
Subject 4	36	44	18	20	11	100	57	49	38
Subject 5	20	79	74	46	38	55	11	36	100
Subject 6	74	38	79	20	11	14	100	18	44
Subject 7	100	74	79	57	44	24	20	18	44
Subject 8	11	14	36	44	46	55	74	79	100
Subject 9	55	74	100	18	14	15	73	49	38
Subject 10	20	74	38	79	11	14	100	18	44
Subject 11	38	20	74	79	37	49	46	55	5
Subject 12	20	46	55	11	14	74	100	79	44
Subject 13	55	79	37	38	5	4	46	36	12

Table A14.2 Rankings for query 2

Subjects	Ranking results								
Subject 1	30	29	77	47	92	96	97	47	98
Subject 2	30	27	96	48	47	29	92	2	66
Subject 3	31	30	77	27	47	82	92	48	28
Subject 4	77	80	96	97	31	30	2	48	47
Subject 5	27	77	48	30	97	2	47	29	52
Subject 6	27	30	48	47	2	31	52	77	97
Subject 7	31	96	99	91	98	80	77	66	52
Subject 8	77	64	52	27	47	1	18	67	2
Subject 9	48	47	52	77	80	97	2	31	32
Subject 10	27	30	48	47	2	31	52	77	97
Subject 11	30	47	2	52	77	97	98	27	66
Subject 12	80	62	53	77	52	64	47	2	18
Subject 13	66	52	28	2	56	16	27	1	76

Table A14.3 Rankings for query 3

Subjects	Ranking results								
Subject 1	3	35	51	39	7	19	17	50	34
Subject 2	3	50	51	35	13	7	39	19	34
Subject 3	3	39	35	51	7	13	6	61	50
Subject 4	51	50	3	13	7	39	19	35	94
Subject 5	13	3	7	35	34	39	50	51	19
Subject 6	3	13	39	51	35	34	50	7	19
Subject 7	13	51	39	35	7	3	13	35	34
Subject 8	3	39	35	13	50	7	51	13	34
Subject 9	3	13	7	51	39	35	50	17	34
Subject 10	3	13	35	34	51	39	50	7	19
Subject 11	13	35	51	50	3	39	7	34	19
Subject 12	3	50	51	7	39	13	34	35	12
Subject 13	3	7	50	51	39	35	24	13	59

Table A14.4 Rankings for query 4

Subjects	Ranking results								
Subject 1	87	69	85	4	5	89	46	14	11
Subject 2	69	87	90	26	84	85	89	4	5
Subject 3	69	87	86	88	23	84	15	75	81
Subject 4	85	90	87	84	86	69	4	89	88
Subject 5	69	87	88	86	85	84	15	22	23
Subject 6	69	87	86	23	81	88	84	85	11
Subject 7	59	85	84	86	87	59	11	15	60
Subject 8	15	85	49	87	69	79	11	69	14
Subject 9	84	85	89	57	87	88	46	38	69
Subject 10	69	87	86	23	11	81	88	84	85
Subject 11	69	87	86	85	23	100	73	4	5
Subject 12	5	69	79	15	49	85	14	11	22
Subject 13	86	69	87	88	84	85	78	14	15

Table A14.5 Rankings for query 5

Subjects	Ranking results								
Subject 1	31	30	58	97	27	48	47	29	96
Subject 2	47	48	29	30	27	97	66	77	80
Subject 3	31	96	30	66	97	77	29	98	30
Subject 4	77	67	64	48	47	31	30	29	98
Subject 5	31	29	48	77	47	97	67	27	30
Subject 6	29	31	27	30	47	48	77	52	97
Subject 7	31	21	91	92	96	64	66	77	28
Subject 8	47	28	31	27	21	48	29	30	97
Subject 9	31	27	48	2	52	66	58	47	28
Subject 10	31	21	27	30	47	48	77	52	97
Subject 11	31	47	77	97	29	30	16	2	66
Subject 12	64	16	21	27	31	48	30	97	47
Subject 13	66	67	76	52	48	2	28	31	80

Table A14.6 Rankings for query 6

Subjects	Ranking results								
Subject 1	95	74	37	49	100	79	45	44	75
Subject 2	74	49	55	10	4	5	73	70	15
Subject 3	37	55	95	4	24	38	44	49	74
Subject 4	37	95	49	15	55	46	24	13	8
Subject 5	37	55	95	74	10	18	44	75	49
Subject 6	37	55	49	75	74	44	1	24	53
Subject 7	37	95	32	15	10	12	41	74	95
Subject 8	37	13	44	74	55	70	81	95	49
Subject 9	37	70	81	44	74	79	55	1	36
Subject 10	37	55	75	74	49	44	1	24	53
Subject 11	37	74	55	14	95	70	75	49	1
Subject 12	37	1	49	13	44	55	74	95	70
Subject 13	37	79	6	55	70	36	71	78	100

Table A14.7 Rankings for query 7

Subjects	Ranking results								
Subject 1	63	93	33	62	56	75	99	42	32
Subject 2	32	41	54	53	63	1	93	43	33
Subject 3	32	63	33	53	54	43	72	41	93
Subject 4	33	91	41	72	33	41	29	43	53
Subject 5	32	29	30	53	63	99	33	93	1
Subject 6	32	29	63	30	53	33	1	99	93
Subject 7	32	41	43	42	53	54	72	98	63
Subject 8	56	64	82	77	92	48	32	33	1
Subject 9	32	60	98	64	33	41	77	30	53
Subject 10	32	29	63	30	53	76	99	1	93
Subject 11	63	32	75	53	1	41	92	72	48
Subject 12	63	62	56	64	82	48	32	33	1
Subject 13	63	62	32	33	64	91	99	72	93

Table A14.8 Rankings for query 8

Subjects	Ranking results								
Subject 1	18	78	57	20	79	11	4	5	46
Subject 2	44	18	14	100	74	49	55	5	4
Subject 3	44	18	14	57	74	75	81	79	100
Subject 4	100	18	57	36	38	11	20	14	7
Subject 5	18	44	14	74	100	78	70	10	75
Subject 6	44	18	14	100	74	37	70	75	99
Subject 7	18	14	36	44	75	74	57	88	100
Subject 8	79	74	57	88	75	46	49	44	20
Subject 9	74	15	49	73	14	18	70	11	71
Subject 10	44	18	14	100	74	37	70	75	99
Subject 11	74	18	44	49	14	37	70	81	12
Subject 12	14	18	44	100	36	23	75	79	1
Subject 13	44	14	18	74	100	73	79	78	41

Table A14.9 Rankings for query 9

Subjects	Ranking results								
Subject 1	79	20	11	38	46	12	5	4	18
Subject 2	38	12	46	79	20	4	5	11	57
Subject 3	79	20	57	18	38	45	5	14	55
Subject 4	20	57	79	38	36	11	18	46	100
Subject 5	79	38	20	55	46	5	4	11	57
Subject 6	79	20	38	55	74	46	49	11	100
Subject 7	20	79	46	57	46	38	49	89	90
Subject 8	79	74	57	88	75	46	49	44	20
Subject 9	79	20	11	38	46	57	12	5	95
Subject 10	79	20	38	55	74	49	46	11	100
Subject 11	79	38	20	55	5	4	46	11	49
Subject 12	38	20	14	44	46	49	88	57	74
Subject 13	79	20	38	46	36	15	12	75	11

Appendix 15: Image Rankings for Nine Queries in One Hundred Images by Subjects

Contents:

- Figure A15.1 Image rankings for query 1 by subjects
- Figure A15.2 Image rankings for query 2 by subjects
- Figure A15.3 Image rankings for query 3 by subjects
- Figure A15.4 Image rankings for query 4 by subjects
- Figure A15.5 Image rankings for query 5 by subjects
- Figure A15.6 Image rankings for query 6 by subjects
- Figure A15.7 Image rankings for query 7 by subjects
- Figure A15.8 Image rankings for query 8 by subjects
- Figure A15.9 Image rankings for query 9 by subjects

In Tables A15.1-A15.9, images are displayed in order of visual similarity from most similar to least similar to each query image. The number above the image is the ID number of the image in the 100 image dataset as seen in Appendix 13, and the corresponding accumulated histogram is showed below each image.

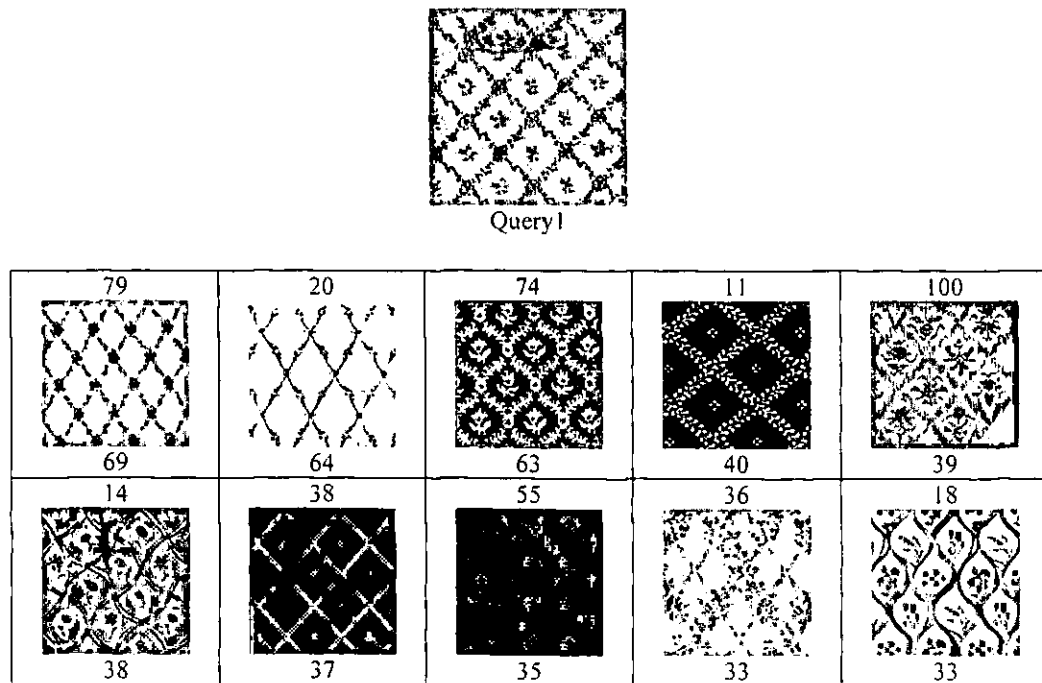


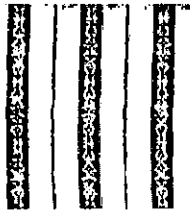
Figure A15.1 Image rankings for query 1 by subjects



Query 2

77 64	30 61	47 58	27 52	52 41
48 40	2 38	31 33	96 26	80 26

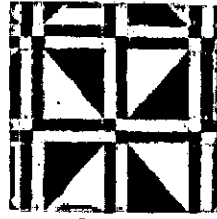
Figure A15.2 Image rankings for query 2 by subjects



Query 3

3 105	13 83	51 79	35 74	39 70
7 63	50 57	34 25	19 13	17 5

Figure A15.3 Image rankings for query 3 by subjects



Query 4

69 90	87 87	85 66	86 54	84 45
88 31	15 24	23 23	89 16	5 16

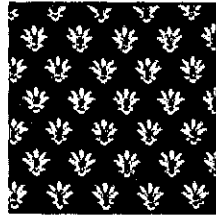
Figure A15.4 Image rankings for query 4 by subjects



Query 5

31 89	48 53	47 52	30 47	27 46
29 39	77 36	97 30	21 28	66 26

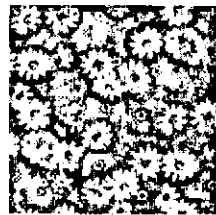
Figure A15.5 Image rankings for query 5 by subjects



Query 6

<p>37</p> <p>106</p>	<p>55</p> <p>69</p>	<p>74</p> <p>59</p>	<p>95</p> <p>49</p>	<p>49</p> <p>46</p>
<p>44</p> <p>34</p>	<p>70</p> <p>24</p>	<p>75</p> <p>19</p>	<p>1</p> <p>17</p>	<p>79</p> <p>16</p>

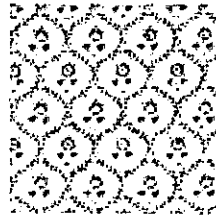
Figure A15.6 Image rankings for query 6 by subjects



Query 7

<p>32</p> <p>85</p>	<p>63</p> <p>69</p>	<p>33</p> <p>51</p>	<p>53</p> <p>41</p>	<p>41</p> <p>37</p>
<p>29</p> <p>27</p>	<p>64</p> <p>25</p>	<p>62</p> <p>22</p>	<p>56</p> <p>21</p>	<p>30</p> <p>21</p>

Figure A15.7 Image rankings for query 7 by subjects



Query 8

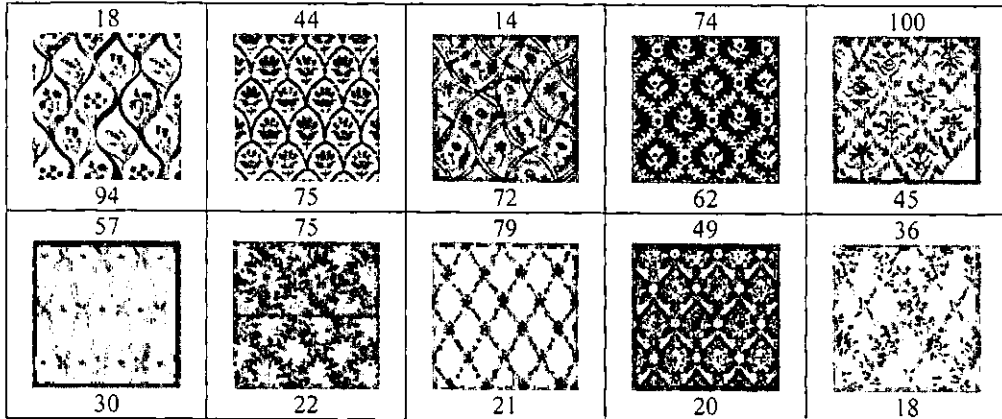
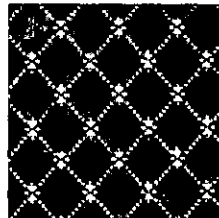


Figure A15.8 Image rankings for query 8 by subjects



Query 9

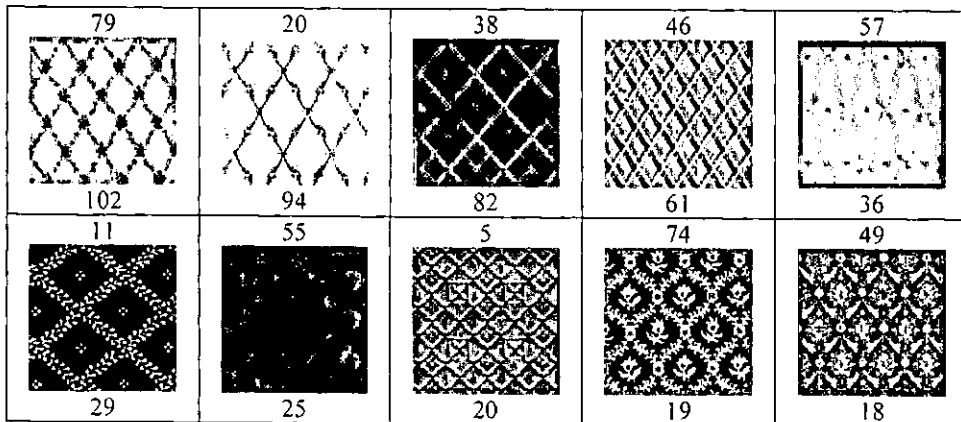


Figure A15.9 Image rankings for query 9 by subjects

Appendix 16: Precision-Recall Graphs for Nine Queries in One Hundred Images by Using Five Computational Methods

Contents:

- Figure A16.1 Precision-recall graphs for query 1
- Figure A16.2 Precision-recall graphs for query 2
- Figure A16.3 Precision-recall graphs for query 3
- Figure A16.4 Precision-recall graphs for query 4
- Figure A16.5 Precision-recall graphs for query 5
- Figure A16.6 Precision-recall graphs for query 6
- Figure A16.7 Precision-recall graphs for query 7
- Figure A16.8 Precision-recall graphs for query 8
- Figure A16.9 Precision-recall graphs for query 9

In Figures A16.1 - A16.9, the horizontal axis expresses recall and vertical axis expresses the corresponding precision at standard recall points 10%, 20%,...,100%. The curve with (-*-) expresses precision-recall by using the method of *GLCM*, (-o-) expresses *MRSAR*, (-x-) expresses *FT*, (-□-) expresses *WT*, and (-◇-) expresses *GT*. Figure(a) shows precision-recall before classification and Figure(b) shows precision-recall after classification.

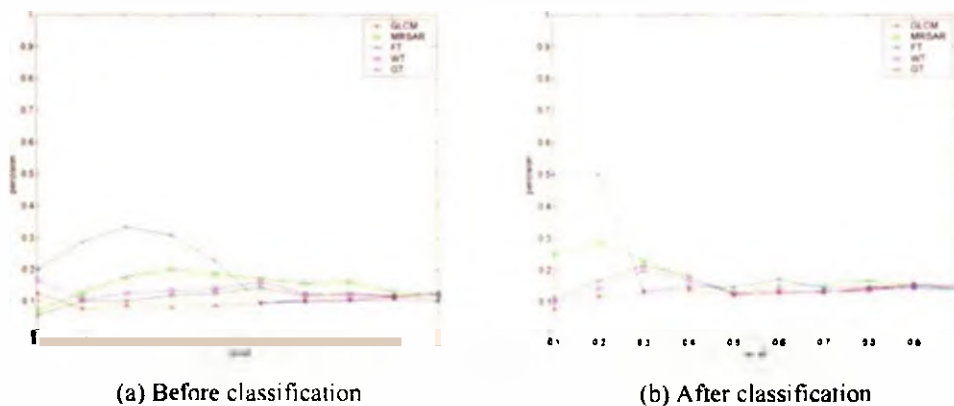


Figure A16.1 Precision-recall graphs for query 1

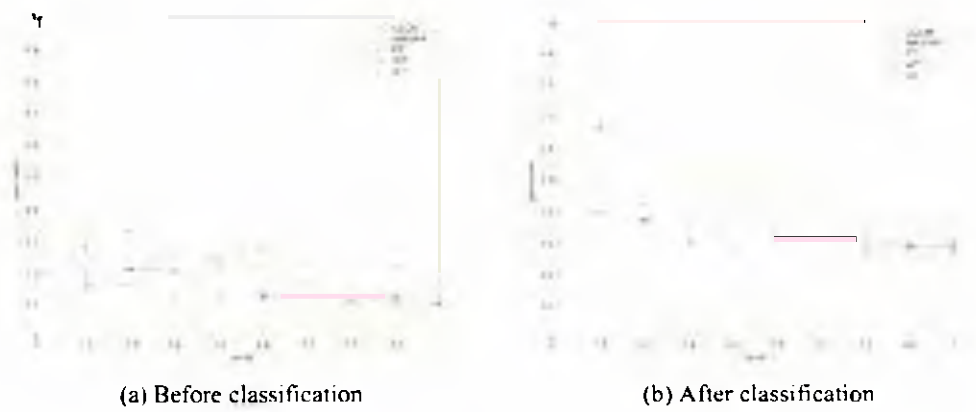


Figure A16.2 Precision-recall graphs for query 2

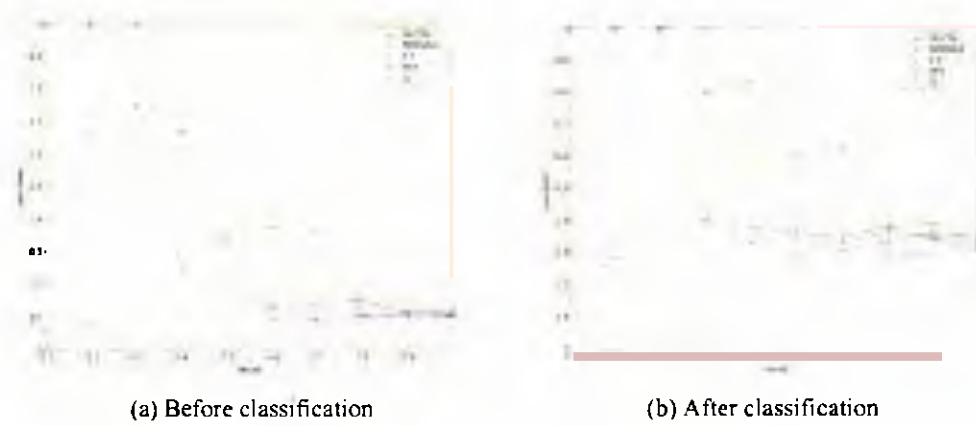


Figure A16.3 Precision-recall graphs for query 3

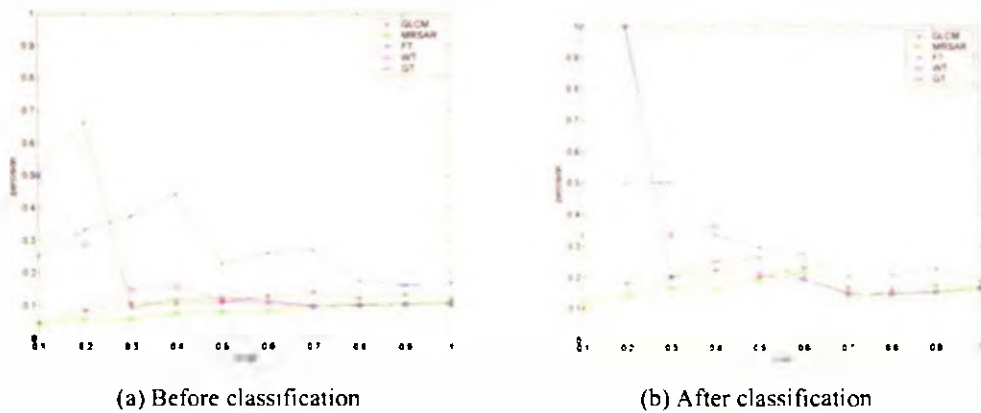
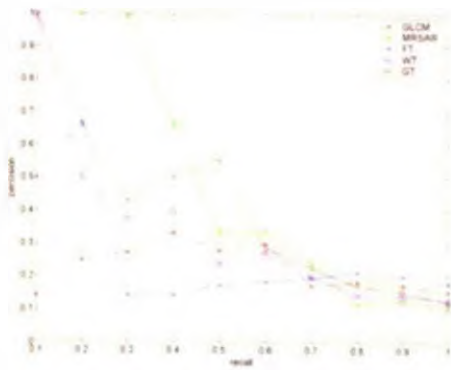
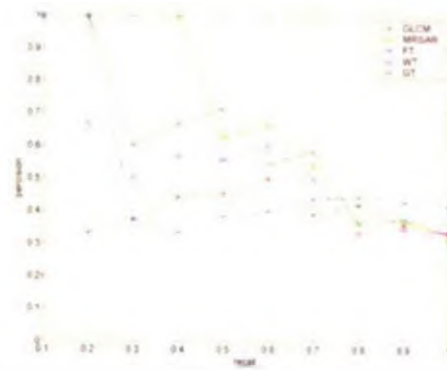


Figure A16.4 Precision-recall graphs for query 4

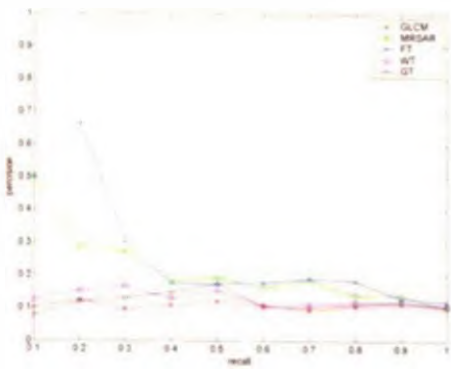


(a) Before classification

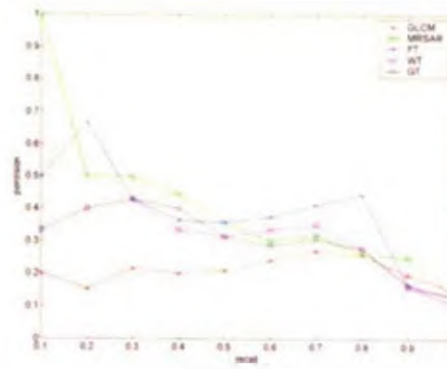


(b) After classification

Figure A16.5 Precision-recall graphs for query 5

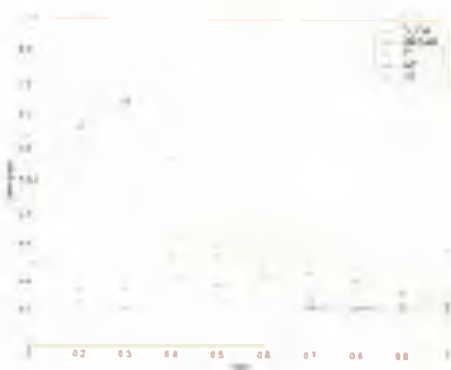


(a) Before classification

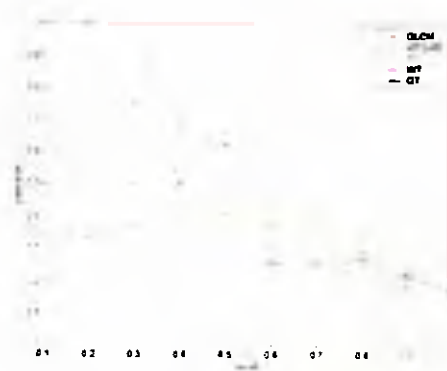


(b) After classification

Figure A16.6 Precision-recall graphs for query 6

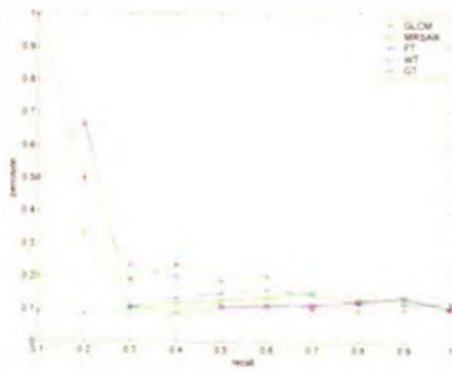


(a) Before classification

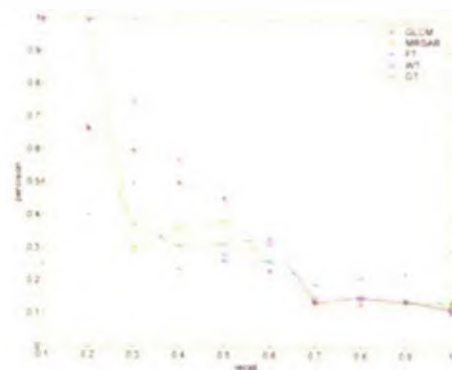


(b) After classification

Figure A16.7 Precision-recall graphs for query 7

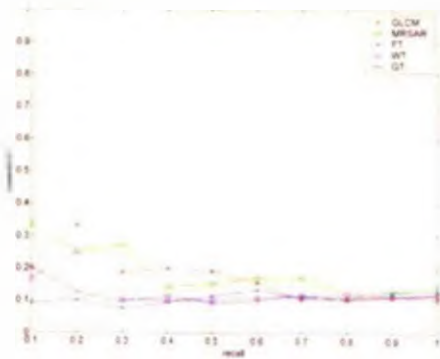


(a) Before classification

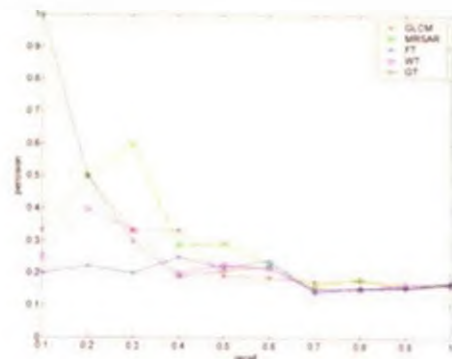


(b) After classification

Figure A16.8 Precision-recall graphs for query 8



(a) Before classification



(b) After classification

Figure A16.9 Precision-recall graphs for query 9